PHARMACEUTICALS AND PERSONAL CARE PRODUCTS IN THE TIDAL FRESHWATER POTOMAC RIVER

by

Arion Leahigh

A Dissertation
Submitted to the
Graduate Faculty
of
George Mason University
in Partial Fulfillment of
The Requirements for the Degree
of
Doctor of Philosophy
Chemistry and Biochemistry

Committee:

_____	Dr. Gregory D. Foster, Committee Chair
_____	Dr. Gerald Weatherspoon, Committee Member
_____	Dr. Benoit Van Aken, Committee Member
_____	Dr. Thomas Huff, Committee Member
_____	Dr. Gerald Weatherspoon, Department Chairperson
_____	Dr. Donna M. Fox, Associate Dean, Office of Student Affairs & Special Programs, College of Science
_____	Dr. Ali Andalibi, Interim Dean, College of Science

Date: 25 Nov 2019

Fall Semester 2019
George Mason University
Fairfax, VA

Pharmaceuticals and Personal Care Products in the Tidal Freshwater Potomac River

A Dissertation submitted in partial fulfillment of the requirements for the degree of Doctor of Philosophy at George Mason University

by

Arion Leahigh
Bachelor of Science
University of Pittsburgh, 2013

Director: Gregory D. Foster, Professor
Department of Chemistry and Biochemistry

Fall Semester 2019
George Mason University
Fairfax, VA

Copyright 2019 Arion Leahigh
All Rights Reserved

DEDICATION

This dissertation is dedicated to my husband, Jack. None of this would have been possible without your continual support, patience, and love for the past 10 years. Thank you for always believing in me, even, and especially, when I didn't believe in myself. I look forward to every day knowing that it's another day I get to spend with you.

I love you.

ACKNOWLEDGEMENTS

This project would not have been seen to successful completion without the help of a multitude of people in my life.

My sincerest gratitude and appreciation go to:

My parents, Beth and Matt, who taught me from day one that I could be and do anything I wanted, if I worked hard enough. While I am sure they are relieved that my dreams have shifted from cheerleader and mail carrier (in the off season), I know that they would have and will continue to support me in every way possible no matter what I choose to do with my life.

My committee chair and research advisor, Dr. Gregory D. Foster for taking a chance on me when few others would have done so. I have gained so much experience and knowledge these past few years and I will be forever grateful for your guidance throughout this journey.

My brother, Matt, for providing an example of someone who gets back up even after being knocked down and reminding me to lighten up and live a little. His strength to persevere inspires me every day.

My grandparents, Matt, Marilyn, Earl, and Kay, for great memories, great recipes, and great examples of how to live a life full of love for each other.

My in-laws, Maureen and Craig, for accepting me into the family, your continual support and encouragement, and, most importantly, never once asking when I'd be finished with this dissertation. I appreciate that more that you will ever know.

My Team Foster lab mates, Elizabeth Lang and Carol Ajjan, for braving the elements to help me collect samples, helping process samples during some particularly long days in the lab, and providing valuable insights and advice regarding this research project.

My fellow graduate students: Kathryn Holguin, Andrew Evangelista, and Haley Ball for always reminding me that I'm not alone in the madness that is grad school.

My friends, Colleen Wertz, Amanda Vayda, Sarah Drost, and all the others for so many years of friendship and continually reminding me that there is a great life waiting for me after school ends.

The remainder of my lab mates, Tovga Haji, Lisa McAnulty, Tabitha King, and Julia Czarnecki, who were always available to lend a helping hand regarding this research and keeping our lab running (and clean).

The field work crew from Environmental Science and Policy Department, under the supervision of Dr. Chris Jones.

Dr. Megan Devine, for paving the way for the rest of us and providing a brilliant example of what it means to be a woman and scientist.

Ivel Lee Collins, our 3D printing and software and information acquisition specialist, for spending a lot of his free time making sure we had everything necessary to collect and process data.

Dr. Tom Huff, for continual technical support with every instrument and serving on my committee.

Dr. Benoit Van Aken, for continual support and serving on my committee.

Dr. Gerald Weatherspoon, for providing me with countless opportunities that allowed me to grow as both a scientist and an individual and for serving on my committee.

The entire George Mason University, Department of Chemistry and Biochemistry for their support and guidance in my time as a graduate student.

Melissa Hayes, Director of Graduate Programs for the College of Science, for answering numerous emails and solving more problems that I could count and every single one that I managed to create.

Greg Bliss and Dr. Randy McBride from the GMU Coastal Geology Lab at Potomac Science Center for providing grain size data.

Michelle Gannon and Dr. David Velinsky from the Drexel University, Department of Biodiversity, Earth & Environmental Science for providing total organic carbon and total organic nitrogen data.

Alexandria Renew Enterprises and Arlington Water Pollution Control Plant for providing effluent samples.

The Office of the Provost at George Mason University for providing me with a Summer Research Fellowship and Dissertation Completion Grant.

The Patriot Green fund for the ability to purchase the SDI Vibecore-Mini and all other coring paraphernalia through Specialty Devices, Inc.

TABLE OF CONTENTS

Page
List of Tables x
List of Figures xii
List of Equations xvi
List of Abbreviations and Symbols xvii
Abstract xx
Chapter 1: Presence and Geospatial Distribution of Pharmaceuticals and Personal Care Products in Water and Sediments Across The Tidal Freshwater Potomac River 1
1.1 Introduction 1
1.1.1 Environmental Presence and Sources of PPCPs 1
1.1.2 Importance of the TFWPR as an area of study 7
1.2 Study Objectives 9
1.3 Materials and Methods 9
1.3.1 Study Area 9
1.3.2 Sampling Sites 11
1.3.3 Field Sampling 17
1.3.4 Materials 18
1.3.5 Sample Processing 21
1.3.6 LC-MS/MS Analysis 24
1.3.7 Quality Assurance 26
1.3.8 Ancillary Measurements 31
1.4 Results 33
1.4.1 Ancillary Data 33
1.4.2 PPCP Quantitation Frequencies 38
1.4.3 Spatial Analysis of PPCPs by Site Grouping for Water Samples 41
1.4.4 PPCP Concentrations in WTP Effluents 52
1.4.5 Distribution of PPCPs between water and sediment 57

1.5 Discussion 60
1.5.1 Comparison of PPCPs in the TFWPR to Other Sites Worldwide 60
1.5.2 Sources of PPCPs to the TFWPR 65
1.5.3 Comparison of PPCPs among WTPs 69
1.5.4 PPCP Dispersal in the TFWPR 69
1.5.5 PPCPs in Sediment 71
1.5.6 Seasonality of PPCPs 74
1.6 Conclusion 78
Chapter 2: Distribution and Flux of Pharmaceuticals and Personal Care Products between water and sediment from the Hunting Creek Region of the Tidal Freshwater Potomac River 81
2.1 Introduction 81
2.2 Study Objective 83
2.3 Materials and Methods 84
2.3.1 Sampling Sites 84
2.3.2 Materials 86
2.3.3 Field Sampling 88
2.3.4 Sample Processing 89
2.3.5 LC-MS/MS Analysis 92
2.3.6 Quality Assurance 94
2.3.7 Ancillary Measurements 99
2.3.8 Boundary Layer Model and Flux Calculations 100
2.4 Results 108
2.4.1 Ancillary Data 108
2.4.2 PPCPs in Surface Water, Pore-water, and Sediment 109
2.4.3 Flux Results 114
2.5 Discussion 118
2.5.1 Comparison of PPCP fluxes in the TFWPR to PCB and PAH fluxes 118
2.5.2 Contribution of MTCs to the Flux of individual PPCP 119
2.5.3 Comparison of PPCP fluxes throughout the TFWPR 120
2.6 Conclusion 125

Chapter 3: Occurrence of Pharmaceuticals and Personal Care Products in Riverine Sediment Cores from the Gunston Cove Region of the Tidal Freshwater Potomac River 127
3.1 Introduction 127
3.2 Study Objective 129
3.3 Materials and Methods 129
3.3.1 Sample Sites 129
3.3.2 Materials 130
3.3.3 Field Sampling 131
3.3.4 Sample Processing 132
3.3.5 LC-MS/MS Analysis 134
3.3.6 GC-MS Analysis 135
3.3.7 Quality Assurance 137
3.3.8 Ancillary Measurements 139
3.3.9 Data Processing 141
3.4 Results 141
3.4.1 Ancillary Data 141
3.4.2 PPCPs in Sediment Cores 145
3.5 Discussion 147
3.5.1 Age of Sediment Core based on Pesticide profiles 147
3.5.2 Correlation Between PPCPs, Pesticides, TOC, and PSA 149
3.5.3 Cs-137 Depth Data 150
3.5.4 PPCP vs Pesticide Depth Profiles 151
3.5.5 Comparison to other PPCP vs Pesticide Depth Profiles 152
3.6 Conclusion 152
4 Appendix 156
5 References 191

LIST OF TABLES

Table Page
Table 1.1: Pertinent Information on WTPs in the TFWPR that were of interest to this study 8
Table 1.2: Sampling Site Locations. The colors correspond to site designations in Figure 1.3 13
Table 1.3: Chemicals and their corresponding vendors used to make Internal and Surrogate Standard Solutions for LC-MS/MS Analysis 19
Table 1.4: Chemicals and their corresponding vendors used to make Calibration Standard Solutions for LC-MS/MS Analysis 19
Table 1.5: LC-MS/MS Instrument Parameters 25
Table 1.6: Flow Data for Upstream locations on the day of each sampling session. 37
Table 1.7: Percent quantitation frequencies (%QF) of the 85 target chemicals found in water and sediment. 38
Table 1.8: Sorption properties of PPCPs in sediment and surface water in the TFWPR. 71
Table 2.1: LC-MS/MS Instrument Parameters 93
Table 2.2: % TOC and %TON of HC1, HC2, and HC4 Sediment Samples 108
Table 2.3: Moisture, % Sand, % Silt, and % Clay for HC1, HC2, and HC4 Sediment Samples 109
Table 2.4: Mass Transfer Coefficients and Fluxes for detected PPCPs at HC1, HC2, and HC4 sampling locations 114
Table 3.1: LC-MS/MS Instrument Parameters 134
Table 3.2: GC-MS Instrument Parameters 136
Table 4.1A: Properties, Uses, and Structures of Targeted Pharmaceuticals and Personal Care Products[141] 156
Table 4.2A: List of Compounds, Type, and LC RT (min) for all compounds used in this analysis 163
Table 4.3A: List of PPCP MRM ions and quadrupole voltages used in LC/MS-MS analysis 166
Table 4.4A: Average %RSD values for all PPCPs detected in water samples 173
Table 4.5A: Average %RSD values for all PPCPs detected in sediment samples 174
Table 4.6A: Average Matrix Spike recovery percentages for all PPCPs water samples 175
Table 4.7A: Average Matrix Spike recovery percentages for all PPCPs in sediment samples 178
Table 4.8A: % Moisture, % Sand, % Silt, and % Clay for Sediment Samples 180
Table 4.9A: Total Suspended Matter for all water samples at all sites 181

Table 4.10A: PPCP Concentrations in Effluent sample from Alexandria Renew Enterprises in comparison to downstream of the WTP 183
Table 4.11A: PPCP Concentrations in Effluent sample from Arlington Water Pollution Control Plant in comparison to downstream of the WTP 185
Table 4.12A: Concentrations of PPCPs detected in surface water, pore-water, and sediment samples at sampling sites HC1, HC2 and HC3. 188
Table 4.13A: % Moisture, % Sand, % Silt, and % Clay for GC2 Core Subsection Sediment Samples 189

LIST OF FIGURES

Figure Page
Figure 1.1: Pictorial representation of the water cycle used in the Alexandria Renew Enterprises Wastewater Treatment Plant to transform wastewater into clean water. Information provided by Alexandria Renew Enterprises (AlexRenew) 4
Figure 1.2: Land use of the Potomac River Basin per a 2006 study published by the Interstate Commission on the Potomac River Basin[39] 10
Figure 1.3: Map of Sampling Locations (pins) and Wastewater Treatment Plants (stars) 14
Figure 1.4: Finer resolution view of the Four Mile Run Sampling locations surrounding Arlington Water Pollution Control Plant 15
Figure 1.5: Finer resolution view of the Hunting Creek Sampling locations surrounding Alexandria Renew Enterprises 15
Figure 1.6: Finer resolution view of the Gunston Cove Sampling locations surrounding Noman Cole WTP 16
Figure 1.7: Water and Sediment Processing Flow Diagram courtesy of Lisa McAnulty, George Mason University, Potomac Science Center 24
Figure 1.8: Mean Surrogate %recoveries evaluated in for all the Potomac River surface water samples. Black columns represent the mean recovery and bars represent ± 1 SD. 28
Figure 1.9: Mean Surrogate %recoveries evaluated in for all the Potomac River sediment samples. Black columns represent the mean recovery and bars represent ± 1 SD. 29
Figure 1.10: The Total Organic Carbon as %TOC for each sediment sample obtained throughout the entire TFWPR over the course of the entire sampling season..... 34
Figure 1.11: Summary % Sand, Silt, Clay diagram depicting the average % of sand, silt, clay for each site over the entire sampling season. 35
Figure 1.12: TSM for all surface water samples at all sites along the TFWPR sites throughout the entire sampling season. Black columns represent the mean recovery and bars represent ± 1 SD. 36
Figure 1.13: Median PPCP concentrations found in water (black) and sediment (white) samples at each site along the TFWPR. Water was collected at all sites. Sediment samples were not collected at CB1, CR1, GC1, FMR1, an FMR2. The Kruskal-Wallis test ($p<0.05$ for both water and sediments samples) indicate a statistical difference among the individual sample concentrations. 42
Figure 1.14: Median ΣPPCP concentrations found in surface water (black) and sediment (white) samples at each site in Hunting Creek. The Kruskal-Wallis test ($p>0.05$ for both water and sediments samples) indicate no statistical difference among the individual sample concentrations. 43

Figure 1.15: Median ΣPPCP concentrations found in surface water (black) and sediment (white) samples at each site in Gunston Cove. The Kruskal-Wallis test (p>0.05 for both water and sediments samples) indicate no statistical difference among the individual sample concentrations. 44
Figure 1.16: Median all ΣPPCP concentrations found in surface water and sediment samples at each site in Four Mile Run. Black bars represent median PPCPs in surface water samples. White bars with black outlines represent median PPCPs in sediment samples. The Kruskal-Wallis test (p>0.05 for both water and sediments samples) indicate no statistical difference among the individual sample concentrations. 45
Figure 1.17: %Composition of 18 individual PPCPs found in surface water samples at each site throughout the TWFPR. Legend color read from left to right, top to bottom. .. 47
Figure 1.18: %Composition of 16 individual PPCPs found in sediment samples at each site throughout the TWFPR. Legend color reads from left to right, top to bottom. 48
Figure 1.19: Concentrations of 9 detected PPCPs (QF >50%) (in order of decreasing median detected concentration) in surface water samples (n = 119) from all downstream sampling locations throughout the TFWPR. Boxes, centerlines, and whiskers indicate interquartile range, median, and 5th and 95th percentiles, respectively. 50
Figure 1.20: Concentrations of 14 detected PPCPs (QF >50%) (in order of decreasing median detected concentration) in sediment samples (n = 91) from all downstream sampling locations throughout the TFWPR. Boxes, centerlines, and whiskers indicate interquartile range, median, and 5th and 95th percentiles, respectively. 51
Figure 1.21: PPCPs found in Alexandria Renew effluent water samples. Black columns represent the mean concentrations (ng/L) and bars represent ± 1 SD. 53
Figure 1.22: PPCPs found at extremely high concentrations in Alexandria Renew effluent water samples. Black columns represent the mean concentrations (ng/L) and bars represent ± 1 SD. 54
Figure 1.23: PPCPs found in Arlington Pollution Control Plant effluent water samples. Black columns represent the mean concentrations (ng/L) and bars represent ± 1 SD. 56
Figure 1.24: PPCPs found at high concentrations in Arlington Pollution Control Plant effluent water samples. Black columns represent the mean concentration (ng/L) and bars represent ± 1 SD. 57
Figure 1.25: Linear regression of Log K_d versus Log D for all compounds that were found in both water and sediment samples at each site along the TFWPR. Each point represents the average Log K_d value at a particular site for one trip. 59
Figure 1.26: Radar Plot of the individual PPCPs found in the TFWPR. The plot is based on mole fraction concentrations. 66
Figure 1.27: Radar Plot of the individual PPCPs found in the WTP effluent samples. The plot is based on mole fraction concentrations. 67
Figure 1.28: Radar Plot of the individual PPCPs found in samples taken upstream of the WTPs. The plot is based on mole fraction concentrations. 68
Figure 1.29: Depiction of the interaction of mineral surfaces with the PPCPs Triamterene (left) and Desvenlafaxine (right). 74

Figure 1.30: Concentration of the PPCP DEET in surface water samples at the downstream Hunting Creek locations over the course of the entire sampling season..... 76
Figure 1.31: Concentration of the PPCP Fexofenadine in surface water samples at the downstream Hunting Creek locations over the course of the entire sampling season..... 77
Figure 1.32: Concentration of the PPCP Nicotine in surface water samples at the downstream Hunting Creek locations over the course of the entire sampling season..... 78
Figure 2.1: Map of the Upper and Lower Hunting Creek Region and the Drainage Point in the TFWPR. 85
Figure 2.2: Mean Surrogate %recoveries evaluated in for all the Potomac River surface water samples. Black columns represent the mean recovery and bars represent ± 1 SD. 95
Figure 2.3: Mean Surrogate %recoveries evaluated in for all the Potomac River pore-water samples. Black columns represent the mean recovery and bars represent ± 1 SD. 96
Figure 2.4: Mean Surrogate %recoveries evaluated in for all the Potomac River sediment samples. Black columns represent the mean recovery and bars represent ± 1 SD. 97
Figure 2.5: Processes governing the deposition and burial of PPCPs in sediments. The BBL is depicted in the diffusive flux process at the sediment-water interface and is bidirectional. Deposition and resuspension represent bulk one-way processes. 102
Figure 2.6: PPCPs concentrations in surface water, pore-water, and sediment samples at HC1 sampling location. Black bars, gray bars, and white bars represent surface water, pore-water, and sediment concentrations, respectively. In some instances, the PPCP listed was not found in sediment and, as such, no white bar is present. The y-axis was transformed to a log scale in order to be able to view all values on a simple graph. 112
Figure 2.7: PPCPs concentrations in surface water, pore-water, and sediment samples at HC2 sampling location. Black bars, gray bars, and white bars represent surface water, pore-water, and sediment concentrations, respectively. The y-axis was transformed to a log scale in order to be able to view all values on a simple graph..... 113
Figure 2.8: PPCPs concentrations in surface water, pore-water, and sediment samples at HC2 sampling location. Black bars, gray bars, and white bars represent surface water, pore-water, and sediment concentrations, respectively. The y-axis was transformed to a log scale in order to be able to view all values on a simple graph..... 114
Figure 2.9: The difference in concentration of each PPCP found in surface waters and pore-water at HC1, HC2, and HC4. Black dots represent HC1, gray dots represent HC2, and white dots with black outlines represent HC4..... 117
Figure 2.10: The three mass transfer coefficients (K_L, K_{LDOC}, and K_{BIO}) for each of the 14 individual PPCPs detected at HC1. Black dots represent K_{BIO}, gray dots represent K_L, and white dots outlined in black represent K_{LDOC}. 120
Figure 2.11: The sediment-water fluxes for each of the 14 individual PPCPs detected at HC1. Black bars represent the flux with bioturbation and white bars represent the flux without bioturbation..... 121
Figure 2.12: The sediment-water fluxes for each of the 7 individual PPCPs detected at HC2. Black bars represent the flux with bioturbation and white bars represent the flux without bioturbation..... 122

Figure 2.13: The sediment-water fluxes for each of the 5 individual PPCPs detected at HC4. Black bars represent the flux with bioturbation and white bars represent the flux without bioturbation. 123
Figure 2.14: The mass transfer coefficients K_{LTOTAL} for each of the 14 individual PPCPs detected. Black dots represent HC1, gray dots represent HC2, and white dots outlined in black represent HC4. 125
Figure 3.1: Map of the Gunston Cove Region. 130
Figure 3.2: Mean Surrogate %recoveries evaluated in for core samples. Black columns represent the mean recovery and bars represent ± 1 SD. 138
Figure 3.3: The %TOC (black bars), PSA (black dots), and %Moisture (black dashes) for each sub-sample obtained for the GC sediment core. 142
Figure 3.4: Summary % Sand, Silt, Clay diagram depicting the %Sand, %Silt, and %Clay for each subsection of the GC2 sediment core 143
Figure 3.5: C^{137} Specific Activity for each sub-sample of the GC2 sediment core. 144
Figure 3.6: The average concentration of each individual PPCP found throughout the GC2 sediment core. The y-axis is present in a log scale in order to be able to include a wide range of concentrations. 145
Figure 3.7: The Σ_{30}PPCPs (black) and $\Sigma_4$pesticides (gray, dashed) (normalized to the sub-samples with the highest concentrations) that were detected in each sub-sample of the GC2 sediment core. 146
Figure 3.8: The concentrations of OPs (black), OCs (gray), DDE (black, dotted), and DDD (gray, dashed) detected in each sub-sample of the GC2 sediment core expressed as a ratio of the concentration of each subsection to the highest concentration found throughout the core. 149

LIST OF EQUATIONS

Equation Page
Equation 1.1: Quantitation Limit for all PPCPs 26
Equation 1.2: Moisture Content in Sediment 32
Equation 1.3: Total Suspended Matter 33
Equation 1.4: The mass-based distribution coefficient 58
Equation 2.1: Flux of PPCPs 102
Equation 2.2: Pore-water concentration corrected for DOC 103
Equation 2.3: DOC correction factor for Pore-water concentrations 103
Equation 2.4: DOC-water partition coefficient 104
Equation 2.5: The sediment to water mass transfer coefficient 104
Equation 2.6: The mass transport coefficient of freely dissolved PPCPs 105
Equation 2.7: The Diffusion Coefficient 105
Equation 2.8: Molar Volume 105
Equation 2.9: The mass transfer coefficient of the DOC-bound PPCPs 106
Equation 2.10: The sediment to water partition coefficient 106
Equation 2.11: The bioturbation factor 107
Equation 2.12: Pore-water concentrations for HC2 and HC4 where pore-water was not able to be isolated 107

LIST OF ABBREVIATIONS AND SYMBOLS

% Carbon ..... %C
% Moisture ..... %M
% Quantitation Frequency ..... %QF
% Recovery ..... %R
% Relative Standard Deviation ..... %RSD
3,4-Methylenedioxy-N-ethylamphetamine ..... MDEA
3,4-Methylenedioxyamphetamine ..... MDA
3,4-Methylenedioxymethamphetamine ..... MDMA
Aluminum ..... Al
Attention Deficit Hyperactivity Disorder ..... ADHD
Benthic Boundary Layer ..... BBL
Calcium ..... Ca
Carbon C
Carbon-Nitrogen ..... CN
Celsius ..... ºC
Centers for Disease Control and Prevention ..... CDC
Centimeter ..... cm
Cesium-137 ..... Cs-137
Combined sewer outfalls ..... CSOs
Dichlorodiphenyldichloroethane ..... DDD
Dichlorodiphenyldichloroethylene ..... DDE
Dichlorodiphenyltrichloroethane ..... DDT
Dispersive Solid Phase Extraction ..... dSPE
Distribution Coefficient ..... K_d
Dual Ion Source ..... DUIS
Electrospray Ionization ..... ESI
Ethyl Acetate ..... EtOAc
George Mason University ..... GMU
Gram ..... g
Hour ..... hr
Hydrogen ..... H
Iron ..... Fe
Kilometer ..... km
Kilometer ..... km
Liquid Chromatography-Mass Spectrometry/Mass Spectrometry ..... LC-MS/MS
Liter L

Magnesium ..... Mg
Mass Transfer Coefficient ..... MTC
Matrix Spike ..... MS
Matrix Spike Recovery ..... MSR
Measured Distribution Coefficient ..... $K_{d\text{-}meas}$
Meter ..... m
Methanol ..... MeOH
Micrometer ..... µm
Milli-Q type-3 Water ..... UPW
Milligram ..... mg
Milliliter ..... mL
Millimeter ..... mm
Minute ..... min
Mixed-mode, strong **A**nion-e**X**change ..... MAX
Mixed-mode, strong **C**ation-e**X**change ..... MCX
Multiple Reaction Monitoring ..... MRM
n-octanol-water partition coefficient ..... K_{OW}
N,N-Diethyl-meta-toluamide ..... DEET
Nanogram ..... ng
Nitrogen ..... N_2
Non-Steroidal Anti-Inflammatory Drugs ..... NSAIDs
Not Applicable ..... N/A
Organochlorines ..... OCs
Organophosphates ..... OPs
Over the Counter Medications ..... OTCs
Particle Size Analysis ..... PSA
Parts Per Million ..... ppm
Pharmaceuticals and Personal Care Products ..... PPCPs
Phosphorus ..... P
Potassium ..... K
Principal Investigator ..... PI
Quantitation Frequency ..... QF
Quantitation Limit ..... QL
Quick Easy Cheap Effective Rugged Safe ..... QuEChERS
Relative Standard Deviation ..... RSD
Revolutions per minute ..... rpm
Silicon ..... Si
Sodium ..... Na
Solid Phase Extraction ..... SPE
Standard Deviation ..... SD
The District of Colombia, Maryland, and Virginia ..... DMV
Tidal Freshwater Potomac River ..... TFWPR
Total Organic Carbon ..... TOC
Total Suspended Matter ..... TSM

Total Suspended Matter ..... TSM
Ultra-High-Pressure Liquid Chromatography ..... UHPLC
United States of America ..... USA
Volts V
Volume/Volume ..... v/v
Volume/Volume/Volume ..... v/v/v
Wastewater Treatment Plant ..... WTP

ABSTRACT

PHARMACEUTICALS AND PERSONAL CARE PRODUCTS IN THE TIDAL FRESHWATER POTOMAC RIVER

Arion Leahigh, Ph.D.

George Mason University, 2019

Dissertation Director: Dr. Gregory D. Foster

It is believed that the principal source of pharmaceuticals and personal care products (PPCPs) in rivers and streams is directly linked to the high consumption rate of drugs in our society. As such, PPCPs and their metabolites are inadvertently released into the rivers and streams through reclaimed water and waste treatment plant (WTP) discharge. Understanding the sources, emissions, and effects of PPCPs in surface waters is essential to managing public health and enlightening our society about the environmental implications of overprescribed drug therapy. The goals of the present study were to (i) characterize the presence, spatial distribution, and temporal variability in the concentrations of PPCPs in water and sediments throughout the tidal freshwater Potomac River (TFWPR), (ii) evaluate the interfacial dynamics of PPCPs in the TFWPR through the quantification of sediment-water fluxes along a downstream transect near a high capacity waste treatment facility, and (iii) investigate the burial profiles of PPCPs in river

sediments. PPCPs (96 individual constituents) were analyzed in river samples using solid phase (water) and solvent extraction (QuEChERS) techniques coupled with liquid chromatography-mass spectrometry (LC-MS/MS). Approximately 42 PPCPs were quantified in river samples by LC-MS/MS at 14 individual sampling sites. Spatial analysis revealed that PPCP export from the TFWPR exceeded input, showing that the major WTPs markedly increase river concentrations. In addition, the greatest PPCP concentrations were generally found nearest the WTP outfalls. Seasonality in PPCP water concentrations was directly related to use patterns. Determination of PPCP sediment-water distribution constants indicated that mineral sorption likely plays a significant role sediment uptake. Results from sediment-water fluxes showed that bed sediments near the WTP outfalls were accumulating PPCPs, and that fluxes reversed direction further downstream. It was determined that sediment can serve as either a sink or a source of PPCPs into the water column depending upon the location and distance from the outfall studied. In addition, it was found that bioturbation had a significant role in overall fluxes. Lastly, the study also determined the nature of sediment burial and historical deposition profiles of PPCPs present in a sediment core taken from a location downstream of a high-capacity WTP in the Gunston Cove region. It was concluded that PPCPs have a significantly different historical depth profile when compared to other legacy micropollutants such as organochlorine pesticides because of the differences in their deposition rates, degradation processes, and different physical and chemical properties. Furthermore, the depth profiles suggested that PPCPs do not persist in sediments. The present study demonstrated that understanding the sources, emissions, and effects of

PPCPs in surface waters is essential to managing public health and enlightening our society about the environmental implications of overprescribed drug therapy. In addition, valuable information concerning the presence, spatial distribution, and temporal variability in the concentrations of PPCPs in water and sediments, the interfacial dynamics of PPCPs, and the burial profiles of PPCPs in river sediments was obtained as part of the effort to understand these matters.

CHAPTER 1: PRESENCE AND GEOSPATIAL DISTRIBUTION OF PHARMACEUTICALS AND PERSONAL CARE PRODUCTS IN WATER AND SEDIMENTS ACROSS THE TIDAL FRESHWATER POTOMAC RIVER

1.1 Introduction

1.1.1 Environmental Presence and Sources of PPCPs

In recent years, it has come to light that surface waters are becoming increasingly contaminated by manufactured pharmaceutical and personal care products (PPCPs).[1–5] Particularly concerning is the emergence of high levels of prescription drugs, illicit/recreational drugs, and over the counter medications (OTCs) found in surface waters and fluvial sediments worldwide.[6–8] It is believed that the principal source of these micropollutants into rivers and streams is directly linked to the high consumption rate of drugs in our society. In the USA, approximately 50% of the population has used one or more prescription drugs within the past 30 days, and the use of drugs increases with age, especially over age 60. The most commonly used types of prescription drugs include bronchodilators (children aged 0–11 years), central nervous system stimulants (adolescents aged 12–19 years), antidepressants for adults aged 20–59, and lipid-lowering drugs for adults aged 60 and over.[9] The number of prescriptions dispensed in the USA has increased between 2009 and 2018. In 2009 the number of drug prescriptions dispensed was near 3.95 billion, while in 2018 the number of prescriptions dispensed was approximately 4.21 billion. Administered drugs are released into private and public sewer

systems. When public sewer discharge enters the waste treatment stream it undergoes the process illustrated in Figure 1.1, which includes primary, secondary, and often tertiary treatment technologies. It should be noted that WTPs are not responsible for and are not efficient at removing PPCPs (and their metabolites) from wastewater during this process. There are no existing federal or state discharge regulations covering the emissions of PPCPs in the wastewater stream. As such, PPCPs and their metabolites are inadvertently released into the rivers and streams through reclaimed water. Understanding the sources, emissions, and effects of PPCPs in surface waters is essential to managing public health and enlightening our society about the environmental implications of overprescribed drug therapy.

While WTP discharge is considered a large source of PPCPs in the aquatic environment, there are several other sources that need to be acknowledged. In some instances, the treated sludge from WTPs may be released into the environment and applied as fertilizer across agricultural lands. Similarly, the PPCPs used in veterinary medicine can enter the environment when animal wastes are used as fertilizer. The run-off from these lands can then enter the water cycle. The wastewater from the facilities that produce the PPCPs is discharged to public sewers and may contain significant amounts of PPCPs, more so even than wastewater from normal households and commercial buildings. Furthermore, PPCPs can also leach into freshwater from leaky septic systems, sewer pipes, and runoff from combined sewer outfalls (CSOs).[2] While this project does not specifically focus on sources beyond WTP discharge, it is important

to note that those sources may be contributing to the overall magnitude of PPCPs found in the aquatic environment.

In general, it is known that many PPCPs can be environmentally persistent, demonstrate bioactivity, and potentially bioaccumulate in aquatic organisms.[3,10,11] These compounds pose a potential risk to ecosystem and public health because they are specifically designed to have biological effects even at low concentrations. The effects of PPCPs on aquatic organisms are of particular concern because of risk from exposure in areas surrounding WTPs. At this time the long-term effects of the exposure of aquatic organisms to PPCPs remains largely unknown; however, some studies indicate that the possibilities include delayed development, unusual behavior, and altered reproduction.[1,12] Numerous studies have been conducted to determine the bioaccumulation of PPCPs with endocrine disrupting capabilities.[2,4,10] In the majority of these studies focusing on endocrine disrupting PPCPs the research reveals that the levels of these compounds are present at concentrations high enough to pose an ecological risk in most environmental matrices (water and sediment).[7,13,14] However, fewer studies have specifically targeted opioids, amphetamines, antidepressants, anti-inflammatory, OTC medicants, and the PPCPs of interest in field studies. The proposed research will help to fill the knowledge gap in this area by focusing on a more focused subset of PPCPs in both surface waters and sediments.

Figure 1.1: Pictorial representation of the water cycle used in the Alexandria Renew Enterprises Wastewater Treatment Plant to transform wastewater into clean water. Information provided by Alexandria Renew Enterprises (AlexRenew)

When determining the list of PPCPs targeted for analysis in this study, several factors were taken into consideration. First and foremost, the majority of the compounds in this study were found to be in the comprehensive list of the top 200 most commonly prescribed drugs in the United States. In addition, it was important to select PPCPs that were detected in surface waters in previous studies conducted in different aquatic systems.[15–19] This will provide for the ability to compare the TFWPR with other aquatic systems in the United States and across the globe.

A major subgroup of PPCPs are opiate based prescription pain medications. Due to the potency and accessibility of these substances, they have been popular for both

medical treatment and recreational use despite the associated high risk of addiction and overdose.[20,21] In fact, the use (and abuse) of these substances has become so prevalent that the U.S. Drug Enforcement Administration has declared that deaths via overdose have reached epidemic levels, with almost half of all opioid related deaths in 2016 involving prescription opioids. As the opioid epidemic continues to flourish, it is estimated that the overall life expectancy of Americans will continue to drop and as many as 500,000 will die from opioid related deaths over the next decade.[23]

Another subset of PPCPs are amphetamine-based prescription medications and illicit/recreational drugs. Amphetamine is found in most Attention Deficit Hyperactivity Disorder (ADHD) medication, which has seen an exponential increase in prescriptions over the past decade. This medication is incredibly useful for individuals who have been properly diagnosed with ADHD as it stimulates their brain chemistry such that they gain improved focus. However, the recreational use of this type of medication has become increasingly attractive to young adults, specifically students, who use this medication to better focus on their school work, professional work, or other activities without the proper guidance of a physician.[24]

Additional substances of this class, methamphetamine and phentermine, share these stimulant properties while others, MDA, MDEA, and MDMA have hallucinogenic, psychedelic, and euphoric effects. These substances are extremely addictive and highly abused by a growing number of the population and their addictive nature has led to an increase in deaths related to psycho-stimulant abuse, specifically methamphetamine, over the past decade.[25]

In addition to amphetamines and opiates, this work also focused on antibiotics, antimicrobial, antibacterial, antiviral, and antiparasitic medications. While the majority of these PPCPs are prescription medications, studies have shown that the United States is currently experiencing an issue of patients being overprescribed medications. In regard to antibiotics, it was shown that in the United States in 2016 at least 30 percent were prescribed unnecessarily.[26–28] Research conducted by the Centers for Disease Control and Prevention (CDC) found that the majority of these prescriptions were given to patients to treat conditions caused by viruses, which do not respond to antibiotics.[26] This over and non-therapeutic prescription of antibiotics (and other medications) has caused an excess of antibiotics, and other prescription medications, to end up in our sewage systems and, eventually, waterways.

In addition to PPCPs that can help treat physical issues, there are several classes of PPCPs that can treat mental health issues.[29] These classes include, antianxiety, sedative, antidepressant, and selective serotonin reuptake inhibitors. The recent focus on mental health in society today has led to a great increase in the quantity of these substances being prescribed to patients. However, like other PPCPs, these medications eventually end up in our waterways. Several other classes of PPCPs were studied, including - bronchodilators, statins, beta blockers, antihypertensives, diuretics, non-steroidal anti-inflammatory drugs (NSAIDs), OTCs, and personal use/personal care products.

The Clean Water Act, originally enacted in 1972 as the Federal Water Pollution Control Act, is a U.S. Federal law that regulates the pollutants discharged into surface

waters across the country.[30] While this act has changed and grown in many ways since initially enacted, it does not currently detail any regulatory specifications regarding pharmaceuticals.[31] However, given the increase of the consumption of these substances, it can be expected that the concentrations of these substances will continue to increase in the aquatic environment. Therefore, monitoring the concentrations, and subsequent remediation, of these contaminants is more of a concern as they may cause multiple issues in the aquatic environment as time moves forward. This study utilized a schedule of 91 PPCPs representing the diverse classes of pharmaceuticals mentioned previously with the goal of obtaining a deeper understanding of the presence and distribution of these compounds and better determine if they are a threat to ecological and public health. The structure, uses, and relevant properties of each of the PPCPs studied herein are listed in Table 4.1A.

1.1.2 Importance of the TFWPR as an area of study

The Potomac River is an approximately 610-kilometer (km) long tributary of the Chesapeake Bay, that originates in the Allegheny Mountains, West Virginia and is the second largest tributary of the Chesapeake Bay.[32] The TFWPR is a 174-km stretch that begins below the Fall Line, a steep slope where the Atlantic coastal plain meets the Piedmont plateau, and extends to the Chesapeake Bay.[33] The flow of this section of the Potomac River is influenced by the tides, hence the name, and is the region of the watershed that supports the greatest human population.

The tidal rivers and their estuaries are unique due to the proximity to large urban areas as well as the biodiversity of their ecosystems. The estuaries of tidal rivers are areas that experience the influence of both nature and humankind as the need for food, water, WTPs, and urban and agricultural products create stress on all coastal resources.[34] This project focused on an approximately 60 km stretch of the upper TFWPR starting at Chain Bridge, McLean, VA and ending at Leesylvania State Park, Woodbridge, VA illustrated in Figure 1.3. This area was of particular interest for several reasons, including multiple high-capacity WTP plants discharging into a small area and the very large overall population served by those WTPs. Table 1.1 provides pertinent information on the scale of the four largest WTPs of interest in this study. The accumulation of PPCPs in the surface water and sediment beds of the TFWPR and the combination of population size and WTP discharge made this area ideal for this study. The TFWPR is a highly WTP-impacted region in the Potomac River watershed.

Table 1.1: Pertinent Information on WTPs in the TFWPR that were of interest to this study

WTP Name	Tributary of Discharge	Discharge Capacity[35–38] *(million gallons per day)*	Sewershed Population
Alexandria Renew Enterprises	Hunting Creek	25	~315,000
Arlington Water Pollution Control Plant	Four Mile Run	10	~300,000
Noman Cole Wasterwater Treatment Plant	Gunston Cove	67	~372,000
Blue Plains Advanced Wastewater Treatment Plant	Potomac River	300	~681,000

1.2 Study Objectives

The goal of this study was to characterize the presence, spatial distribution, and temporal variability in the concentrations of PPCPs in water and sediments throughout the TFWPR associated with WTP discharge. These are the first critical steps in framing the ecological and public health risks of PPCPs in the fluvial-estuarine boundary. The primary objective of this study was to identify major-use PPCPs in water and sediments, where applicable, from all sampling locations to quantify the presence and concentrations of PPCPs in the TFWPR. The secondary objectives of this study were to assess the geospatial differences between the different embayment areas and compare the water and sediment profiles for all PPCPs to ascertain the distribution between the two matrices.

1.3 Materials and Methods

1.3.1 Study Area

The 37,996 square kilometer (km) watershed of the Potomac River, including areas of Maryland, West Virginia, Virginia, and the District of Columbia (illustrated in Figure 1.2), contains 57.6% forested land, 31.8% agricultural land, 4.8% developed land, and 5.2% water and wetlands. As of the 2010 census, the population of the Potomac River watershed was estimated to be 6.11 million people, with 81% of the population living in urban areas.[32] The District of Colombia, Maryland, and Virginia (DMV) area is the focus of this study. The population of this area is 5.1 million, roughly 84% of the basin population, with an average population density of 8,470 per square km. The average flow recorded on the Potomac River in this area is approximately 26.5 billion liters per day.[32]

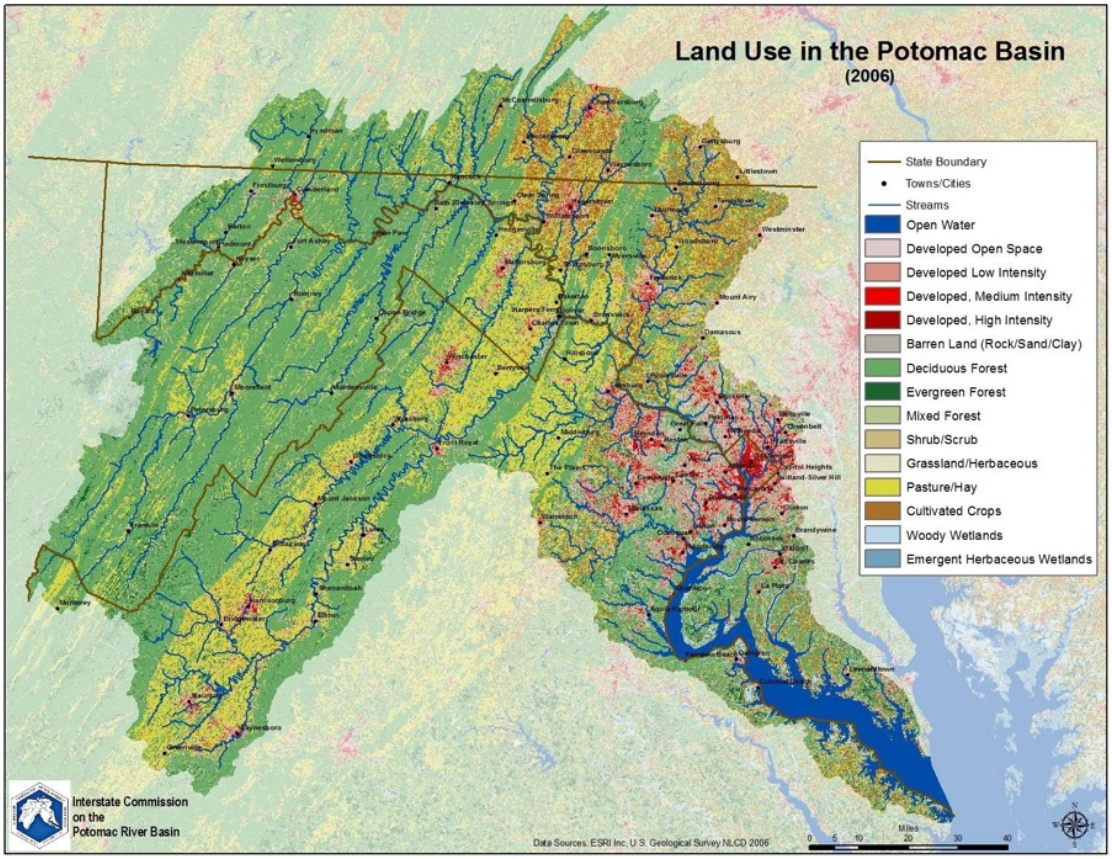

Figure 1.2: Land use of the Potomac River Basin per a 2006 study published by the Interstate Commission on the Potomac River Basin[39]

The TFWPR is an estuary that contains several embayments at the fluvial-estuarine boundary that were the focus areas of present study. An estuary can be defined as a body of water in which seawater is significantly diluted by freshwater,[34] and fluvial-estuarine boundary as the transition between the upland river and the estuary. The Potomac River connects not to the sea, but to the Chesapeake Bay and therefore, the estuaries of the TFWPR are a mix of freshwater and the brackish water of the

Chesapeake Bay. Brackish water is water that has more salinity than freshwater but less than seawater. Embayments are recesses in a coastline that form areas of water that are smaller than what could be considered a gulf but larger than what could be considered a cove. These shoals are somewhat protected from the full force of the flow of the main body of water, in this case the TFWPR, and exceedingly biodiverse, providing habitats for a variety of species. In addition, these areas have been known to be host to recreational activities such as boating, fishing, and other water sports.[34,40,41] The WTPs of focus in this area all discharge into streams that eventually flow into these embayments making them ideal locations for collection of samples and detection of PPCPs.

The specific area of this study, illustrated in Figure 1.3, is characterized by fresh water flows and riverine chemistry.[33] Riverine chemistry describes the process in which a river can transport dissolved ions that have been introduced into the system from surface runoff and groundwater. The average amount of dissolved solids in rivers is approximately 100 mg/L; for comparison, the total dissolved solids in rain water is roughly 5 mg/L.[41,42] The amount of dissolved solids in rivers can be attributed to the weathering of minerals into clays, which most commonly contain Al, Ca, Fe, K, Mg, Na, P, and Si, which contributes to the overall makeup of the sediment in these areas.[43]

1.3.2 Sampling Sites

Water and sediment samples were collected from several locations (Table 1.2) throughout the TFWPR. These locations were chosen based on their proximity to large WTPs, location within embayments, and accessibility for ease of sampling.

In addition, it was necessary to have a broad coverage of the TFWPR that included both upstream and downstream sites as well as a more detailed geospatial profile near the WTP discharge. Chain Bridge was selected as the most upstream site since this location is the beginning of the TFWPR and is upstream of all WTP discharges in the area of study. The areas of Hunting Creek, Four Mile Run, and Gunston Cove consisted of at least one site upstream of the WTP discharge, a site immediately downstream of the WTP discharge, and at least on additional site further downstream. The Lower Potomac was selected as the most downstream site and the terminus of the tidal freshwater river before entering the oligohaline tidal zone (characterized by higher salinity) of the Potomac River and is downstream of all WTP discharge in the sampling area.

More detailed maps of each geospatial regions surrounding the WTP plants of interest can be found in Figure 1.4, Figure 1.5, and Figure 1.6. In these maps, all sites, upstream and downstream are designated with their labeling code listed in Table 1.2. The WTPs are indicated with a star icon and are also labeled according to their given names. The Chain Bridge and Lower Potomac sites are not present on any of the finer resolution maps but are included in Figure 1.3, as the most upstream and most downstream points, respectively.

Table 1.2: Sampling Site Locations. The colors correspond to site designations in Figure 1.3.

Sampling Site Name	# of Sites	Sampling Cite Location	Labeling Code	Sample Cite Coordinates	Nearby Wastewater Treatment Plant
Chain Bridge	1	Arlington, VA	CB1	38.9296, -77.11682	Upstream of ALL WTP
Upper Hunting Creek	1	Alexandria, VA	CR1	38.80543, -77.10747	Upstream Alexandria Renew Enterprises
Hunting Creek	5	Alexandria, VA	HC1 HC2 HC3 HC4 HC5	38.79367, -77.05887 38.78546, -77.05128 38.77958, -77.04911 38.77815, -77.0345 38.79839, -77.03847	Alexandria Renew Enterprises
Upper Four Mile Run	1	Arlington, VA	FMR1	38.84884, -77.10265	Upstream Arlington Water Pollution Control Plant
Four Mile Run	2	Arlington, VA	FMR2 FMR3	38.8405, -77.05262 38.83284, -77.04018	Arlington Water Pollution Control Plant
Upper Gunston Cove	1	Lorton, VA	GC1	38.70129, -77.21021	Upstream Noman-Cole WTP
Gunston Cove	2	Lorton, VA	GC2 GC3	38.67514, -77.15645 38.67399, -77.12894	Noman-Cole WTP
Potomac Science Center	1	Woodbridge, VA	-	38.65800, -77.23632	Location of Lab
Lower Potomac	1	Woodbridge, VA	LP1	38.5911, -77.24595	Downstream of ALL WTP

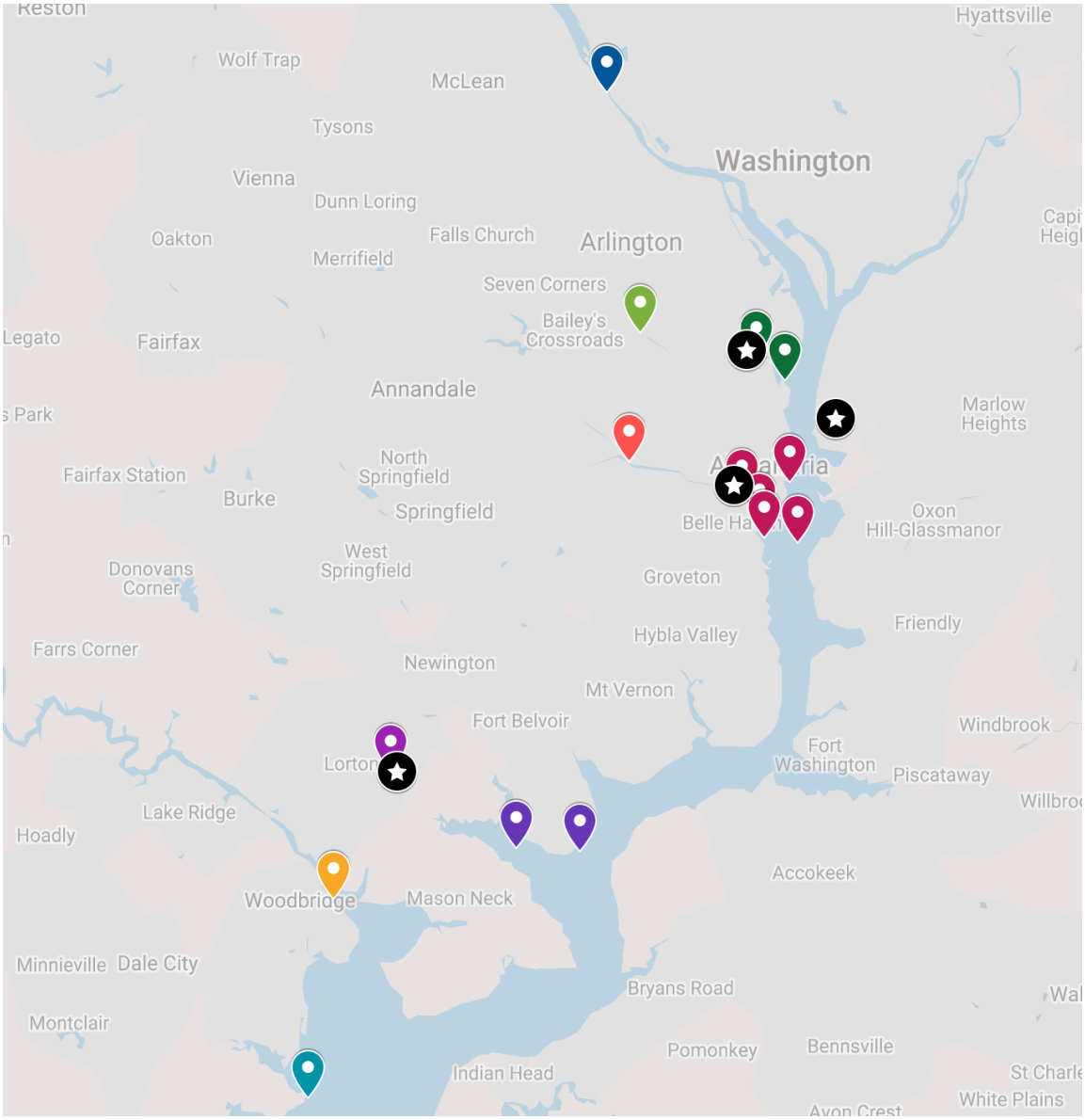

Figure 1.3: Map of Sampling Locations (pins) and Wastewater Treatment Plants (stars)

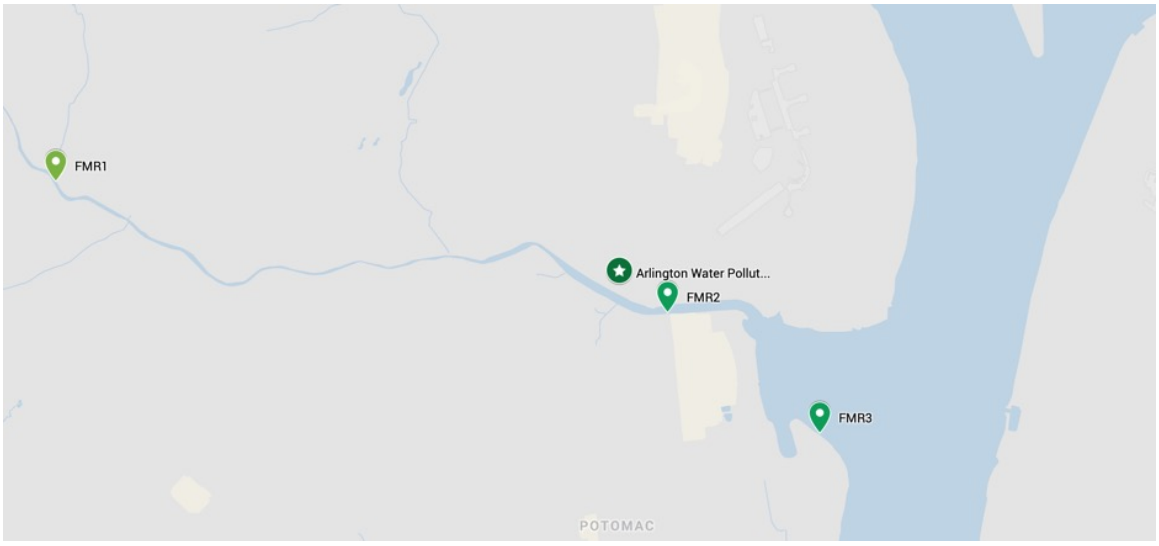

Figure 1.4: Finer resolution view of the Four Mile Run Sampling locations surrounding Arlington Water Pollution Control Plant

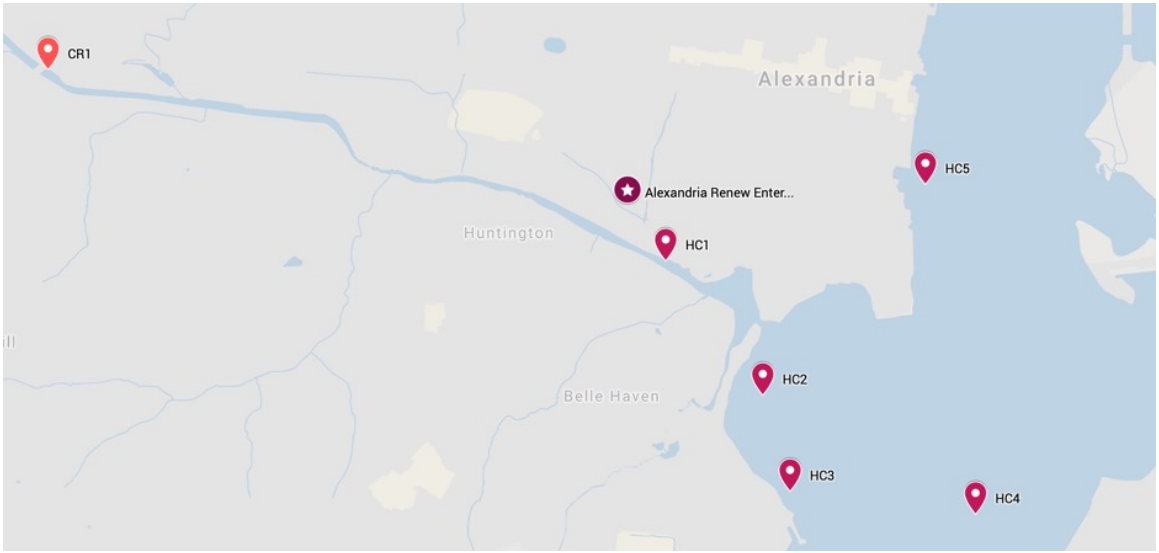

Figure 1.5: Finer resolution view of the Hunting Creek Sampling locations surrounding Alexandria Renew Enterprises

Figure 1.6: Finer resolution view of the Gunston Cove Sampling locations surrounding Noman Cole WTP

The three wastewater treatment plants serve different geographical areas with minor variations in population size. Alexandria Renew Enterprises serves approximately 169,000 and 146,000 people from Fairfax County and the City of Alexandria, respectively, for a total of 315,000 customers. Arlington Water Pollution Control plant serves approximately 226,400 people from Arlington County, Fairfax County, and some portions of Falls Church and Alexandria. The population served can swell to approximately 306,500 during the daytime as commuters enter treatment zones for work and other activities. Noman Cole WTP serves approximately 372,000 people, making up 40% of the population of Fairfax County. As the population size for each WTP is within approximately 20% of the average, the overall magnitude of PPCPs found within each region exhibited a similar distribution. However, the differences in geographical areas treated by each WTP was evident in the distinct PPCPs found in each geospatial region.

1.3.3 Field Sampling

River water samples were obtained as surface grabs onboard a skiff or on foot in shallow water using a submersible pump (12 V, Max Flow 8.7 L/min, Model No. 75509-55, Cole Parmer, Mt Vernon Hills, IL). Each water sample (~20 liters (L)) was collected in a vertically integrated fashion when the depth was greater than 2 meters (m) (an interval from 0.5 m below the surface to 0.5 m above the river bottom). The water was collected in 20-L sealed stainless-steel kegs and labeled for transportation to the Environmental Chemistry Laboratory at the Potomac Science Center (George Mason University). Upon return to the laboratory, the water samples were immediately filtered and stored for less than 24 – 48-hr at 10˚C prior to analytical processing. At each sampling site two additional 1-L water samples were collected in polypropylene bottles using the same pump method for the analysis of total suspended matter (TSM) at each site. All sample containers were pre-rinsed three times with sample water prior to filling.

Riverbed sediments were obtained onboard a skiff or via shoreline sampling coincident with water sampling when available fine-grained sediment was present (i.e., primarily silt-clay composition). Upstream sites were often rocky bottom and sediments were not obtained. The sediments were collected using a Petite Ponar grab sampler tethered by rope. The sediment obtained in the Ponar was taken aboard the boat or shore and expelled into a stainless-steel tray, while being careful not to disturb the sediment. Approximately 10 g of the top 2 – 4-cm surficial layer was removed and placed directly into a pre-cleaned amber glass jar using a stainless-steel spoon. The jar was sealed using a Teflon-lined lid and stored on ice for transportation to the Environmental Chemistry

Laboratory at the Potomac Science Center. The samples were stored at -20˚C until analytical processing could be performed.

1.3.4 Materials

Whatman® glass microfiber filters, GF/F and GF/D, sizes 47 mm and 150 mm, were used for water filtration for small and large volume water samples, respectively, and were purchased from Sigma Aldrich (St. Louis, MO). Oasis MAX (**M**ixed-mode, strong **A**nion-e**X**change) and MCX (**M**ixed-mode, strong **C**ation-e**X**change) 6 cc Vac Cartridges (500 mg Sorbent per Cartridge, 60 μm Particle Size) used in the extraction of all water samples were purchased from Waters Corporation (Milford, MA). QuEChERS (Agilent Technologies, Santa Clara, CA) extraction and dispersive solid phase extraction (dSPE) salts and kits, used to process all sediment samples for LC-MS/MS analysis, were purchased from Agilent Technologies (Santa Clara, CA). Acetonitrile and formic acid, used to make the LC-MS/MS mobile phases, was purchased from Thermo Fisher Scientific (Waltham, MA). Other bulk solvents used for analysis and supply preparation included methanol, acetone, and ethyl acetate were purchased from Thermo Fisher Scientific (Waltham, MA). Milli-Q type-3 water (UPW), used to make an LC-MS/MS mobile phase and for cleaning purposes was made in house by a MilliQ Direct 18/6 system. LCMS liquid nitrogen and compressed argon and nitrogen gasses were purchased from Roberts Oxygen (Rockville, MD).

The PPCPs were purchased as isotopically labeled chemicals to make up the LC-MS/MS internal/surrogate (Table 1.3) and target (Table 1.4) analytes in the analytical

standards (>97% purity). The chemicals purchased initially were used to make up the three individual working mixes, which were then combined and diluted into acetonitrile for mixtures used as calibration standards.

Table 1.3: Chemicals and their corresponding vendors used to make Internal and Surrogate Standard Solutions for LC-MS/MS Analysis

Internal Standard Mixture		Surrogate Standard Mixture	
Chemical	**Vendor**	**Chemical**	**Vendor**
Caffeine-$^{13}C_3$	Cerilliant	Bisphenol A-$^{13}C_{12}$	Cambridge Isotope Labs
Ibuprofen-d_3	Sigma-Aldrich	Ethyl paraben-$^{13}C_6$	Cambridge Isotope Labs
17b-Estradiol-d_5	Sigma-Aldrich	Desethylatrazine-$^{13}C_3$	Cambridge Isotope Labs
Ciprofloxacin-d_8	Sigma-Aldrich	Estrone-$^{13}C_3$	Cambridge Isotope Labs
Sulfamethazine-$^{13}C_6$	Cambridge Isotope Labs	Progesterone-$^{13}C_3$	Sigma-Aldrich
Fluoxetine-d_6	Sigma-Aldrich	Norsertraline-$^{13}C_6$	Sigma-Aldrich
Diazepam-d_5	Sigma-Aldrich	Alprazolam-d_5	Sigma-Aldrich
Testosterone-$^{13}C_3$	Sigma-Aldrich	Benzophenone-d_{10}	Sigma-Aldrich
Oxybenzone-d_5	Sigma-Aldrich	Sulfamethoxazole-$^{13}C_6$	Cambridge Isotope Labs
n-Propyl Paraben-$13C_6$	Cambridge Isotope Labs	Hydrocodone-d_6	Sigma-Aldrich
Oxycodone-d_3	Sigma-Aldrich	(+\-)-MDA-d_5	Sigma-Aldrich
(±)-Methamphetamine-d_5	Sigma-Aldrich		

Table 1.4: Chemicals and their corresponding vendors used to make Calibration Standard Solutions for LC-MS/MS Analysis

Working Mix A		Working Mix B		Working Mix C	
Chemical	**Vendor**	**Chemical**	**Vendor**	**Chemical**	**Vendor**
4-Aminobenzoic acid	Sigma-Aldrich	(+)-Propoxyphene	Cerilliant	(±)-Amphetamine	Sigma-Aldrich
Acetaminophen	Sigma-Aldrich	1,7-Dimethylxanthine	Sigma-Aldrich	MDA	Sigma-Aldrich
Azithromycin	Sigma-Aldrich	Acyclovir	Cerilliant	(±)-MDEA	Sigma-Aldrich
Caffeine	Sigma-Aldrich	Amlodipin besylate	Sigma-Aldrich	(±)-MDMA	Sigma-Aldrich
Chloramphenicol	Sigma-Aldrich	Benztropine mesylate	Sigma-Aldrich	(±)-Methamphetamine	Sigma-Aldrich
Ciprofloxacin	Sigma-Aldrich	Bupropion HCl	Cerilliant	Phentermine	Sigma-Aldrich
Dextromethorphan hydrobromide monohydrate	Sigma-Aldrich	Clonidine	Cerilliant	Buprenorphine	Sigma-Aldrich
N,N-Diethyl-m-toluamide	Sigma-Aldrich	Diltiazem HCl	Cerilliant	Codeine	Sigma-Aldrich
Diphenhydramine hydrochloride	Sigma-Aldrich	Enalapril Maleate	Sigma-Aldrich	Fentanyl	Sigma-Aldrich
Enrofloxacin	Sigma-Aldrich	Fexofenadine HCl	Sigma-Aldrich	Hydrocodone	Sigma-Aldrich
Erythromycin	Sigma-Aldrich	Lisinopril	Sigma-Aldrich	Hydromorphone	Sigma-Aldrich

Sulfadimethoxine	Sigma-Aldrich	Loratadine	Santa Cruz Biotech	Meperidine	Sigma-Aldrich
Sulfamethazine	Sigma-Aldrich	Metformin (1,1-Dimethylbiguanide) HCl	Santa Cruz Biotech	(±)-Methadone	Sigma-Aldrich
Sulfamethoxazole	Sigma-Aldrich	Nadolol	Santa Cruz Biotech	Morphine	Sigma-Aldrich
Sulfaquinoxaline	Sigma-Aldrich	Promethazine HCl	Cerilliant	Naloxone	Sigma-Aldrich
Sulfathiazole	Sigma-Aldrich	Ranitidine HCl	Sigma-Aldrich	Naltrexone	Sigma-Aldrich
trans-3′-Hydroxycotinine	Cerilliant	S(-)-Nicotine	Cerilliant	Oxycodone	Sigma-Aldrich
Trazadone	Cerilliant	Verapamil HCl	Cerilliant	Oxymorphone	Sigma-Aldrich
Triclocarban (3.4.4'-Trichlorocarbanilide)	Sigma-Aldrich	2-Hydroxy Ibuprofen	Sigma-Aldrich	cis-Tramadol	Sigma-Aldrich
Trimethoprim	Sigma-Aldrich	Atrazine Mercapturate	Toronto Research Chems	Alprazolam	Sigma-Aldrich
Albuterol (Salbutamol)	Sigma-Aldrich	Celecoxib	Santa Cruz Biotech	Clonazepam	Sigma-Aldrich
Amoxicillin Trihydrate	Sigma-Aldrich	Diclofenac Sodium Salt	Sigma-Aldrich	Diazepam	Sigma-Aldrich
Atenolol	Sigma-Aldrich	Furosemide	Cerilliant	Flunitrazepam	Sigma-Aldrich
Atorvastatin Calcium Salt Trihydrate	Sigma-Aldrich	Glipizide	Sigma-Aldrich	(±)-Lorazepam	Sigma-Aldrich
Ethyl 4-Aminobenzoate (Benzocaine)	Sigma-Aldrich	Ketoprofen	Sigma-Aldrich	Nitrazepam	Sigma-Aldrich
Chlorotetracycline HCl	Sigma-Aldrich	Perfluorooctanoic Acid	Sigma-Aldrich	Oxazepam	Sigma-Aldrich
Cimetidine	Sigma-Aldrich	Theophylline	Cerilliant	Temazepam	Sigma-Aldrich
Cotinine	Sigma-Aldrich	Triclocarban	Sigma-Aldrich	Citalopram HBr	Sigma-Aldrich
(±)-Metoprolol (+)-Tartrate Salt	Sigma-Aldrich	Warfarin	Cerilliant	Desmethylene Paroxetine HCl	Sigma-Aldrich
Oxytetracycline HCl	Sigma-Aldrich	Ibuprofen	Cerilliant	Duloxatine HCl	Sigma-Aldrich
Penicilliin G Sodium Salt	Sigma-Aldrich	Naproxen	Cerilliant	Escitalopram oxalate	Sigma-Aldrich
Propanolol HCL	Sigma-Aldrich	Triclosan		Fluoxetine HCl	Sigma-Aldrich
Simvastatin	Sigma-Aldrich	Gabapentin	Cerilliant	Norfluoxetine oxalate	Sigma-Aldrich
Tetracycline HCl	Sigma-Aldrich	Bezafibrate	Sigma-Aldrich	Norsertraline HCl	Sigma-Aldrich
Triamterene	Sigma-Aldrich	Hydrochlorothiazide	Cerilliant	Desmethylvenlafaxine HCl	Sigma-Aldrich
		Aspartame	Sigma-Aldrich	Paroxetine HCl hemihydrate	Sigma-Aldrich
		Potassium clavulanate	Sigma-Aldrich	Sertraline HCl	Sigma-Aldrich
		Budesonide	Sigma-Aldrich	Venlafaxine HCl	Sigma-Aldrich
		Formoterol	Sigma-Aldrich	Amitriptyline HCL	Sigma-Aldrich
				Nortriptyline HCL	Sigma-Aldrich
				Nordiazepam	Sigma-Aldrich
				10,11-Carbamazepine epoxide	Sigma-Aldrich
				Carbamazepine	Sigma-Aldrich

All glassware used for sample storage and preparation were cleaned by washing with soap, rinsing with UPW and fired at 400°C overnight to ignite any interfering

organic residues on surfaces that may interfere with quantitative analysis. All laboratory materials were made of glass, stainless steel, or Teflon to avoid sample contamination. The Teflon materials were cleaned the same way as glass, but without firing. All non-glass items were rinsed with methanol and air dried before use.

1.3.5 Sample Processing

The 20-L river water samples were initially filtered through GF/D and GF/F glass fiber filters to isolate the suspended particles from water, which is summarized in Figure 1.7. The filtered water was aliquoted into 1-L glass jars for subsequent extraction. The filtered water was spiked with 50 – 100 ng each of the internal and surrogate standards (Table 1.3) prior to extraction.

The PPCPs were extracted from the filtered water samples via a solid phase extraction (SPE) technique using Oasis MAX and MCX SPE cartridges. The cartridges were loaded onto a Supelco vacuum manifold (Sigma Aldrich, St. Louis, MO). The MCX cartridges were connected directly to the manifold. The MAX cartridges were stacked on top of the MCX cartridges via a SPE Tube Adapter (Sigma Aldrich, St. Louis, MO). The vacuum manifold was rinsed with methanol prior to the loading of the cartridges. The Oasis MAX and MCX cartridges were conditioned twice with 5 mL of 70:30 (volume/volume – v/v) methanol (MeOH):ethyl acetate (EtOAC), 5 mL of MeOH, and 5 mL of UPW. The filtered samples were then loaded onto the cartridges using large volume sample tubing at a rate of 2 – 3 drops per second. Upon the conclusion of the extraction, the cartridges were washed twice with 95:5 (v/v) UPW:MeOH. The cartridges

were dried on the manifold for 30 minutes prior to elution. Following the drying step, the cartridges were eluted into 40 mL amber vials. The MAX cartridges were eluted with 6 mL of 69:29:2 (v/v/v) MeOH:EtOAC:Formic Acid. The MCX cartridges were eluted with 6 mL of 67.5:27.5:5 (v/v/v) MeOH:EtOAC:Ammonium Hydroxide. The SPE extracts are reduced in volume to approximately 0.5 mL using a TurboVap (Zymark Corp., Hopkinton, MA) evaporator (employing dry N_2 gas), transferred to 1.5 mL amber glass LC-MS/MS vials, and stored in a -20°C freezer prior to quantitative analysis.

The sediment samples were initially pre-sieved through a 500-µm stainless steel mesh into a 50-mL centrifuge tube. The tubes were placed in the centrifuge at 2200 rpm for 10 minutes to collect the solids. Once removed from the centrifuge, any supernatant water was discarded. Each sample was sub-sampled for LC-MS/MS, % moisture (%M), particle size analysis (PSA), and total organic carbon (TOC) analysis.

In LC-MS/MS analysis, the sediment samples (precisely weighted to 2 g) were spiked with internal and surrogate standards and the samples were extracted via the QuEChERS (**Q**uick-**E**asy-**Ch**eap-**E**ffective-**R**ugged-**S**afe) method[44–47] as summarized in Figure 1.7. The 2 g of sediment were transferred to a 50-mL centrifuge tube and 10 mL of Optima grade acetonitrile was added to each tube. Each sample was then spiked with 50 – 100 ng each of the internal and surrogate standards (Table 1.3). The tubes were vortexed for 10 minutes. After vortexing each sample, 10 mL of UPW was added to every sample. The samples were vortexed again for 1 min. QuEChERS packets containing 6 g of anhydrous magnesium sulfate and 1.5 g of sodium acetate were added to each sample. This step created a phase separation between the water and acetonitrile

and forced the PPCPs to partition into the organic phase. The tubes were centrifuged for 10 min at 2200 rpm. An 8-10 mL aliquot of the organic phased was then transferred via glass pipette to a 15-mL dSPE tube containing 1.2 g of magnesium sulfate and 0.4 g of primary-secondary amine, removing any interfering matrix components. The tubes were vortexed and centrifuged for 10 min at 220 rpm. The supernatant of each sample was transferred to a clean 40-mL amber glass vial using a glass pipette. The SPE extracts were reduced in volume to approximately 0.5 mL using a TurboVap (Zymark Corp., Hopkinton, MA) evaporator (employing dry N_2 gas) and transferred to 1.5 mL amber glass LCMS vials. The extracts were stored in a -20°C freezer prior to quantitative analysis.

All samples were analyzed in triplicate. The water and sediment processes are depicted in the flow diagram in Figure 1.7. In addition, grain size and TOC were also analyzed in all sediment samples using a Beckman-Coulter (Brea, CA) laser diffraction (LS 13320) particle size analyzer and a Carlo Erba Model 1112 Flash Elemental Analyzer (Egelsbach, Germany), respectively.

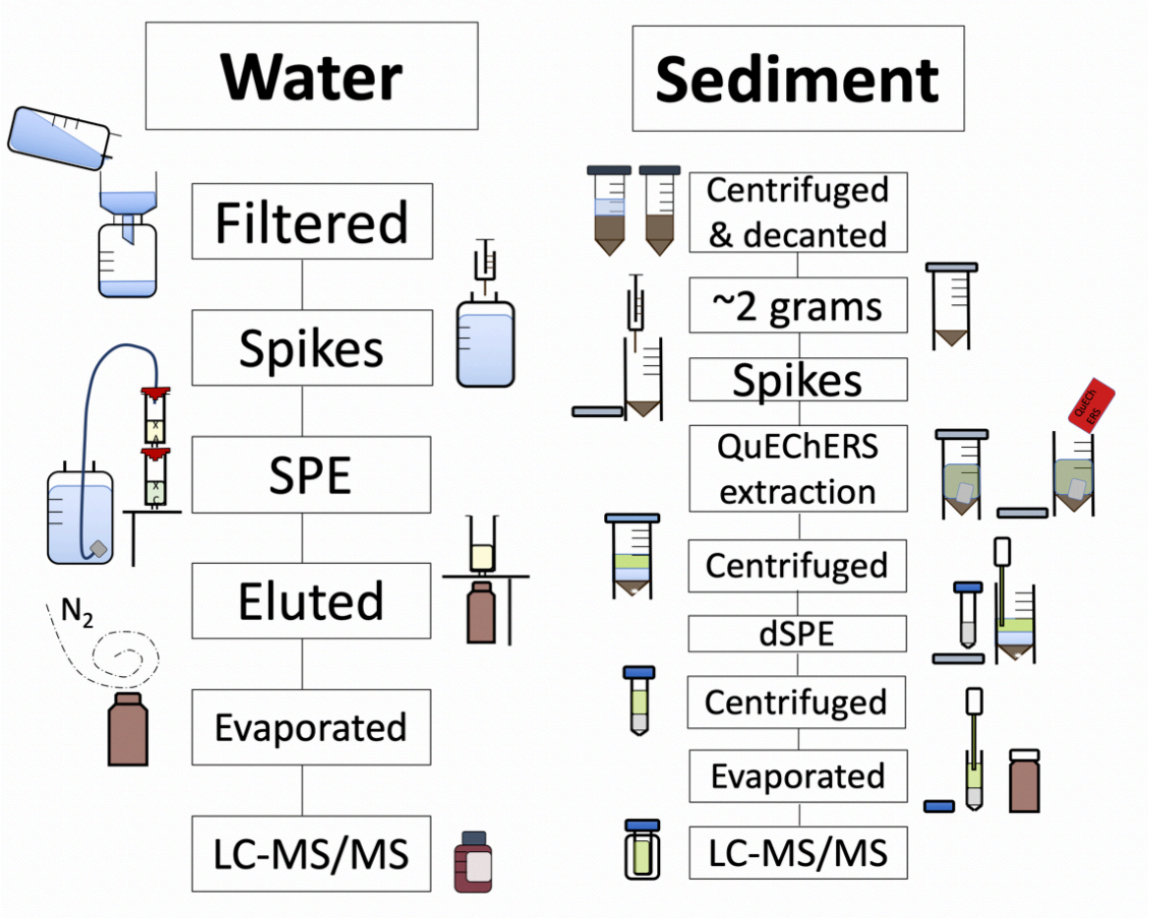

Figure 1.7: Water and Sediment Processing Flow Diagram courtesy of Lisa McAnulty, George Mason University, Potomac Science Center

1.3.6 LC-MS/MS Analysis

The PPCPs in the water and sediment extracts were analyzed for the compounds of interest using a Shimadzu Model 8050 liquid chromatograph triple-quadrupole mass spectrometer (LC-MS/MS) configured with a SIL-20ACXR autosampler (Columbia, MD). The LC-MS/MS interface was operated in electrospray ionization (ESI) mode in the presence of a Corona needle (DUIS) in both positive and negative ionization. LC-MS/MS separation of the PPCPs was performed using a 50 mm x 2.1 mm (id), 1.8 µm

(particle diameter) Forced Biphenyl reversed-phase UHPLC column (Restek, Bellefonte, PA) in conjunction with a raptor Biphenyl guard column, with a binary mobile phase consisting of Type I Milli-Q water (solvent A), and acetonitrile (solvent B), both containing 0.1% formic acid as a phase modifier. Operating conditions for the LC-MS/MS are listed in Table 1.5. The gradient elution program allowed for a total run time of approximately 10 min. The retention times for the PPCPs are in Table 4.2A.

Table 1.5: LC-MS/MS Instrument Parameters

Parameter	Operating Conditions
Total Flow Rate	0.40 mL/min
Gradient Elution Program	10% B at 0 min
	50% to 95% B 0-6 min
	100% B 6-7 min
	100% to 30% B 7-9 min
	10% B 9-10 min
Nebulizing Gas Flow	2 L/min
Heating Gas Flow	10 L/min
Drying Gas Flow	10 L/min
Oven Temperature	40°C
Interface Temperature	300°C

The LC-MS/MS quantitation of the PPCPs was accomplished in the multiple reaction monitoring (MRM) mode. Three MRM ions were established for each PPCP (with the exception of cis-tramadol which only had one MRM) through automated MRM optimization procedures following manual precursor ion identification using the full scan mode. The quantifier (primary) and qualifier (secondary and tertiary) product ions and the various quadrupole voltages for the PPCPs are listed Table 4.3A. Quantitation was

performed using the internal standardization method with isotopically labelled internal standards (^{2}H or ^{13}C analogues as shown in Table 1.3) that were added prior to the extraction step. Quantitation was completed using a ten-point calibration curve based on the primary product MRM ion abundance for each PPCP relative to that of an associated internal standard. The retention times and qualifier MRM ions relative abundances were used to confirm the chemical identity of the PPCP. Data analysis and quantitation was performed using LabSolutions software (ver. 5.91).

1.3.7 Quality Assurance

Method recoveries were tested for extraction and analyte recovery through the use of blanks, surrogate standard recoveries, relative standard deviation (RSD) of triplicate samples, and quantitation limit (QL) determination for both water and sediment samples, as calculated in Equation 1.1, where α is the coefficient 10.

Equation 1.1: Quantitation Limit for all PPCPs

$$Quantitation\ Limit\ (QL) = \alpha \times Peak\ Concentration \times \frac{Noise}{Peak\ Height}$$

The method blanks were prepared using UPW and clean sand for water and sediment, respectively. This allowed for the evaluation of the contamination from the SPE and QuEChERS solid phase extraction and analytical procedures. Matrix spikes (MS) were composed of its own method blank and were performed for samples at

specific locations. The Matrix Spikes were used to calculate accuracy by using the matrix spike recoveries (MSR). The surrogate spike was added to the method blanks and all the samples. It was used to determine the percent recovery (%R) of the analytes throughout the method. All samples had duplicates run and their RSD calculated.

Surrogate Spike recoveries are summarized in Figure 1.8 and Figure 1.9. All water and sediment samples were spiked with surrogate standards prior to the individual extraction processes. This allowed for the ability to determine the performance of the groups of analytes. The surrogates consisted of isotopically labeled homologues of compounds that were being targeted for analysis. Out of eight total surrogate standards, five exceeded 70% recovery, indicating high performance. The reported concentrations of targeted chemicals were not corrected for surrogate recoveries.

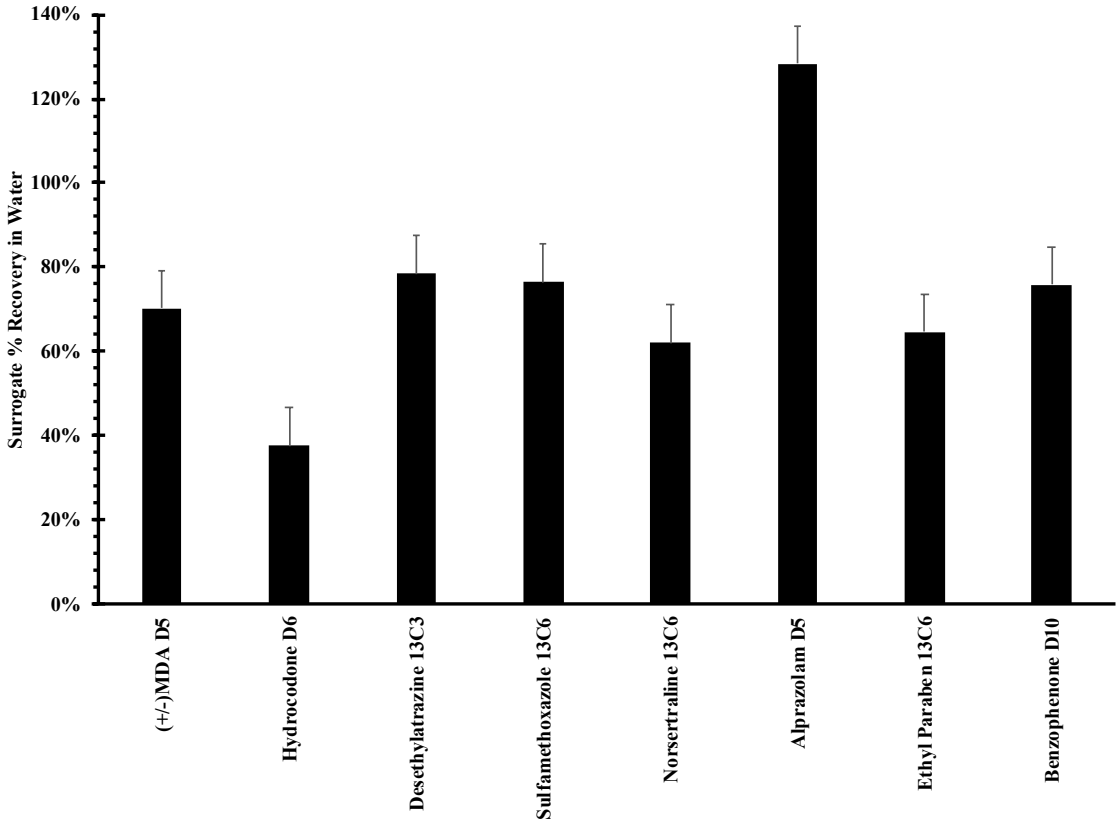

Figure 1.8: Mean Surrogate %recoveries evaluated in for all the Potomac River surface water samples. Black columns represent the mean recovery and bars represent ± 1 SD.

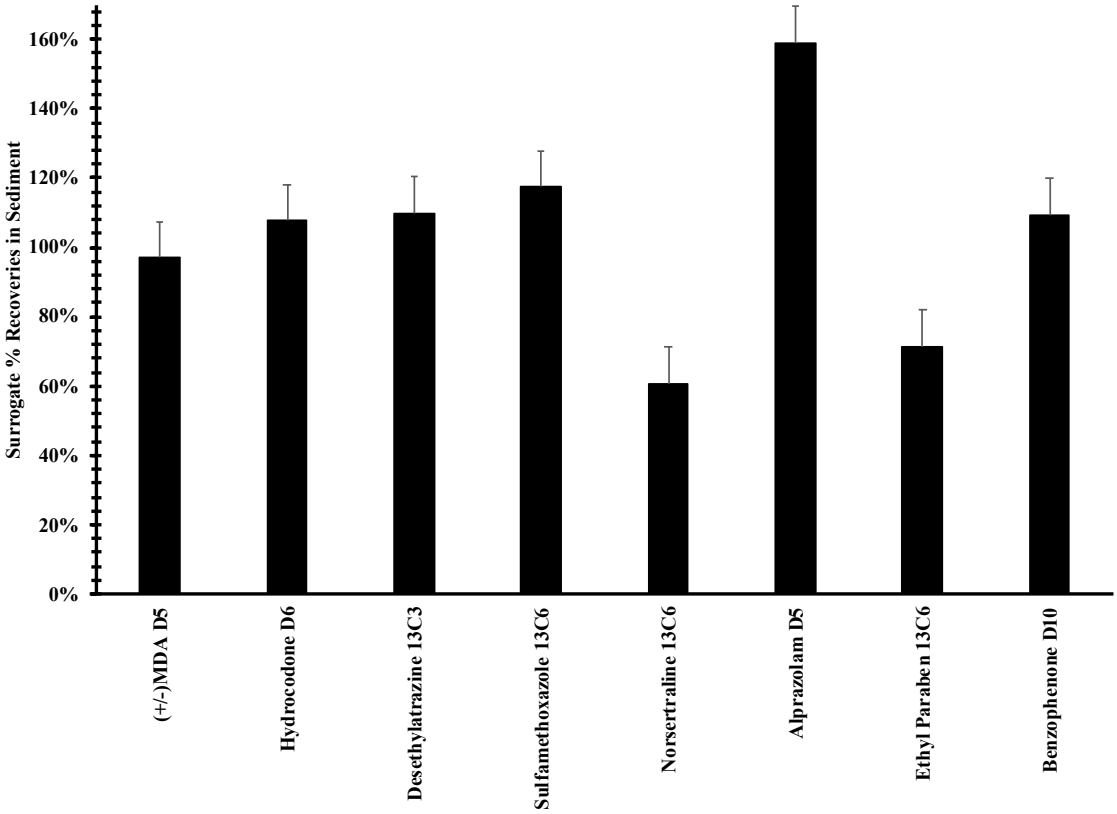

Figure 1.9: Mean Surrogate %recoveries evaluated in for all the Potomac River sediment samples. Black columns represent the mean recovery and bars represent ± 1 SD.

Laboratory blanks were run for both water and sediment samples. In both cases, the blanks were processed in such a way that they encountered all reagents and containers that a normal sample would be in contact with over the entire course of sample processing. Only two of the 91 targeted chemicals were found in lab blanks at concentrations above the QL. Nicotine was found in several water lab blanks at an average concentration of 4.4 ng/L. DEET was found in several sediment lab blanks at an average of 4.7 ng/g. This value is very low in comparison to the concentration found in actual samples. The QL for all PPCPs ranged from 0.053 ng/L to 32 ng/L.

Field blanks were run for water samples. A 20-L can of UPW was taken out into the field, run through the pump, and pumped back into the can prior to sampling at the first location of each trip. The blanks were processed in such a way that they also encountered all reagents and containers that a normal sample would be in contact with over the entire course of sample processing. Only seven of the 91 targeted chemicals were found in lab blanks at concentrations above the QL. Of those seven chemicals, only caffeine and DEET were detected in more than 14% of all field blank samples with caffeine and DEET being detected in 100% and 96% of field blanks, respectively. The other compounds detected were nicotine (14%), sulfamethoxazole (4%), sulfaquinoxaline (4%), fexofenadine (12%), and carbamazepine (10%). Caffeine and DEET were found in several field blanks at an average concentration of 28 ng/L and 33 ng/L, respectively.

Each water or sediment sample was collected and analyzed in triplicate. For each triplicate, the %RSD was calculated whenever a PPCP was detected. The %RSD for detected PPCPs ranged from 4.4% to 76% (30% overall mean) for water and 2.3% to 134% (42% overall mean) for sediment. The %RSD are listed in full in Table 4.4A and Table 4.5A.

Matrix spikes included all targeted chemicals in water and sediment samples and were used as an evaluation of the performance of the method overall. They were performed by spiking every approximately 1-L of water and approximately 2 g of wet sediment with 80 ng of each target chemical. The MSRs ranged from to 4.5% to 607% in surface water with an average of 70%. There were percent recoveries of 0% for metformin, azithromycin, gabapentin, 2-hydroxy-ibuprofen, hydromorphone, penicillin

G, (±)-methamphetamine, codeine, ciprofloxacin, phentermine, naproxen, budesonide, triclocarban, lisinopril, and, tetracycline, and perfluorooctanoic Acid. The MSRs ranged from to 0.08% to 227% in sediment with an average of 71%. There were percent recoveries of 0% for atorvastatin, lisinopril, and tetracycline. The results of all MSRs are reported in Table 4.6A and Table 4.7A. Those majority of compounds that exhibited a MSR of 0% were not detected in any samples. However, those that were found to have a 0% recovery and were reported in this data set have been to have higher recoveries (~50%) in the overall data set of the research group as a whole.

1.3.8 Ancillary Measurements

Ancillary measurements were conducted to determine total organic carbon (TOC), %moisture (%M), particle size analysis (PSA), and total suspended matter (TSM). TOC content was performed by Drexel University, using a Carlo Erba Model 1112 Flash Elemental Analyzer. Approximately 1 g of sediment from each sampling location and trip was dried in an oven at approximately 60^{o}C overnight, and then ground to a fine powder using a mortar and pestle. The samples were placed in a ceramic crucible and fumigated with concentrated HCl for 24 hours to degas carbon dioxide derived from inorganic carbon (primarily as carbonates) following the method of Ramnarine.[48] The treated sediment was re-dried in a 60˚C oven for one week to ensure that no excess HCl was present. The sample was then placed into a tin boat, weighed, and combusted at 1000˚C for total C and N content.

Sediment moisture was determined by measuring out approximately 1–2 g of wet sediment into a tared aluminum boat and measuring mass. The aluminum was placed in an oven at 60°C for 48 – 72 hr until a constant weight. The mass of the sample was recorded again after the drying period. The moisture content was evaluated by determining the loss of mass after drying as described in Equation 1.2. The moisture content was used to correct and convert wet weight of the sediment samples to dry weight. The dry weight of all sediment samples was used when expressing PPCP sediment concentrations.

Equation 1.2: Moisture Content in Sediment

$$Moisture\ Content\ (\%M) = \left(\frac{Mass\ of\ Water\ Lost\ Upon\ Heating\ (g)}{Mass\ of\ Wet\ Sediment\ Prior\ to\ Heating\ (g)}\right) \times 100$$

Sediment grain size, in terms of percent sand, silt and clay content, for all the collected riverbed sediments was determined using a Beckman-Coulter (Brea, CA) laser diffraction (LS 13320) particle size analyzer in the GMU Coastal Geology Lab at the Potomac Science Center, PI Dr. Randy McBride with assistance from Greg Bliss and Elizabeth Lang. Sediment initially was passed through a 0.5-mm stainless-steel sieve to remove large particles followed by disaggregation with 5% aqueous hexametaphosphate prior to analysis. Grain size results were provided by the Excel program GRADISTAT for ternary diagrams.

TSM, the dry mass of the suspended particles, that are not dissolved, in a sample of water is a water quality parameter that can be used to assess the quality of any sample

of water. TSMs was determined by vacuum filtration of the 1-L river water samples through stacked, pre-weighed 47 mm (diameter) GF/D and GF/F glass fiber filters. The filters were dried at 60°C and analyzed gravimetrically The TSM concentration (mg/L) was determined using Equation 1.3 below.

Equation 1.3: Total Suspended Matter

$$Total\ Suspended\ Matter = \frac{Mass\ of\ Filtered\ Particles\ (mg)}{Sample\ Volume\ (L)}$$

1.4 Results

1.4.1 Ancillary Data

In hydrologic environments, geochemical variables such as TSM, river flow, sediment grain size, sediment percent moisture and sediment total organic carbon (TOC) are all important parameters to consider when evaluating the presence, dispersal and distribution of micropollutants. Each of these parameters where characterized or recorded in the present study.

TOC varied minimally both spatially and temporally in the TFWPR, ranging from 0.90 - 2.56 %TOC with a median value of 1.62 %TOC. The %TOC of each the sediment samples are depicted in Figure 1.10. There was no statistical difference in TOC among all the sites (Kruskal-Wallis, $p>0.05$).

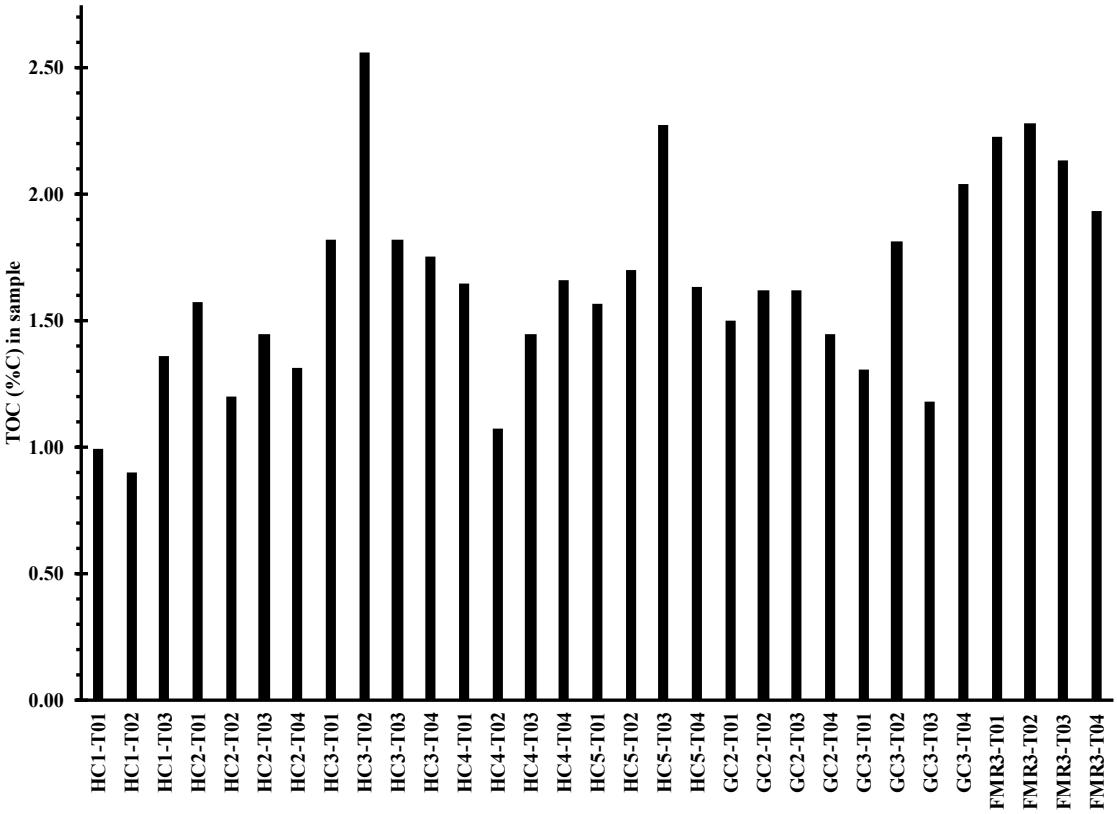

Figure 1.10: The Total Organic Carbon as %TOC for each sediment sample obtained throughout the entire TFWPR over the course of the entire sampling season

Sediment moisture and texture varied both spatially and temporally in the TFWPR. The summary sand, silt, and clay texture diagram for all sites is shown below in Figure 1.11. The numerical % silt, sand, clay values for each trip are compiled in Table 4.8A. The sediments were predominantly classified as sandy silt for the Hunting Creek and silt for the Four Mile Run and Gunston Cove regions (Figure 1.11). However, there was no significant difference in grain size among the sediments from all sites (Kruskal-Wallis, $p>0.05$). The sediments taken from the HC1 location, which is the furthest upstream after the WTP, were sandier than those taken downstream at HC2, HC3, HC4, and HC5.

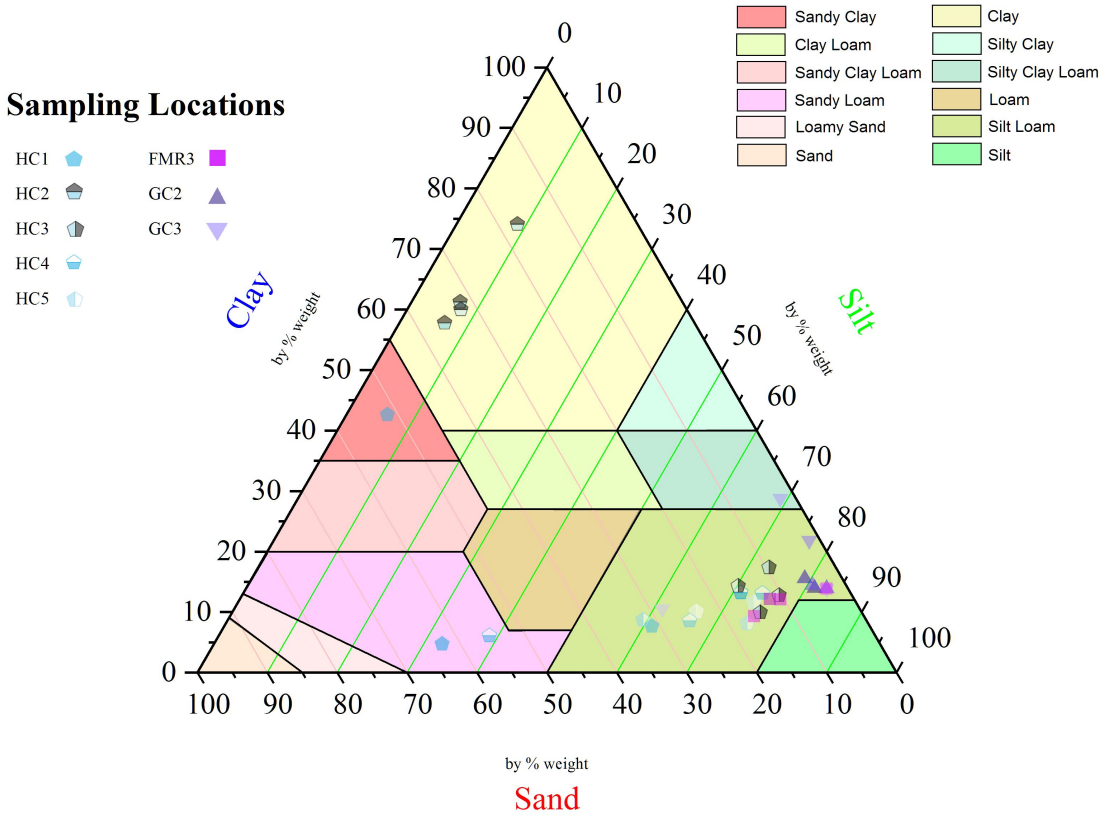

Figure 1.11: Summary % Sand, Silt, Clay diagram depicting the average % of sand, silt, clay for each site over the entire sampling season.

The TSM was measured at all sites where water was collected. The results are summarized in Table 4.9A and Figure 1.12. In some instances, the final mass of the filters was smaller than the initial mass and the mass of TSM particles could not be calculated. It is believed that this is a result of the clean filers not being dried prior to usage and having absorbed water leading to an error when recording the initial mass.

These results are reported as Not Applicable (N/A). The detection limit for TSM was determined to be approximately 0.1 mg/L. TSM values ranged from 0.11–261.15 mg/L with a median value of 26.32 mg/L. It was determined there was no significant difference in the TSM values between the sites (Kruskal-Wallis, $p>0.05$).

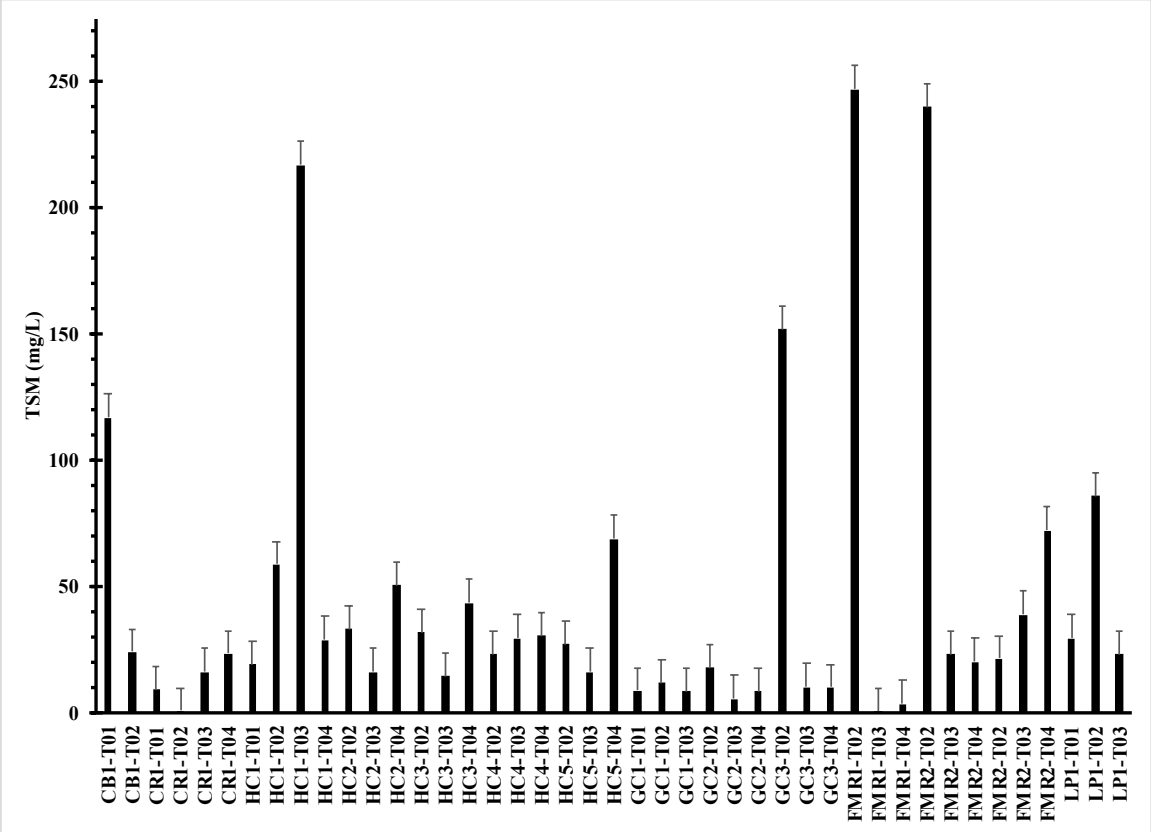

Figure 1.12: TSM for all surface water samples at all sites along the TFWPR sites throughout the entire sampling season. Black columns represent the mean recovery and bars represent ± 1 SD.

The TSM values for HC1-T03, FMR1-T02, and FMR2-T02 are significantly higher than other trips at the same location. The sampling trip for HC1-T03 occurred the day after a major storm in the area. Similarly, the sampling trip T03 for the Four Mile

Run sites experienced a storm while in the field sampling. The samples at FMR3 were collected before the storm started and into the first few minutes of the storm. The samples collected at FMR1 and FMR2 were collected after the storm had passed. In these instances, the storms severely impacted the overall flow and turbidity of the areas being sampled.

The flow and precipitation conditions for the upstream sites at each location is compiled below in Table 1.6.

Table 1.6: Flow Data for Upstream locations on the day of each sampling session.

Sampling Location	Sampling Trip	Daily Average Flow (m^3/s)	Longterm Historical Avergage Flow (m^3/s)	Days since previous storm event
CB1[49] (Little Falls)	T01	129	82.41 (89 years of record)	0
	T02	1097		3
	T03	372		13
CR1[50]	T01	0.212	0.283 (56 years of record)	5
	T02	0.416		4
	T03	0.151		18
	T04	0.852		4
GC1[51] (Accotink Cr)	T01	0.263	0.290 (71 years of record)	12
	T02	0.759		2
	T03	0.430		11
	T04	0.145		3
FMR1[52]	T01	2.20	0.142 (44 years of record)	9
	T02	3.25		0
	T03	6.17		0
	T04	2.69		0

1.4.2 PPCP Quantitation Frequencies

The percent quantitation frequencies (%QF) observed for PPCPs are shown for both surface water and sediment (Table 1.7). Quantitation frequency is defined as number of reported concentrations above the QL of the chemical relative to the total number of analyses. Overall, 36 out of 91 total PPCPs were quantified in water and 40 out of 91 PPCPs were quantified in sediments in the Potomac River. All others were undetected in either matrix. The PPCPs were grouped by quantitation frequency into high (>70%), moderate (>25%), and low (>0%) categories to characterize presence and abundance. High frequency PPCPs were those commonly quantified in both matrices, moderate frequency PPCPs were those quantified in high frequency in one, but not both, matrices, and low frequency PPCPs were those quantified <25% in either matrices.

Table 1.7: Percent quantitation frequencies (%QF) of the 85 target chemicals found in water and sediment.

PPCP	%QF Water	%QF Sediment	Mean %QF
High Detection Frequency PPCPs			
Fexofenadine	79%	70%	75%
Moderate Detection Frequency PPCPS			
Nicotine	95%	16%	55%
Caffeine	99%	6%	53%
Triamterene	43%	27%	35%
Metoprolol	61%	66%	63%
cis-Tramadol HCl	65%	68%	66%
Desvenlafaxine	37%	54%	45%
Sulfamethoxazole	65%	0%	32%
Propranolol	23%	51%	37%
Dextromethorphan	31%	46%	39%
Venlafaxine	48%	52%	50%
Diphenhydramine hydrochloride	38%	90%	64%
DEET	97%	42%	70%

Escitalopram	0%	89%	45%
Carbamazepine	64%	6%	35%
Fluoxetine	0%	60%	30%
Methadone	28%	62%	45%
Sertraline	3%	60%	3%
Low Detection Frequency PPCPS			
3'-Hydroxy cotinine	0%	0 %	0%
Acyclovir	0%	0 %	0%
Cimetidine	3%	0 %	1%
Cotinine	20%	0 %	10%
Albuterol	0%	0 %	0%
Atenolol	22%	0 %	11%
Ranitidine	5%	0 %	2%
Azithromycin	0 %	0 %	0 %
Gabapentin	0 %	0 %	0 %
Morphine	0 %	0 %	0 %
Oxymorphone	0 %	28%	14%
Clonidine	0 %	0 %	0 %
2-Hydroxy-Ibuprofen	0 %	0 %	0 %
Hydromorphone	0 %	0 %	0 %
Nadolol	0 %	0 %	0 %
Metformin	31%	5%	18%
Sulfathiazole	0 %	0 %	0 %
Aspartame	0 %	0 %	0 %
Penicillin G	0 %	0 %	0 %
Methamphetamine	0 %	0 %	0 %
Naloxone	0 %	2%	1%
MDA	13%	0%	6%
Codeine	0 %	0 %	0 %
Ciprofloxacin	0 %	0 %	0 %
Phentermine	0 %	0 %	0 %
Sulfamethazine	0%	3%	2%
Naltrexone	0 %	0 %	0 %
MDMA	0 %	0 %	0 %
Enrofloxacin	0 %	0 %	0 %
Formoterol	0 %	0 %	0 %
Atrazine Mercapturate	0 %	0 %	0 %
Hydrocodone	0 %	0 %	0 %
MDEA	0 %	3%	2%
Bupropion	54%	5%	30%
Enalapril	0 %	0 %	0 %
Meperidine	0 %	3%	2%

Sulfadimethoxine	0 %	0 %	0 %
Sulfaquinoxaline	0 %	3%	2%
Diltiazem	12%	11%	11%
10_11-Carbamazepine epoxide	46%	3%	25%
Promethazine	1%	0%	0.65%
Propoxyphene	0 %	0 %	0 %
Fentanyl	0 %	15%	8%
Verapamil	0 %	16%	8%
Benztropine	1%	3%	2%
Buprenorphine	0 %	0 %	0 %
Loratadine	0 %	0 %	0 %
Naproxen	0 %	0 %	0 %
Oxazepam	0 %	0 %	0 %
Paroxetine	0 %	4%	2%
Nordiazepam	0.65%	3%	2%
Bezafibrate	0 %	0 %	0 %
Nitrazepam	0 %	0 %	0 %
(±)-Lorazepam	0 %	0 %	0 %
Budesonide	0 %	0 %	0 %
Nortriptyline	0 %	11%	5%
Amitriptyline	0 %	43%	22%
Clonazepam	0 %	3%	2%
Alprazolam	3%	0%	2%
Temazepam	6%	3 %	5%
Flunitrazepam	0 %	0 %	0 %
Diazepam	0 %	0 %	0 %
Atorvastatin	3%	0 %	2%
Triclocarban	0 %	35%	18%
Lisinopril	0 %	3%	2%
Tetracycline	0 %	0 %	0 %
Hydrochlorothiazide	21%	0 %	11%
Furosemide	28%	11%	19%
Perfluorooctanoic Acid	0 %	0 %	0 %
Glipizide	1.%	0 %	0.65%
Warfarin	0 %	0 %	0 %
Diclofenac	3.%	0 %	2%
Celecoxib	31%	2%	1%
High Mean %QF ≥ 75% | **Medium** 75% > Mean %QF > 25% | **Low** Mean %QF ≤ 25%			

1.4.3 Spatial Analysis of PPCPs by Site Grouping for Water Samples

The PPCP concentrations in water (ng/L) within the entire TFWPR showed that concentrations increased across the upstream-to-downstream end members, from Chain Bridge to the Lower Potomac River site, signifying that PPCPs concentrations increased in the downstream direction within the TFWPR. The maxima in the sum of all 91 PPCP (Σ_{91}PPCP) concentrations occurred nearest the WTP outfalls (Figure 1.13), both at Alexandria Renew Enterprises and Arlington Water Pollution Control Plant. The lowest ΣPPCP concentrations generally were found in the upland creeks or in the mainstem Potomac River, with the exceptions being the lower Potomac River location and Four Mile Run. In the Hunting Creek region, the lowest concentrations of PPCPs were found upstream of the WTP outfall. Immediately following the WTP outfall, the concentrations and quantities of PPCPs detected increased. Immediately downstream of the outfall, the ΣPPCP concentrations were generally greater relative to other proximal upstream or downstream locations. Downstream of the outfalls, the Σ_{91}PPCP concentrations in water decreased until bottoming out within the mainstem of the TFWPR (i.e., HC4).

ΣPPCP concentrations in sediments (ng/g) showed a more variable trend relative to water along the downstream transect from Chain Bridge to the Lower Potomac River site (Figure 1.13) reflecting the heterogeneous spatial distribution of fine grained sediments, along with the fact that sediment were not collected at each sampling site.

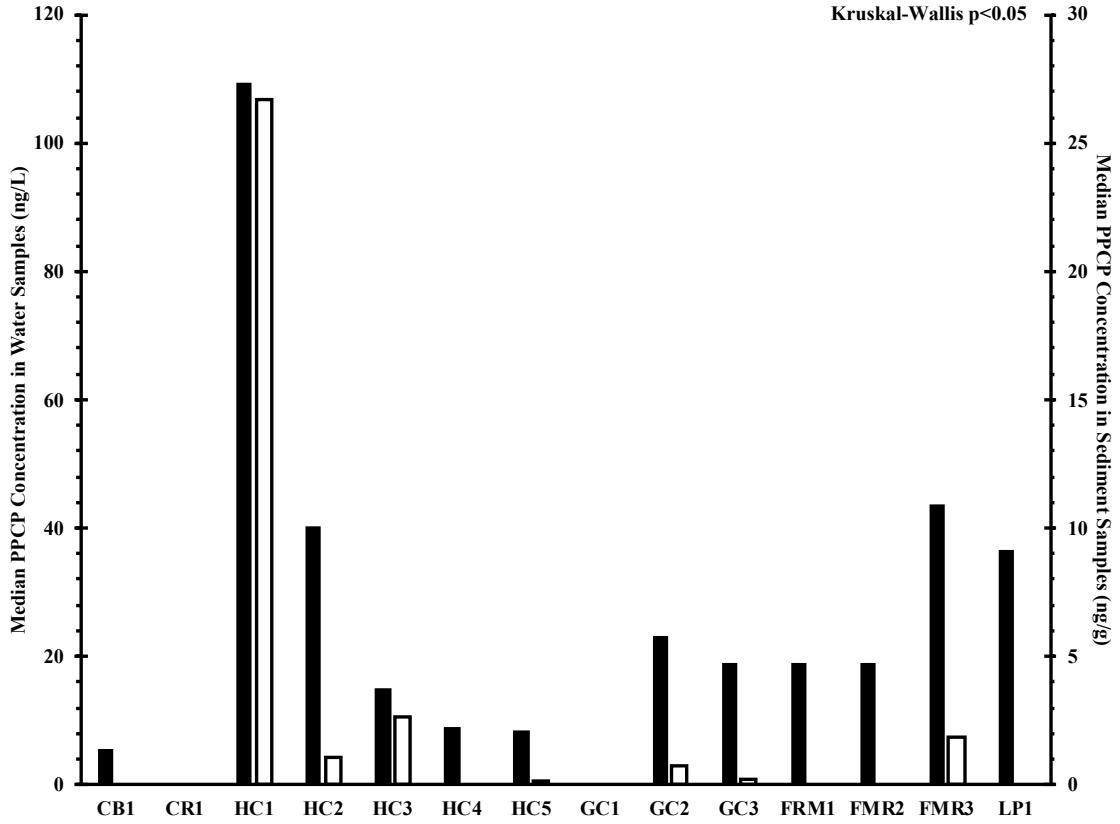

Figure 1.13: Median PPCP concentrations found in water (black) and sediment (white) samples at each site along the TFWPR. Water was collected at all sites. Sediment samples were not collected at CB1, CR1, GC1, FMR1, an FMR2. The Kruskal-Wallis test ($p<0.05$ for both water and sediments samples) indicate a statistical difference among the individual sample concentrations.

The spatial profile of ΣPPCP concentrations in Hunting Creek water and sediments is shown in Figure 1.14. CR1 (Cameron Run) was the site upstream of Alexandria Renew Enterprises WTP in this area. HC1 (Upper Hunting Creek) is immediately downstream of the outfall for Alexandria Renew Enterprises. Sites HC2 and HC3 (Lower Hunting Creek) are downstream of the outfall but still within Hunting Creek while sites HC4 and HC5 are downstream of the outfall in the mainstem TFWPR. The

median concentration for ΣPPCPs upstream of the WTP outfall was zero because the quantitation frequency was much less than 50%.

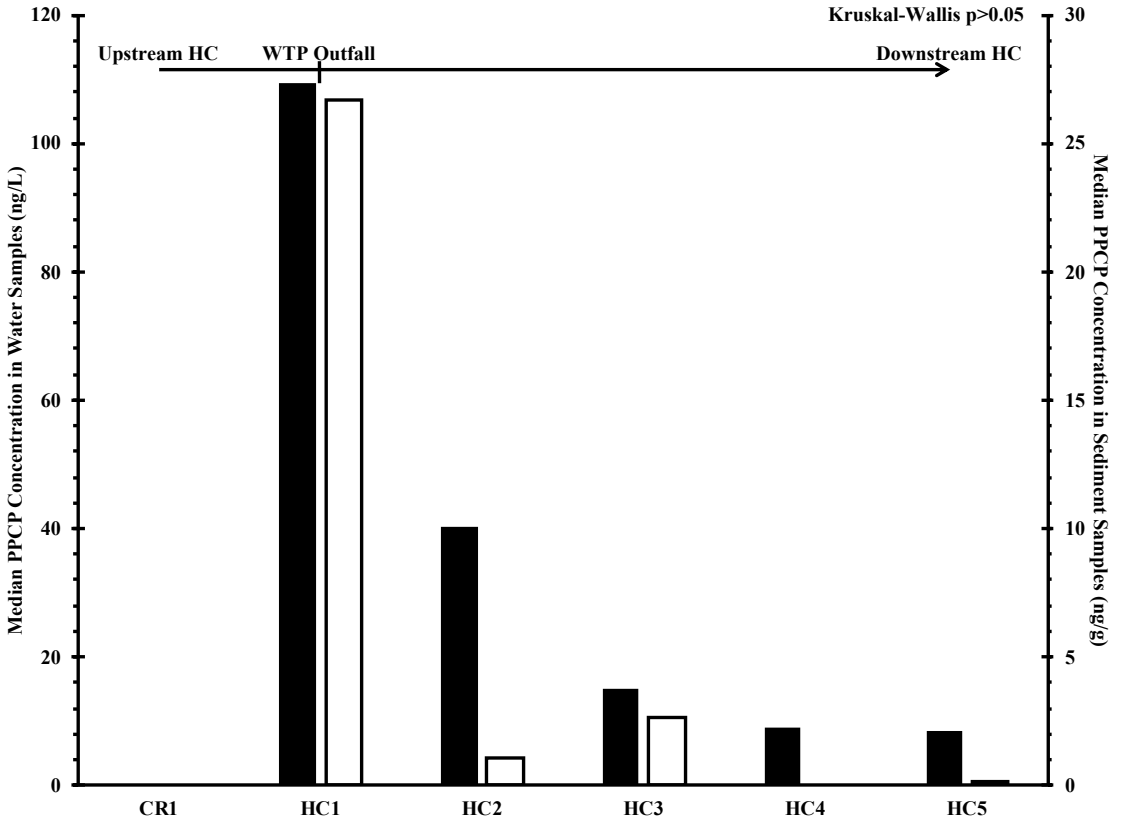

Figure 1.14: Median ΣPPCP concentrations found in surface water (black) and sediment (white) samples at each site in Hunting Creek. The Kruskal-Wallis test (p>0.05 for both water and sediments samples) indicate no statistical difference among the individual sample concentrations.

Shown in Figure 1.15 is the spatial profile of ΣPPCP concentrations in Gunston Cove water and sediments. GC1 (Pohick Creek) is the non-tidal site upstream for the Noman Cole Wastewater Treatment Plant, the WTP in this area. ΣPPCP concentrations at GC1 were below quantification limits. Riverbed sediments could not be collected at GC1;

therefore, sediment concentrations are not available. GC2 (Gunston Cove) is tidal and was downstream of the outfall for the Noman Cole Wastewater Treatment Plant and downstream of the confluence of Pohick Creek with Pohick Bay, and the ΣPPCP concentrations in water and sediment were highest at this location. Site GC3 was downstream of the outfall within the mainstem TFWPR

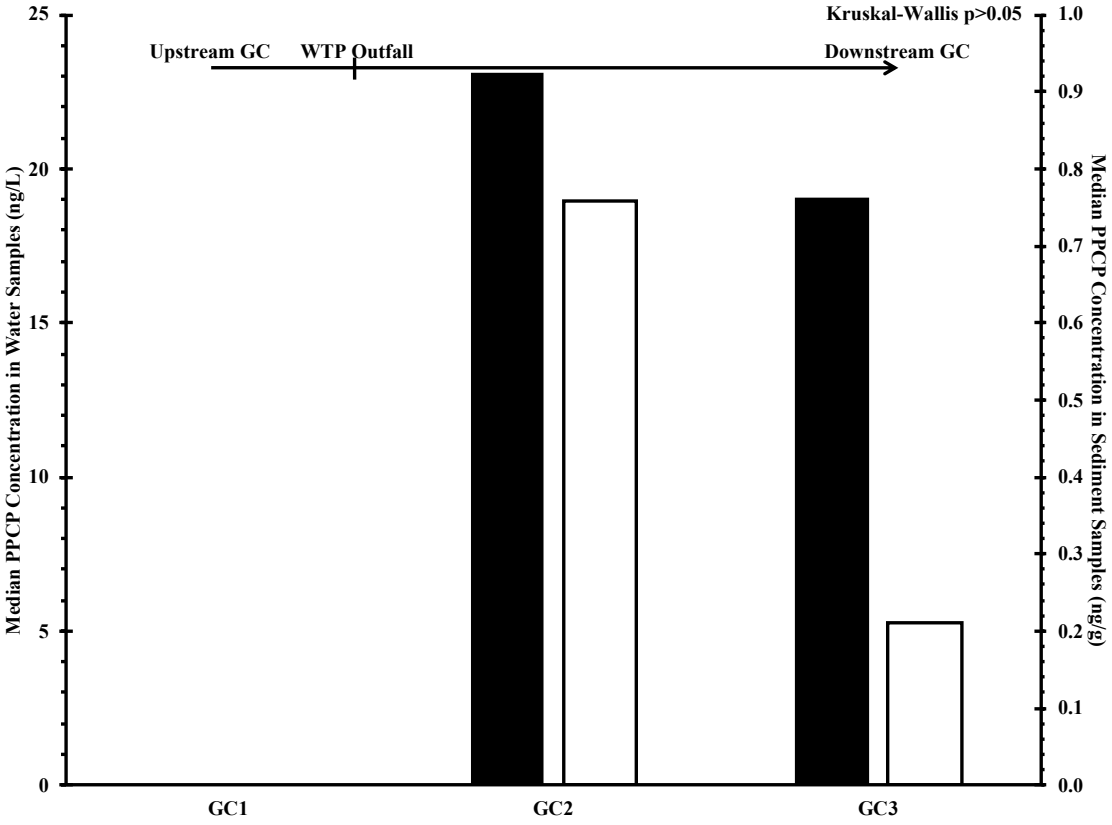

Figure 1.15: Median ΣPPCP concentrations found in surface water (black) and sediment (white) samples at each site in Gunston Cove. The Kruskal-Wallis test (p>0.05 for both water and sediments samples) indicate no statistical difference among the individual sample concentrations.

The spatial profile of ΣPPCP concentrations in Four Mile Run water and sediment is shown in Figure 1.16. FMR1 is the non-tidal site upstream of Arlington Water

Pollution Control Plant along Four Mile Run, where only water was collected. FMR2 was positioned in Four Mile Run immediately downstream of the outfall for Arlington Water Pollution Control Plant, and sediments were not collected at this site. Site FMR3 is downstream of the outfall in the main body of the TFWPR, where water and sediments were collected.

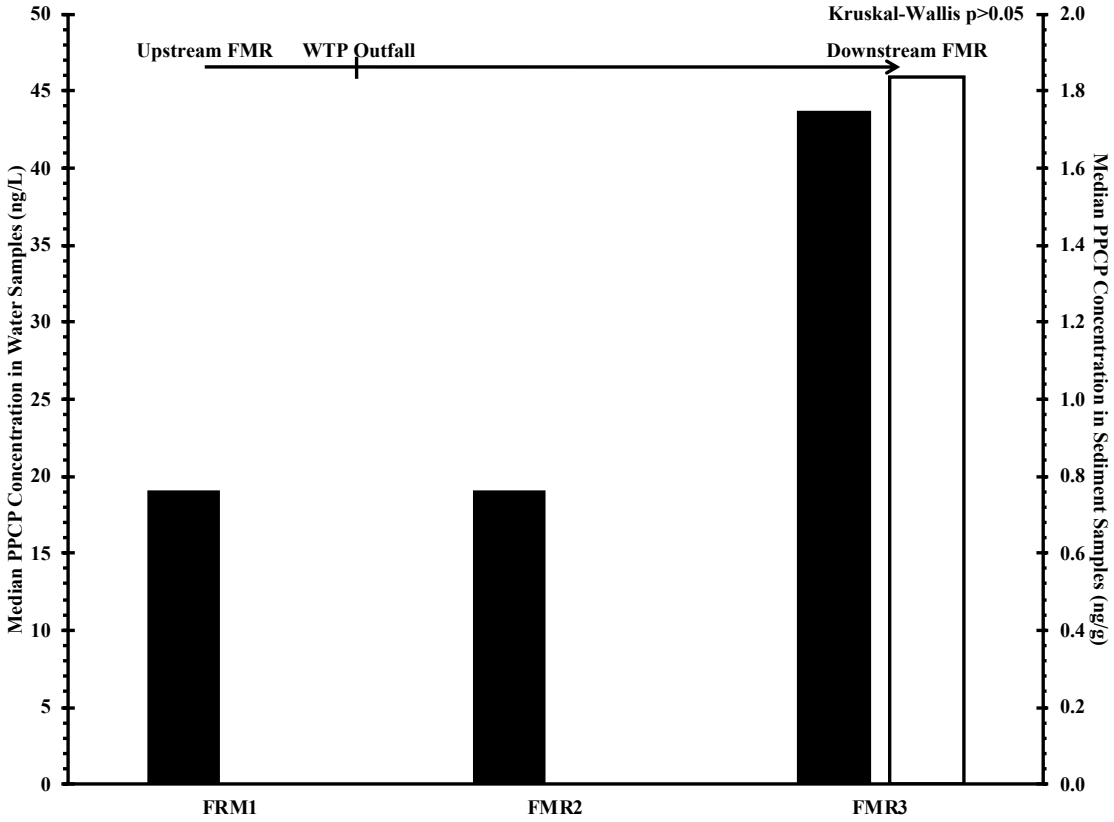

Figure 1.16: Median all ΣPPCP concentrations found in surface water and sediment samples at each site in Four Mile Run. Black bars represent median PPCPs in surface water samples. White bars with black outlines represent median PPCPs in sediment samples. The Kruskal-Wallis test (p>0.05 for both water and sediments samples) indicate no statistical difference among the individual sample concentrations.

The median concentrations of ΣPPCPs detected upstream of the WTP outfall were greater than zero for this particular sampling area (FMR1) and was a unique observation in this study. At this site, the non-tidal stream was located within a heavily used city park in densely populated Arlington, VA (i.e., Four Mile Run Park), which likely contributed to an increase in the type and quantity of PPCPs present in upstream surface water.

There were 18 individual PPCPs detected at concentrations above the QL in the surface water samples at multiple sites throughout the TFWPR, which included metformin, nicotine, caffeine, triamterene, metoprolol, tramadol, desvenlafaxine, bupropion, sulfamethoxazole, dextromethorphan, venlafaxine, diphenhydramine, carbamazepine epoxide, DEET, fexofenadine, carbamazepine, methadone, and celecoxib. In addition, there were several PPCPs that were present in the Hunting Creek and Four Mile Run areas, but not at Gunston Cove. These PPCPs included cotinine, atenolol, propranolol, diltiazem, hydrochlorothiazide, and furosemide. The PPCP MDA was found exclusively in surface water samples from the Four Mile Run area. There were no PPCPs that were unique to only the Gunston Cove area. The composition of PPCPs that made up the ΣPPCP concentrations in surface water at each site is illustrated in Figure 1.17.

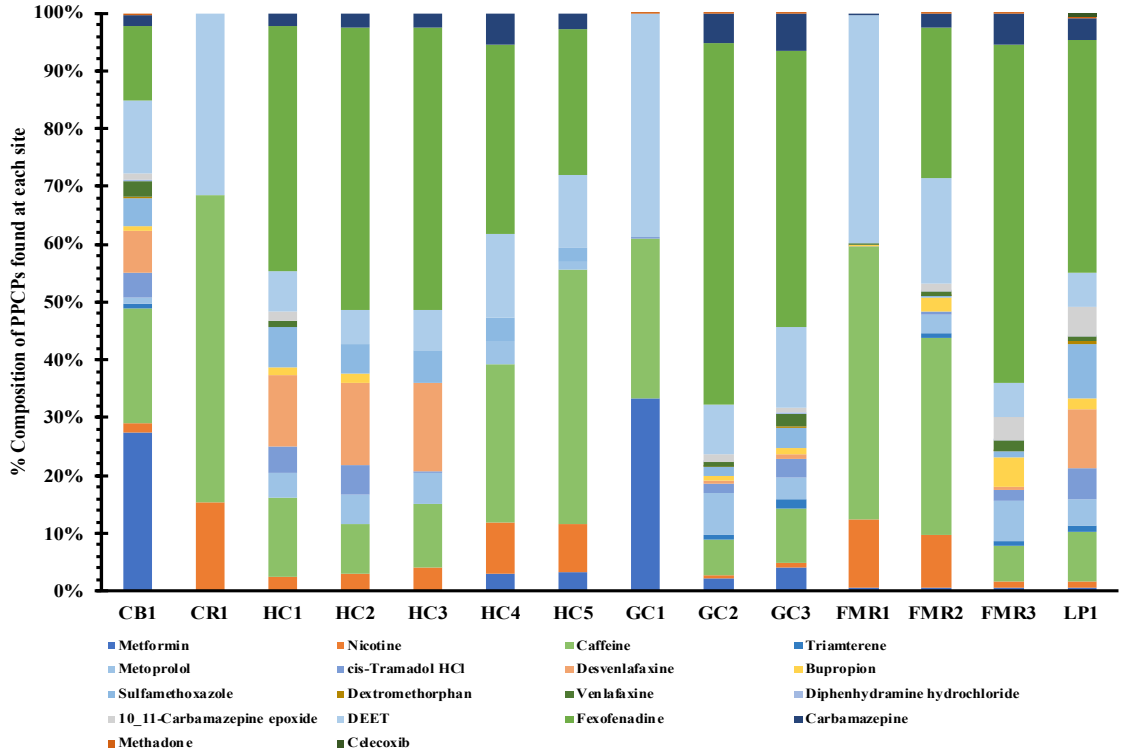

Figure 1.17: %Composition of 18 individual PPCPs found in surface water samples at each site throughout the TWFPR. Legend color read from left to right, top to bottom.

Similarly, there were 16 PPCPs detected in concentrations above the QL in sediment samples at multiple sites throughout the TFWPR. These include: oxymorphone, triamterene, metoprolol, tramadol, desvenlafaxine, propranolol, dextromethorphan, venlafaxine, diphenhydramine, DEET, escitalopram, fexofenadine, fluoxetine, amitriptyline, methadone, and sertraline. This list of PPCPs present throughout the TFWPR in sediments was similar to those found in the surface water samples.

Hunting Creek and Four Mile Run exhibited an overlap of sedimentary PPCPs including bupropion, nortriptyline, and triclocarban. Unlike what was found in water samples, where there were no PPCPs unique to only the Hunting Creek region, there were

several PPCPs that were unique to the Hunting Creek area sediments, particularly at the sampling location immediately downstream of the WTP outfall. These PPCPs included metformin, nicotine, caffeine, diltiazem, fentanyl, verapamil, carbamazepine, temazepam, furosemide, glipizide, diclofenac, and celecoxib. The significant number of PPCPs exclusive to this area was likely due to the sediment's proximity to the WTP outfall, which was closer here than at the other two tributaries. Again, there were no PPCPs unique to the Gunston Cove area sediments. The differences in PPCPs that make up the total PPCP concentration at each site is shown in Figure 1.18.

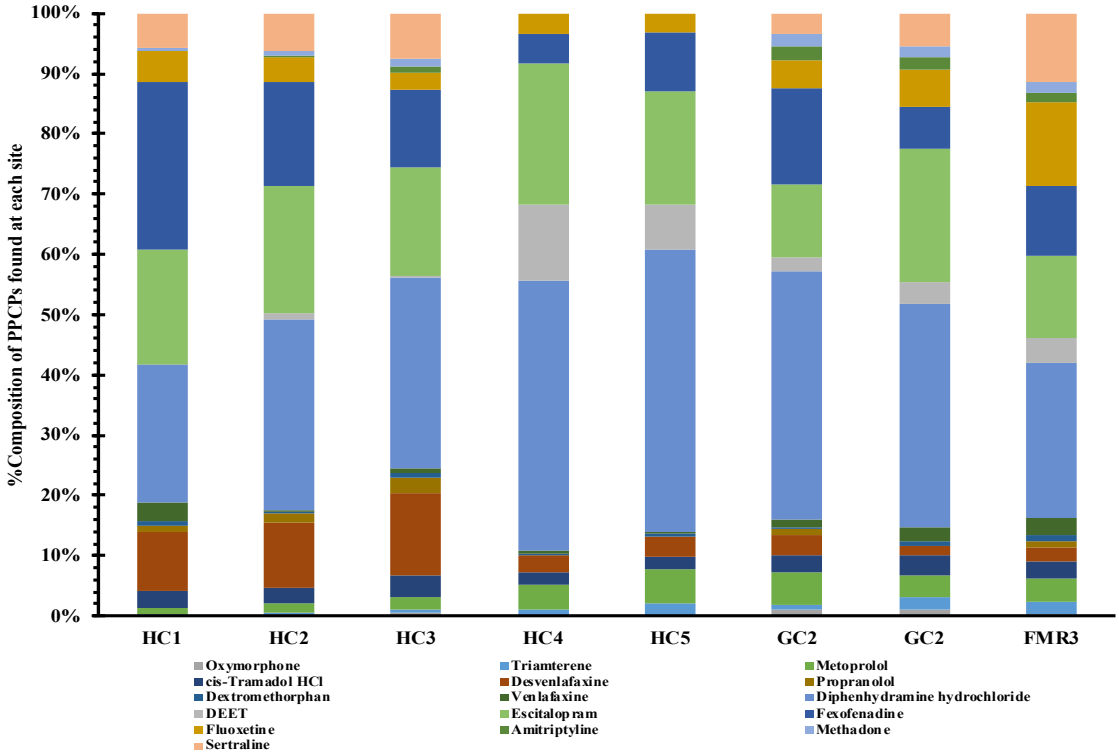

Figure 1.18: %Composition of 16 individual PPCPs found in sediment samples at each site throughout the TWFPR. Legend color reads from left to right, top to bottom.

In general, the median PPCP concentrations were found to be highest in the Hunting Creek region for both surface water and sediments. Four Mile Run exhibited the second highest median PPCP concentrations and Gunston Cove experienced the lowest median PPCP concentration in surface water samples. The inability to collect sediment samples throughout the Four Mile Run and Gunston Cove areas does not allow for comparison to the median concentration of PPCPs found in the Hunting Creek region, which was more extensively sampled.

Out of the 36 total PPCPs that were detected in all TFWPR surface water samples, 9 showed quantitation frequencies >50%. These compounds exhibited some of the highest median concentrations of all PPCPs detected in surface water samples. The concentrations for these 9 PPCPs for all locations throughout the TFWPR are summarized below in the box and whisker plot below (Figure 1.19). The PPCPs are listed from highest to lowest concentrations when combined across all sites.

Fexofenadine, an antihistamine, was found in the greatest concentration in surface water samples followed closely by caffeine, DEET, and nicotine. Carbamazepine (anticonvulsant), sulfamethoxazole (antibiotic), metoprolol (beta blocker), tramadol (opioid), and bupropion (antidepressant) were also found in surface waters. There was no single class of PPCPs that dominated in presence or concentrations throughout the northern Potomac River watershed.

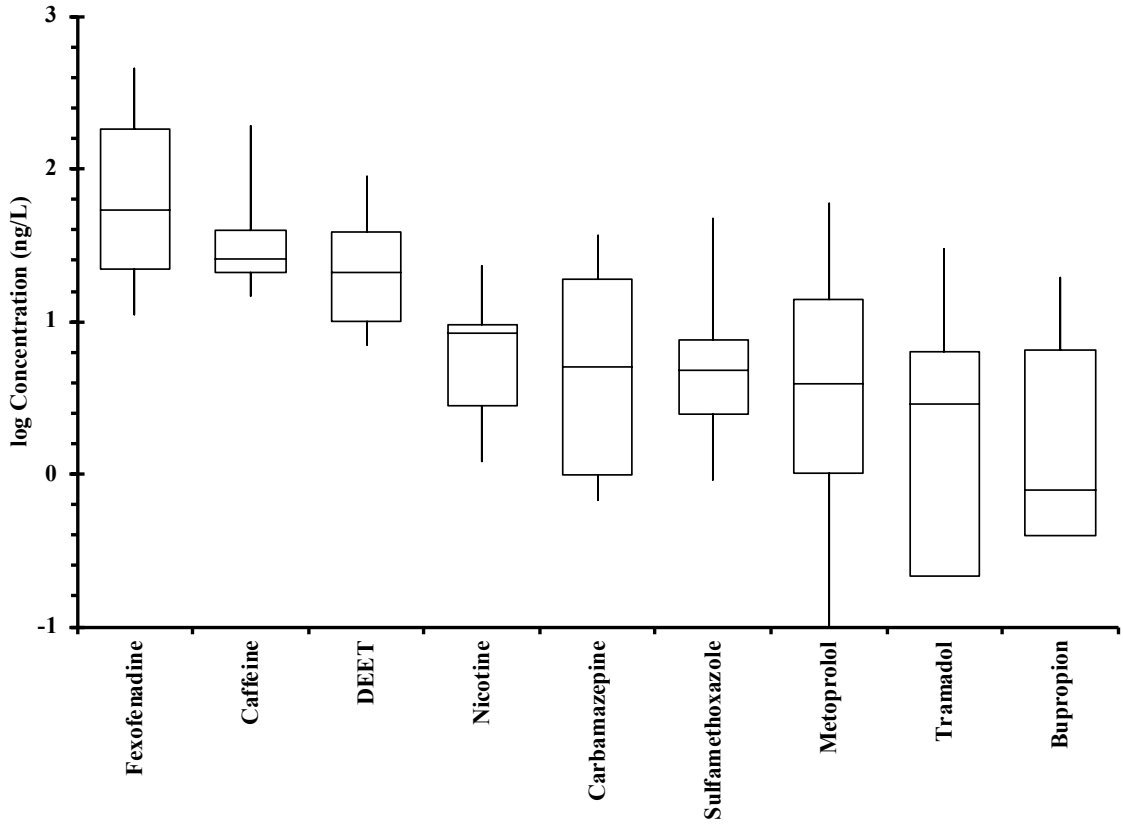

Figure 1.19: Concentrations of 9 detected PPCPs (QF >50%) (in order of decreasing median detected concentration) in surface water samples (n = 119) from all downstream sampling locations throughout the TFWPR. Boxes, centerlines, and whiskers indicate interquartile range, median, and 5th and 95th percentiles, respectively.

Out of the 40 PPCPs detected in sediment samples, 14 had a detection frequency >50%. These compounds exhibited some of the highest median concentrations of all PPCPs detected in the sediment samples. The concentrations for these 14 PPCPs across all locations in the TFWPR are summarized below in Figure 1.20. The PPCPs are listed from highest to lowest concentrations when combined across all sites.

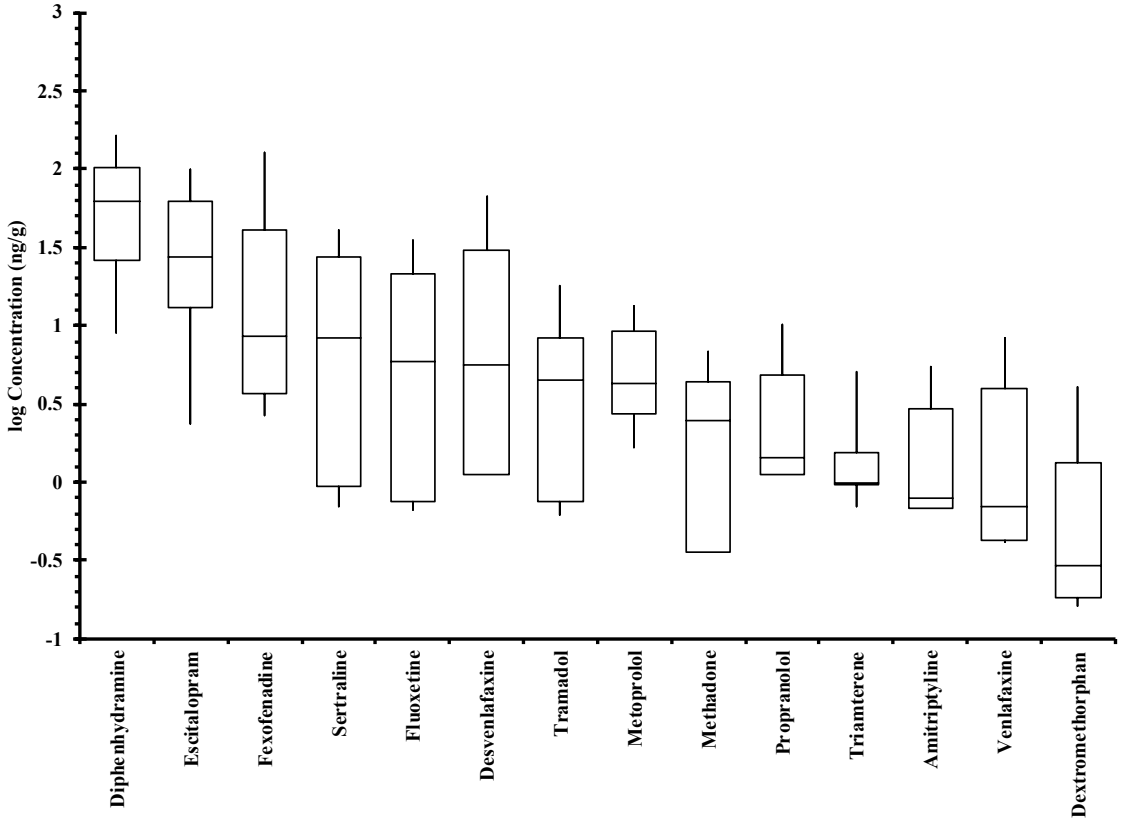

Figure 1.20: Concentrations of 14 detected PPCPs (QF >50%) (in order of decreasing median detected concentration) in sediment samples (n = 91) from all downstream sampling locations throughout the TFWPR. Boxes, centerlines, and whiskers indicate interquartile range, median, and 5th and 95th percentiles, respectively.

Interestingly, diphenhydramine, another antihistamine, was found in the highest concentration in sediment samples. Fexofenadine and metoprolol were also found in sediment samples at lower concentrations in respect to the surface water samples. Aside from these two PPCPs there was not any crossover of PPCPs found in water and sediment samples. This is believed to be due to the different physiochemical properties of the PPCPs.

1.4.4 PPCP Concentrations in WTP Effluents

Wastewater effluent samples were obtained for LC-MS/MS analysis from two of the three WTPs discharging in proximity to the sampling sites at Hunting Creek and Four Mile Run, including Alexandria Renew Enterprises and Arlington Water Pollution Control Plant. The individual PPCPs quantified in effluent water from each WTP are depicted in Figure 1.21, Figure 1.22, Figure 1.23, and Figure 1.24. In each instance, the concentrations found in the effluent samples were compared to those found in water and sediment immediately downstream of the effluent. A linear regression was used to analyze this data and determine if there was a specific correlation between the concentration of a compound in the effluent samples and the concentration found downstream.

The Alexandria Renew Enterprises effluent sample was found to contain 43 of the 91 target PPCPs. Of the 43 compounds detected, 22 were not found to be present in water or sediment samples downstream. This indicates that these compounds are not persistent in the environment. In regard to the 21 compounds that were found downstream in either water or sediment (or both) samples, the concentrations were significantly lower in downstream surface water relative to effluent concentrations, on the order of magnitude from 10 – 1000 times lower depending on the PPCP in question. A full list of the PPCPs found in effluent versus downstream surface waters and sediments can be found in Table 4.10A.

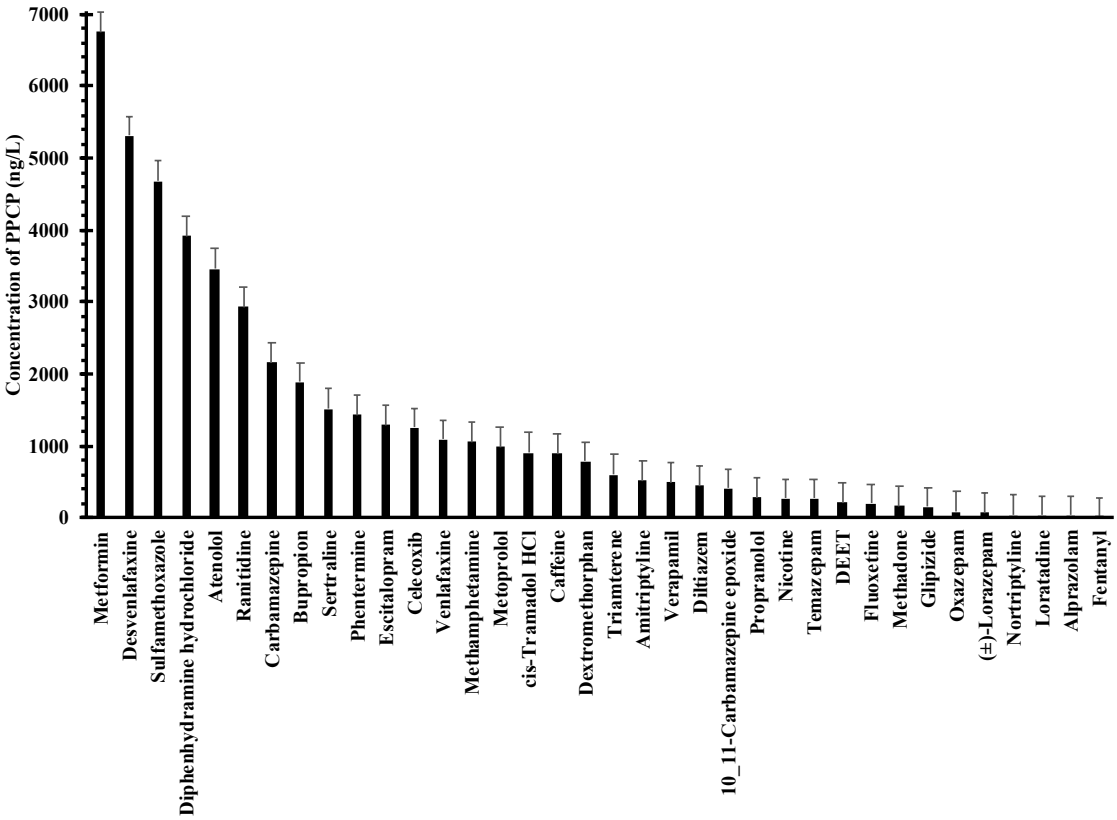

Figure 1.21: PPCPs found in Alexandria Renew effluent water samples. Black columns represent the mean concentrations (ng/L) and bars represent ± 1 SD.

The concentrations of PPCPs found in effluent water from Alexandria Renew Enterprise were significantly greater than those found in surface water and sediment samples from Hunting Creek. However, there does not appear to be any correlation between concentration of PPCPs found in the effluent and concentration of PPCPs found downstream in either surface water or sediment samples ($R^2 = 0.064$ and $R^2 = 0.4501$, respectively).

There were five PPCPs found at concentrations substantially above the linear range of the LC-MS/MS calibration curve used for analysis. Those PPCPs are depicted separately in Figure 1.22.

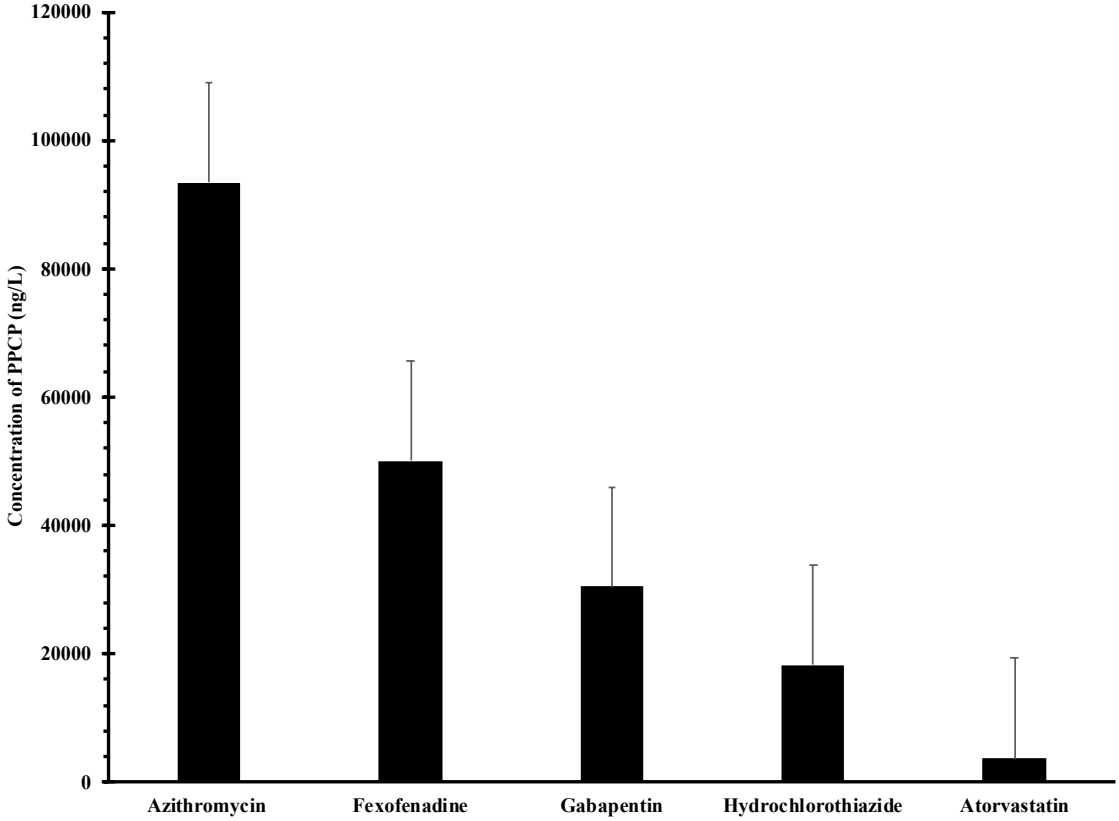

Figure 1.22: PPCPs found at extremely high concentrations in Alexandria Renew effluent water samples. Black columns represent the mean concentrations (ng/L) and bars represent ± 1 SD.

A dilution study was carried was carried out to obtain values for these compounds that were more in line with the scope of the rest of the study. This consisted of a 1:100 and 1:1000 dilution of the effluent samples. However, after dilution, the internal standards were unable to be found in the samples and quantitation could not be carried out on the diluted samples.

The Arlington Water Pollution Control Plant effluent sample was found to contain 40 of the 91 target PPCPs. Of the 40 compounds detected, 11 were not found to be

present in water or sediment samples downstream. This indicates that these compounds are not persistent in the environment. In regard to the 29 compounds that were found downstream in either water or sediment (or both) samples, the concentrations were significantly lower in downstream surface water relative to effluent concentrations, on the order of magnitude from 10 – 1000 times lower depending on the PPCP in question. A full list of the PPCPs found in effluent versus downstream surface waters and sediments can be found in Table 4.11A.

The concentrations of PPCPs found in effluent from Arlington Pollution Control Plant were significantly higher than those found in water and sediment samples from Four Mile Run. However, there does not appear to be any correlation between concentration of PPCPs found in the effluent and concentration of PPCPs found downstream in either surface water or sediment samples ($R^2 = 0.0415$ and $R^2 = 0.00012$, respectively).

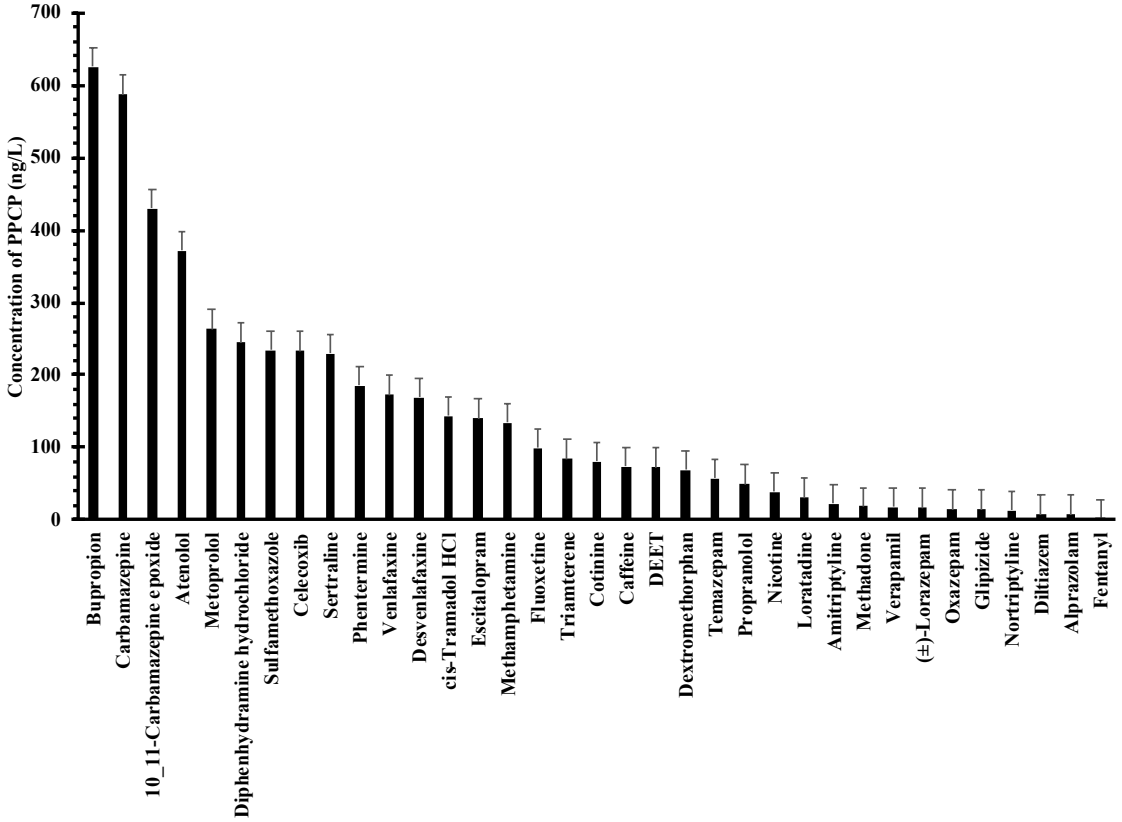

Figure 1.23: PPCPs found in Arlington Pollution Control Plant effluent water samples. Black columns represent the mean concentrations (ng/L) and bars represent ± 1 SD.

There were four PPCPs found at high concentrations but still within the linear range of the calibration curve used for analysis. Those PPCPs are depicted separately in Figure 1.24. A dilution study was carried was carried out to obtain values for these compounds that were more in line with the scope of the rest of the study. This consisted of a 1:100 and 1:1000 dilution of the effluent samples. However, after dilution, the internal standards were unable to be found in the samples and quantitation could not be carried out on the diluted samples.

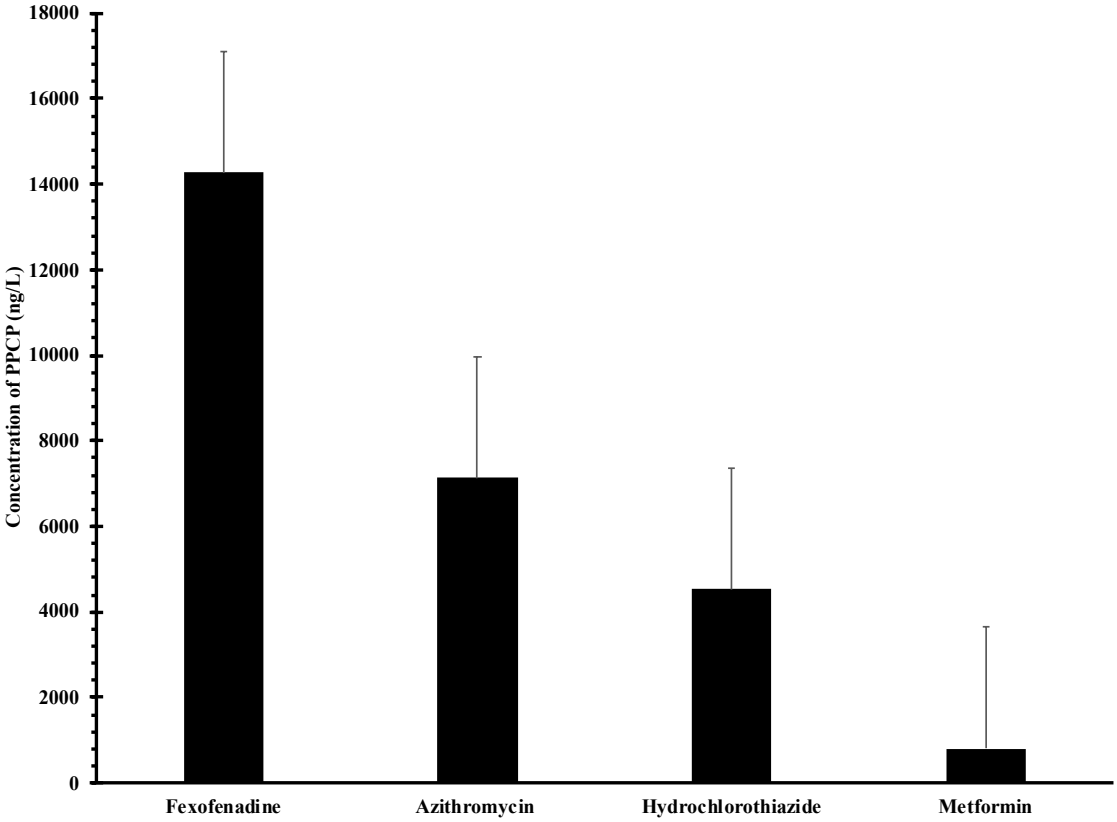

Figure 1.24: PPCPs found at high concentrations in Arlington Pollution Control Plant effluent water samples. Black columns represent the mean concentration (ng/L) and bars represent ± 1 SD.

1.4.5 Distribution of PPCPs between water and sediment

The mass-based distribution coefficient, K_d, was calculated for PPCPs in which concentrations were measured in water (C_w) and sediment (C_s) at a particular site during each individual trip as given in Equation 1.4.

Equation 1.4: The mass-based distribution coefficient

$$K_d = \frac{C_s}{C_w}$$

The K_d values for a compound can be used to estimate the distribution of the compound between the water and sediment compartments. However, this value is dependent upon other factors such as, characteristics of the compound, matrix of each compartment, temperature, and recent rainfall, and is only an estimate of the sediment-water distribution of each compound.

The n-octanol-water partition coefficient, K_{ow}, is helpful in determining the partitioning of compounds between different compartments in the environment. The properties of octanol allow it to serve as a solvent that can mimic total organic carbon found in sediments. The K_{ow} values for compounds have been previously determined, corrected for pH dependence, and reported in the literature. The pH-corrected log K_{ow} values are expressed as log Distribution Coefficient, or log D, as D varies with pH.

A regression of log K_d vs log D was performed to determine if there was any correlation between the two values that would allow for the prediction of whether the compound in question would partition into the sediment or remain in the water column. The results of this analysis are shown in Figure 1.25. A Spearman's rank correlation was conducted on log K_d vs log D values. This regression resulted in a Spearman's Rho value of 0.459 indicating that both variables are increasing monotonically.

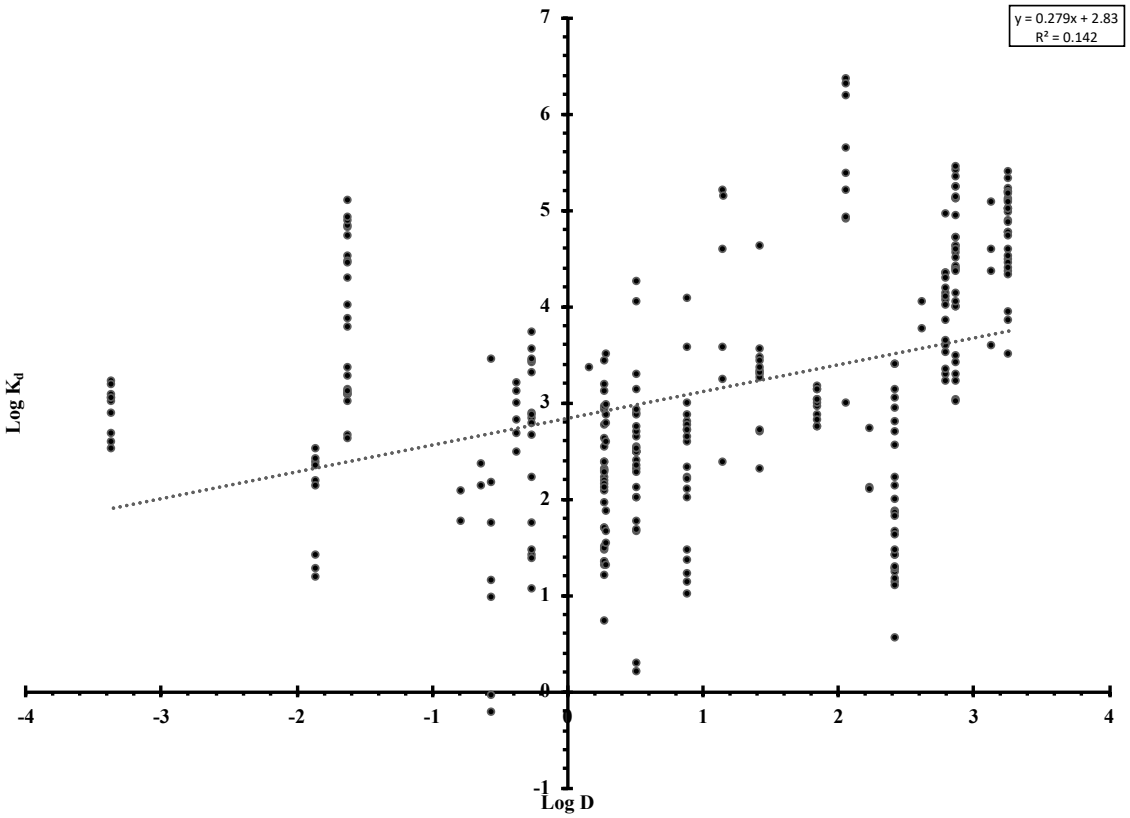

Figure 1.25: Linear regression of Log K_d versus Log D for all compounds that were found in both water and sediment samples at each site along the TFWPR. Each point represents the average Log K_d value at a particular site for one trip.

This regression illustrates that as the D increases, the K_d increases as well, as suggested by the Spearman's rank correlation. This is in agreement with the literature which has determined that compounds with higher D values will partition into the sediment.[53,54]

1.5 Discussion

1.5.1 Comparison of PPCPs in the TFWPR to Other Sites Worldwide

Twenty PPCPs were observed in water and/or sediment samples with a QF >50%. Of those twenty, three were detected in both surface water and sediment, and included: fexofenadine, metoprolol, and tramadol. The presence of these PPCPs in surface waters and sediments was universally prominent across to the TFWPR.

Fexofenadine, an antihistamine sold under the name Allegra, was detected at the highest concentration of all PPCPs in this study in surface water samples. According to the FDA, only 5% of the total oral dose of fexofenadine is metabolized. The remaining 95% is excreted as waste which explains the high concentrations found in surface waters.[55] Fexofenadine was detected in surface waters across the globe at concentrations ranging from 4 – 3,000 ng/L.[16,56–58] Fexofenadine concentrations in sediment were not reported. The average concentration of fexofenadine found in surface water samples in this study was 119 ng/L. This value is in line with studies done elsewhere in the United States and in Europe, where usage of pharmaceuticals are more heavily regulated.[56,57] In addition, studies have reported that the highest concentration of fexofenadine was found in surface water samples immediately after the WTP outfall.[16,56] This was found to be true in this study as well, with the sites HC1, GC2, and FMR2 having concentrations of 387 ng/L, 191 ng/L, and 276 ng/L, respectively.

Metoprolol, a beta-blocker that is used to treat high blood pressure, is metabolized extensively in the body with less than 5% of an oral dose recovered in the urine.[59] Metoprolol is detected globally in surface waters at concentrations ranging from 11 – 77

ng/L.[60–63] The average concentration of metoprolol in this study was 13 ng/L was in agreement with the literature. The aforementioned studies did not report concentrations of metoprolol in the sediment; however, these studies also reported that metoprolol demonstrated a tendency to persist in the surface water downstream of the WTP. The results of this study also demonstrated this trend with metoprolol found in the downstream sites at concentrations varying from 1.3 – 33 ng/L.

Tramadol, an opioid, has been detected globally in surface waters and sediments throughout the US and globally. The concentration of tramadol in surface water samples a ranged from 9 – 2,774 ng/L.[64–66] The studies that analyzed sediment samples for the presence of tramadol were able to detect the compound but not at concentrations above their limit of quantitation of 2 – 5 ng/g.[64] The average concentration of tramadol detected in this study was 8 ng/L and 17 ng/g in surface waters and sediment, respectively. Tramadol was often detected in water and sediment samples, however, this study also experienced the issue of tramadol being detected at concentrations lower than the quantitation limit as reported in other studies.[64]

Six out of twenty PPCPs observed with a QF >50% were found only in surface water samples. Those PPCPs include caffeine, DEET, nicotine, carbamazepine, sulfamethoxazole, and bupropion.

Caffeine, DEET, and nicotine are some of the most widely used personal care products across the globe and have been found in surface waters in concentrations ranging from 4 – 47,500 ng/L[67–70], 13 – 660 ng/L[71–73], and 5 – 815 ng/L[74–77], respectively. In this study, caffeine, DEET, and nicotine were found in >98% of all surface water

samples at an average concentration of 70 ng/L, 47 ng/L, and 16 ng/L, respectively. Their persistence throughout the entire region of sampling agrees with the aforementioned studies.

Bupropion, an antidepressant used to treat major depressive disorder and seasonal affective disorder. This pharmaceutical has been found in surface waters throughout the United States and parts of Europe in concentrations ranging from 10 – 1,160 ng/L.[15,78–80] Bupropion was also found in riverbed sediments in the United States at concentrations of approximately 2 ng/g, when detected.[81] While bupropion was found in sediment samples in this study, it was detected in <50% of all samples and was not included in this analysis. The average concentration of bupropion in surface water samples in this study was 5.2 ng/L. Bupropion was found to be most prevalent at sites closest to the WTP outfall.

Sulfamethoxazole is an antibiotic used to treat a wide variety of bacterial infections. It has been found in surface waters throughout the United States at concentrations ranging from 28 – 57 ng/L.[17,60,82] In this study, sulfamethoxazole was found in surface water samples at an average concentration of 12 ng/L. As was the case with bupropion, sulfamethoxazole was most prominent in surface water samples immediately following the WTP outfall.

Carbamazepine is an anticonvulsant used primarily to treat epilepsy. This PPCP and its metabolite, carbamazepine epoxide, has been detected in surface waters throughout the majority of Europe and in some parts of the United States with concentrations ranging from 12 – 250 ng/L.[15,60,83–85] In most instances, the concentration of the metabolite was not reported separately from the primary compound. In this study

the average concentration of carbamazepine and its metabolite in surface waters was found to be 9.7 and 5.5 ng/L, respectively.

Eleven out of twenty PPCPs were observed with a QF >50% and these were found only in sediment samples. Those PPCPs included: escitalopram, sertraline, fluoxetine, desvenlafaxine, venlafaxine, amitriptyline, methadone, propranolol, triamterene, dextromethorphan, and diphenhydramine.

Escitalopram, fluoxetine, and sertraline are SSRIs while desvenlafaxine, venlafaxine, and amitriptyline are antidepressants. The majority of studies concerning SSRIs focus on their occurrence and concentrations in surface waters.[15,86,87] However, the studies that have looked at these compounds have reported concentrations ranging from 0.291 – 4.42 ng/g, 2.58 – 2.53 ng/g, and 1.56 – 6.35 ng/g for escitalopram, fluoxetine, and sertraline, respectively.[88] In this study escitalopram, fluoxetine, and sertraline were found at average concentrations of 1.37 ng/g, 1.07 ng/g, and 1.163 ng/g, respectively, in sediment.

Venlafaxine, an antidepressant and nerve pain medication, has been reported at concentrations both nationally and globally in concentrations ranging from 2 – 690 ng/L[56,89–91] in surface water samples and 1.6 – 26 ng/g[81] in sediment samples. In this study venlafaxine was found at an average concentration of 12.6 ng/g in sediment, which falls well within the normal ranges reported in the literature. Venlafaxine has not been shown to persist in the surface water downstream of the WTP outfall and, instead, settles into the sediment bed at the downstream locations.

Similarly, desvenlafaxine and amitriptyline has been found in surface waters and sediments globally at concentrations ranging from 1.1-7.6 ng/g[92] and <1.4 ng/g[93], respectively. Desvenlafaxine was found at an average concentration of 0.80 ng/g in this study, which is slightly lower than what has been reported in the literature. Amitriptyline was found at an average concentration of 0.51 ng/g, which is consistent with values reported elsewhere.[92]

Triamterene is a diuretic that can also treat high blood pressure. It has been found in surface waters and sediment samples across the US at concentrations ranging from 1.1 – 12 ng/L[4,60,94] and 0.3 – 11 ng/g, respectively.[94] Triamterene was found at in surface water and sediment samples throughout the TFWPR. The average concentration of triamterene was 8.3 ng/g for sediments. Metoprolol and propranolol are beta-blockers that are used to treat high blood pressure. These compounds were found in concentrations in the US ranging from 0.01 – 17 ng/g[95] and 0.1 – 3.4 ng/g[96,97], respectively in sediments. The concentrations of metoprolol and propranolol found in this study were on the low end of those reported in the literature with average concentrations of 0.70 ng/g and 0.41 ng/g, respectively.

Methadone is an opioid that can be used to treat moderate to severe pain and drug addiction. The vast majority of studies concerning methadone in the environment focus on its concentration in surface and groundwater samples where it has been reported at concentrations of 10 – 90 ng/L[98–100] and have not measured the concentration in sediments. In this study methadone was found at an average concentration of 0.60 ng/g. It is unknown how this compares to other sediments.

Diphenhydramine and dextromethorphan are OTCs used to treat allergies and a cough, respectively. Diphenhydramine has been widely studied and has been reported at concentrations of 0.63 – 48.6 ng/g[101,102], while dextromethorphan has not be reported elsewhere. The average concentrations for these compounds in sediment were found to be 1.7 ng/g and 0.47 ng/g, respectively.

1.5.2 Sources of PPCPs to the TFWPR

While there are several sources of PPCPs to the TFWPR, this study focused specifically on WTP and upstream contributions. In order to determine if the PPCPs in questions were being contributed by the WTPs, effluent samples were obtained from two of the WTPs in the area. In addition, samples were taken upstream of the WTP to determine which PPCPs, if any, occurred in the surface water prior (upstream) to the WTP discharge.

The radar plot in Figure 1.26 illustrates the PPCPs present in the TFWPR. Fexofenadine, metformin, DEET, caffeine, nicotine, and desvenlafaxine are the most prominent PPCPs in the TWFPR. This result was as expected give that those PPCPs were found in the majority of all samples. However, this study determined that not all these PPCPs were exclusively contributed by WTPs. This plot, and the subsequent radar plots are based on mole fraction concentrations. The data was analyzed in this way to avoid large concentrations biasing the multivariate factors.

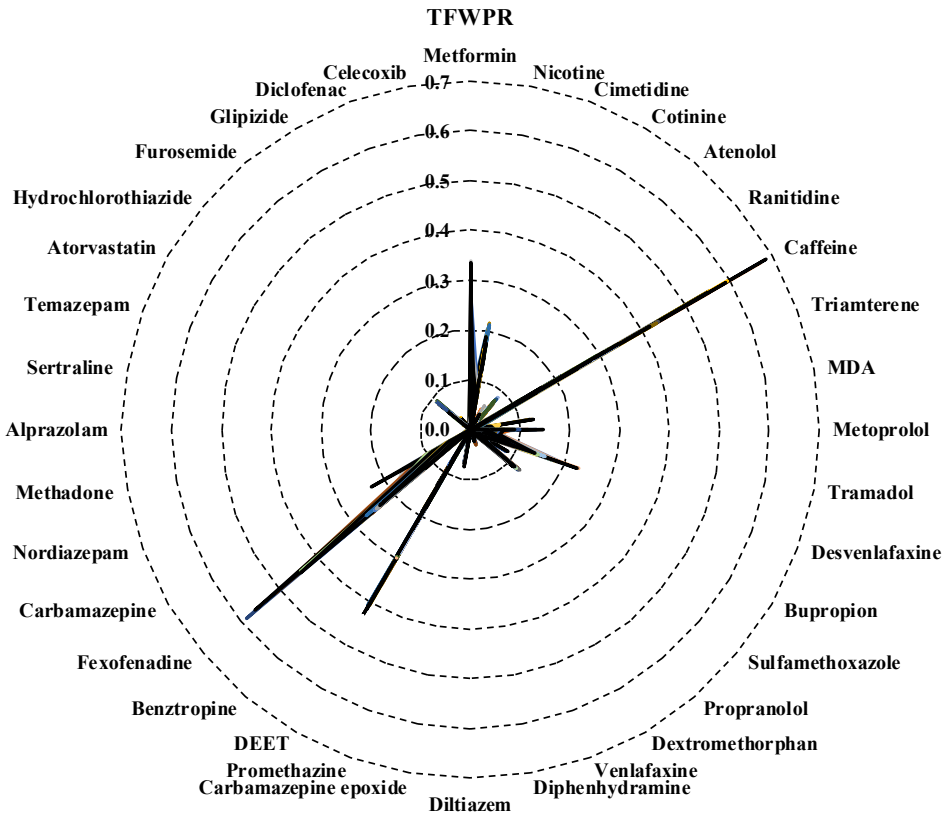

Figure 1.26: Radar Plot of the individual PPCPs found in the TFWPR. The plot is based on mole fraction concentrations.

Figure 1.27 is a radar plot of the PPCPs found in effluent samples from the WTPs. Fexofenadine was the most prominent PPCP found in effluent samples, followed by hydrochlorothiazide and metformin. WTPs also contributed desvenlafaxine, sulfamethoxazole, and atenolol. The large amount of hydrochlorothiazide is interesting as this was not observed in any significant levels downstream of the WTPs. However, research into the matter has shown that hydrochlorothiazide is highly susceptible to photodegradation.[103,104] It is believed that this compound reacts very shortly after being discharged into the TFWPR to form different transformation products.[105] Also of importance to note is the lack of DEET, caffeine, and nicotine. The absence of their

presence in this radar plot suggests that these particular PPCPs are being contributed to the TFWPR by another, unidentified source.

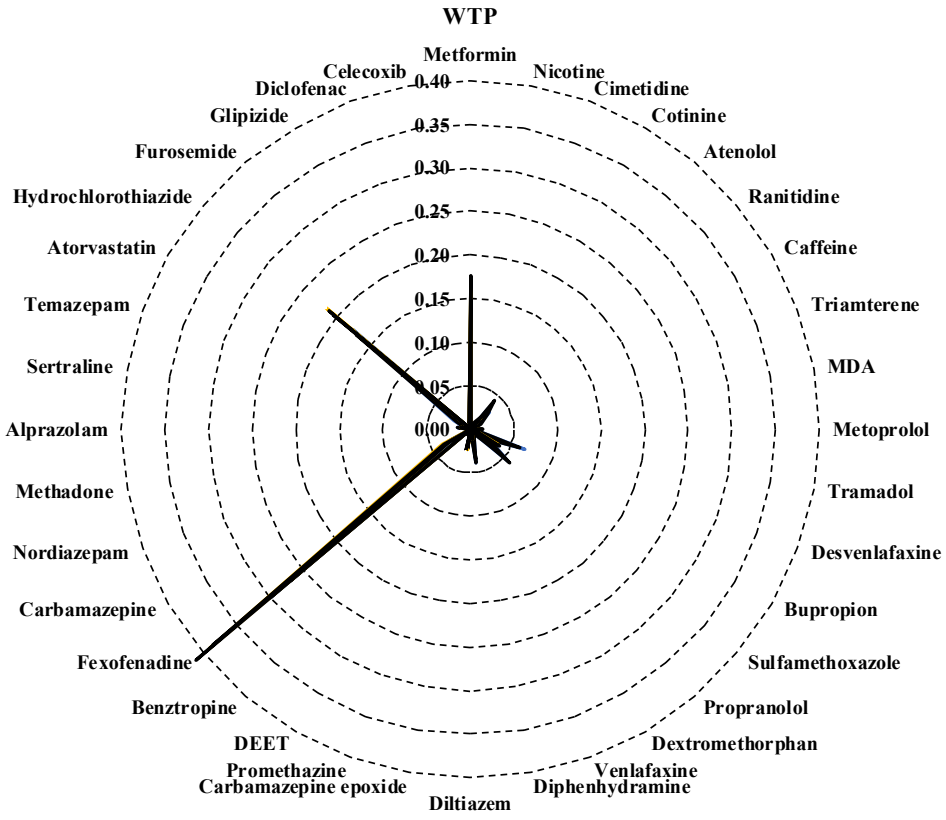

Figure 1.27: Radar Plot of the individual PPCPs found in the WTP effluent samples. The plot is based on mole fraction concentrations.

The samples taken upstream of the WTPs were also analyzed in this manner to determine which PPCPs were present in the TWFPR prior to WTP discharge. The resulting radar plot, Figure 1.28, shows that DEET, caffeine, nicotine, and metformin are the most prominent PPCPs upstream of the WTP discharge zone. The majority of upstream locations were in parks or wooded areas. As such, the large amount of DEET is

unsurprising. Similarly, the presence of caffeine and nicotine in such heavily populated areas would not be unexpected. However, the significant presence of metformin indicates another source of PPCPs into these environments. While the specific source is unknown at this time, these analyses have demonstrated that WTPs are not the only source of PPCPs into the TWFPR.

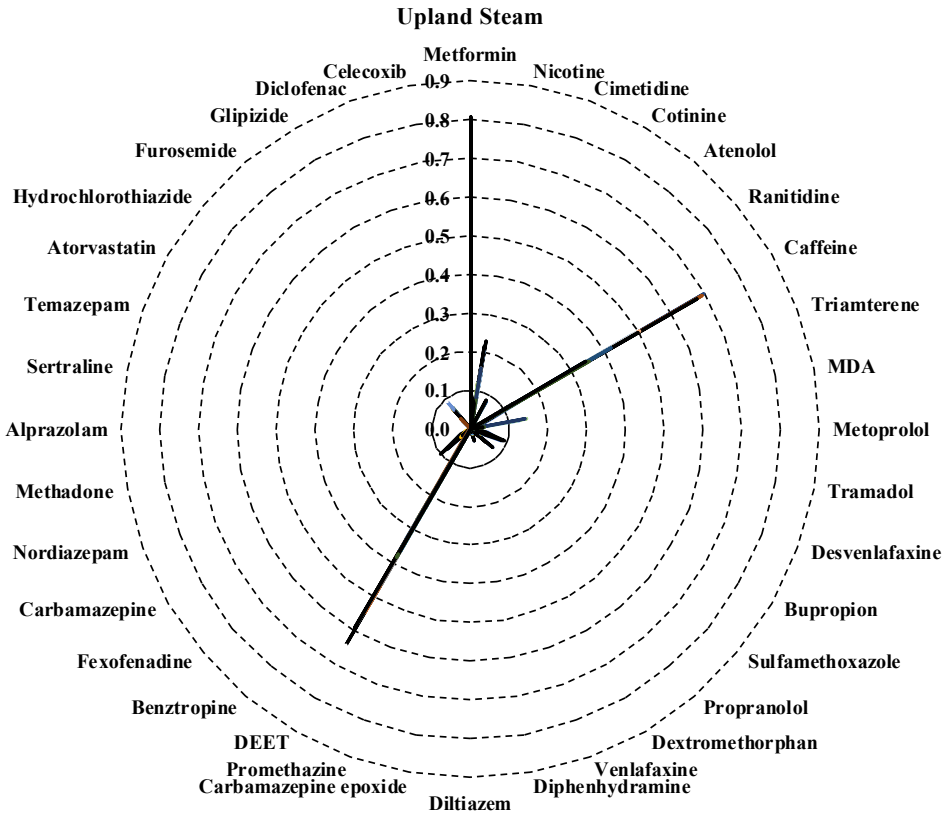

Figure 1.28: Radar Plot of the individual PPCPs found in samples taken upstream of the WTPs. The plot is based on mole fraction concentrations.

1.5.3 Comparison of PPCPs among WTPs

Alexandria Renew Enterprises and Arlington Pollution Control Plant, two of the WTPs of interest in this study, provided effluent samples. The PPCPs found in each effluent sample were discussed previously and depicted in Figure 1.21, Figure 1.22, Figure 1.23, and Figure 1.24. A Spearman's Rank Correlation showed significant correlation in mole fraction concentrations (Rho = 0.76, $p<0.05$) between the PPCPs found in both effluent samples, indicating that these two high-capacity WTPs are discharging similar PPCPs into the TFWPR. This may be due to the similar demographics each WTP serves in their distinct areas of service and it is likely that all WTPs in the area are discharging similar PPCPs. Future analysis of effluent from all WTPs may provide more insight into fine-resolution therapeutic PPCP usage and population demographics within the area surrounding the TFWPR.

1.5.4 PPCP Dispersal in the TFWPR

A distinct difference between the concentration of PPCPs in the effluent versus the concentration in the discharge zone was observed in this study. In regard to the effluent sample from Alexandria Renew Enterprises, of the forty-three PPCPs found in measurable concentrations, twenty-nine were not detected in surface waters in the discharge zone. The fourteen PPCPs that were detected in the discharge zone were detected at concentrations ranging from 3 – 481 times lower than they were found in the effluent samples. The full list of PPCPs and their concentrations in the effluent sample and surface water in the discharge zone may be found in Table 4.10A.

In regard to the effluent sample from Arlington Pollution Control Plant, of the forty PPCPs found in measurable concentrations, nineteen were not detected in surface waters in the discharge zone. The eighteen PPCPs that were detected in the discharge zone were detected at concentrations ranging from 8 – 410 times lower than they were found in the effluent samples. Interestingly, three PPCPs (caffeine, nicotine, and DEET) were found in the discharge zone at higher concentrations than present in the effluent samples. This data agrees with the previous observation that there is an additional, unknown source of those PPCPs into the environment. The full list of PPCPs and the concentrations in the effluent sample and surface water in the discharge zone may be found in Table 4.11A.

These results indicate that the PPCPs in question, specifically those not found in the surface waters of the discharge zones, do not persist in the environment. One of the major differences in concentration may be due to the dilution of the PPCPs. When the effluent samples were collected it was from a controlled environment. Once the effluent is discharged into the TFWPR it is rapidly diluted in surface waters. Furthermore, it is known that the majority of these PPCPs can undergo transformations to different products via photodegradation or other processes.[2,103–106] The scope of this study had limited transformative product evaluations of PPCPs. As such, it is possible that these PPCPs were present at the discharge site at greater concentrations than reported. In addition, these PPCPs may react with other substances found in surface waters or, in some instances, fall out of the water column and partition into the sediment.[60,92,107]

1.5.5 PPCPs in Sediment

Several PPCPs were observed in sediment samples collected over the course of the sampling season. This was of interest to note as most PPCPs have low to moderate K_{ow} values. Overall, there were thirty-two PPCPs found in sediment compared to thirty-six found in surface water samples. In some instances, there was an overlap of twenty-four PPCPs found in both surface water and sediment samples. These PPCPs were used in the regression analysis between log K_d and log D values found in Figure 1.25. In this instance log D values were used in place of log K_{ow} values, as D is corrected for pH. A comparison of K_{ow} versus D values for these compounds is found in Table 1.8.

Table 1.8: Sorption properties of PPCPs in sediment and surface water in the TFWPR.

PPCP	Log K_{ow}	Log D_{ow} pH 7.4	Log K_d measured median	Log K_d predicted	ΔLog K_d (meas-pred)	Functional Group	Expected Charge	#N Atoms	H bond A/D	pKa
Metformin	-1.40	-3.36	3.02	-3.31	6.34	Amine	+	5	5/5	12.40
Nicotine	1.17	-0.37	2.90	-0.74	3.64	Amine	+	2	6/0	3.04, 7.84
Atenolol	0.16	-1.85	2.18	-1.75	3.93	Amine	+	2	5/4	9.60
Ranitidine	0.27	-0.63	2.12	-1.64	3.77	Amine	+	4	7/2	2.70, 8.20
Caffeine	-0.07	0.28	2.21	-1.98	4.20	Ar Amine	+	4	2/0	10.40
Triamterene	0.98	-1.61	3.86	-0.93	4.79	Amine	+	7	7/6	6.20
Metoprolol	1.88	-0.25	2.84	-0.03	2.87	Amine	+	1	4/2	9.70
Tramadol	2.51	0.52	2.47	0.60	1.88	Amine	+	1	3/1	9.41
Desvenlafaxine	2.72	0.89	2.45	0.81	1.65	Amine	+	1	3/2	na
Bupropion	3.85	2.88	4.51	1.94	2.58	Amine	+	1	2/1	na
Sulfamethoxazole	0.89	-0.56	1.14	-1.02	2.16	Ar Amine	+	3	6/3	na
Propranolol	3.48	1.15	4.07	1.57	2.51	Amine	+	1	3/2	9.42
Dextromethorphan	3.60	1.86	2.99	1.69	1.31	Amine	+	1	2/0	na
Venlafaxine	3.28	1.43	3.31	1.37	1.95	Amine	+	1	3/1	na
Diphenhydramine	3.27	2.34	4.87	1.36	3.52	Amine	+	1	2/0	8.98
Diltiazem	2.70	2.06	5.37	0.79	4.58	Amine	+	2	6/0	8.06
Fexofenadine	4.80	2.43	1.81	2.89	-1.08	Carboxyacid	-	1	5/3	4.28, 8.76
Carbamazepine	2.45	0.29	2.58	0.54	2.05	Urea	+	2	3/2	13.90
Methadone	3.93	2.80	4.05	2.02	2.03	Amine	+	1	2/0	8.94
[1]log K_d (pred) = log K_{ow} + log 0.61 + log f_{oc} (Karickoff et al. 1969)										
[2]Exceptionally large differences between measured and predicted K_d										

There was no apparent trend in the differences between log K_{ow} and log D for these PPCPs. The values did not change in the same way for all the PPCPs once corrected for pH. However, the correction for pH did have a significant effect (i.e. difference) on eighteen of the twenty-four PPCPs, with the values either changing sign (+ vs -) or changing magnitude by a value of log 1 or greater. The differences between these values indicate that acid-base chemistry plays a significant role in the fate of PPCPs in the environment and that PPCPs may acquire formal charge at ambient pHs.

A Spearman's Rank Correlation was run using the log D and log K_d values. The results (Rho = 0.45, $p<0.05$) indicate a significant correlation between the set of values. While the linear regression indicates a weak correlation between the two values (Figure 1.25), it may be improved upon by further refinement of the K_d values. It was observed that the measured distribution constants $K_{d\text{-}meas}$ were much larger than what would have been expected based on their corresponding K_{ow} values for certain PPCPs. One possible reason for this discrepancy is because this model does not take into account any rapid decomposition that may be taking place in the environment (yielding low water concentrations). Furthermore, the sediment concentrations were not normalized to organic carbon levels because there was no observed correlation between $K_{d\text{-}meas}$ and %TOC. It is generally assumed that organic micropollutants primarily partition into natural organic matter based on polarity and the (increasing) magnitude of K_{ow}.

In addition, the K_d values do not take into account any distribution of compounds between suspended sediments and water or organisms, such as plankton, and water. Several other studies that have taken these distributions into account and have determined

that interactions of compounds between water and sediments is not straightforward and that the larger organic carbon cycle plays a significant role in distribution of compounds between compartments.

In general, the weak, yet significant, correlation between the log D and log $K_{d\text{-}meas}$ values indicates that mechanism of sorption of PPCPs in sediment is not driven solely by organic matter as most partitioning models predict. Another possible mechanism is sorption of PPCPs to exposed (i.e., not coated with organic matter) mineral surfaces found in sediment. Several studies have focused on the interaction between PPCP and PPCP-like compounds to mineral surfaces within the sediments and have found that these sorptive activities can play a major role in PPCPs partitioning into the sediment. Furthermore, it has been reported that up to 70% of sorption in the sediment could be attributed to interaction with mineral surfaces.[108–111]

It is known that the mineral surfaces can readily react with certain functional groups present in a number of PPCPs. For example, the mineral surfaces contain a large number of alcohol (-OH) groups that can interact with certain functional groups on the PPCP via hydrogen bonding. The majority of the PPCPs in this study possessed some form of amine functional group. The hydrogen from the alcohol group on the mineral surfaces would be attracted to the electronegative nitrogen found in the amine group. Furthermore, many of the PPCPs also have carbonyl function groups. When this is the case the alcohol groups on the mineral surfaces can interact with these functional groups as well. These interactions are depicted in Figure 1.29. It appeared that one of the best indicators of the uptake of PPCPs by sediment was the number of H-acceptor/donor sites

that exist on the PPCP molecule. Those PPCPs with the greatest number of H-acceptor/donor sites showed the greatest positive deviation from the predicted line in Figure 1.25. Information concerning the H-acceptor/donor sites can be found in Table 1.8.

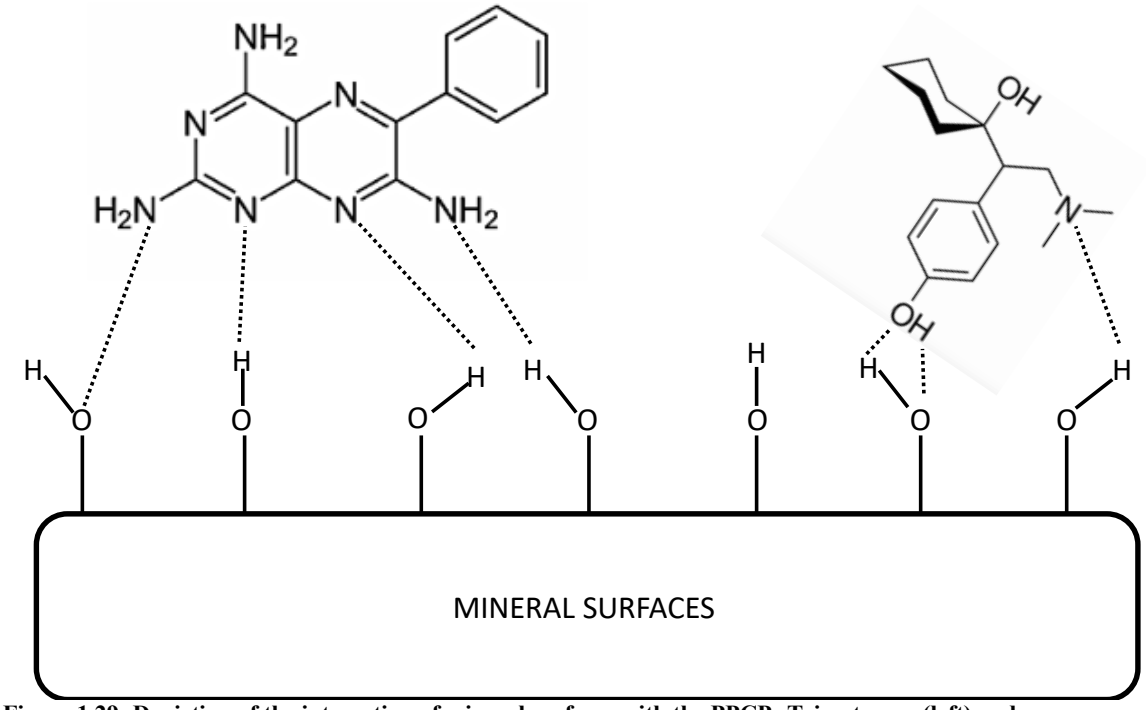

Figure 1.29: Depiction of the interaction of mineral surfaces with the PPCPs Triamterene (left) and Desvenlafaxine (right).

1.5.6 Seasonality of PPCPs

The seasonality, or how the change and variation in seasons affects the usage of and, therefore, the concentration of PPCPs in the environment has been of recent interest to the scientific community. Several studies have been conducted to monitor these changes across the globe.[17,112–115]

In this study the sampling period extended from May to September 2018, and as such a comprehensive four-season comparison (fall, winter, spring, and summer) of all the PPCPs could not be evaluated. However, there were seasonal trends observed over the course of the spring, summer, and near-fall (i.e., mid-September) sampling times for a few of the PPCPs.

DEET, a common ingredient in insect repellents, is often utilized in the summer months for both agricultural use and as a personal care product as more people take part in outdoor recreation.[115,116] Given the temporal use expected of this product, it follows that the concentrations found would increase over the course of the summer and decline with ambient temperature and daylight periodicity as autumn begins. This trend was observed in water samples collected in the Hunting Creek region as seen in Figure 1.30.

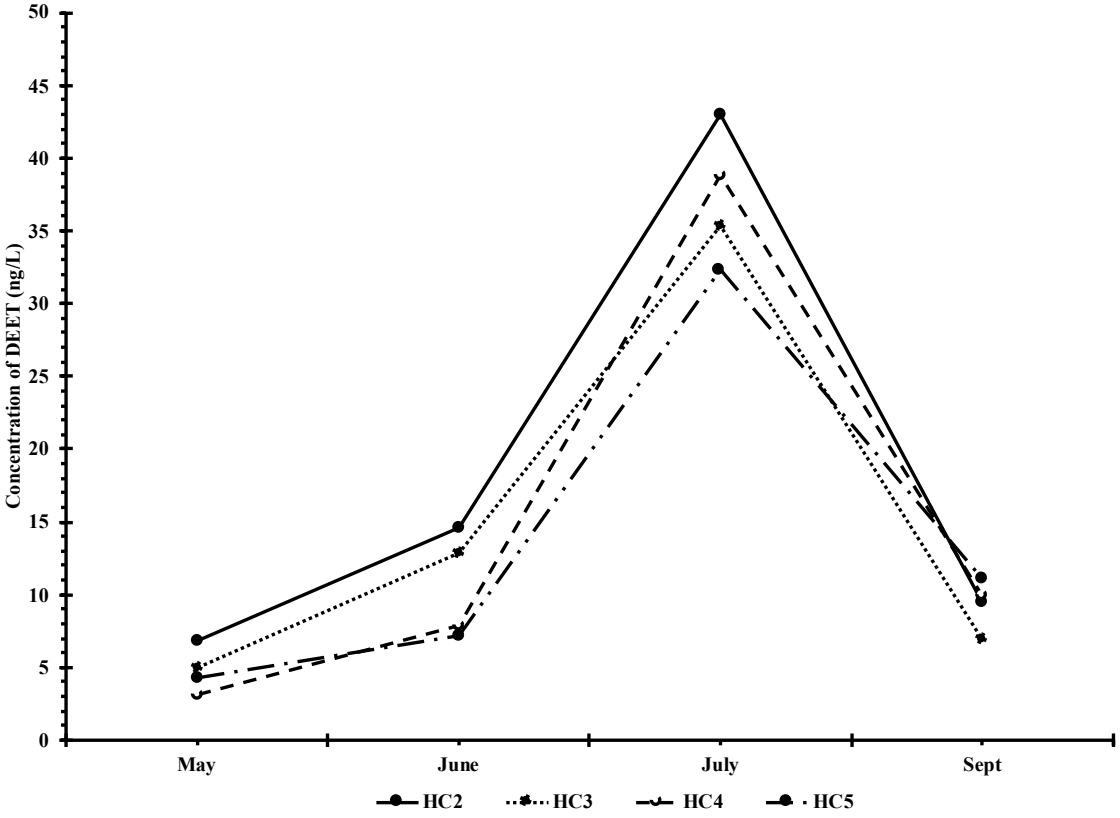

Figure 1.30: Concentration of the PPCP DEET in surface water samples at the downstream Hunting Creek locations over the course of the entire sampling season

Fexofenadine is the main ingredient in the allergy medication Allegra. In the United States, the spring allergy season often begins in February and lasts until the early summer months. With approximately 50 million American experiencing various types of allergies every year[117], it was expected that the rise and fall of the concentration of Fexofenadine would correspond to the start and end of allergy season. This trend was observed in water samples collected in the Hunting Creek region as seen in Figure 1.31.

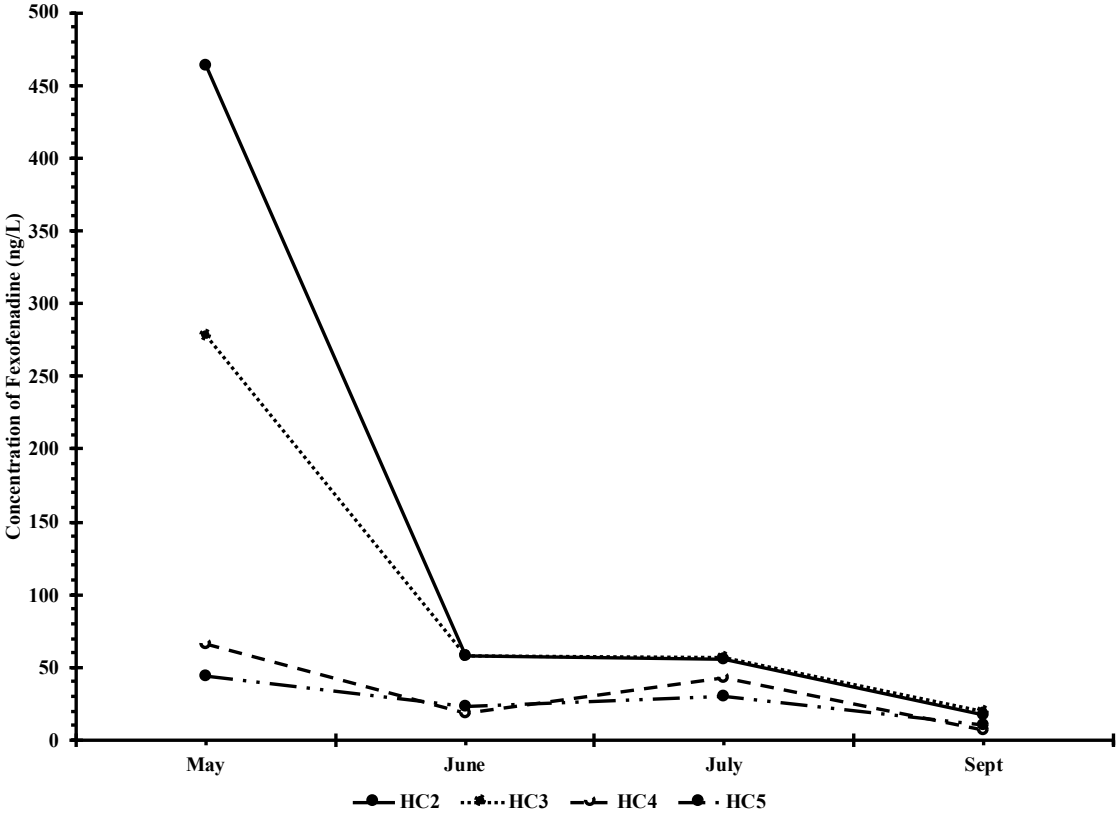

Figure 1.31: Concentration of the PPCP Fexofenadine in surface water samples at the downstream Hunting Creek locations over the course of the entire sampling season

Nicotine is an addictive substance found in tobacco products.[118,119] There is no known seasonality of tobacco usage, and as such, the concentration of nicotine found in samples should remain consistent through the course of the sampling season. This trend was observed in water samples collected in the Hunting Creek region as seen in Figure 1.32.

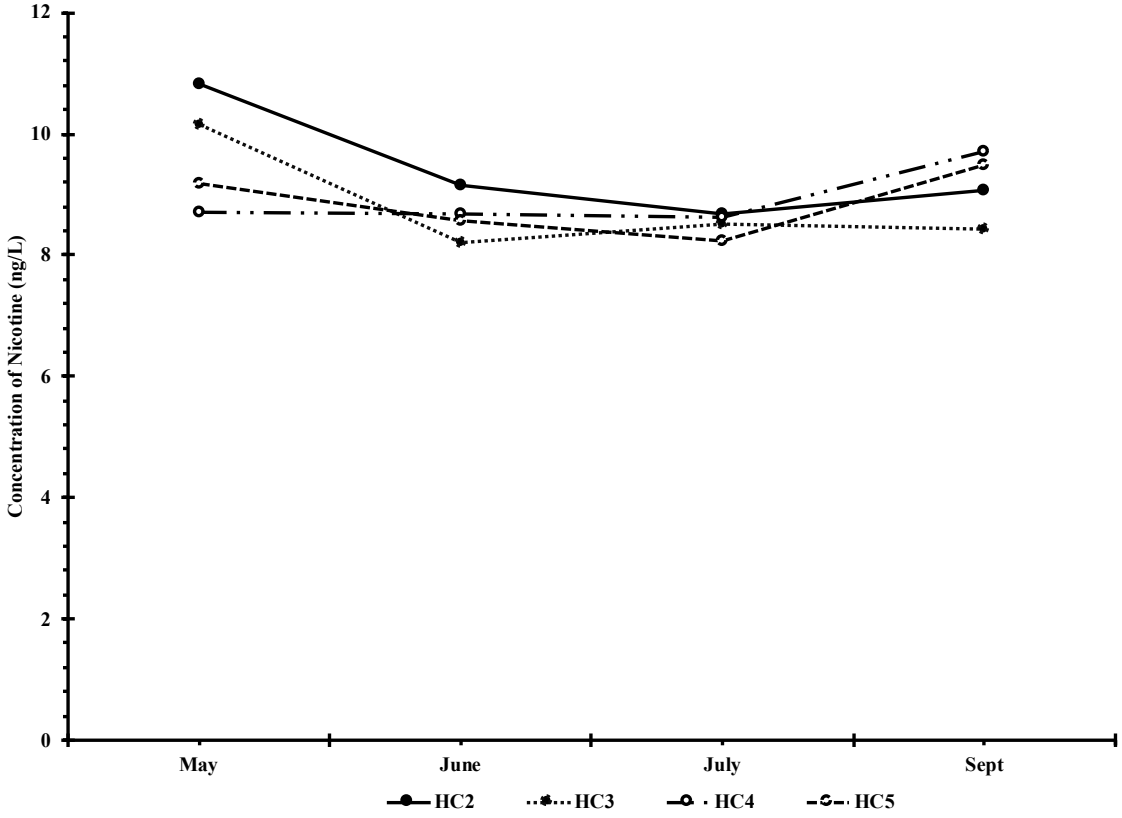

Figure 1.32: Concentration of the PPCP Nicotine in surface water samples at the downstream Hunting Creek locations over the course of the entire sampling season

1.6 Conclusion

PPCPs have been found in surface waters and fluvial sediments at several sites in the TWFPR. The presence and concentration of these PPCPs is due to a number of factors including, but not limited to, temporal variations, spatial distributions, flow rate, and weather conditions.

The major source of PPCPs to the TFWPR was found to be WTPs along with upstream inputs. The overall amount of PPCPs found at the most upstream site (CB1) was significantly lower than that which was found at the most downstream site (LP1).

This indicates that the WTPs are delivering a signifanct level of PPCPs into the TFWPR. In addition, data from sites upstream of the discharge zone showed several PPCPs not prominent in WTP effluent. This indicates that there are other, unknown sources of PPCPs to the environment.

Furthermore, PPCPs were found to drop out of the water column and partition into the sediment. While this may have been unexpected based solely on experimental constants and the organic carbon model of sorption, this is consistent with interactions of the mineral surfaces in the sediments with the PPCPs. Specifically, it was determined that the PPCPs that are positively charged and that have the most nitrogen bonding sites will follow this mineral sorption model.

The greatest concentrations of PPCPs were found near the WTP discharge zones, with the exception of Four Mile Run where the greatest concentration of PPCPs was found at the downstream site FMR3. While the specific reason for this is unknown at this time, is likely due to the nature of that sampling location as it is at a high-traffic marina where numerous other sources of PPCPs may be present.

Overall, the present study was able to establish that WTPs are a significant source of PPCPs to the TFWPR, the PPCPs are found in highest concentrations near the WTP, and that PPCPs follow a mineral sorption model when partitioning between the water and the sediment. These results are significant in that they have contributed to the understanding of the sources, emissions, and effects of PPCPs in surface waters, which is essential to managing public health and enlightening our society about the environmental implications of overprescribed drug therapy. Future steps in continuing this study will be

to expand the scope of the study to include more PPCPs and their metabolites and transformed products, obtain effluent from all WTPs in the area, and increasing the samples season for a more robust sample set.

CHAPTER 2: DISTRIBUTION AND FLUX OF PHARMACEUTICALS AND PERSONAL CARE PRODUCTS BETWEEN WATER AND SEDIMENT FROM THE HUNTING CREEK REGION OF THE TIDAL FRESHWATER POTOMAC RIVER

2.1 Introduction

Coastal sediments serve as a repository for organic micropollutants following discharge into the aquatic environment from land-based sources. Riverbed sediments may serve as sources or sinks for micropollutants in areas receiving high emission rates, such as sewer outfalls, storm drains, industrial discharges, and drainage ponds. Sediments can sequester micropollutants via sorption between the micropollutants in the water phase and the organic matter and mineral surfaces within the sediment. Because sorption is a reversible process, micropollutants may be sorbing or desorbing, depending on the conditions within the sediment micro-environment, which includes sediment pore-water, overlying water, and the sediment particles at the sediment-water interface. The role of source or sink may change spatially in a river environment, and have lead to important implications regarding chemical dispersal and toxicity.

Evaluation of sediment-water fluxes is critical to determining source or sink behavior of micropollutants. The most common approach used to determine sediment-water fluxes is by using a diffusion-based boundary layer model, which evaluates mass transfer coefficients (MTCs) between sediment pore-water and overlying water through a stagnant thin film at the interface.[120,121] A few studies have been conducted evaluating

this behavior in regard to the legacy micropollutants polychlorinated biphenyls (PCBs) and polycyclic aromatic hydrocarbons (PAHs).[122–127] However, much less is known regarding the sediment-water fluxes of PPCPs at the fluvial-estuarine boundary in coastal environments. As the sediment-water flux is critical to assessing the persistence and cycling of micropollutants in the aquatic environment, the present study sought to fill this gap and investigate the flux of PPCPs in the TFWPR.

The TFWPR has several unique attributes that make it ideal for a study on the flux of PPCPs between water and sediments. Tidal rivers at their fluvial-estuarine boundaries (i.e. the river Fall Line) represent the common nexus of large urban areas at this particular geographic location with the biodiversity of the freshwater estuarine ecosystem. The estuaries of tidal rivers are areas that experience the influence of both nature and humankind as the need for food, water, WTPs, urban, and agricultural products create stress on all coastal resources.[34]

The present investigation focused on the Cameron Run-Hunting Creek region (Alexandria, VA) of the TFWPR near a high-capacity WTP (Figure 2.1), which is one of the largest Potomac River WTPs discharging into a highly populated region of metropolitan Washington, DC. Additionally, the Hunting Creek location yielded access to the greatest number of sites along a downstream transect from a large WTP where surface water and sediment (along with corresponding pore-water) could be sampled by boat as part of an ongoing monitoring study.[128] Specifically of interest in this project was the flux of PPCPs in the surface water and sediment beds of the TFWPR. While there is not a significant abundance of heavy industry surrounding the TFWPR, the population

density is exceedingly large (>6 million inhabitants) with a high level of PPCP input derived through seven high-capacity WTPs. The combination of large population size, population density, and WTP discharge make the TFWPR a region of concern for the chemical fate and health risks related to PPCPs in the aquatic environment.

Pore-water is the free water naturally present in soils and sediments. Due to the nature of pore-water being in close contact with solid surfaces, it may exchange solutes quickly over a short time period; therefore, the concentrations in pore-water may change rapidly and, with those changes, bring about changes in what is absorbed in each compartment.[127,129–133] As such, pore-water plays a crucial role in determining whether sediments will be a sink or a source for PPCPs in the water column. While it was demonstrated (see Chapter 1) that the presence of PPCPs was prominent in both sediments and overlying water in the Hunting Creek region of the TFWPR, there has been no study to date detailing the direct flux of PPCPs from sediments to the overlying water. This study aims to enhance our understanding of the sediment-water fluxes of several PPCPs in the TFWPR as a function of distance from the WTP source.

2.2 Study Objective

The goal of this study was to evaluate sediment-water fluxes of PPCPs in sediments near a high capacity WTP in the Washington, DC region. Sediments were sampled along the transect beginning in a tributary of the Potomac River near the WTP discharge point and continuing downstream for 3.44 km into the mainstem Potomac River. A boundary layer model was used to describe the sediment-water interfacial

diffusion of PPCPs in flux estimates. Such a model was crucial in understanding whether or not sediments serve as a sink or source for PPCPs in this region. The primary objectives were to:

1. Quantify PPCP concentrations in water, sediment, and sediment pore-water;
2. Develop a boundary layer diffusion model for PPCPs;
3. Estimate sediment-water fluxes in terms of direction and magnitude; and
4. Compare the characteristics of PPCP fluxes along the transect.

2.3 Materials and Methods

2.3.1 Sampling Sites

Hunting Creek was chosen as the location for this study due to the extensively sampled sites found within this region as well as the WTP discharge zone. Hunting Creek begins in what is known as Cameron Run. The Cameron Run watershed is an approximately forty-two square mile watershed that drains into the TFWPR. This watershed is highly developed and includes several large communities, strip malls, commercial areas, and roadway systems.[134] The long term historical average flow for Cameron Run is 0.283 m^3/s.

Cameron Run becomes Upper Hunting Creek shortly before the Alexandria Renew discharge zone but maintains the same sewer shed demographics. The area after the WTP discharge zone is referred to as Lower Hunting Creek which eventually drains into the mainstem of the TFWPR. This portion of the study required a sample site in each

of the three zones: upper Hunting Creek, lower Hunting Creek, and mainstream TFWPR. These sites, referred to as HC1, HC2, and HC4, respectively, are shown in Figure 2.1. Each site has unique hydrology and sedimentology that can affect the flux of PPCPs between water and sediment. These three sites were chosen in order to be able to assess the change in the flux of PPCPs throughout the entire Hunting Creek region.

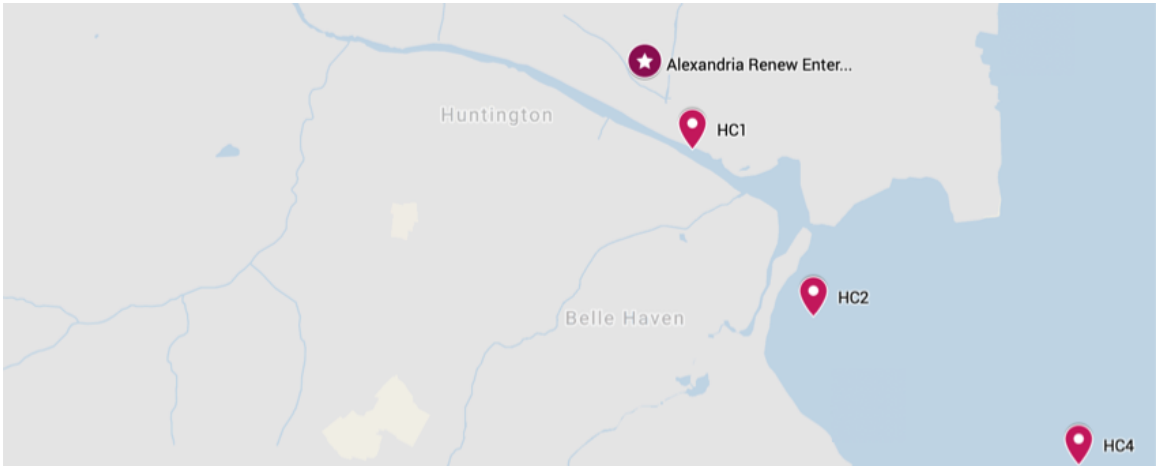

Figure 2.1: Map of the Upper and Lower Hunting Creek Region and the Drainage Point in the TFWPR.

The HC1 sampling sites was chosen as the primary site (surface water, sediments, and pore-water) for this project. This site was chosen due the accessibility of the site, the ability to collect both surface water and sediment, and the ability to collect the large quantities of sediment that were necessary to isolate pore-water. In addition, this site has previously proved to be a location where a significant amount of PPCPs have been found

in both surface waters and sediments due to its proximity to the WTP discharge zone, making it was an ideal location for this study.

The HC2 and HC4 sampling sites were chosen as secondary (surface water and sediments) locations for this study. The HC2 sampling location is in the Lower Hunting Creek region. This location was used to represent the entire Lower Hunting Creek region where the PPCPs have had the opportunity to undergo dilution and degradation but is not fully subjected to the flow of the mainstream TWFPR. The HC4 sampling site was chosen to represent the drainage of Hunting Creek in the mainstream of the TFWPR. This zone is largely influenced by the tidal cycles and the rate of flow of the water can greatly impact the presence and detection of PPCPs in the water column and sediment samples.

Pore-water was collected exclusively at the HC1 sampling location. This site was the only location that provided enough sediment to isolate the pore-water in the laboratory. While no pore-water was collected at HC2 or HC4, the information gained from the study at HC1 allowed for the determination of the PPCP fluxes at these locations.

2.3.2 Materials

Whatman® glass microfiber filters, GF/F and GF/D, sizes 47 mm and 150 mm, were used for water filtration for or small and large volume water samples, respectively, and were purchased from Sigma Aldrich (St. Louis, MO). Oasis MAX (**M**ixed-mode, strong **A**nion-e**X**change) and MCX (**M**ixed-mode, strong **C**ation-e**X**change) 6 cc Vac Cartridges (500 mg Sorbent per Cartridge, 60 um Particle Size) used in the extraction of

all water samples were purchased from Waters Corporation (Milford, MA). QuEChERS (Agilent Technologies, Santa Clara, CA) extraction and dispersive solid phase extraction (dSPE) salts and kits, used to process all sediment samples for LC-MS/MS analysis, were purchased from Agilent Technologies (Santa Clara, CA). Acetonitrile and formic acid, used to make the LC-MS/MS mobile phases, was purchased from Thermo Fisher Scientific (Waltham, MA). Other bulk solvents used for analysis and supply preparation included methanol, acetone, and ethyl acetate were purchased from Thermo Fisher Scientific (Waltham, MA). Milli-Q type-3 water (UPW), used to make an LC-MS/MS mobile phase and for cleaning purposes was made in house by a MilliQ Direct 18/6 system. LCMS liquid nitrogen and compressed argon and nitrogen gasses were purchased from Roberts Oxygen (Rockville, MD).

The PPCPs were purchased as isotopically labeled chemicals to make up the LC-MS/MS internal/surrogate (Table 1.3) and target (Table 1.4) analytes in the analytical standards. The chemicals were purchased initially to make up the three individual working mixes, which were then combined and diluted into acetonitrile for mixtures used as calibration standards.

All glassware used for sample and preparation were cleaned by washing with soap, rinsing with UPW and fired at 400°C overnight to ignite any interfering organic residues on surfaces that may interfere with quantitative analysis. All laboratory materials were made of glass, stainless steel, or Teflon to avoid sample contamination. The Teflon materials were cleaned the same way as glass, but without firing. All non-glass items were rinsed with methanol and air dried before use.

2.3.3 Field Sampling

River water samples were obtained as surface grabs onboard a skiff or on foot in shallow water using a submersible pump (12 V, Max Flow 8.7 L/min, Model No. 75509-55, Cole Parmer, Mt Vernon Hills, IL). Each water sample (~20 liters (L)) was collected in a vertically integrated fashion when the depth was greater than 2 meters (m) (an interval from 0.5 m below the surface to 0.5 m above the river bottom). The water was collected in 20-L sealed stainless-steel kegs and labeled for transportation to the Environmental Chemistry Laboratory at the Potomac Science Center (George Mason University). Upon return to the laboratory, the water samples were immediately filtered and stored for less than 24 – 48 hr in a refrigerator (10˚C) prior to analytical processing. At each sampling site two additional 1-L water samples were collected in polypropylene bottles using the same pump method for the analysis of total suspended matter (TSM) at each site. All sample containers were pre-rinsed three times with sample water prior to filling.

Riverbed sediments were obtained onboard a skiff or shoreline sampling coincident with water sampling when available fine-grained sediment was present (i.e., primarily silt-clay composition). Upstream sites were often rocky bottom and sediments were not obtained. The sediments were collected using a Petite Ponar grab sampler tethered by rope. The sediment obtained in the Ponar was taken aboard the boat or shore and expelled into a stainless-steel tray, while being careful not to disturb the sediment. Approximately 10 g of the top 2 – 4 cm surficial layer was removed and placed directly

into a pre-cleaned amber glass jar using a stainless-steel spoon. The jar was sealed using a Teflon-lined lid and stored on ice for transportation to the Environmental Chemistry Laboratory at the Potomac Science Center. The samples were stored in the freezer (-20˚C) until analytical processing.

A large quantity of sediment, enough to fill two stainless steel trays, was obtained in the same manner as traditional riverbed sediment sampling. This tray was taken back to the lab where the pore-water was isolated from the sediment.

2.3.4 Sample Processing

The 20-L river water samples were initially filtered through GF/D and GF/F glass fiber filters to isolate the suspended particles from water, which is summarized in Figure 1.7. The filtered water was aliquoted into 1-L glass jars for subsequent extraction. The filtered water was spiked with 50 – 100 ng each of the internal and surrogate standards (Table 1.3) prior to extraction.

The PPCPs were extracted from the filtered water samples via a solid phase extraction (SPE) technique using Oasis MAX and MCX SPE cartridges. The cartridges were loaded onto a Supelco vacuum manifold (Sigma Aldrich, St. Louis, MO). The MCX cartridges were connected directly to the manifold. The MAX cartridges were stacked on top of the MCX cartridges via a SPE Tube Adapter (Sigma Aldrich, St. Louis, MO). The vacuum manifold was rinsed with methanol prior to the loading of the cartridges. The Oasis MAX and MCX cartridges were conditioned twice with 5 mL of 70:30 (volume/volume – v/v) methanol (MeOH):ethyl acetate (EtOAC), 5 mL of MeOH, and 5

mL of UPW. The filtered samples were then loaded onto the cartridges using large volume sample tubing at a rate of 2 – 3 drops per second. Upon the conclusion of the extraction, the cartridges were washed twice with 95:5 (v/v) UPW:MeOH. The cartridges were dried on the manifold for 30 minutes prior to elution. Following the drying step, the cartridges were eluted into 40 mL amber vials. The MAX cartridges were eluted with 6 mL of 69:29:2 (v/v/v) MeOH:EtOAC:Formic Acid. The MCX cartridges were eluted with 6 mL of 67.5:27.5:5 (v/v/v) MeOH:EtOAC:Ammonium Hydroxide. The SPE extracts are reduced in volume to approximately 0.5 mL using a TurboVap (Zymark Corp., Hopkinton, MA) evaporator (employing dry N_2 gas), transferred to 1.5 mL amber glass LC-MS/MS vials, and stored in a -20°C freezer prior to quantitative analysis.

The sediment samples were initially pre-sieved through a 500-µm stainless steel mesh into a 50-mL centrifuge tube. The tubes were placed in the centrifuge at 2200 rpm for 10 minutes to collect the solids. Once removed from the centrifuge, any supernatant water was discarded. Each sample was sub-sampled for LC-MS/MS, % moisture (%M), particle size analysis (PSA), and total organic carbon (TOC) analysis.

In LC-MS/MS analysis, the sediment samples (precisely weighted to 2 g) were spiked with internal and surrogate standards and the samples were extracted via the QuEChERS (**Q**uick-**E**asy-**Ch**eap-**E**ffective-**R**ugged-**S**afe) method[44–47] as summarized in Figure 1.7. The 2 g of sediment were transferred to a 50-mL centrifuge tube and 10 mL of Optima grade acetonitrile was added to each tube. Each sample was then spiked with 50 – 100 ng each of the internal and surrogate standards (Table 1.3). The tubes were vortexed for 10 minutes. After vortexing each sample, 10 mL of UPW was added to

every sample. The samples were vortexed again for 1 min. QuEChERS packets containing 6 g of anhydrous magnesium sulfate and 1.5 g of sodium acetate were added to each sample. This step created a phase separation between the water and acetonitrile and forced the PPCPs to partition into the organic phase. The tubes were centrifuged for 10 min at 2200 rpm. An 8-10 mL aliquot of the organic phased was then transferred via glass pipette to a 15-mL dSPE tube containing 1.2 g of magnesium sulfate and 0.4 g of primary-secondary amine, removing any interfering matrix components. The tubes were vortexed and centrifuged for 10 min at 220 rpm. The supernatant of each sample was transferred to a clean 40-mL amber glass vial using a glass pipette. The SPE extracts were reduced in volume to approximately 0.5 mL using a TurboVap (Zymark Corp., Hopkinton, MA) evaporator (employing dry N_2 gas) and transferred to 1.5 mL amber glass LCMS vials. The extracts were stored in a -20°C freezer prior to quantitative analysis.

All samples were analyzed in triplicate. The water and sediment processes are depicted in the flow diagram in Figure 1.7. In addition, grain size and TOC were also analyzed in all sediment samples using a Beckman-Coulter (Brea, CA) laser diffraction (LS 13320) particle size analyzer and a Carlo Erba Model 1112 Flash Elemental Analyzer (Egelsbach, Germany), respectively.

Pore-water was isolated from sediment using aliquot centrifugation. In this procedure, individual 50-mL centrifuge tubes were filled to the 40 mL mark with wet sediment. The tubes were centrifuged at 2200 rpm for 10 minutes. Upon removal from the centrifuge, the supernatant water, in this instance, the pore-water, was poured off into

a 1-L glass bottle. Approximately 5 – 15 mL of pore-water was isolated from each 40 mL portion of wet sediment. The centrifugation step was repeated approximately 250 times to draw off a sufficient quantity of pore-water for chemical analysis. After approximately 1000 mL of pore-water was obtained through centrifugation, the supernatant was filtered through stacked, pre-weighed glass fiber GF/D and GF/F glass fiber filters to isolate the suspended particles from water in a Millipore filtration apparatus. The water samples were passed through the filters under an applied vacuum. At this point, the pore-water samples were processed in the same way as the surface water samples.

2.3.5 LC-MS/MS Analysis

The PPCPs in the water and sediment extracts were analyzed for the compounds of interest using a Shimadzu Model 8050 liquid chromatograph triple-quadrupole mass spectrometer (LC-MS/MS) configured with a SIL-20ACXR autosampler (Columbia, MD). The LC-MS/MS interface was operated in electrospray ionization (ESI) mode in the presence of a Corona needle (DUIS) for both positive and negative ionization. LC-MS/MS separation of the PPCPs was performed using a 50 mm x 2.1 mm (id), 1.8 μm (particle diameter) Forced Biphenyl reversed-phase UHPLC column (Restek, Bellefonte, PA) in conjunction with a raptor Biphenyl guard column, with a binary mobile phase consisting of Type I Milli-Q water (solvent A), and acetonitrile (solvent B), both containing 0.1% formic acid as a phase modifier. Operating conditions for the LC-MS/MS are listed in Table 2.1. The gradient elution program allowed for a total run time of approximately 10 min. The retention times for the PPCPs are in Table 4.2A.

Table 2.1: LC-MS/MS Instrument Parameters

Parameters	Operating Conditions
Total Flow Rate	0.40 mL/min
Gradient Elution Program	10% B at 0 min
	50% to 95% B 0-6 min
	100% B 6-7 min
	100% to 30% B 7-9 min
	10% B 9-10 min
Nebulizing Gas Flow	2 L/min
Heating Gas Flow	10 L/min
Drying Gas Flow	10 L/min
Oven Temperature	40°C
Interface Temperature	300°C

The LC-MS/MS quantitation of the PPCPs was accomplished in the multiple reaction monitoring (MRM) mode. Three MRM ions were established for each PPCP (with the exception cis-tramadol which only had one MRM) through automated MRM optimization procedures following manual precursor ion identification using the full scan mode. The quantifier (primary) and qualifier (secondary and tertiary) product ions and the various quadrupole voltages for the PPCPs are listed Table 4.3A. Quantitation was performed using the internal standardization method with isotopically labelled internal standards (^{2}H or ^{13}C analogues as shown in Table 1.3 – Chapter 1) that were added prior to the extraction step. Quantitation was completed using a ten-point calibration curve based on the primary product MRM ion abundance for each PPCP relative to that of an associated internal standard. The retention times and qualifier MRM ions relative

abundances were used to confirm the chemical identity of the PPCP. Data analysis and quantitation was performed using LabSolutions software (ver. 5.91).

2.3.6 Quality Assurance

Surrogate Spike recoveries are summarized in Figure 2.2, Figure 2.3, and Figure 2.4. All water and sediment samples were spiked with surrogate standards prior to the individual extraction processes. This allowed for the determination of the method performance of PPCP analysis with respect to individual samples. The surrogates consisted of isotopically labeled homologues of compounds that were being targeted for analysis. Out of eight total surrogate standards, five (surface water) and six (sediment) exceed 70% recovery, indicating high performance..

The reported concentrations of targeted chemicals were not corrected for surrogate recoveries. The high surrogate recoveries found in the pore-water samples, is an indication of the complex matrix found in these samples.

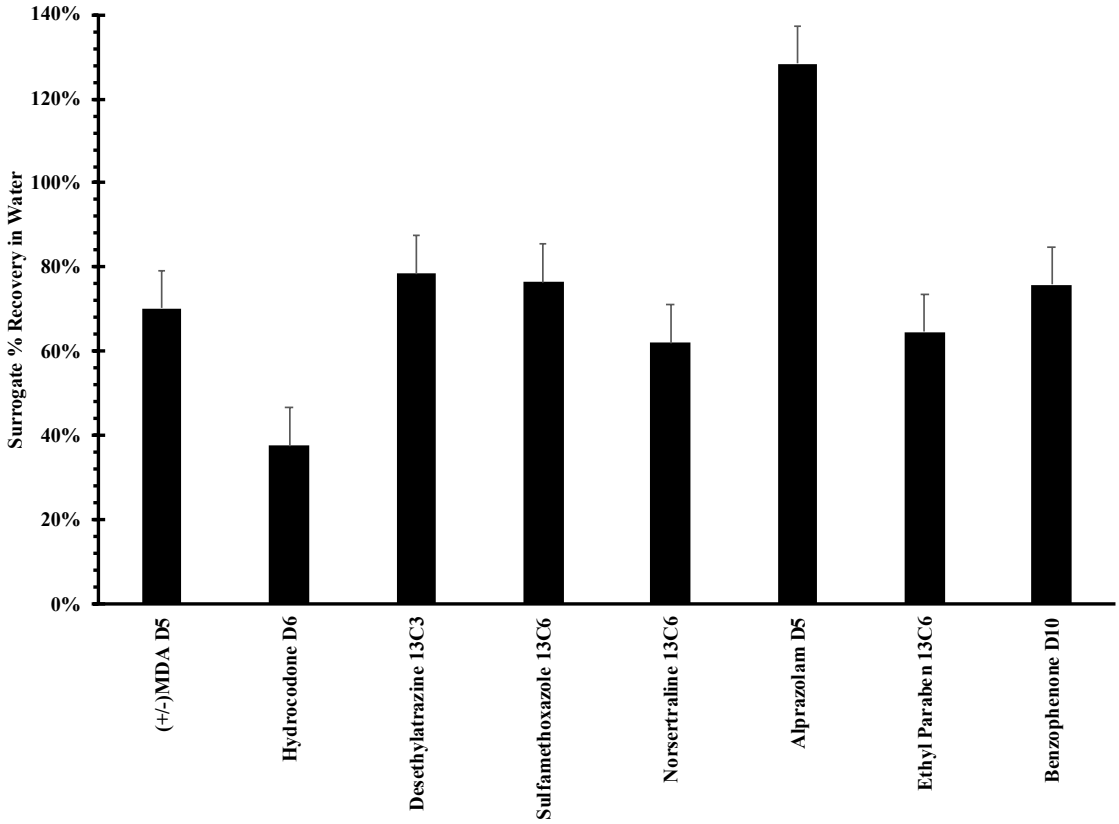

Figure 2.2: Mean Surrogate %recoveries evaluated in for all the Potomac River surface water samples. Black columns represent the mean recovery and bars represent ± 1 SD.

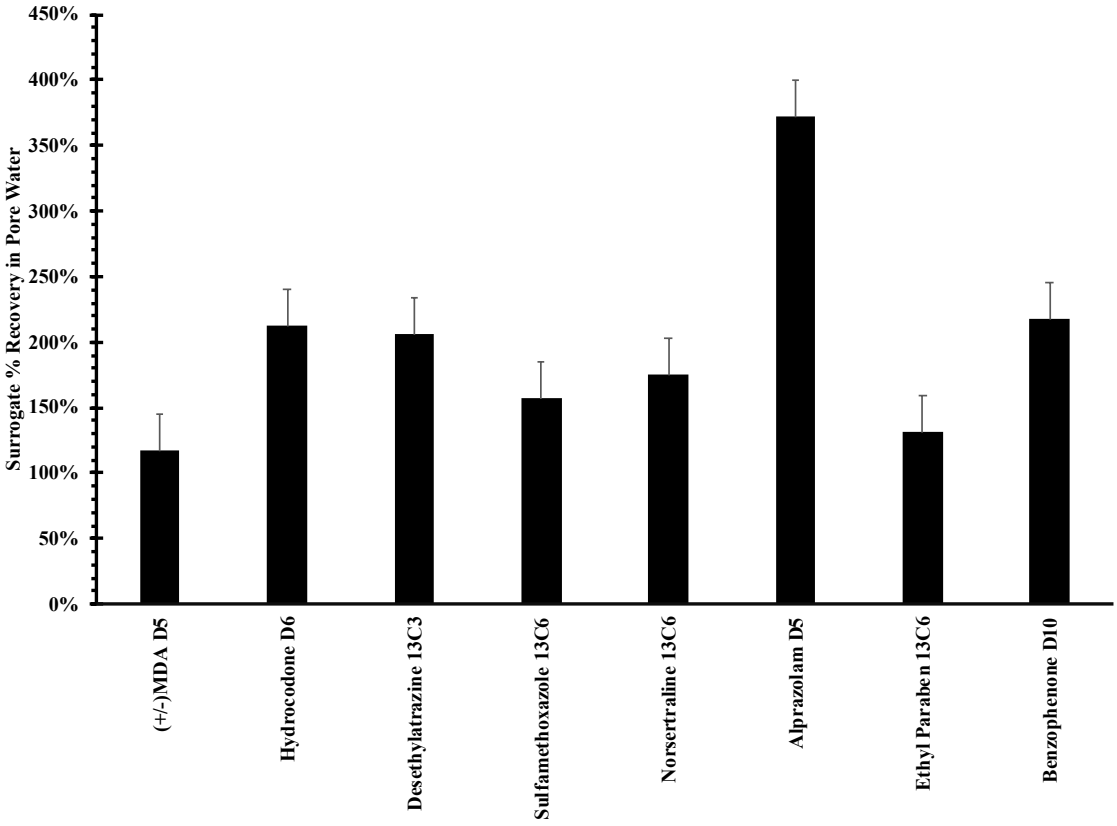

Figure 2.3: Mean Surrogate %recoveries evaluated in for all the Potomac River pore-water samples. Black columns represent the mean recovery and bars represent ± 1 SD.

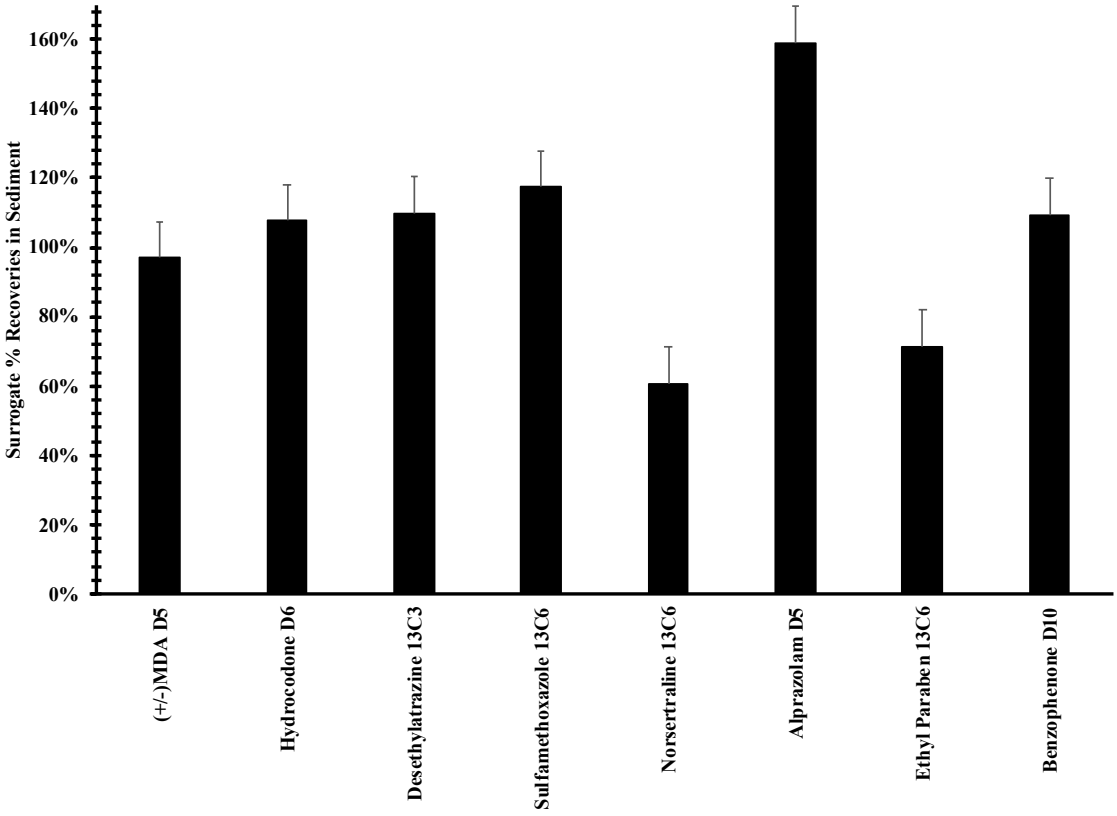

Figure 2.4: Mean Surrogate %recoveries evaluated in for all the Potomac River sediment samples. Black columns represent the mean recovery and bars represent ± 1 SD.

Laboratory blanks were run for both water and sediment samples. In both cases, the blanks were processed in such a way that they were exposed to all reagents and containers that a normal sample would be in contact with over the entire course of sample processing. Only two of the 91 targeted chemicals were found in lab blanks at concentrations above the QL. Nicotine was found in several water lab blanks at an average concentration of 4.4 ng/L. DEET was found in several sediment lab blanks at an average of 4.7 ng/g. This value is very low in comparison to the concentration found in actual samples. The QL for all PPCPs ranged from 0.053 ng/L to 32 ng/L.

Field blanks were run for water samples. A 20-L can of UPW was taken out into the field, run through the pump, and pumped back into the can prior to sampling at the first location of each trip. The blanks were processed in such a way that they were also exposed to all reagents and containers that a normal sample would be in contact with over the entire course of sample processing. Only seven of the 91 targeted chemicals were found in lab blanks, at concentrations above the QL. Of those seven chemicals, only caffeine and DEET were detected in more than 14% of all field blank samples with caffeine and DEET being detected in 100% and 96% of field blanks, respectively. The other compounds detected were Nicotine (14%), Sulfamethoxazole (4%), Sulfaquinoxaline (4%), Fexofenadine (12%), and Carbamazepine (10%). Caffeine and DEET were found in several field blanks at an average concentration of 28.494 ng/L and 32.964 ng/L, respectively.

Matrix spikes included all targeted chemicals in water and sediment samples and were used as an evaluation of the performance of the method overall. They were performed by spiking every approximately 1-L of water and approximately 2 g of wet sediment with 80 ng of each target chemical. The matrix spike recoveries ranged from to 4.5% to 607% in surface water with an average of 70%. There were percent recoveries of 0% for metformin, azithromycin, gabapentin, 2-hydroxy-ibuprofen, hydromorphone, penicillin G, (±)-methamphetamine, codeine, ciprofloxacin, phentermine, naproxen, budesonide, triclocarban, lisinopril, and, tetracycline, and perfluorooctanoic Acid. The matrix spike recoveries ranged from to 0.08% to 227% in sediment with an average of 71%. There were percent recoveries of 0% for atorvastatin, lisinopril, and tetracycline.

The results of all matrix spike recoveries are reported in Table 4.6A and Table 4.7A. Due to the limited amount of pore-water isolated for analysis, it was not possible to perform an analysis with matrix spikes on pore-water samples.

The surface water and sediment samples were prepared and analyzed in triplicate. The pore-water sample was run in duplicate due to the limited amount of pore-water available for analysis. For each triplicate, the %RSD was calculated whenever a PPCP was detected. The %RSD for detected PPCPs ranged from 4.4% to 76% (30% overall mean) for water and 2.3% to 134% (42% overall mean) for sediment. The %RSD are listed in full in Table 4.4A and Table 4.5A.

2.3.7 Ancillary Measurements

Ancillary measurements were conducted on bed sediment to determine total organic carbon (TOC), %moisture (%M), and particle size analysis (PSA). TOC content was performed by Drexel University, using a Carlo Erba Model 1112 Flash Elemental Analyzer. Approximately 1 g of sediment from each sampling location and trip was dried in an oven at approximately 60˚C overnight, and then ground to a fine powder using a mortar and pestle. The samples were placed in a ceramic crucible and fumigated with concentrated HCl for 24 hours to degas carbon dioxide derived from inorganic carbon (primarily as carbonates) following the method of Ramnarine.[48] The treated sediment was re-dried at 60˚C oven for one week to ensure that no excess HCl was present. The sample was placed into a tin boat, weighed, and combusted at 1000˚C for total C and N content.

Sediment moisture was determined by measuring out approximately 1 – 2 g of wet sediment into a tared aluminum boat and measuring mass. The aluminum was placed in an oven at 60°C for 48 – 72 hr. The mass of the sample was recorded again after the drying period. The moisture content was evaluated by determining the loss of mass after drying as described in Equation 1.2 (Chapter 1). The moisture content was used to correct and convert wet weight of the sediment samples to dry weight. The dry weight of all sediment samples was used when expressing PPCP sediment concentrations.

Sediment grain size, in terms of percent sand, silt and clay content, for all the collected riverbed sediments was determined using a Beckman-Coulter laser diffraction (LS 13320) particle size analyzer in the GMU Coastal Geology Lab at the Potomac Science Center. Sediment initially was passed through a 0.5-mm stainless-steel sieve to remove large particles followed by disaggregation 5% aqueous hexametaphosphate prior to analysis. Grain size results were provided by the Excel program GRADISTAT for ternary diagrams.

2.3.8 Boundary Layer Model and Flux Calculations

Sediment-water fluxes were evaluated using a simple bottleneck boundary layer model.[121] The benthic boundary layer (BBL) consists of the thin stagnant layer of water at the sediment-water interface formed by the lack of mixing.[135] The BBL is an important zone as it represents a diffusion-limited boundary layer between the water column and sediment bed.[129] Figure 2.5 describes the BBL along with other depositional and

resuspension processes. Of particular importance to the BBL is the pore-water that is present in the sediments.

The three main mechanisms of interest are sorption between the sediment and water, diffusion facilitated by dissolved organic carbon (DOC) across the sediment-water interface, and bioturbation. Sorption between sediment and water is a chemical process that controls the distribution of chemicals between these two compartments. Due to a variety of complex properties, both chemical and physical, some PPCPs have a stronger affinity to the solid phase while others prefer to remain dissolved in the surrounding water column. This process is described by K_L, the mass transport coefficient of the freely dissolved PPCPs.

In addition to freely dissolved PPCPs, PPCPs can interact with the DOC found in the sediment. During the course of this interaction, the PPCPs may become bound to the DOC and move with the DOC across the sediment-water interface. This process is described by $K_{L\ DOC}$, the mass transfer coefficient of the DOC-bound PPCPs.

The final mechanism for consideration is the transport of PPCPs across the sediment-water interface via bioturbation. Bioturbation refers to the mixing of sediments by living creatures that reside in the sediment. Some creatures may move sediment from the surface to the bottom of the active layer while others may reverse that process. This process is described by K_{BIO}, the bioturbation mass transfer coefficient.

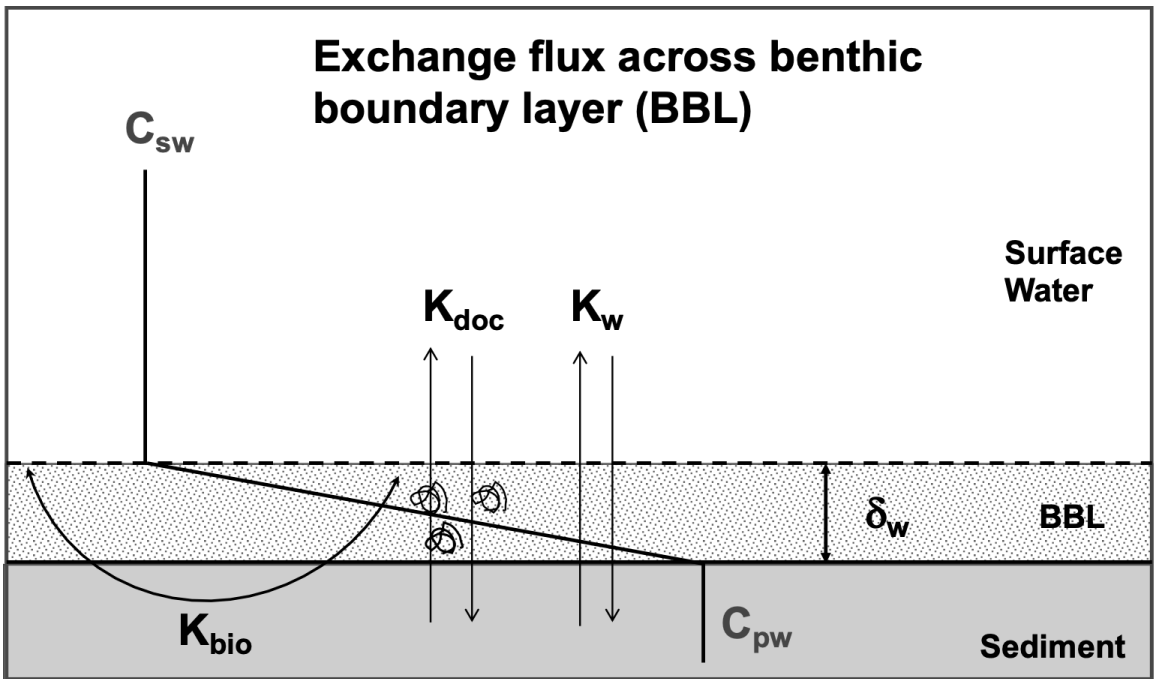

Figure 2.5: Processes governing the deposition and burial of PPCPs in sediments. The BBL is depicted in the diffusive flux process at the sediment-water interface and is bidirectional. Deposition and resuspension represent bulk one-way processes.

PPCP sediment-water flux was evaluated through Equation 2.1[126,136],

Equation 2.1: Flux of PPCPs

$$F = K_{L_{Total}}\left(C_{PW_{Corrected}} - C_{SW}\right)$$

where F is flux (ng/m^2-s), K_{Ltotal} is the overall mass transport coefficient, $C_{PWcorrected}$ is the concentration of PPCP found in pore-water corrected for any sorption to pore-water DOC, and C_{SW} is the concentration of the PPCP found in surface water above the sediment and diffusion boundary layer. C_{sw} is assumed to be constant from turbulent mixing in the water column, which is only 1 meter or less in depth in Hunting Creek.

The C_{PW} correction was performed using the water-DOC fractional distribution constant (α_w) as illustrated in Equation 2.2.[126,136].

Equation 2.2: Pore-water concentration corrected for DOC

$$C_{PW_{Corrected}} = \alpha_W \times C_{PW}$$

The C_{PW} term refers to the measured concentrations of PPCPs in this study. The fractional distribution constant (α_w) represents the mass fraction of PPCP associated with the dissolved phase of pore-water and was estimated according to Equation 2.3,[126]

Equation 2.3: DOC correction factor for Pore-water concentrations

$$\alpha_W = \frac{1}{\left(1 + (K_{DOC} \times [DOC])\right)}$$

where K_{DOC} and [DOC] have units of L/kg and kg/L, respectively.

[DOC] is the concentration of dissolved organic carbon (kg/L) in the aqueous phase of the sample and was estimated in this study. This parameter can be measured if appropriate instrumentation is available. However, when unavailable, as was the case in this project, the [DOC] can be estimated from the measured sediment %TOC values. Previous research has demonstrated that the DOC constitutes approximately 90% of the TOC found in all sediment samples in bodies of water similar to rivers and estuaries.[137–140] Therefore, sediment %TOC values were converted to pore-water DOC values by

multiplying the TOC values by 0.9 (i.e. $[DOC]_{pore\text{-}water}$ (mg/L) = 0.90 x $\%TOC_{sediment}$). K_{DOC}, the DOC-water partition coefficient, was approximated by Equation 2.4.

Equation 2.4: DOC-water partition coefficient

$$K_{DOC} = 0.41 \times K_{OW}$$

The K_{ow} values for each PPCP were obtained through ChemSpider, which is based on the US EPA EPIsuite database.[141] The log K_{ow} values for each PPCP targeted in this analysis are compiled in Table 4.1A.

K_{LTotal} is the sediment-water mass transport coefficient. It is the reciprocal sum of the three individual mass transport coefficients and takes into account independent molecular diffusional processes that influence transport across the BBL. The molecular diffusion of PPCPs occurs through the BBL via dissolved phase (K_L), sorbed to DOC (K_{LDOC}), and bioturbation (K_{BIO}) mechanisms. It is given by Equation 2.5.[126]

Equation 2.5: The sediment to water mass transfer coefficient

$$1/K_{L_{Total}} = 1/K_L + 1/\left(K_{L_{DOC}} \times K_{DOC} \times [DOC]\right) + \frac{K_D}{\lambda}$$

K_L, the mass transport coefficient of the freely dissolved PPCPs, was derived by Equation 2.6.[126]

Equation 2.6: The mass transport coefficient of freely dissolved PPCPs

$$K_L = \frac{D}{\delta_0}$$

The D term represents the aqueous phased molecular diffusion coefficient and was estimated from Equation 2.7.

Equation 2.7: The Diffusion Coefficient

$$D = \frac{1.326 \times 10^4 \eta^{1.14}}{V^{0.589}}$$

The BBL thickness, δ_o, was an applied constant (0.06 cm) in this study, This estimation is based on previous reports that have found δ_o to be consistently be in the range of 0.02 – 0.12 cm, with the median value of 0.06 cm.[136,142,143] This estimation was used for all PPCPs in this project as it was not possible to asses δ_o experimentally

The viscosity of water, η, can either be measured directly in the experiment, or, as is the case for this project, can be found in the literature.[141] The molar volumes, V, is unique to each PPCP and was determined according to Equation 2.8.

Equation 2.8: Molar Volume

$$V = \frac{Molar\ Mass}{Density}$$

The molar mass and density are were derived from the literature.[141]

$K_{L\,DOC}$, the mass transfer coefficient of the DOC-bound PPCPs, is given by Equation 2.9.

Equation 2.9: The mass transfer coefficient of the DOC-bound PPCPs

$$K_{L_{DOC}} = 0.02K_L$$

This relationship between $K_{L\,DOC}$ and K_L is based on previously conducted experiments and has been documented in the literature.[126,136]

K_D, the sediment-water distribution constant, is given by Equation 2.10.[126]

Equation 2.10: The sediment to water partition coefficient

$$K_D = \frac{C_{SED}}{C_{PW_{Corrected}}}$$

The C_{SED} term in Equation 2.10 refers to the measured concentrations of PPCPs in this study.

For the bioturbation mass transport component in Equation 2.5, the factor λ is based on bioturbation depth (h), sediment density (ρ_b), and an average biodiffusion coefficient (D_b). The relationship between these values and the factor is given in Equation 2.11.

Equation 2.11: The bioturbation factor

$$\lambda = \frac{h}{D_b \rho_b}$$

The factor, estimated to be approximately 11060 days liter per meter kilogram based on typical values for h, ρ_b, and D_b, and was based on previous experimentally derived constants documented in the literature.[126,136,144] This estimation was used for this portion of the project. The K_D/λ ratio in Equation 2.5 is regarded as K_{BIO}.

As previously stated, the majority of research concerning fluxes of micropollutants in the water-sediment interface has been conducted on PAHs, PCBs, and similar compounds. The estimation of constants and assumptions used for this study were based off of PAH and PCB data. However, PPCPs are quite similar to these compounds, with comparable molar masses, which are prominent factors in diffusion constants. Therefore, it was determined that those estimations to remain valid.

In addition, pore-water was not obtained from sites HC2 and HC4. Instead the C_{pw} was calculated via Equation 2.12, where C_{sed} was taken directly from the measured concentrations of PPCPs in this study and K_D was calculated using the pore-water data from the site HC1.

Equation 2.12: Pore-water concentrations for HC2 and HC4 where pore-water was not able to be isolated.

$$C_{pw} = \frac{C_{sed}}{K_d}$$

In all cases, the sign (+ or -) of the flux indicates the direction of the PPCPs. If the flux is positive (+) this indicates that concentration of PPCPs is greater in the pore-water than in the surface water and the sediments are serving as a source for the PPCPs from the sediment to the water column. If the flux is negative (-) this indicates that concentration of PPCPs is smaller in the pore-water than in the surface water and the sediments are serving as a sink for the PPCPs from the water column to the sediment.

2.4 Results

2.4.1 Ancillary Data

The TOC analysis was performed in triplicate on the sediment collected for flux measurements in this portion of the project. The %TOC and %TON results are summarized in Table 2.2. TOC varied minimally across all three sites, ranging from 1.01 – 1.66 %TOC with a median value of 1.31 %TOC. TON varied minimally across all three sites, ranging from 0.09 – 1.67 %TON with a median value of 0.12 %TON. There was no statistical difference in TOC or TON among all the sites (Kruskal-Wallis, $p>0.05$).

Table 2.2: % TOC and %TON of HC1, HC2, and HC4 Sediment Samples

Sampling Location	%TOC	%TON
HC1	1.01	0.09
	1.10	0.09
	1.16	0.08
HC2	1.58	0.12
	1.20	0.09
	1.44	0.13
	1.31	0.12
HC4	1.65	0.17
	1.07	0.08
	1.45	0.14
	1.66	0.15

The sediment % moisture, % sand, % silt, and % clay results are summarized in Table 2.3. The % moisture, % sand, % silt, and % clay varied minimally across all three sites. There was no statistical difference in % moisture, % sand, % silt, and % clay among all the sites (Kruskal-Wallis, $p>0.05$).

Table 2.3: Moisture, % Sand, % Silt, and % Clay for HC1, HC2, and HC4 Sediment Samples

Sampling Locaiton	% Moisture	% Sand	% Silt	% Clay
HC1	38.14%	55.69%	39.04%	5.27%
HC2	51.91%	22.98%	67.15%	9.90%
HC4	54.41%	27.20%	62.55%	10.25%

2.4.2 PPCPs in Surface Water, Pore-water, and Sediment

The individual PPCP concentrations in surface water, pore-water and sediment at site HC1, HC2, and HC3 are shown below (Figure 2.6, Figure 2.7, and Figure 2.8). Only those PPCPs that were found in both surface water and pore-water are depicted in these figures because fluxes could only be evaluated if PPCPs were present in both of these environmental sub-compartments. The values of all measured concentrations for HC1 (sediments, pore-water, and surface water), HC2, and HC4 (sediments and surface waters) are reported in Table 4.12A.

The concentrations of PPCPs in surface water ranged from 0.14 – 124 ng/L for HC1, 0.18 – 15.1 ng/L for HC2, and 0.62 – 3.8 ng/L for HC4. The median values were

10.1, 3.7, and 0.95 ng/L for sites HC1, HC2, and HC4, respectively. Caffeine (124 ng/L) was the PPCP found at the highest concentration in surface water at HC1 but was not present in surface waters at HC2 or HC4. The PPCP found at the lowest concentration in surface waters at HC1 and HC2, dextromethorphan (0.14 and 0.18 ng/L, respectively), was not found at HC4. Desvenlafaxine was the PPCP found in highest concentration at HC2 (44.2 ng/L) and second highest at HC1 (113 ng/L) but was not present in surface waters at HC4. Metformin (3.1 ng/L) was the PPCP found at the highest concentration in surface waters at HC4 and in similar concentrations at HC1 and HC2.

The concentrations of PPCPs in pore-water ranged from 2.3 – 522 ng/L for HC1, 0.01 – 4642 ng/L for HC2, and 0.04 – 1724 ng/L for HC4. The median values were 45.4, 211, and 6.9 ng/L for sites HC1, HC2, and HC4, respectively. Desvenlafaxine (522 ng/L) was the PPCP found in highest concentration at HC1 but was found at much smaller concentrations in pore-water at HC2 (12.0 ng/L) and HC4 (1.9 ng/L). The PPCP found at the lowest concentration in pore-waters at HC1 and HC4, diphenhydramine (2.3 ng/L and 0.04 ng/L, respectively), was not found at HC2. Metformin was the PPCP found in highest concentration in pore-water at HC2 (4642 ng/L) and HC4 (1724 ng/L). The PPCP found at the lowest concentration in pore-water at HC2, dextromethorphan (0.014 ng/L), was not found at HC4.

The concentrations of PPCPs in sediments ranged from 0.2 – 79.2 ng/g for HC1, 0.32 – 127 ng/g for HC2, and 0.33 – 14.8 ng/g for HC4. The median values were 3.1, 6.3, and 0.89 ng/g for sites HC1, HC2, and HC4, respectively. The PPCP found at the highest concentrations in sediment at HC1 and HC4, diphenhydramine (79.2 ng/g and 14.8 ng/g,

respectively), was not found at HC2. Dextromethorphan, the PPCP found in highest concentration in sediments at HC2 (127 ng/g) was found at much smaller concentrations at HC1 (2.4 ng/g) and not at all at HC4. The PPCP found at the lowest concentration in pore-waters at HC1 and HC4, diphenhydramine (2.3 ng/L and 0.04 ng/L, respectively), was not found at HC2. Metformin was the PPCP found in highest concentration in pore-water at HC2 (4642 ng/L) and HC4 (1724 ng/L). The PPCP found at the lowest concentration in sediments at HC1, bupropion (0.20 ng/g), was found at similar concentrations at HC2 (0.89 ng/g) and not found at all at HC4. The PPCP found at the lowest concentration in sediments at HC2, tramadol (0.32 ng/g), was found at similar concentrations at HC4 (0.72 ng/g) and not found at all at HC4 and at higher concentrations HC1 (10.0ng/g). Triamterene, the PPCP found at lowest concentration at HC4 (0.33 ng/g), was found in similar concentrations at HC1 (0.72 ng/g) and higher concentrations at HC2 (9.9 ng/g).

The majority of PPCPs were found to have concentrations higher in the pore-water than in the surface waters. In addition, the change in concentrations for different PPCPs in surface waters and sediments down the transect is consistent with what was reported in Chapter 1.

At the HC1 sampling location, the concentration of PPCPs was greater in pore-water samples compared to the concentration in surface water samples for the majority of PPCPs detected.

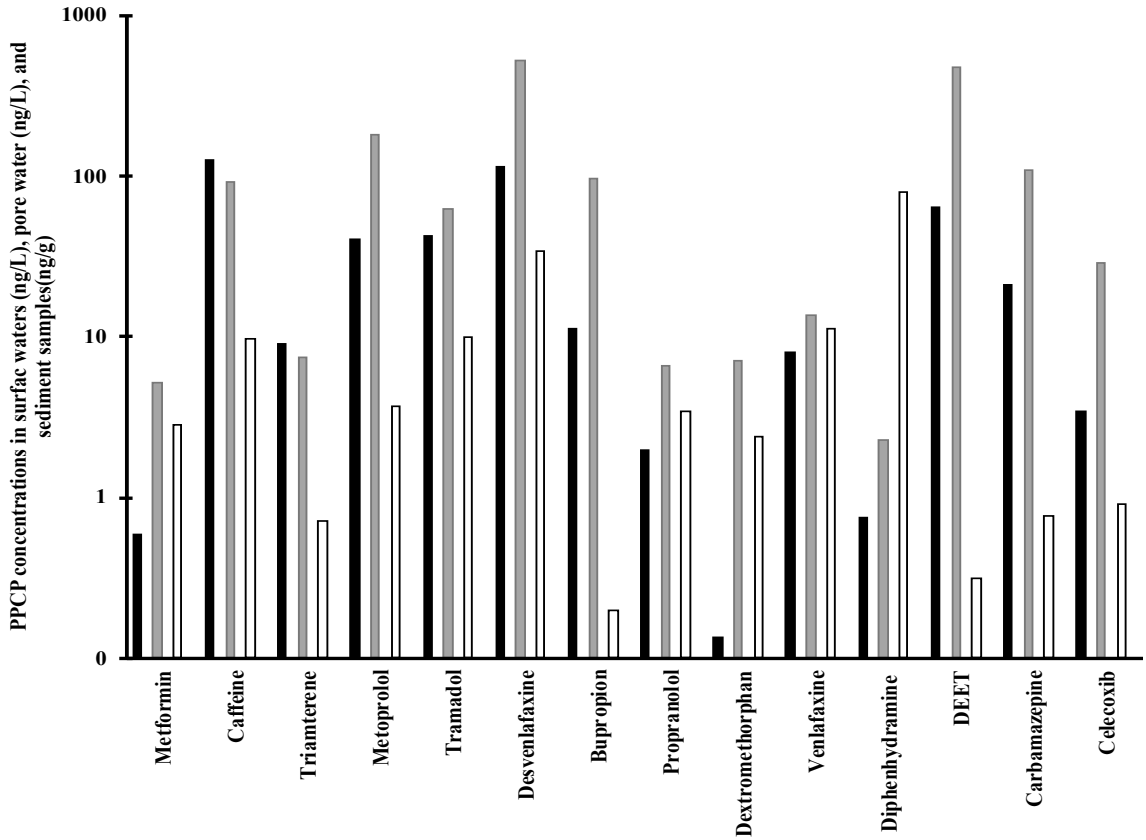

Figure 2.6: PPCPs concentrations in surface water, pore-water, and sediment samples at HC1 sampling location. Black bars, gray bars, and white bars represent surface water, pore-water, and sediment concentrations, respectively. In some instances, the PPCP listed was not found in sediment and, as such, no white bar is present. The y-axis was transformed to a log scale in order to be able to view all values on a simple graph.

At the HC2 sampling location, there was a mix of concentration differences for the PPCPs detected. Approximately 60% of PPCPs detected were found at higher concentrations in the pore-water compared to the surface water. The remaining 40% were found at higher concentrations in the surface water.

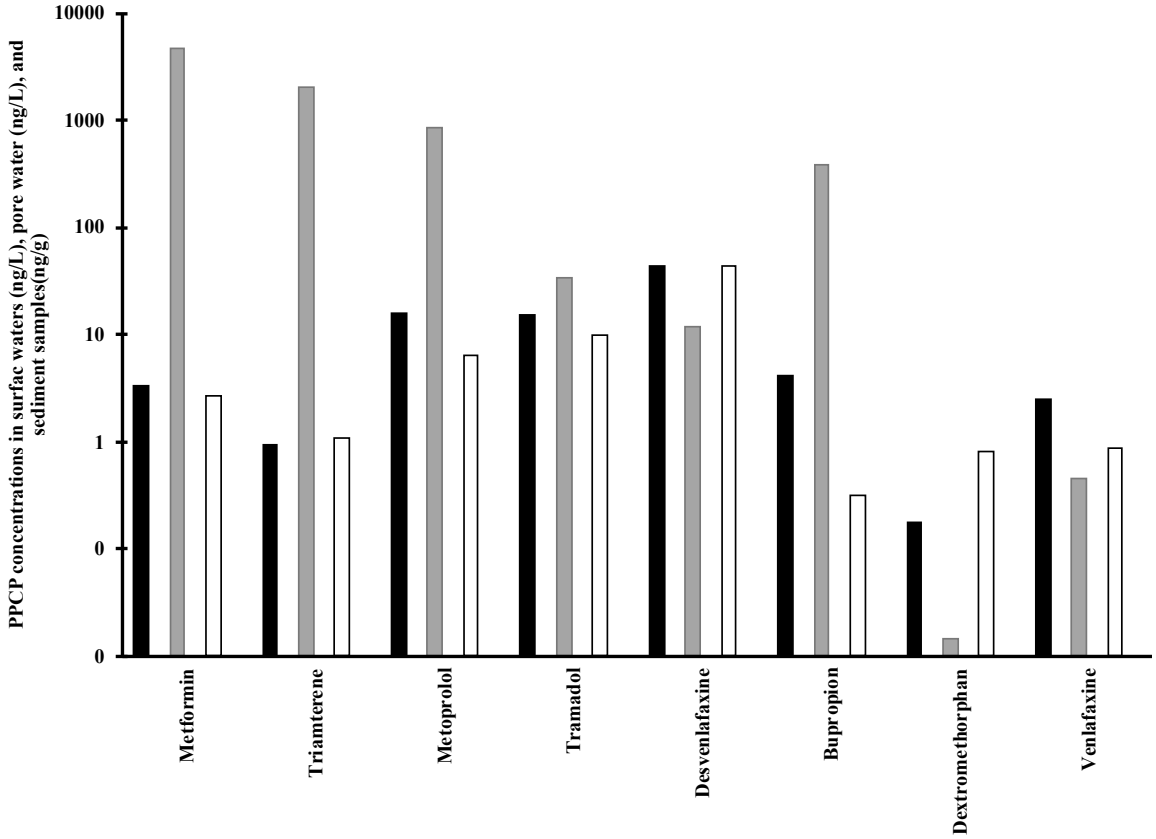

Figure 2.7: PPCPs concentrations in surface water, pore-water, and sediment samples at HC2 sampling location. Black bars, gray bars, and white bars represent surface water, pore-water, and sediment concentrations, respectively. The y-axis was transformed to a log scale in order to be able to view all values on a simple graph.

At the HC4 sampling location, there was a mix of concentration differences for the PPCPs detected. Approximately 90% of PPCPs detected were found at higher concentrations in the pore-water compared to the surface water. The remaining 10% were found at higher concentrations in the surface water.

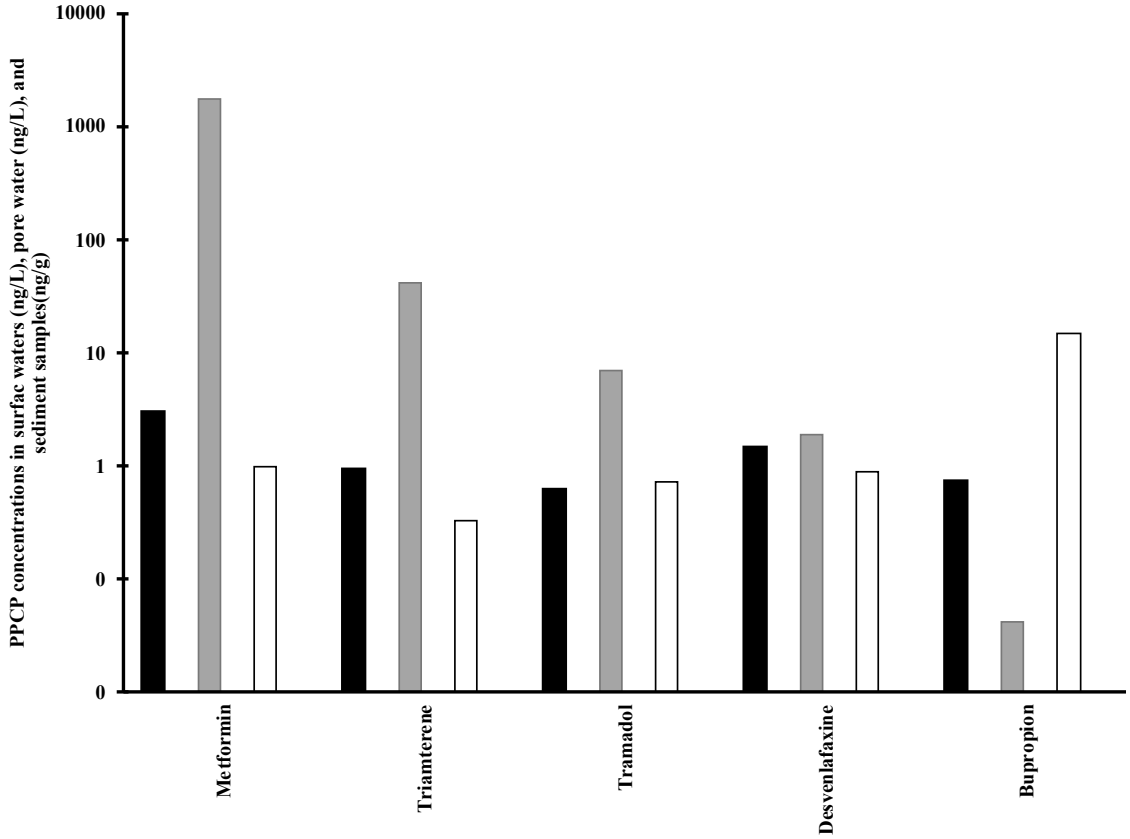

Figure 2.8: PPCPs concentrations in surface water, pore-water, and sediment samples at HC2 sampling location. Black bars, gray bars, and white bars represent surface water, pore-water, and sediment concentrations, respectively. The y-axis was transformed to a log scale in order to be able to view all values on a simple graph.

2.4.3 Flux Results

The results of the flux calculations are found below in Table 2.4 for HC1, HC2, and HC4.

Table 2.4: Mass Transfer Coefficients and Fluxes for detected PPCPs at HC1, HC2, and HC4 sampling locations

PPCP	Calculation Result	HC1	HC2	HC4
Metformin	K_L *(m/s)*	2.57×10^{-04}	2.57×10^{-04}	2.57×10^{-04}
	$K_{L\ DOC}$ *(m/s)*	5.14×10^{-06}	5.14×10^{-06}	5.14×10^{-06}
	K_{BIO} *(m/s)*	4.97×10^{-02}	5.21×10^{-05}	5.21×10^{-05}
	$K_{L\ TOTAL}$ *(m/s)*	5.00×10^{-02}	3.14×10^{-04}	3.14×10^{-04}
	Flux (F) *(ng/m²s)*	-2.28×10^{-04}	$1.46\times10^{+03}$	-4.83×10^{-03}

Caffeine	K_L *(m/s)*	2.20×10^{-04}		
	$K_{L\ DOC}$ *(m/s)*	4.40×10^{-06}		
	K_{BIO} *(m/s)*	1.06×10^{-02}		
	$K_{L\ TOTAL}$ *(m/s)*	1.09×10^{-02}		
	Flux (F) *(ng/m²s)*	-4.49×10^{-04}		
Triamterene	K_L *(m/s)*	2.03×10^{-04}	2.03×10^{-04}	2.03×10^{-04}
	$K_{L\ DOC}$ *(m/s)*	4.05×10^{-06}	4.05×10^{-06}	4.05×10^{-06}
	K_{BIO} *(m/s)*	1.85×10^{-02}	5.15×10^{-04}	7.08×10^{-04}
	$K_{L\ TOTAL}$ *(m/s)*	1.87×10^{-02}	7.21×10^{-04}	9.14×10^{-04}
	Flux (F) *(ng/m²s)*	-1.05×10^{-04}	1.45×10^{-03}	3.71×10^{-05}
Metoprolol	K_L *(m/s)*	1.44×10^{-04}	1.44×10^{-04}	
	$K_{L\ DOC}$ *(m/s)*	2.87×10^{-06}	2.87×10^{-06}	
	K_{BIO} *(m/s)*	1.79×10^{-02}	4.54×10^{-03}	
	$K_{L\ TOTAL}$ *(m/s)*	1.81×10^{-02}	4.69×10^{-03}	
	Flux (F) *(ng/m²s)*	-3.92×10^{-04}	3.94×10^{-03}	
Tramadol	K_L *(m/s)*	1.34×10^{-04}	1.34×10^{-04}	1.34×10^{-04}
	$K_{L\ DOC}$ *(m/s)*	2.68×10^{-06}	2.68×10^{-06}	2.68×10^{-06}
	K_{BIO} *(m/s)*	5.60×10^{-01}	8.51×10^{-04}	9.55×10^{-03}
	$K_{L\ TOTAL}$ *(m/s)*	5.61×10^{-01}	9.88×10^{-04}	9.69×10^{-03}
	Flux (F) *(ng/m²s)*	-2.26×10^{-02}	1.83×10^{-05}	6.04×10^{-05}
Desvenlafaxine	K_L *(m/s)*	1.53×10^{-04}	1.53×10^{-04}	
	$K_{L\ DOC}$ *(m/s)*	3.06×10^{-06}	3.06×10^{-06}	
	K_{BIO} *(m/s)*	3.66×10^{-01}	6.21×10^{-03}	
	$K_{L\ TOTAL}$ *(m/s)*	3.66×10^{-01}	6.21×10^{-03}	
	Flux (F) *(ng/m²s)*	-3.84×10^{-02}	-2.05×10^{-04}	
Bupropion	K_L *(m/s)*	1.62×10^{-04}	1.62×10^{-04}	1.53×10^{-04}
	$K_{L\ DOC}$ *(m/s)*	3.24×10^{-06}	3.24×10^{-06}	3.06×10^{-06}
	K_{BIO} *(m/s)*	1.53×10^{-01}	2.06×10^{-04}	4.21×10^{-02}
	$K_{L\ TOTAL}$ *(m/s)*	1.54×10^{-01}	3.71×10^{-04}	4.23×10^{-02}
	Flux (F) *(ng/m²s)*	-1.69×10^{-03}	1.43×10^{-04}	1.69×10^{-05}
Propranolol	K_L *(m/s)*	1.55×10^{-04}		
	$K_{L\ DOC}$ *(m/s)*	3.09×10^{-06}		
	K_{BIO} *(m/s)*	$1.63\times10^{+01}$		
	$K_{L\ TOTAL}$ *(m/s)*	$1.63\times10^{+01}$		
	Flux (F) *(ng/m²s)*	-3.14×10^{-02}		
Dextromethorphan	K_L *(m/s)*	1.50×10^{-04}	1.50×10^{-04}	
	$K_{L\ DOC}$ *(m/s)*	3.01×10^{-06}	3.01×10^{-06}	
	K_{BIO} *(m/s)*	$1.38\times10^{+01}$	$8.02\times10^{+02}$	
	$K_{L\ TOTAL}$ *(m/s)*	$1.38\times10^{+01}$	$8.02\times10^{+02}$	
	Flux (F) *(ng/m²s)*	-1.65×10^{-03}	-1.33×10^{-01}	

Venlafaxine	K_L *(m/s)*	1.49×10^{-04}	1.49×10^{-04}	
	$K_{L\ DOC}$ *(m/s)*	2.97×10^{-06}	2.97×10^{-06}	
	K_{BIO} *(m/s)*	$1.64\times10^{+01}$	$1.38\times10^{+01}$	
	$K_{L\ TOTAL}$ *(m/s)*	$1.64\times10^{+01}$	$1.38\times10^{+01}$	
	Flux (F) *(ng/m²s)*	-1.29×10^{-01}	-2.78×10^{-02}	
Diphenhydramine	K_L *(m/s)*	1.36×10^{-04}		1.62×10^{-04}
	$K_{L\ DOC}$ *(m/s)*	2.73×10^{-06}		3.24×10^{-06}
	K_{BIO} *(m/s)*	$6.79\times10^{+02}$		2.96×10^{-02}
	$K_{L\ TOTAL}$ *(m/s)*	$6.79\times10^{+02}$		2.98×10^{-02}
	Flux (F) *(ng/m²s)*	-4.97×10^{-01}		1.32×10^{-03}
DEET	K_L *(m/s)*	1.75×10^{-04}		
	$K_{L\ DOC}$ *(m/s)*	3.50×10^{-06}		
	K_{BIO} *(m/s)*	1.09×10^{-03}		
	$K_{L\ TOTAL}$ *(m/s)*	1.27×10^{-03}		
	Flux (F) *(ng/m²s)*	-4.82×10^{-05}		
Carbamazepine	K_L *(m/s)*	1.72×10^{-04}		
	$K_{L\ DOC}$ *(m/s)*	3.44×10^{-06}		
	K_{BIO} *(m/s)*	2.15×10^{-02}		
	$K_{L\ TOTAL}$ *(m/s)*	2.17×10^{-02}		
	Flux (F) *(ng/m²s)*	-3.89×10^{-04}		
Celecoxib	K_L *(m/s)*	1.42×10^{-04}		
	$K_{L\ DOC}$ *(m/s)*	2.84×10^{-06}		
	K_{BIO} *(m/s)*	9.85×10^{-01}		
	$K_{L\ TOTAL}$ *(m/s)*	9.85×10^{-01}		
	Flux (F) *(ng/m²s)*	-3.27×10^{-03}		

There were fourteen PPCPs detected in the course of this study. Fourteen were detected at HC1, eight detected at HC2, and five detected at HC4. This was consistent with expectations based on the locations of each sampling site. The three mass transfer coefficients (MTCs) were calculated for each PPCP and each site where it was found. In all instances, the $K_{L\ DOC}$ was the smallest MTC, indicating that this process contributed the least to the overall flux, and therefore, fate of each PPCP. K_{BIO} was the largest MTC

for all PPCPs detected. K_L was the second largest MTC for all PPCPs detected. There did not appear to be any trend that would indicate which MTC would be the major contributor to the overall flux.

As previously stated, the difference between the concentration of the PPCPs found in the surface waters versus the concentration in the pore-water would determine if the sediment was serving as a sink or a source. Figure 2.9 depicts the difference between those concentrations for each PPCP detected at each site.

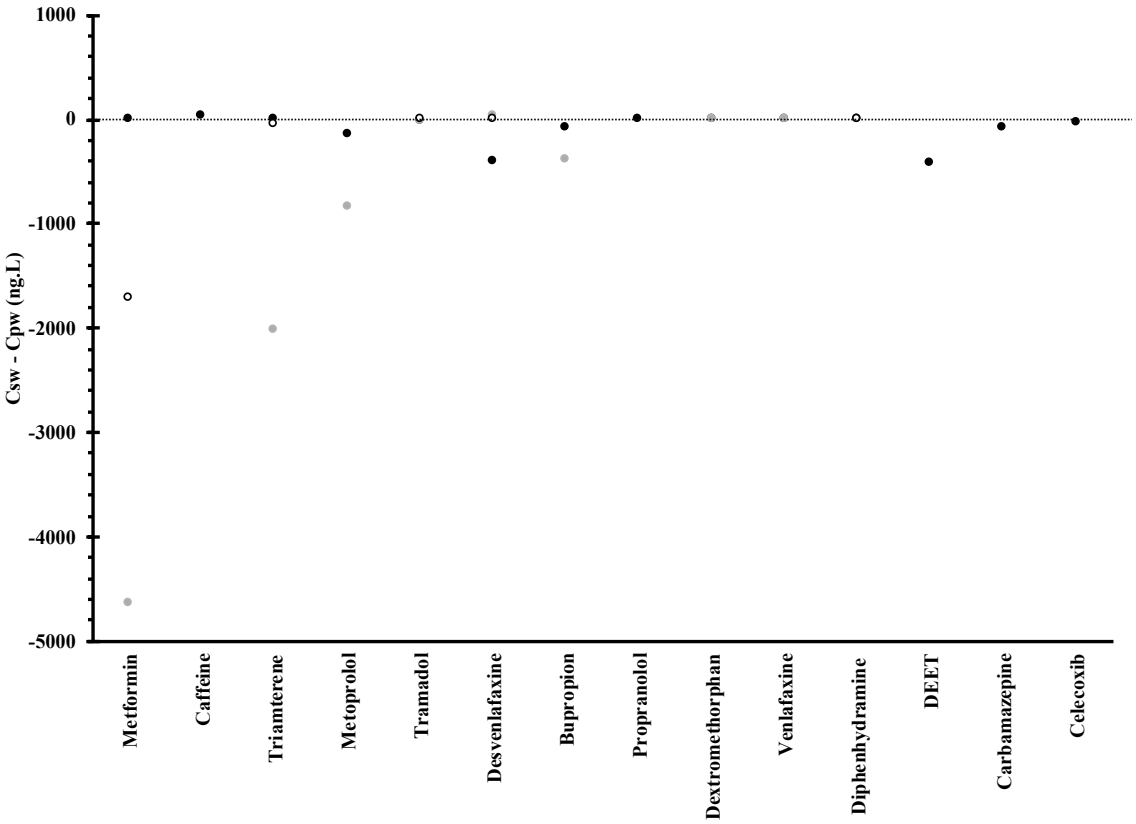

Figure 2.9: The difference in concentration of each PPCP found in surface waters and pore-water at HC1, HC2, and HC4. Black dots represent HC1, gray dots represent HC2, and white dots with black outlines represent HC4.

It was observed that all fourteen PPCPS detected at HC1 indicating had a negative flux. Three out of seven PPCPs detected at HC2 were also found to have negative fluxes and the remaining five were found to have positive fluxes. This indicates that the sediment can serve as both a source and a sink of PPCPs at those sites. All five of PPCPs detected at HC4 were found to have positive fluxes, indicating that the sediment serves primarily as a source in this area. The magnitude of the flux for each PPCP was relatively small, similar to what has been reported in the literature for PAHs and PCBs.[136,144–146]

2.5 Discussion

2.5.1 Comparison of PPCP fluxes in the TFWPR to PCB and PAH fluxes

There is currently limited information available concerning the fluxes of PPCPs between the water-sediment interface. However, extensive studies have been conducted concerning the fluxes of PAHs and PCBs at the water-sediment interface.[126,136,145,147–150] Given the structural similarities between PPCPs, PAHs, and PCBs, including comparable molecular masses, they may be compared for the purposes of this study. The range of fluxes for the PPCPs in this study was found to be -4.97×10^{-1} – 3.94×10^{-3} ng/m^{2}s. Several studies reported varying fluxes of PAHs that ranged from 3.70×10^{-4} – 4.54 ng/m^{2}s[122,123,145,146] while the fluxes of PCBs ranged from 3.17×10^{-6} – 9.95 ng/m^{2}s.[124,145,147,149,150] The reported fluxes of PPCPs are well within the ranges reported for PAHs and PCBs. It is of importance to note that in the studies mentioned, there were no reported negative flux values, indicating that the sediment was always a source for PAHs and PCBs. This was different from what was found in this study as the sediment

acted as both a source and sink for PPCPs depending upon the sampling location. This difference may be due to the slight structural differences between PPCPs and PAHs and PCBs or it may be due to other factors not yet investigated.

2.5.2 Contribution of MTCs to the Flux of individual PPCP

The calculated flux consists of three separate MTCs: K_L, K_{LDOC}, and K_{BIO}. In all instances K_{LDOC} was the smallest MTC. In comparison to the other MTCs, it was so small that it did not have any significant effect on the flux. As previously mentioned, K_{BIO} was the largest MTC for all PPCPs detected and K_L was the second largest MTC. This indicates that the flux of each PPCP is primarily driven by bioturbation within the BBL and somewhat driven by molecular diffusion and transport across the BBL. The diffusion of PPCPs through the sediment water interface due to sorption of PPCPs to the DOC does not appear to have any significant effect on the overall fluxes. A comparison of the three MTCs for each of the fourteen individual PPCPs detected is depicted in Figure 2.10.

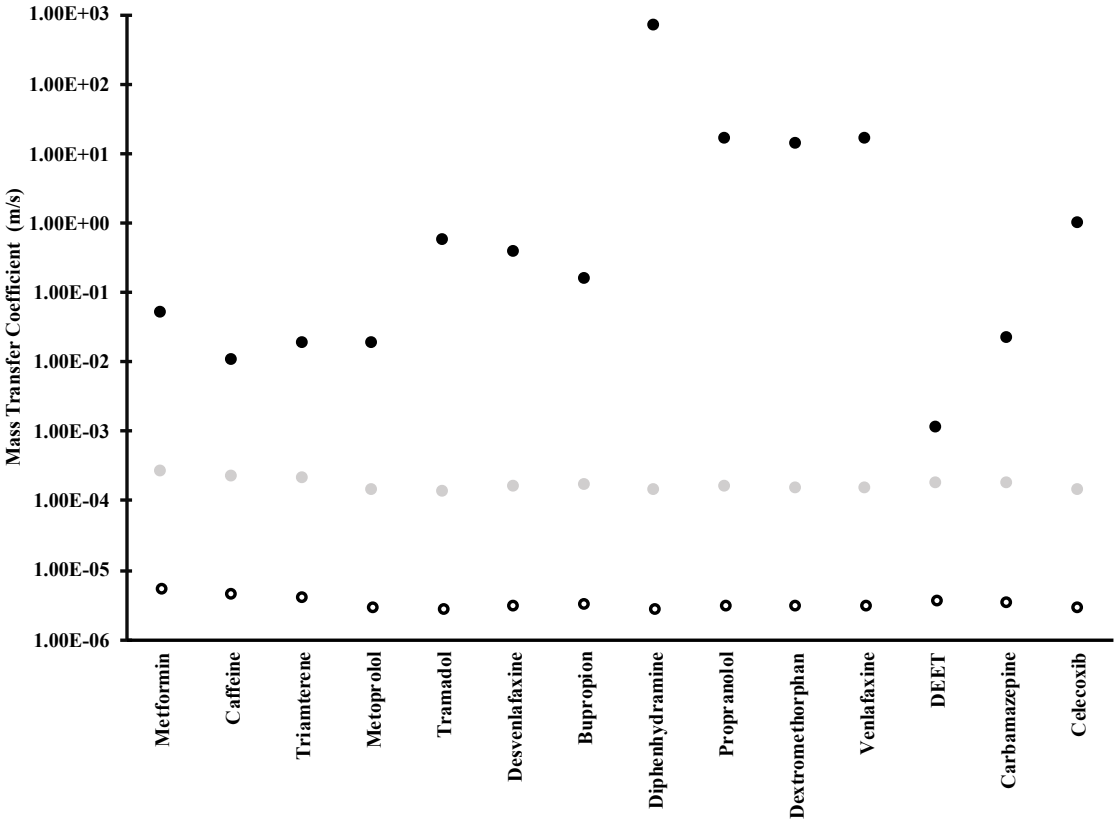

Figure 2.10: The three mass transfer coefficients (K_L, K_{LDOC}, and K_{BIO}) for each of the 14 individual PPCPs detected at HC1. Black dots represent K_{BIO}, gray dots represent K_L, and white dots outlined in black represent K_{LDOC}.

A Spearman's Rank Correlation was performed to determine the correlation between K_{ow} and K_{LTOTAL}. The results (Rho=-0.59) indicate that there is a negative moderate correlation between the two values and that K_{ow} may have a significant impact on the overall K_{LTOTAL}.

2.5.3 Comparison of PPCP fluxes throughout the TFWPR

The most PPCPs were detected at sampling site HC1, located in the Upper Hunting Creek region within the discharge zone of the WTP. The concentrations of the

PPCPs are at their greatest in the surface waters at this sampling site due to the WTP effluent discharge. As such, the sediment in this location served primarily as a sink for all PPCPs (Figure 2.11).

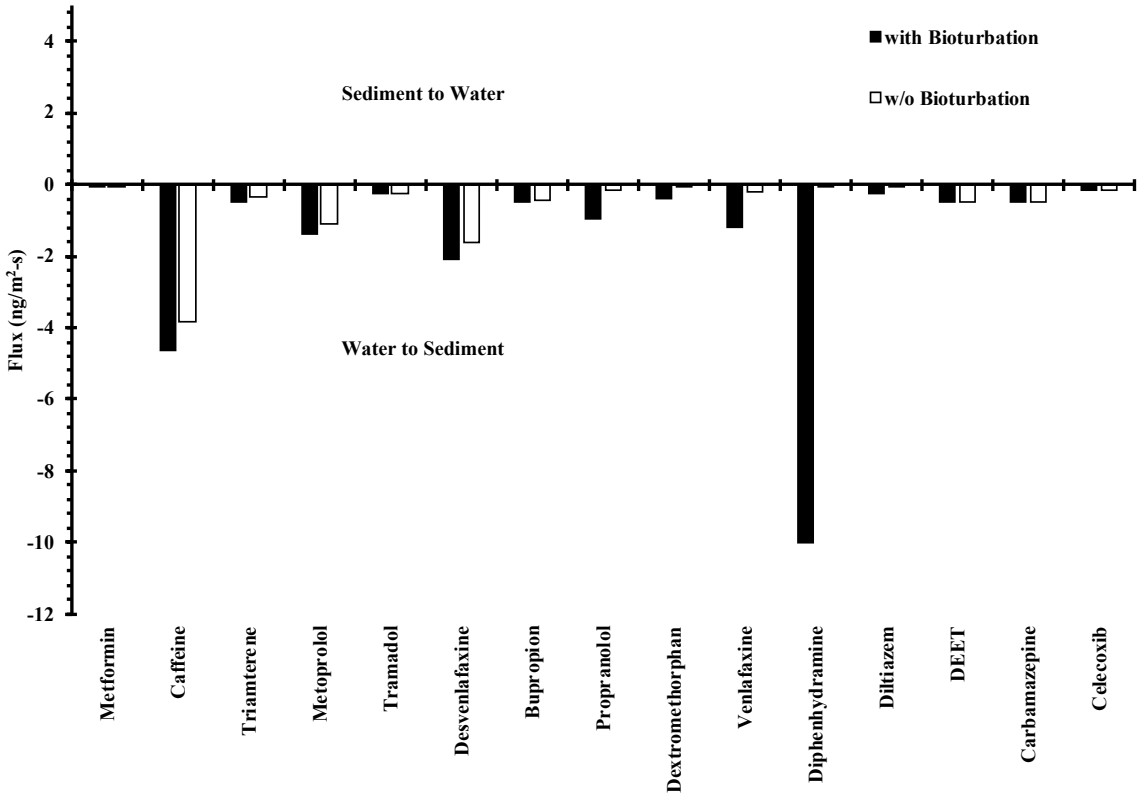

Figure 2.11: The sediment-water fluxes for each of the 14 individual PPCPs detected at HC1. Black bars represent the flux with bioturbation and white bars represent the flux without bioturbation.

Continuing downstream to the Lower Hunting Creek region, there were several PPCPs found at HC2. The concentrations of PPCPs in the surface waters at HC2 were decreased from those found at HC1. In addition, the concentrations found in the pore-water increased for some PPCPs. As previously mentioned, three out of eight PPCPs

detected at HC2 were found to have negative fluxes and the remaining five were found to have positive fluxes (Figure 2.12). This is consistent with the decrease in surface water and increase in pore-water concentrations. The decrease in surface water concentrations is due to several factors, including but not limited to, degradation/decomposition and transformation into metabolites or other products. These processes are also responsible for the smaller amount of PPCPs detected at this site in comparison to HC1.

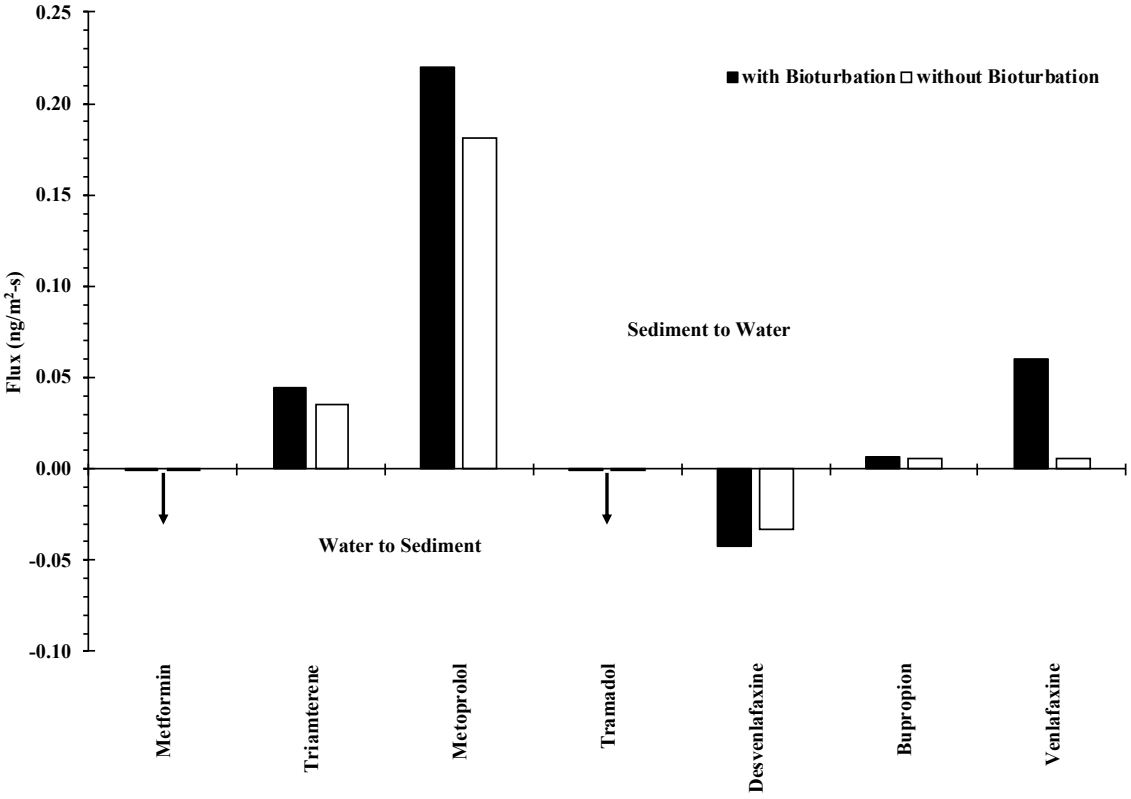

Figure 2.12: The sediment-water fluxes for each of the 7 individual PPCPs detected at HC2. Black bars represent the flux with bioturbation and white bars represent the flux without bioturbation.

Further downstream to the region where Hunting Creek meets the TFWPR, there were few PPCPs found at HC4. The concentrations of PPCPs in the surface waters at HC4 were significantly decreased from those found at HC1. As previously mentioned, four out of five PPCPs detected at HC4 were also found to have positive fluxes (Figure 2.13). This indicates that the sediment serves primarily as a source of PPCPs at this site. Again, this is consistent with the decrease in surface water concentrations similar to what was found at HC2.

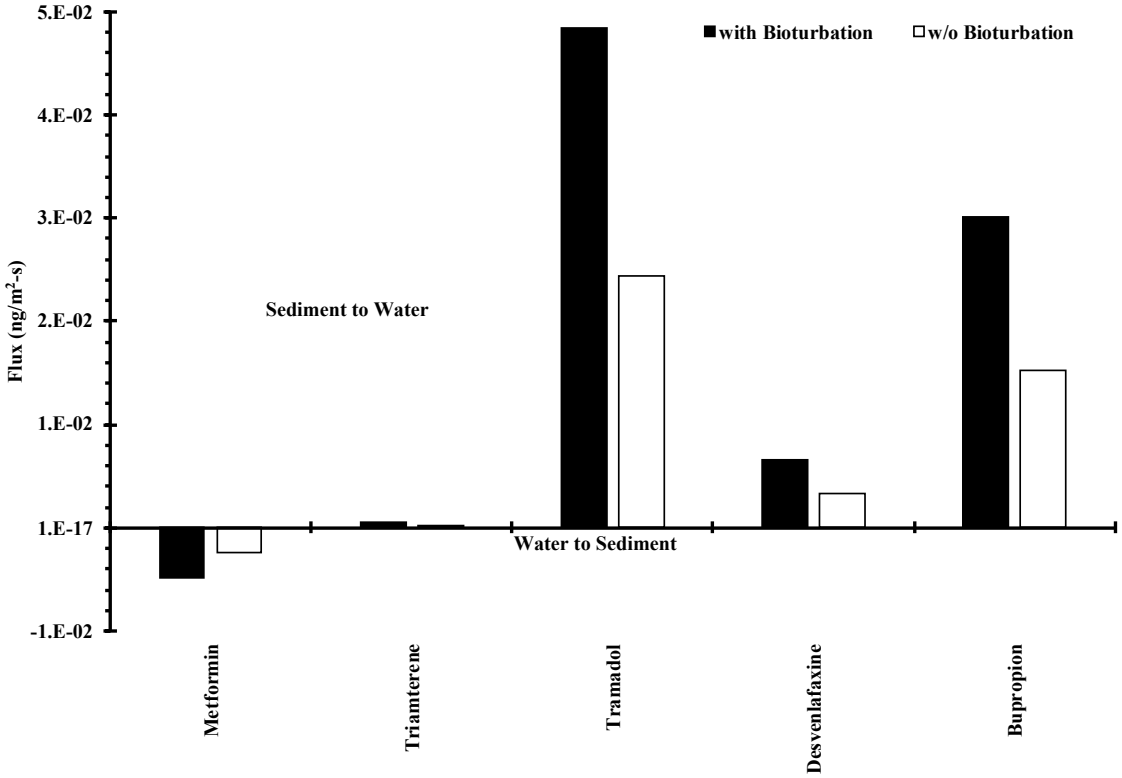

Figure 2.13: The sediment-water fluxes for each of the 5 individual PPCPs detected at HC4. Black bars represent the flux with bioturbation and white bars represent the flux without bioturbation.

There were five PPCPs found at all three sampling locations. Three of those PPCPs (tramadol, desvenlafaxine, and buproprion) followed the same trend regarding their concentration in pore-water. The concentration was the highest at HC1, decreased at HC2, and continued to decrease even further at HC4. In contrast, metformin and triamterene saw the increase in concentration in pore-water from HC1 to HC2 and then a decrease from HC2 to HC4. Their concentrations detected at HC4 were still higher than those detected at HC1. While these trends are important to note, there does not seem to be any connection between these trends and the categories of PPCPs found as they exhibit distinct physiochemical properties dependent on their class.

The K_{LTOTAL} varied for each of these three PPCPs across the three different sampling sites, depicted in Figure 2.14. This is likely due to the significantly different concentrations in pore-water and surface water across all three sites.

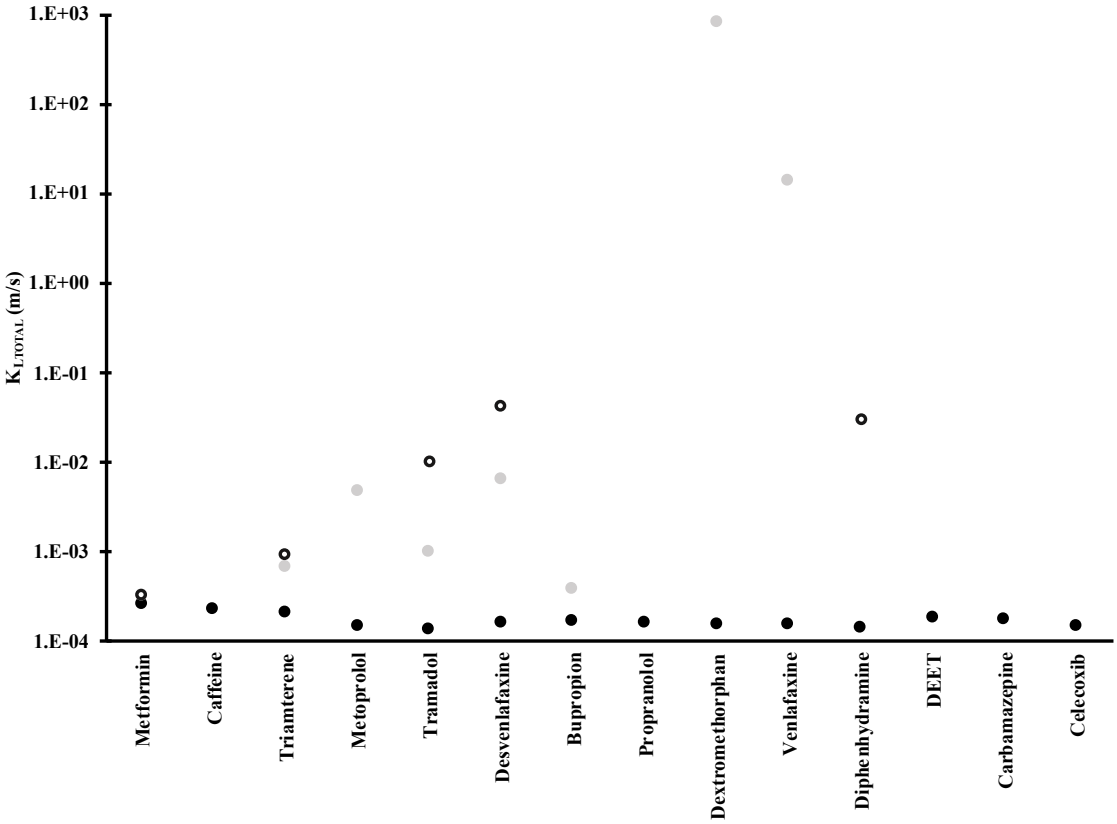

Figure 2.14: The mass transfer coefficients K_{LTOTAL} for each of the 14 individual PPCPs detected. Black dots represent HC1, gray dots represent HC2, and white dots outlined in black represent HC4.

Interestingly, the K_{LTOTAL} values were the smallest at HC1 where all the fluxes were negative. When detected at both HC2 and HC4 the K_{LTOTAL} were always highest at HC4. This indicates that the K_{LTOTAL} will increase down the transect.

2.6 Conclusion

The flux of twenty-three individual PPCPs was calculated at three sites in different zones along Hunting Creek in an effort to determine if the sediments in these zones are serving as a source or a sink of these PPCPs in the environment. It was determined that when surface water concentrations are highest, such as in the zone of the

WTP discharge, the sediment will serve primarily as a sink for the PPCPs. However, PPCPs diffuse rapidly downstream of the WTP outfall. As such, the concentration in surface water decreases down the transect and the sediment will serve primarily as a source of PPCPs to the environment.

Furthermore, the calculated fluxes are in the range of those calculated for other environmental organic compounds such as PAHs and PCBs. It was determined that bioturbation is especially important for PPCPs with high K_d values. The PPCPs did exhibit negative flux values, while other compounds (PAHs and PCBs) did not indicating that their different physiochemical properties play a significant role in their flux between water and sediment. In addition, it was determined that the colloid associated change across the boundary layer was not an important factor in the developed boundary layer model.

Overall, the present study was able to establish a boundary layer model that may be used for the determination of the fluxes of PPCPs throughout the TFWPR and other aquatic environments. These results are significant in that they have contributed to the understanding of the distribution of PPCPs between surface waters and sediments, which is essential to managing public health and enlightening our society about the environmental implications of overprescribed drug therapy. Additional work to increase the sampling area, improve the collection and isolation of pore-water, and expand the scope of analysis to look for transformative products of the PPCPs would greatly improve the project.

CHAPTER 3: OCCURRENCE OF PHARMACEUTICALS AND PERSONAL CARE PRODUCTS IN RIVERINE SEDIMENT CORES FROM THE GUNSTON COVE REGION OF THE TIDAL FRESHWATER POTOMAC RIVER

3.1 Introduction

Geosolids, particularly aluminosilicate particles <63 μm in diameter, undergo fluvial transport in rivers and streams, and as these solids undergo deposition, they convey sorbed micropollutants to riverbed sediment. Deposited sediment progress downstream through a resuspension and re-deposition cycle culminating in eventual discharge into the world's oceans.[151] Alternatively, in certain riverine zones, deposited sediment may undergo long-term burial, thus creating the historical record.[152–156] Marshes have a high rates of sedimentation that produce an enhanced depositional zones for sediments and micropollutants,[157,158] along with bayhead deltas at the confluence of tributaries, creating regions in fluvial and estuarine areas that have much higher rates of sedimentation compared to other riverine zones.[159]

There are regions of the TFWPR where burial may occur including marshes and bayhead deltas. The TFWPR has several unique geographic attributes that make it ideal to study the deposition of PPCPs, including proximity to the large urban, metropolitan Washington, DC area, high ecological biodiversity, and transitional fluvial-estuarine boundary hydrology that creates shoals and embayments. These factors influence both nature and humankind as the need for drinking water, wastewater discharge, flood

management, and agricultural production create stresses on local resources.[160] In the TFWPR there are multiple high-capacity WTPs discharging into a small river zone that services a metropolitan region with 6 million inhabitants. Specifically of interest in this project was the accumulation of PPCPs in the bayhead delta of the Gunston Cove (Lorton, VA) embayment of the TFWPR. The combination of high population size and upstream (Pohick Creek) WTP discharge (>250,000 m^3/day) made this location ideal for study of the sediment record.

PPCPs can provide a useful historical record due to the controlled nature of their availability and use. Each individual pharmaceutical is heavily regulated by multiple agencies, specifically the FDA. As such, records indicating when these PPCPs were first available for use in the environment will provide helpful information as to the age of the sediment layers. In addition, there are several well characterized micropollutants, in this case pesticides, that can be used as a time proxy to compare with the PPCPs. Sediment cores can provide a historic record of PPCPs and pesticides as well as other organic contaminants. This will provide useful and insightful information regarding PPCP deposition. Analysis of these cores results in a concentration/depth record which is utilized in the determination of change in usage of PPCPs through over time. Several studies have been conducted to determine the concentration of pesticide residues in sediment cores in marsh and wetland areas.[161–164] However, very few studies have been conducted to determine the concentration of PPCPs in sediment cores taken from riverine environments.[154,155] To aid with the interpretation of historical deposition within the

sediment core vertical profile, legacy pesticides and Cesium-137 (Cs-137) were employed to establish timelines or burial.

3.2 Study Objective

The primary objective of this study was to determine the nature of burial and historical deposition profiles of PPCPs in riverbed sediments of the TFWPR. The secondary objective was to analyze the sediment core for pesticide residues to determine approximate dates of the core. In addition to pesticide residue analysis, each sub-section of the sediment cores was analyzed via a Gamma Spectrascope for the presences of Cesium-137 to determine an approximate date of each sub section.

3.3 Materials and Methods

3.3.1 Sample Sites

The coring site was selected from the Gunston Cove (GC) embayment formed from the confluence of Pohick Creek with the Potomac River. The intent was to select a site that was located immediately downstream of a large WTP; therefore, site GC2 was selected (Figure 3.1). The GC shoal is isolated from the mainstem Potomac River. The high capacity Noman Cole WTP in this area discharges into Pohick Creek, which flows into this embayment approximately 1 km upstream of the sampling site. The coordinates for the GC were 38.67514, -77.15645.

Figure 3.1: Map of the Gunston Cove Region.

3.3.2 Materials

QuEChERS (Agilent Technologies, Santa Clara, CA) extraction and dispersive solid phase extraction (dSPE) salts and kits, used to process all sediment samples for LC-MS/MS analysis, were purchased from Agilent Technologies (Santa Clara, CA). Acetonitrile and formic acid, used to make the LC-MS/MS mobile phases, was purchased from Thermo Fisher Scientific (Waltham, MA). Other bulk solvents used for analysis and supply preparation included methanol and acetone and were purchased from Thermo Fisher Scientific (Waltham, MA). Milli-Q type 3 water (UPW), used to make an LC-MS/MS mobile phase and for cleaning purposes was made in house by a MilliQ water purifier (18.2 MΩ-cm). LCMS liquid nitrogen and compressed argon and nitrogen gasses were purchased from Roberts Oxygen (Rockville, MD).

The materials for the gas chromatograph-mass spectrometer (GC-MS) included internal standards acenaphthene-d10, chrysene-d12, and phenanthrene-d10 (Restek Corporation, Bellefonte, PA). Surrogate standard 2,4,5,6-tetrachloro-m-xylene was purchased from Supelco – Sigma-Aldrich (St. Louis, MO) and surrogate standard triphenylphosphate was purchased from Restek. Calibration standards were purchased from several vendors: permethrin (Pestanal – Sigma-Aldrich), PBDE congener mix (Accustandard, New Haven, CT), GC-MS pesticide standards for calibration were obtained from Restek, Certified cesium-137, barium-133, and cobalt-60 planar disk calibrated radioisotope sources were manufactured by Spectrum Techniques, LLC (Oak Ridge, TN).

3.3.3 Field Sampling

The sediment core was collected following methods and protocols established by USGS and EPA specifically for marsh sediment coring.[165,166] In summary, the cores were collected on the ebb tide cycle of the TFWPR shortly after high tide. The cores were collected onboard a skiff using an SDI Vibecore-Mini (Specialty Devices Inc., Wylie, Texas) coring device. The Vibecore was powered by a 24 VDC battery. The Vibecore was fitted with a 1-m (length) x 3 cm (diameter) aluminum core tube along with an extension pole for sampling in 1 m-depth of water from the skiff. The core tube also had a core-catcher to aid with core retention during the extraction step of core collection. The Vibecore device helped to minimize sediment compaction within saturated sediments. Core depth, standing water level (if present), and compaction were measured before the

core was closed on each end with Teflon caps. The cores were transported back to the lab where they were stored upright at room temperature until initial processing began within 24 hours.

3.3.4 Sample Processing

The sediment core was split in half, length wise, using a circular saw. One half of the core tube was cut longitudinally at a shallow depth such that the saw blade did not cut into the sediment. Subsequently, the core was separated into two equal halves using a spatula. Each half was photographed, and any aluminum shavings were removed from the surface of the sediment. One half of the core was placed in a plastic bag, vacuum sealed, and placed in a chest freezer at -30°C for storage as an archive. The second half of the core was photographed and sampled starting at the surface of the core to the bottom of the core. In order to sample the core an approximately 2-cm section of the core was removed for each sub sample. A 1 cm strip of sediment was left between each 2 cm sampled section. The pattern for sampling the core was: sample 2 cm, skip 1 cm, sample 2cm, etc. Only the inner portion of each core was sampled, leaving behind any sediment that may have come in contact with the aluminum core wall untouched so as to preserve the chronology of the core. Each individual subsection was labeled, and its depth recorded.

The sediment samples were pre-sieved through a 0.5-mm stainless steel mesh into a 50-mL centrifuge tube. This was done to remove any large particulates that bias the sample mass. The tubes were placed in the centrifuge at 2200 rpm for 10 minutes. Once

removed from the centrifuge, any supernatant water (typically 2 – 10 mL) was discarded. The sub-sampled sediments were placed in glass jars and frozen at -20°C prior to analytical processing.

Each sample was thawed and sub-sampled for LC-MS/MS, GC-MS, % moisture, grain size, TOC, and CS-137 analysis. In LC-MS/MS and GC-MS analysis, sediment (2 g weighed precisely) was spiked with 50 – 100 ng internal and surrogate standards, and the samples were extracted via the QuEChERS (**Q**uick-**E**asy-**Ch**eap-**E**ffective-**R**ugged-**S**afe) method.[45,47] The 2 g sediment samples were transferred to a 50-mL centrifuge tube and 10 mL of acetonitrile was added to each tube and the tubes were subsequently vortexed for 10 minutes. After vortexing each sample, 10 mL of UPW was added to every sample and the samples were vortexed again for 1 min. QuEChERS packets containing 6 g of anhydrous magnesium sulfate and 1.5 g of sodium acetate were added to each sample and the tubes were vortexed for a final time. The tubes were then centrifuged for 10 min at 2200 rpm. An 8 – 10 mL aliquot of the organic phased was transferred via glass pipette to a 15-mL dispersive solid phase extraction (dSPE) tube containing 1.2 g of magnesium sulfate and 0.4 g of primary-secondary amine (PSA), aiding in the removal of LC-MS/MS-interfering matrix components. The tubes were vortexed and centrifuged for 10 min at 2200 rpm. The supernatant of each sample was transferred to a clean 40-mL amber glass vial using a disposable glass pipette. The SPE extracts are reduced in volume to approximately 0.5 mL using a TurboVap (Zymark Corp., Hopkinton, MA) evaporator (employing dry N_2 gas), and transferred to 1.5 mL screw-top amber glass vials for LC-

M/MS and GC-MS analysis. The extracts were stored in a -20°C freezer prior to quantitative analysis.

3.3.5 LC-MS/MS Analysis

The 91 PPCPs in the sediment extracts were analyzed for the compounds of interest using a Shimadzu Model 8050 liquid chromatograph triple-quadrupole mass spectrometer (LC-MS/MS) configured with a SIL-20ACXR autosampler (Columbia, MD). The LC-MS/MS interface was operated in electrospray ionization (ESI) mode in the presence of a Corona needle (DUIS) for both positive and negative ionization. LC-MS/MS separation of the PPCPs was performed using a 50 mm x 2.1 mm (id), 1.8 µm (particle diameter) Forced Biphenyl reversed-phase UHPLC column (Restek, Bellefonte, PA) in conjunction with a raptor Biphenyl guard column, with a binary mobile phase consisting of Type I Milli-Q water (solvent A), and acetonitrile (solvent B), both containing 0.1% formic acid as a phase modifier. Operating conditions for the LC-MS/MS are listed in Table 3.1. The gradient elution program allowed for a total run time of approximately 10 min. The retention times for the PPCPs are in Table 4.2A.

Table 3.1: LC-MS/MS Instrument Parameters

Parameters	Operating Conditions
Total Flow Rate	0.40 mL/min
Gradient Elution Program	10% B at 0 min
	50% to 95% B 0-6 min
	100% B 6-7 min
	100% to 30% B 7-9 min
	10% B 9-10 min
Nebulizing Gas Flow	2 L/min
Heating Gas Flow	10 L/min

Drying Gas Flow	10 L/min
Oven Temperature	40°C
Interface Temperature	300°C

The LC-MS/MS quantitation of the PPCPs was accomplished in the multiple reaction monitoring (MRM) mode. Three MRM ions were established for each PPCP (with the exception cis-tramadol which only had one MRM) through automated MRM optimization procedures following manual precursor ion identification using the full scan mode. The quantifier (primary) and qualifier (secondary and tertiary) product ions and the various quadrupole voltages for the PPCPs are listed Table 4.3A. Quantitation was performed using the internal standardization method with isotopically labelled internal standards (^{2}H or ^{13}C analogues as shown in Table 1.3 – Chapter 1) that were added prior to the extraction step. Quantitation was completed using a ten-point calibration curve based on the primary product MRM ion abundance for each PPCP relative to that of an associated internal standard. The retention times and qualifier MRM ions relative abundances were used to confirm the chemical identity of the PPCP. Data analysis and quantitation was performed using LabSolutions software (ver. 5.91).

3.3.6 GC-MS Analysis

The pesticides of interest (organochlorines (OCs), organophosphates (OPs), dichlorodiphenyldichloroethylene (DDE), and dichlorodiphenyldichloroethane (DDD)) were analyzed using a model 7890A GC System from Agilent Technologies with a CTC Analytics CombiPal autosampler using an Agilent J&W DB-5ms Ultra Inert 25 m

column (part number 122-5522UI), coupled with an Agilent 5975 Inert XL MSD with triple-axis detector. Quantification was carried out in the selected ion monitoring mode (SIM) by selecting at least two characteristic ion fragments for each analyte and monitoring the retention time of each species. The GC-MS conditions and program were built using MSD ChemStation software (ver. G1701EA E.02.02.1431, Agilent Techologies, Santa Clara, CA, USA). The pesticides are quantified using MassHunter Quantitative Analysis software (ver. B.07.00, Agilent Technologies, Santa Clara, CA, USA) from six-point calibration curves via the internal standard method. Operating conditions for the GC-MS were determined prior to beginning the main body of work and are listed in Table 3.2.

Table 3.2: GC-MS Instrument Parameters

Multimodal Inlet	
Initial Temperature; Hold Time	90°C; 0.36 min
Inlet Temperature Ramp Rate	600°C•min^{-1}
Inlet Final Temperature; Hold Time	290°C; 5 min
Pressure	25 psi
Septum Purge Flow	3 ml•min^{-1}
Mode	PTV Solvent Vent
Vent Rate	100 ml•min^{-1} at 5 psi until 0.36 min
Purge Flow to Split Vent	60 ml•min^{-1} at 2.86 min
Agilent Technologies 122-5522UI Column	
Flow	2.9 ml•min^{-1}
Pressure	25 psi – constant pressure
Holdup Time	0.736 min
Post-Run Pressure	1 psi
Agilent Transfer Column to MSD vacuum	
Flow	4.4 ml•min^{-1}
Pressure	1 psi
Holdup Time	0.003 min
Post-Run Pressure	15 psi

Oven Parameters	
Initial Temperature; Hold Time	70°C; 2 min
Ramp 1; Hold Time	25°C•min^{-1} until 150°C; 0 min
Ramp 2; Hold Time	3°C•min^{-1} until 200°C; 0 min
Ramp 3; Hold Time	6°C•min^{-1} until 300°C; 15 min
Post-Run Temperature; Hold Time	310°C; 10 min

3.3.7 Quality Assurance

Surrogate Spike recovers are summarized in Figure 3.2. All sediment samples were spiked with surrogate standards prior to the individual extraction processes. This allowed for the determination of performance of the groups of analytes. The surrogates consisted of isotopically labeled homologues of compounds that were being targeted for analysis. Out of eight total surrogate standards, only one exceeded 70% recovery, indicating low performance. It is believed that a much more complex matrix exists in sediment cores as opposed to regular sediment. The reported concentrations of targeted chemicals were not corrected for surrogate recoveries.

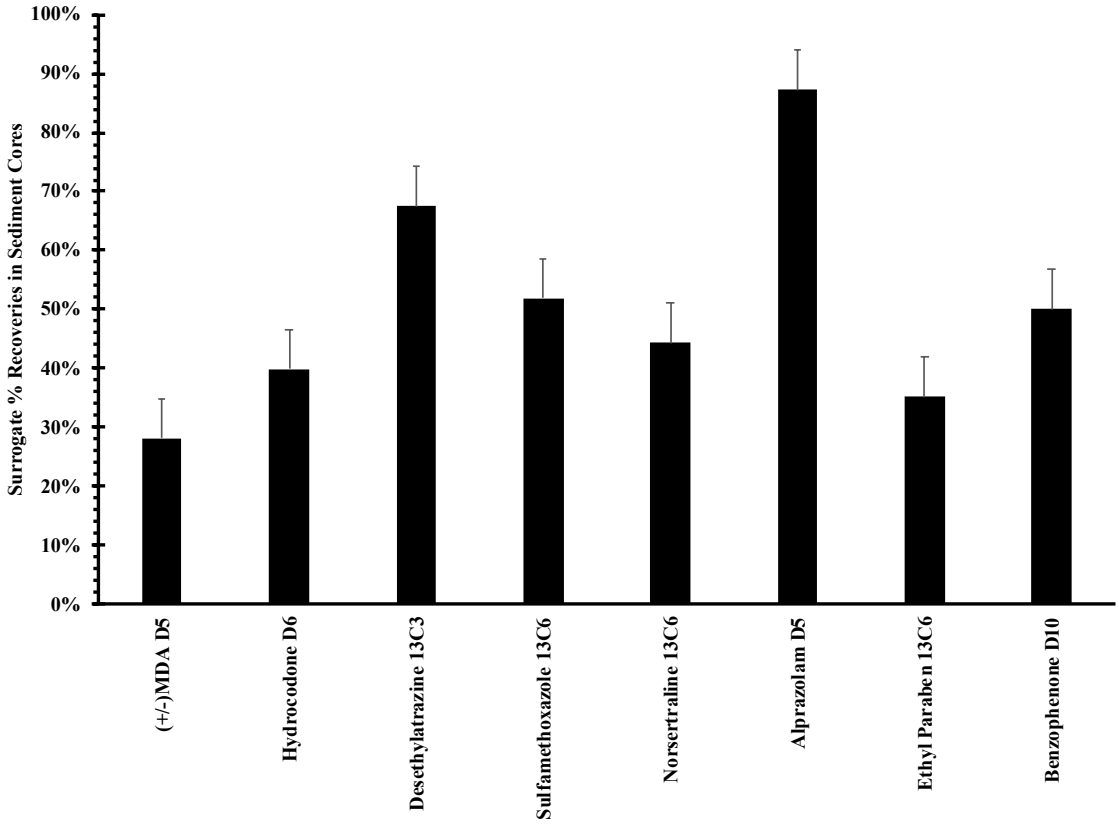

Figure 3.2: Mean Surrogate %recoveries evaluated in for core samples. Black columns represent the mean recovery and bars represent ± 1 SD.

As this analysis was conducted in conjunction with the studies conducted in Chapters 1 and 2, additional lab blanks and matrix spikes were not carried out. Due to the limited amount of sediment available for each subsection and the large amount of analysis needed to be carried out on each subsection, only three samples throughout each core were run in triplicate. The %RSD values for those triplicate runs could not be calculated as the matrix interfered with the quantitation of at the two samples in each triplicate set.

3.3.8 Ancillary Measurements

Ancillary measurements were conducted on bed sediment to determine organic carbon content, moisture content, and grain size.

Total organic carbon (TOC) content was performed using a Carlo Erba Model 1112 Flash Elemental Analyzer (Drexel University, Department of Chemistry, Philadelphia, PA). Approximately 1 g of sediment from each sampling location and trip was dried in an oven at approximately 60˚C overnight, and then ground to a fine powder using a mortar and pestle. The samples were placed in a ceramic crucible and were fumigated with concentrated HCl for 24 hours to degas carbon dioxide derived from inorganic carbon (primarily as carbonates) following the method of Ramnarine.[48] The treated sediment was re-dried at 60˚C oven for one week to ensure that no excess HCl was present. The sample was placed into a tin boat, weighed, and combusted at 1000˚C for total C and N content.

Sediment moisture was determined by measuring out approximately 1 – 2 g of wet sediment into a tared aluminum boat and measuring mass. The aluminum was placed in an oven at 60°C for 48 – 72 hours. The mass of the sample was recorded again after the drying period. The moisture content was evaluated by determining the loss of mass after drying as described in Equation 1.2 (Chapter 1). The moisture content was used to correct and convert wet weight of the sediment samples to dry weight. The dry weight of all sediment samples was used when expressing PPCP sediment concentrations.

Sediment grain size, in terms of percent sand, silt and clay content, for all the collected riverbed sediments was determined using a Beckman-Coulter (Brea, CA) laser

diffraction (LS 13320) particle size analyzer (PSA). Sediment initially was passed through a 0.5-mm stainless-steel sieve to remove large particles followed by disaggregation in 5% aqueous hexametaphosphate prior to analysis by the PSA. Grain size results were provided by the Excel program GRADISTAT for ternary diagrams.

In addition, each subsection of the sediment cores was run on a Gamma Spectrascope to look for the presences of the Cs-137 peak. Approximately 1 – 2 grams of sediment per subsection was dried in an oven at 60°C for 72 – 96 hours. The samples were ground to homologous consistency using a mortar and pestle. The ground samples were transferred to plastic containers with a screw top lid. Prior to running the sediment samples, a background consisting of an empty plastic container with screw top lid was taken. In addition, the standard radioisotopes were run to produce a calibration curve. Each sample was placed in the Gamma Spectrascope, individually, with a run time of 30 minutes. During that 30 minutes time period, the spectrascope counted any radiation detected. There were two goals to this portion of the data collection process. The first was that some subsections would not produce any cesium-137 peak. In this instance, those subsections that did not contain this peak could be dated to prior to 1951. 1951 is the first appreciable amount of cesium-137 detected in soils from nuclear testing. Any subsections that did not contain a cesium-137 peak could be dated as prior to 1951. The second was that a maximum cesium-137 peak would be detected. If this was the case, the sub-sample that contained that peak could be dated to the year 1963. Nuclear testing continued and cesium increased in soils until 1963 when nuclear testing was banned. Therefore, a maximum peak of cesium-137 would indicate the year 1963.

3.3.9 Data Processing

PPCPs and pesticides were detected in the sediment core at significantly different concentrations making it difficult to compare the two groups in similar graphics. For this reason, it was decided that the concentration of the PPCPs in each sub-sample would be normalized to the concentrations in the sub-sample with the highest PPCP concentration. The first layer of the sediment core was found to contain the highest ΣPPCPs concentrations and the ΣPPCPs concentrations in each subsequent sub-sample was divided by that value to obtain the desired ratio. The same process was used to transform the Σpesticide concentrations into ratios. These ratio values were used to make the graphs in the remainder of this chapter.

3.4 Results

3.4.1 Ancillary Data

TOC varied in the sediment core, ranging from 0.85 – 3.45 %TOC with a median value of 1.55 %TOC. The %TOC of each the sediment sub-sample is depicted in Figure 3.3. There was no statistical difference in TOC among all the sub-samples (Kruskal-Wallis, $p>0.05$).

Grain size varied minimally in the sediment core, ranging from 4.5 – 11.3 μm with a median value of 5.4 μm. The PSA measurements of each the sediment sub-sample is depicted in Figure 3.3. There was no statistical difference in grain size among all the sites (Kruskal-Wallis, $p>0.05$).

The %moisture varied minimally in the sediment core, ranging from 51.1-68.1% with a median value of 60.1%. The %moisture measurements of each the sediment sub-sample is depicted in Figure 3.3. There was no statistical difference in %moisture among all the sites (Kruskal-Wallis, $p>0.05$).

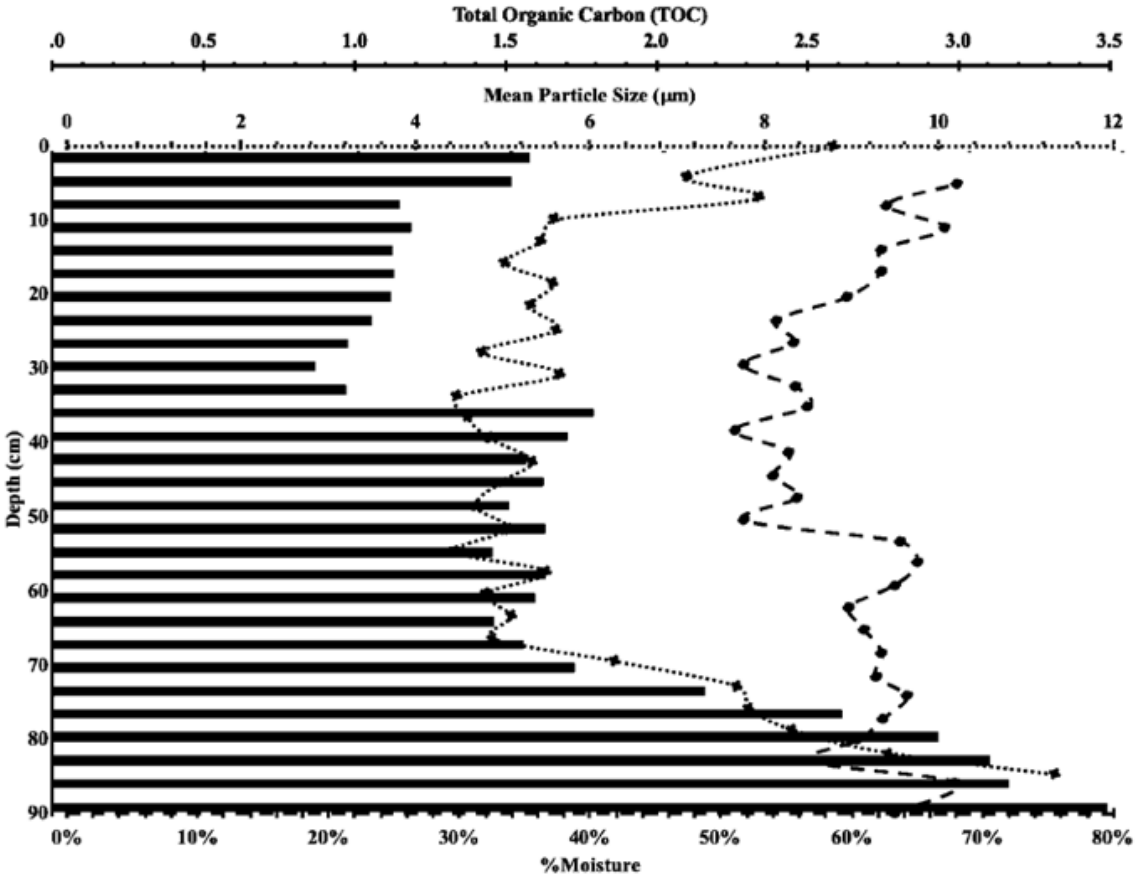

Figure 3.3: The %TOC (black bars), PSA (black dots), and %Moisture (black dashes) for each sub-sample obtained for the GC sediment core.

The TOC increases down core nearly doubling from 50 cm to 80 cm depth. It increases rapidly beginning at 70 cm. This corresponds to a similar increase in grain size at the same depth of 70 cm.

The sediment % moisture, % sand, % silt, and % clay varied minimally across all sub-samples. The results are summarized in Table 4.13A. The summary sand, silt, clay diagram for all sub-samples is found below in Figure 3.4.

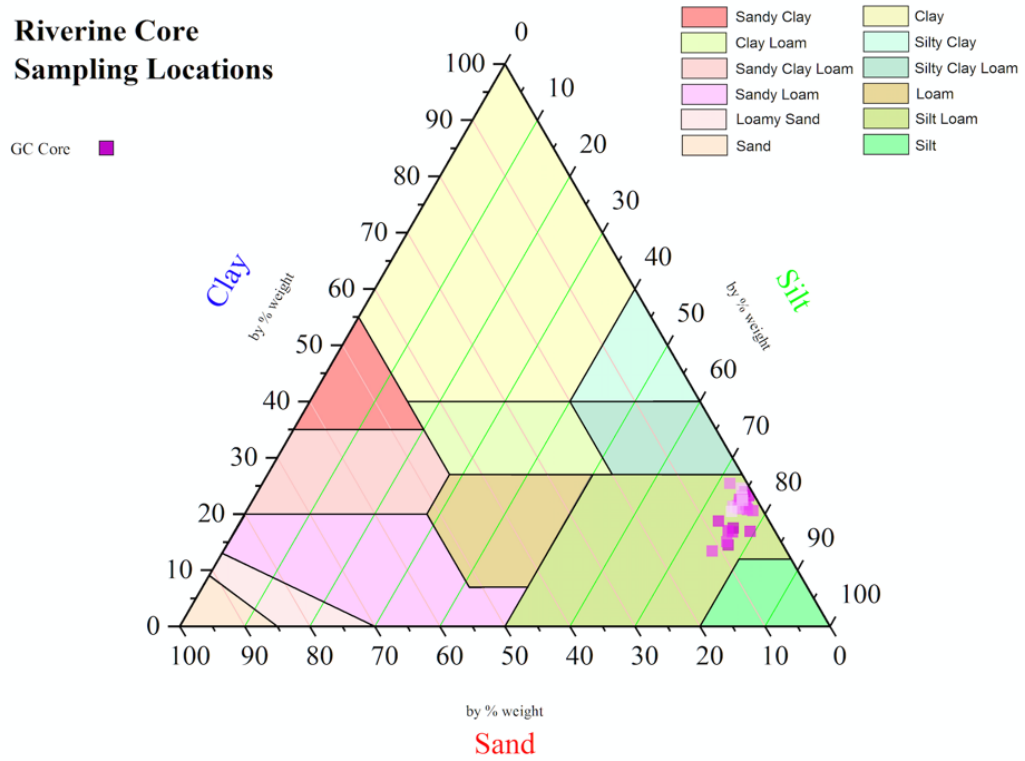

Figure 3.4: Summary % Sand, Silt, Clay diagram depicting the %Sand, %Silt, and %Clay for each subsection of the GC2 sediment core

The Gamma Spectrascope data revealed that all sub-samples contained detectable amounts of Cs-137. This means that the core does not date further back than 1951. In addition, there was no distinct maximum cesium-137 peak or timeline detected in any

subsection (Figure 3.5). Based in the gamma evidence, the entire core is likely to have been deposited post-1963. Given the high deposition rate or sediment in riverine areas, this is to be expected. A deeper core would need to be taken in these areas for the core to be more reliably dated.

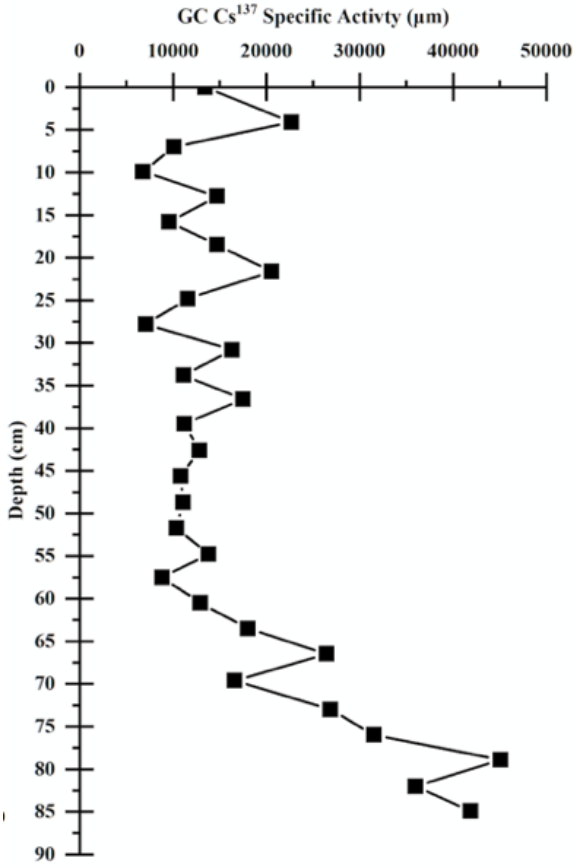

Figure 3.5: C^{137} Specific Activity for each sub-sample of the GC2 sediment core.

3.4.2 PPCPs in Sediment Cores

The types PPCPs found in the sediment cores in all subsections are comparable to those found in surficial sediment found previously (Chapter 1). The quantitation frequency (QF) of PPCPs in the sediment cores ranged from 31% to 98%, with a mean QF of 72%. Most observed PPCPs were detected throughout the core (i.e., 0 – 90 cm depths). The average concentration of each PPCP found in the sediment core is depicted in Figure 3.6.

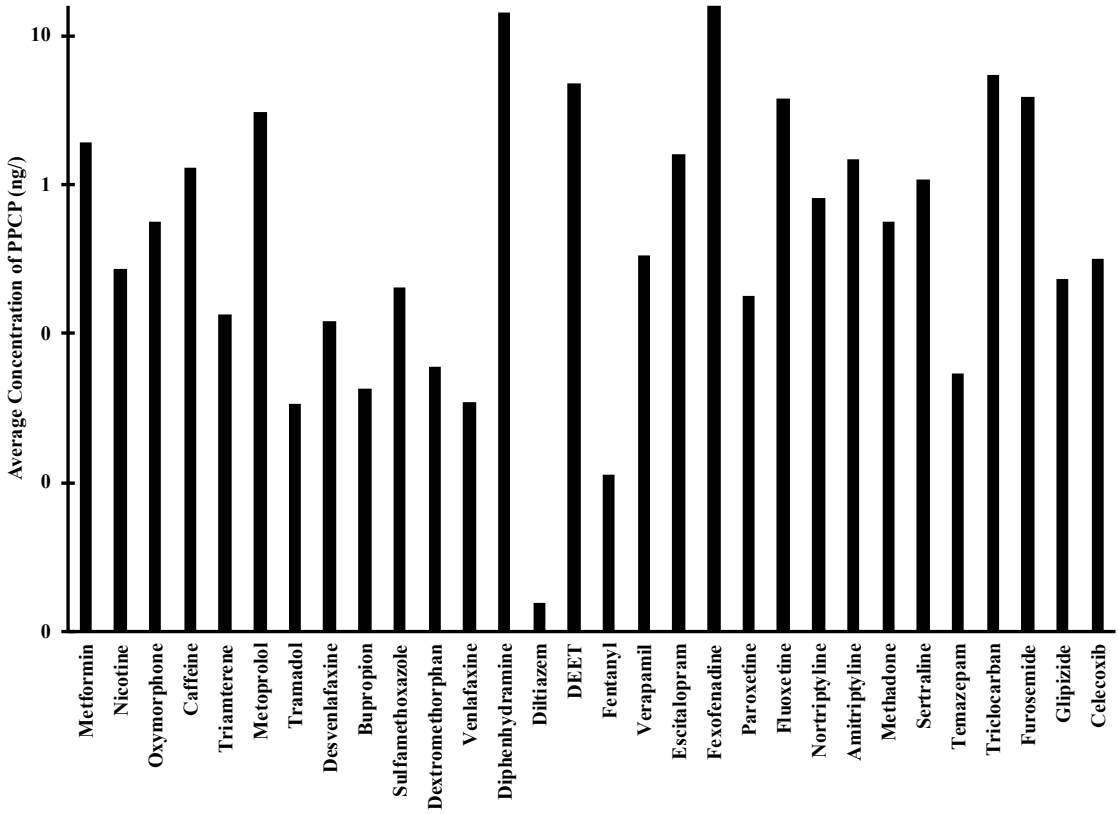

Figure 3.6: The average concentration of each individual PPCP found throughout the GC2 sediment core. The y-axis is present in a log scale in order to be able to include a wide range of concentrations.

The Σ_{30}PPCPs and $\Sigma_4$pesticides, when detected, for each subsection of each sediment core is depicted in Figure 3.7. As previously stated in the section entitled Data Analysis, the PPCPs and pesticide were found at significantly different concentrations. The ratios described in that section were used to construct Figure 3.7.

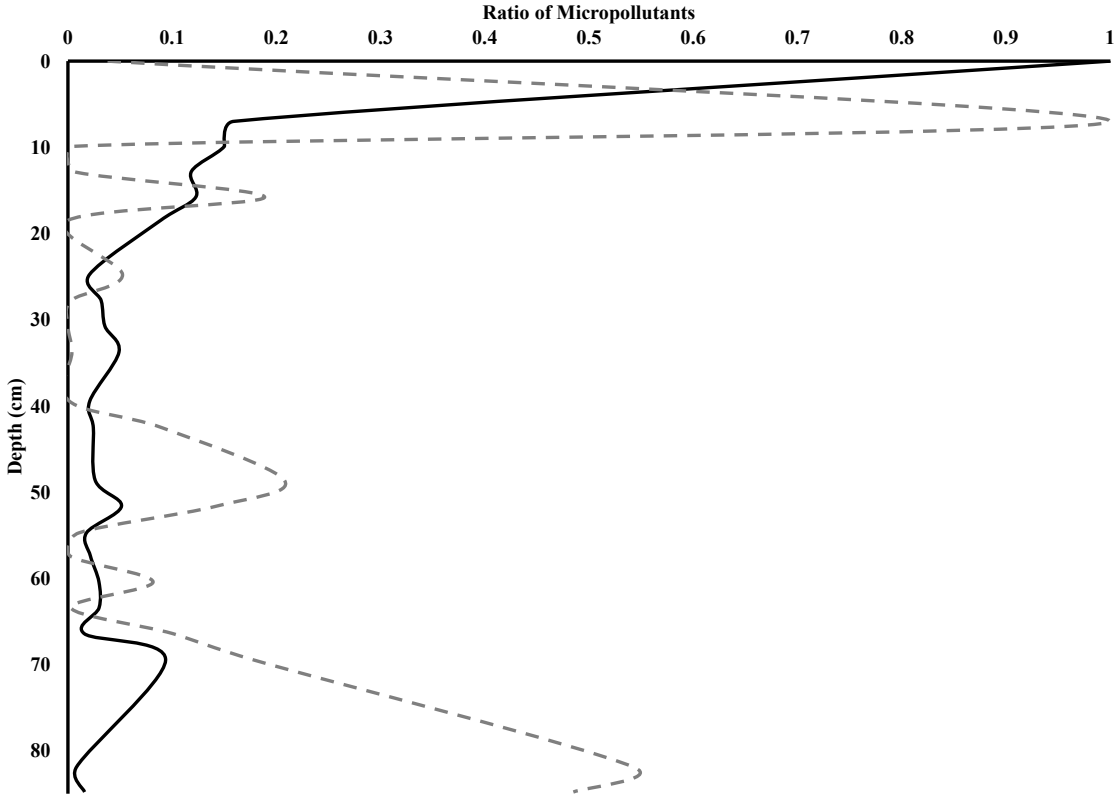

Figure 3.7: The Σ_{30}PPCPs (black) and $\Sigma_4$pesticides (gray, dashed) (normalized to the sub-samples with the highest concentrations) that were detected in each sub-sample of the GC2 sediment core.

The depth profiles for PPCPs differs from that of the pesticides in Gunston Cove. The highest concentrations of PPCPs were present in upper 5 cm of the core, and dropped off significantly with depth below 5 cm. In contrast, the OCs are found at varying

concentrations throughout the core. This is in line with the literature which states that pesticides are more likely to degrade on the top layers of sediment and be retained in lower layers of sediment that are acting as a sink. A Spearman's Rank Correlation (Rho = -0.02) was performed on the PPCP and Pesticide data and it was determined that there was no correlation between the two data sets.

3.5 Discussion

3.5.1 Age of Sediment Core based on Pesticide profiles

Several pesticides that were found as part of this analysis can be useful in determining an approximate date of the including DDE, DDD, OCs, and OPs as the regulation and use of these pesticides is well documented.[167–169]

However, the matrix also affected the detection of the pesticides of interest. For DDE and DDD, the detection was sporadic and with no general trend. DDE and DDD are degradation products of the pesticide, dichlorodiphenyltrichloroethane (DDT) which was introduced in approximately 1940s.[170] DDE was not found to be present in any of the sub-samples at a depth greater than 46 cm. However, DDD was found in almost all samples throughout the core. In addition, both compounds were found at significant concentrations at sub-samples approximately 7 cm deep. Given that DDT was banned for agricultural use in the USA by the EPA in 1972[171], DDE and DDD should not be present at such shallow depths of the core. It is highly likely that the matrix was more complex than anticipated and interfered with the accurate detection of these compounds. This was also evidenced by the concentrations of DDE and DDD found in the sub-sample at

approximately 20 cm. In addition to having the highest concentrations of DDE and DDD, the was the same subsection that included the highest OCs and OPs concentration. It is highly unlikely that all four groups were present at the highest concentration in the same sub-sample. Therefore, that sub-sample was excluded from analysis.

The OCs and OPs were detected in almost every sub-sample of the core. The highest concentration of OCs was found at the top of the core at approximately 10 cm while the highest concentration of OPs was found near the bottom of the core at approximately 82 cm. The presence of OPs and OCs throughout the core indicates that the core includes the 1970s when the majority of OPs and OCs were gaining popularity.[168,169] The depth profiles for DDE, DDD, OCs, and OPs can be found in Figure 3.8.

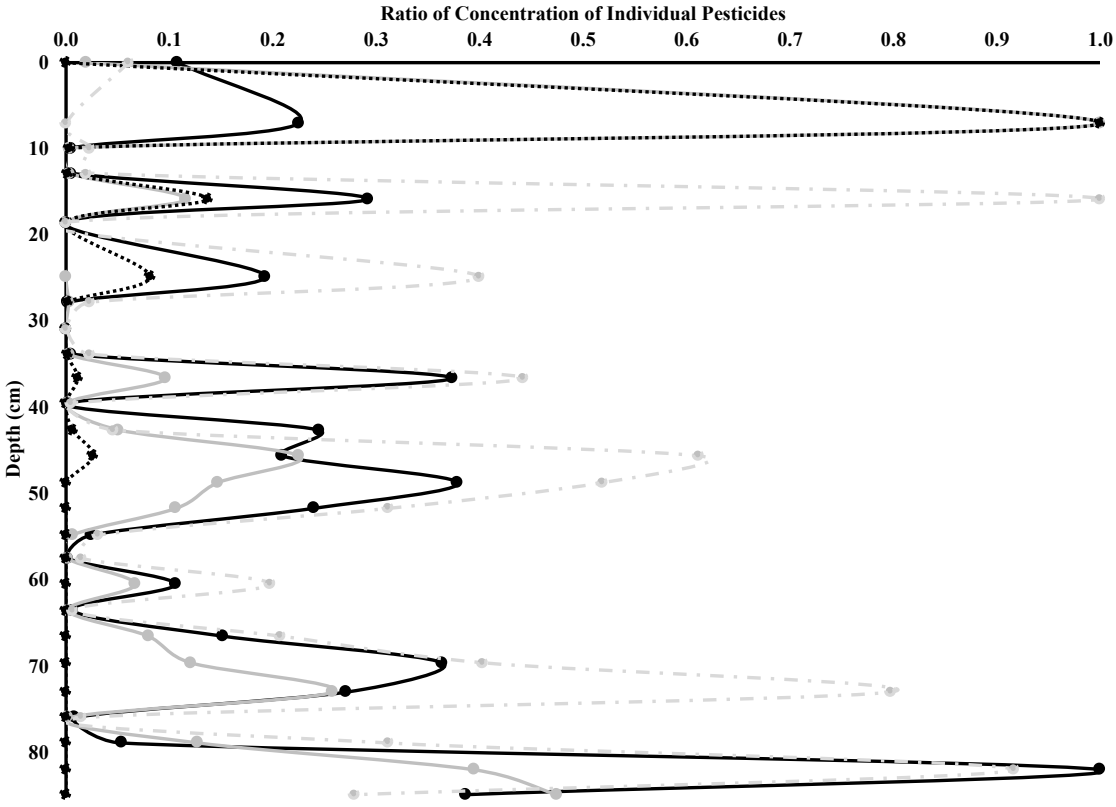

Figure 3.8: The concentrations of OPs (black), OCs (gray), DDE (black, dotted), and DDD (gray, dashed) detected in each sub-sample of the GC2 sediment core expressed as a ratio of the concentration of each subsection to the highest concentration found throughout the core.

3.5.2 Correlation Between PPCPs, Pesticides, TOC, and PSA

Spearman's Rank Correlations were carried out to determine the correlation between PPCPS vs grain size and PPCPs vs TOC. It was determined that PPCPs exhibited weak, positive correlations with grain (Rho = 0.165) and a moderate, negative correlation with TOC (Rho = -0.461). This observation is significant because it is in contrast with the pesticides which exhibited a stronger, positive correlation with grain (Rho = 0.250) and a moderate, positive correlation with TOC (Rho = 0.438).

These results indicate that the deposition of PPCPs is more dependent upon grain size of the sediment whereas, pesticides deposition is most heavily dependent on the TOC of the sediment. These results are in line with previous data that has found pesticides, particularly OCs, and TOC to be positively correlated.[172] This is likely due to the difference in physical properties between PPCPs and pesticides, such as K_{ow}, and the differences in the mode and rate of deposition of each group. Pesticides have much higher K_{ow} values than PPCPs, as such they more highly sorptive than PPCPs. Specifically, pesticides are known to exhibit high rates of sorption to organic matter in the sediment. As the amount of organic matter in the sediment is directly correlated to the TOC of the sediment, it follows that there would be a positive correlation between pesticide sorption and TOC. In contrast, it was previously demonstrated (Chapter 1) that the sorption of PPCPs to sediment was primarily influenced by the mineral surfaces found in the sediment. The stronger correlation between PPCP sorption and sediment grain size is consistent with these findings.

3.5.3 Cs-137 Depth Data

The Cs-137 depth data is the least significant in that the maxima did not yield a more precise date of the sediment core. However, the Cs-137 depth profile was able to provide valuable insight in about the depth profile of the core. If the sediment core was mixed, it would be expected that there would be no change in Cs-137 levels throughout the depth of the core. However, the spike is Cs-137 seen in Figure 3.5 indicates that the core is not mixed and this validates the integrity of the core depth profiles.

3.5.4 PPCP vs Pesticide Depth Profiles

As demonstrated in Figure 3.7, the PPCPs and pesticides have significantly different depth profiles. It is believed that this is due to the different methods of distribution of PPCPs and pesticides. It is known that WTPs are a primary source of PPCPs into the environment, specifically this sampling location. These PPCPs are being released into the aquatic environment at a continuous rate. Once released into the environment they are partitioning between the water column and sediment bed. The likelihood of a particular PPCP to partition into the sediment compartment is driven by the interactions with the mineral surfaces found in the active layer of the sediment bed. These interactions would allow for the PPCPs to remain in the active layer of the sediment where they would undergo different forms of degradation, evidenced by the fact that the PPCPs in the present study were not found to persist in the environment (Chapter 1). This can be seen in Figure 3.7 as the PPCPs were found in the highest concentration on the surface and very low levels throughout the remainder of the sediment core.

In contrast, pesticides often enter the environment as a result of individual applications of pesticides for use in agriculture. When pesticides enter the aquatic environment, they are more likely to undergo sorption to the sediments than remain in the water column due to their different physical properties such as large K_{ow} values. Once the pesticides have been sorbed onto the sediment they will partition with the organic matter over the mineral surfaces in the sediment. This is evidenced by the strong, positive correlation with TOC. These geosolids undergo deposition and carry with them the

sorbed pesticides. Therefore, the pesticides are more likely to experience burial than the PPCPs. This can be seen in Figure 3.7 as the pesticides were found at varying levels throughout the sediment core.

3.5.5 Comparison to other PPCP vs Pesticide Depth Profiles

A recent report was published examining the concentration depth profiles of PPCPs and pesticides in a European river.[155] There was no apparent trend in the depth profile of pesticides and it was stated that the pesticides were introduced into the environment under the same conditions as in the present study. These results are comparable to what was found in the present study

Interestingly, the highest concentrations of PPCPs in that study were found at a significant depth in the sediment core as opposed to being found at the surface in the present study. The high concentrations of PPCPs found at lower depths in the cores were attributed to sediment transported during high-discharge events via unnamed sources prior to sampling. Given the regulation and controls placed on WTPs in the USA, it is unlikely that there would be any unknown high-discharge events in this sampling area that would affect the depth profile in this way. As such, the two PPCP depth profiles are strikingly different.

3.6 Conclusion

The analysis of sediment cores has proven to be exceedingly useful in determining the concentrations and legacy of pesticides. While the methods used here

have been confirmed by multiple sources, the majority of these existing methods are for use in marshes and other low deposition areas. The high deposition rate present at the riverine sampling locations may make these procedures unsuitable for analysis of PPCPs and pesticides. In these high deposition areas, the core length will need to be at least doubled in order to obtain a core that can be dated using conventional methods.

Pesticides such as OCs, OPs, DDE, and DDD are derived mainly from soils that are eroded during episodic high runoff events and are thus shown by the peaks and valleys in the depth plot. These chemicals are legacy pesticides bound up in watershed soils and they are very stable and not subject to rapid biodegradation. Pesticides are also highly sorptive with high K_{ow} values.

PPCPs are deposited at high rates from WTP discharges (via particle deposition), and the profile reflects recent deposition that occurs at a constant steady-state level (thus, not episodic). Rapid decline of PPCPs with depth occurs via biodegradation or rapid desorption. PPCPs have rather low K_{ow} values and, as such, are much more labile than pesticides.

Regarding the matrix in these samples, more analysis will need to be done. The sediment core has an archived half that should be thawed, subsampled, and processed through the QuEChERS extraction process. Each sample should be run in triplicate and matrix spikes should be run on samples at multiple depths.

The goals of the present study were to (i) characterize the presence, spatial distribution, and temporal variability in the concentrations of PPCPs in water and sediments throughout the tidal freshwater Potomac River (TFWPR), (ii) evaluate the

interfacial dynamics of PPCPs in the TFWPR through the quantification of sediment-water fluxes along a downstream transect near a high capacity waste treatment facility, and (iii) investigate the burial profiles of PPCPs in river sediments.

Spatial analysis revealed that PPCP export from the TFWPR exceeded input, showing that the major WTPs markedly increase river concentrations. In addition, the greatest PPCP concentrations were generally found nearest the WTP outfalls. Seasonality in PPCP water concentrations was directly related to use patterns. Determination of PPCP sediment-water distribution constants indicated that mineral sorption likely plays a significant role sediment uptake.

Results from sediment-water fluxes showed that bed sediments near the WTP outfalls were accumulating PPCPs, and that fluxes reversed direction further downstream. It was determined that sediment can serve as either a sink or a source of PPCPs into the water column depending upon the location and distance from the outfall studied. In addition, it was found that bioturbation had a significant role in overall fluxes.

Lastly, the study also determined the nature of sediment burial and historical deposition profiles of PPCPs present in a sediment core taken from a location downstream of a high-capacity WTP in the Gunston Cove region. It was concluded that PPCPs have a significantly different historical depth profile when compared to other legacy micropollutants such as organochlorine pesticides because of the differences in their deposition rates, degradation processes, and different physical and chemical properties. Furthermore, the depth profiles suggested that PPCPs do not persist in sediments.

The present study demonstrated that understanding the sources, emissions, and effects of PPCPs in surface waters is essential to managing public health and enlightening our society about the environmental implications of overprescribed drug therapy. In addition, valuable information concerning the presence, spatial distribution, and temporal variability in the concentrations of PPCPs in water and sediments, the interfacial dynamics of PPCPs, and the burial profiles of PPCPs in river sediments was obtained as part of the effort to understand these matters.

APPENDIX

Table 4.1A: Properties, Uses, and Structures of Targeted Pharmaceuticals and Personal Care Products[141]

Name	CAS Number	Use	K_H (atm m^3 mol^{-1})	log(K_{OW})	Structure
Morphine	57-27-2	Acute and Chronic, Severe Pain Relief Medication	$2.672x10^{-15}$	0.89	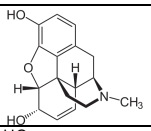
Oxymorphon	76-41-5	Acute and Severe Pain Relief & Preoperative Medication	$7.613x10^{-16}$	0.83	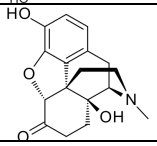
Hydromorphone	466-99-9	Morphine Alternative Pain Medication & Cough Suppressant	$1.109x10^{-13}$	1.60**	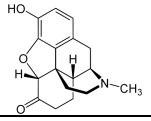
Naloxone	465-65-6	Opioid Blocker & Opioid Misuse Prevention	$1.294x10^{-14}$	2.09	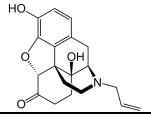
Codeine	76-57-3	Pain Relief, Antitussive, and Sedative Mediation	$6.192x10^{-15}$	1.19	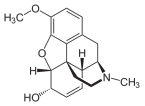
Naltrexone	16590-41-3	Opioid and Alcohol Dependence Management	$8.792x10^{-15}$	1.92	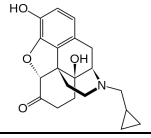
Hydrocodone	125-29-1	Severe Pain Relief and Antitussive Medication	$2.666x10^{-11}$	2.16	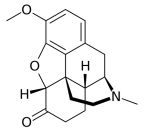
cis-Tramadol HCl	22204-88-2	Moderate to Moderately Severe Pain Relief	$1.376x10^{-10}$	2.51	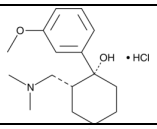
Meperidine	57-42-1	Severe Pain Relief Medication (Labor and Delivery)	$2.315x10^{-10}$	2.72	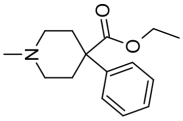
Fentanyl	437-38-7	Chronic Pain Management & Anesthesia and Sedative Medication	$1.111x10^{-8}$	4.05	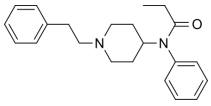

Buprenorphine	52485-79-7	Opioid Withdrawal & Chronic Pain Management	$1.615x10^{-13}$	4.98	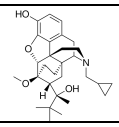
(±)-Methadone	76-99-3	Opioid Dependence/Detoxification & Chronic Pain Management	$9.407x10^{-9}$	3.93	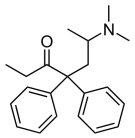
(±)-Amphetamine	300-62-9	Performance Enhancing Stimulant Medication & Recreational Use Illicit Drug	$1.968x10^{-6}$	1.76	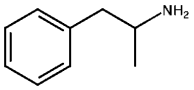
MDA	4764-17-4	Recreational Use Illicit Drug with Hallucinogenic & Psychedelic Effects	$1.771x10^{-8}$	1.64	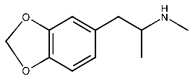
(±)-MDEA	82801-81-8	Recreational Use Illicit Drug with Psychedelic Effects	$8.945x10^{-8}$	2.77**	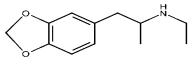
(±)-MDMA	42542-10-9	Recreational Use Illicit Drug with Euphoric & Psychedelic Effects	$1.066x10^{-8}$	2.28**	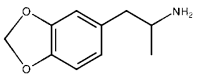
(±)-Methamphetamine	4846-07-5	Recreational Illicit Drug with Euphoric & Stimulant Effects	$6.619x10^{-8}$	2.07	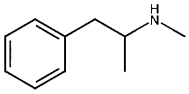
Phentermine	122-09-8	Appetite Suppressant and Enhancing Stimulant Medication	$2.506x10^{-6}$	1.90	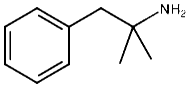
Azithromycin	83905-01-5	Antibiotic	$5.300x10^{-29}$	4.02	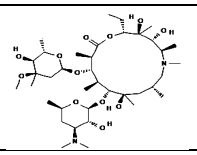
Ciprofloxacin	85721-33-1	Antibiotic	$1.082x10^{-17}$	0.28	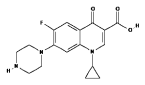
Enrofloxacin	93106-60-6	Antibiotic	$4.260x10^{-16}$	0.70	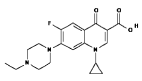
Sulfamethoxazole	723-46-6	Antibiotic	$1.099x10^{-11}$	0.89	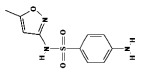

Penicillin G	61-33-6	Antibiotic	$1.884x10^{-13}$	1.83	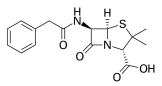
Tetracycline	60-54-8	Antibiotic	$3.137x10^{-25}$	-1.30	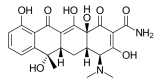
Sulfadimethoxine	122-11-2	Antimicrobial	$1.405x10^{-12}$	1.63	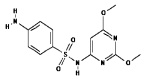
Sulfathiazole	72-14-0	Antimicrobial	$5.434x10^{-13}$	0.05	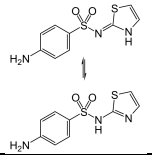
Sulfamethazine	57-68-1	Antibacterial	$8.776x10^{-13}$	0.89	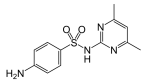
Triclocarban	101-20-2	Antibacterial	$2.314x10^{-09}$	4.90	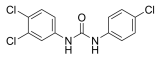
Sulfaquinoxaline	59-40-5	Antiparasitic	$9.853x10^{-14}$	1.68	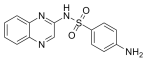
Acyclovir	59277-89-3	Antiviral	$5.749x10^{-19}$	-4.27	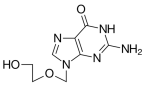
Alprazolam	28981-97-7	Antianxiety Medication	$5.117x10^{-10}$	2.12	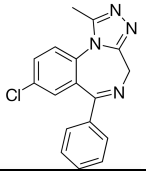
Clonazepam	1622-61-3	Antianxiety Medication	$8.595x10^{-13}$	2.41	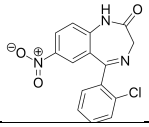
Oxazepam	604-75-1	Antianxiety and Insomnia	$1.098x10^{-13}$	3.35	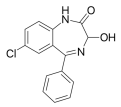
Diazepam	439-14-5	Antianxiety and Sedative	$6.502x10^{-10}$	2.82	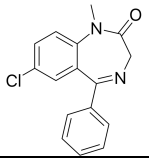

Nordiazepam	1088-11-5	Antianxiety and Sedative	3.942×10^{-10}	3.89	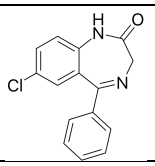
Nitrazepam	146-22-5	Antianxiety and Insomnia	1.482×10^{-12}	2.25	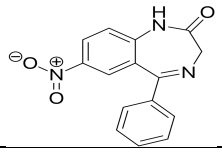
Temazepam	846-50-4	Insomnia	4.105×10^{-13}	2.19	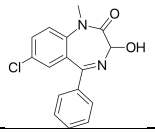
Lorazepam	846-49-1	Sedative and Epileptic Drug	1.475×10^{-13}	3.98	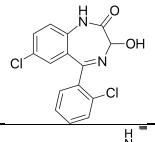
Paroxetine	61869-08-7	Selective Serotonin Reuptake Inhibitor	5.237×10^{-11}	2.57	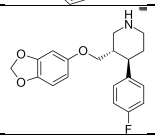
Escitalopram	128196-01-0	Selective Serotonin Reuptake Inhibitor	1.551×10^{-09}	3.74	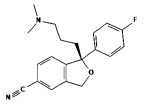
Fluoxetine	54910-89-3	Selective Serotonin Reuptake Inhibitor	2.675×10^{-07}	4.05	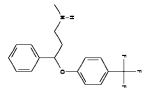
Sertraline	79617-96-2	Selective Serotonin Reuptake Inhibitor	1.340×10^{-07}	5.29	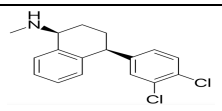
Desvenlafaxine	93413-62-8	Antidepressant	6.468×10^{-12}	2.72	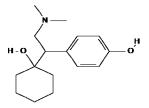
Bupropion	34911-55-2	Antidepressant	7.425×10^{-07}	3.85	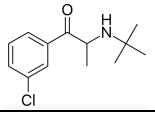
Venlafaxine	93413-69-5	Antidepressant	3.367×10^{-10}	3.28	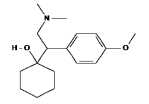
Nortriptyline	72-69-5	Antidepressant	3.456×10^{-07}	4.51	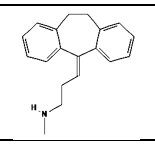

Amitriptyline	50-48-6	Antidepressant	1.604×10^{-07}	4.92	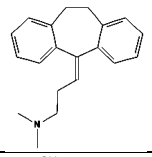
Formoterol	73573-87-2	Bronchodilator	5.164×10^{-18}	1.40	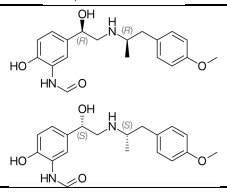
Albuterol	18559-94-9	Bronchodilator	9.325×10^{-15}	0.64	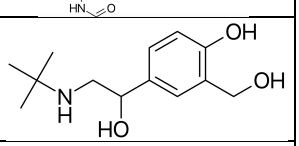
Atorvastatin	134523-00-5	Statin	2.400×10^{-23}	6.36	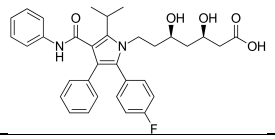
Atenolol	29122-68-7	Beta Blocker	3.933×10^{-13}	0.16	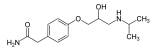
Metoprolol	51384-51-1	Beta Blocker	2.121×10^{-11}	1.88	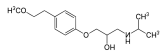
Propranolol	525-66-6	Beta Blocker	1.413×10^{-10}	3.48	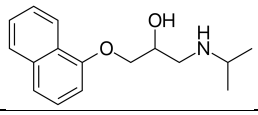
Nadolol	42200-33-9	Beta Blocker	1.794×10^{-15}	0.81	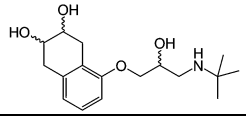
Clonidine	4205-90-7	Antihypertensive and Sedative	1.050×10^{-10}	1.85	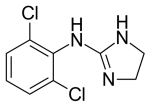
Diltiazem	42399-41-7	Antihypertensive and Calcium Blocker	1.321×10^{-12}	2.70	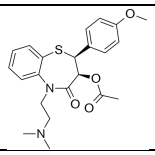
Enalapril	75847-73-3	Antihypertensive	1.505×10^{-14}	2.45	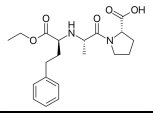
Verapamil	52-53-9	Calcium Channel Blocker and Antihypertensive Drug	5.592×10^{-10}	3.79	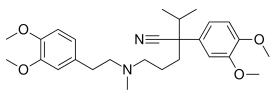

Lisinopril	83915-83-7	ACE Inhibitor	1.621×10^{-16}	-1.22	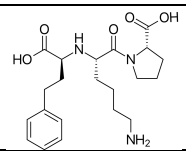
Triamterene	396-01-0	Diuretic	1.100×10^{-15}	0.98	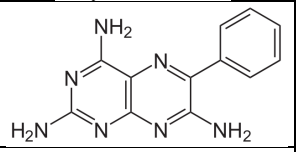
Hydrochlorothiazide	58-93-5	Diuretic	5.397×10^{-14}	-0.07	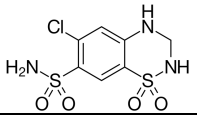
Furosemide	54-31-9	Diuretic	8.919×10^{-14}	2.03	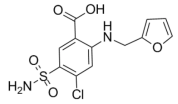
(+)-Propoxyphene	469-62-5	Analgesic	4.590×10^{-08}	4.18	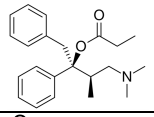
Gabapentin	60142-96-3	Nerve pain medication and anticonvulsant	1.475×10^{-14}	-1.10	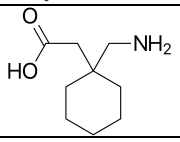
Benztropine	86-13-5	Anti-tremor	1.116×10^{-08}	4.28	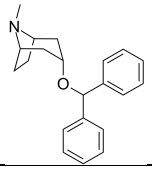
Carbamazepine	298-46-4	Anticonvulsant	1.549×10^{-09}	2.45	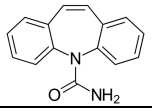
10_11-Carbamazepine epoxide	36507-30-9	Carbamazepine Metabolite	N/A	N/A	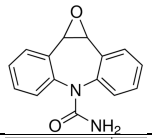
Celecoxib	169590-42-5	Nonsteroidal Anti-inflammatory Drug	1.387×10^{-10}	3.47	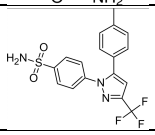
Diclofenac	15307-86-5	Nonsteroidal Anti-inflammatory Drug	5.296×10^{-09}	4.51	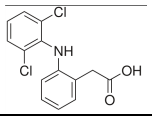
Metformin	657-24-9	Anti-diabetes Medication	2.023×10^{-09}	-1.40	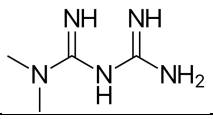

Glipizide	29094-61-9	Anti-diabetes Medication	$4.306x10^{-18}$	1.91	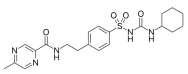
Warfarin	81-81-2	Blood Thinner	$8.373x10^{-14}$	2.70	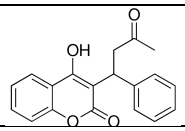
Bezafibrate	41859-67-0	Fibrate Drug	$2.380x10^{-11}$	4.25	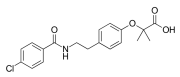
Budesonide	51333-22-3	Steroid	$8.274x10^{-15}$	3.98	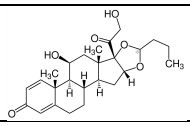
Caffeine	58-08-2	Central nervous system stimulant	$7.116x10^{-13}$	-0.07	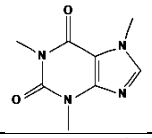
Nicotine	54-11-5	Stimulant	$6.831x10^{-09}$	1.17	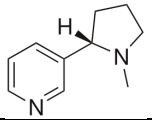
Cotinine	486-56-6	Nicotine Metabolite	$1.806x10^{-09}$	0.07	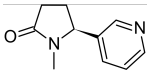
Dextromethorphan	125-71-3	Cough suppressant	$3.129x10^{-08}$	3.60	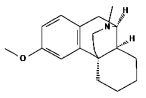
Naproxen	22204-53-1	Nonsteroidal Anti-inflammatory Drug	$2.656x10^{-09}$	3.18	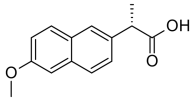
Diphenhydramine hydrochloride	58-73-1	Antihistamine	$5.373x10^{-09}$	3.27	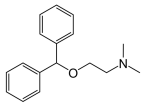
Fexofenadine	83799-24-0	Antihistamine		2.81	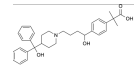
Loratadine	79794-75-5	Antihistamine	$4.176x10^{-07}$	5.20	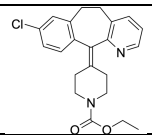
Promethazine	60-87-7	Antihistamine	$4.134x10^{-06}$	4.81	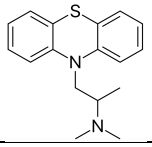

Ranitidine	66357-35-5	Antacid and Antihistamine	$2.349x10^{-11}$	0.27	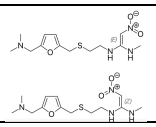
Cimetidine	51481-61-9	Antacid and Antihistamine	$6.215x10^{-14}$	0.57	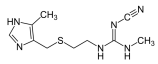
DEET	134-62-3	Insect Repellant	$1.251x10^{-06}$	2.18	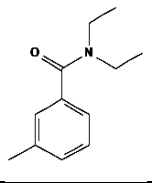
Atrazine Mercapturate	138722-96-0	Metabolite of Atrazine (Herbicide)	$2.253x10^{-14}$	1.88	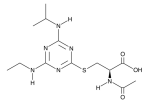
Aspartame	22839-47-0	Artificial Non-Saccharide Sweetener	$1.948x10^{-14}$	0.07	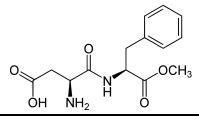
Perfluorooctanoic Acid	335-67-1	Industrial Surfactant	$3.044x10^{00}$	6.30	

Table 4.2A: List of Compounds, Type, and LC RT (min) for all compounds used in this analysis

Chemical	Type	LC RT (min)
Caffeine 13C3	ISTD	2.249
Oxycodone D3	ISTD	2.285
(±)-Methamphetamine D5	ISTD	2.000
Ciprofloxacin D8	ISTD	2.872
Sulfomethazine 13C6	ISTD	3.065
Diazepam D5	ISTD	6.339
Testosterone 13C3	ISTD	6.461
Hydrocodone D6	SSTD	2.436
(+/-)MDA D5	SSTD	1.968
Desethylatrazine 13C3	SSTD	2.848
Sulfomethoxazole 13C6	SSTD	3.735
Ethyl Paraben 13C6	SSTD	4.302
Norsertraline 13C6	SSTD	4.836
Alprazolam D5	SSTD	5.778
Benzophenone D10	SSTD	6.807
Metformin	Target	0.395
Nicotine	Target	0.452

trans-3'-Hydroxycotinine	Target	0.452
Cimetidine	Target	0.456
Cotinine	Target	0.456
Oxymorphone	Target	0.456
Acyclovir	Target	0.457
Albuterol (Salbutamol)	Target	0.457
Atenolol	Target	0.457
Ranitidine	Target	0.457
Morphine	Target	0.457
Hydromorphone	Target	1.000
Gabapentin	Target	1.491
(±)-Amphetamine	Target	1.666
Clonidine	Target	1.762
Naloxone	Target	1.881
Codeine	Target	1.970
MDA	Target	1.981
2-Hydroxy Ibuprofen	Target	1.985
Phentermine	Target	2.006
(±)-Methamphetamine	Target	2.019
Hydrochlorothiazide	Target	2.101
Nadolol	Target	2.119
Azithromycin	Target	2.130
Caffeine	Target	2.248
Naltrexone	Target	2.280
MDMA	Target	2.289
Sulfathiazole	Target	2.409
Aspartame	Target	2.410
Hydrocodone	Target	2.465
MDEA	Target	2.636
Triamterene	Target	2.667
Ciprofloxacin	Target	2.890
Metoprolol	Target	2.984
Sulfamethazine	Target	3.069
cis-Tramadol HCl	Target	3.124
Desvenlafaxine	Target	3.128
Enrofloxacin	Target	3.194
Formoterol	Target	3.277
Atrazine_Mercapturate	Target	3.307
Meperidine	Target	3.542
Penicillin G	Target	3.604
Bupropion	Target	3.651
Sulfamethoxazole	Target	3.732

Venlafaxine	Target	3.798
10_11-Carbamazepine epoxide	Target	4.245
Enalapril	Target	4.251
Propranolol	Target	4.330
Sulfadimethoxine	Target	4.467
Dextromethorphan	Target	4.576
Sulfaquinoxaline	Target	4.587
Diphenhydramine hydrochloride	Target	4.738
Fentanyl	Target	4.772
Escitalopram	Target	4.839
Buprenorphine	Target	4.960
Carbamazepine	Target	5.024
Furosemide	Target	5.100
Perfluorooctanoic Acid	Target	5.108
Diltiazem	Target	5.179
Promethazine	Target	5.228
Oxazepam	Target	5.269
Nitrazepam	Target	5.318
DEET	Target	5.329
Paroxetine	Target	5.344
Nordiazepam	Target	5.373
(±)-Lorazepam	Target	5.398
Fluoxetine	Target	5.541
Nortriptyline	Target	5.557
Propoxyphene	Target	5.577
Clonazepam	Target	5.711
Amitriptyline	Target	5.733
Verapamil	Target	5.737
Alprazolam	Target	5.802
Benztropine	Target	5.828
Fexofenadine	Target	5.850
Methadone	Target	5.885
Glipizide	Target	5.958
Sertraline	Target	5.964
Temazepam	Target	6.021
Loratadine	Target	6.063
Naproxen	Target	6.064
Flunitrazepam	Target	6.170
Bezafibrate	Target	6.197
Budesonide	Target	6.360
Diazepam	Target	6.388
Warfarin	Target	6.623

Diclofenac	Target	7.108
Atorvastatin	Target	7.170
Celecoxib	Target	7.206
Triclocarban	Target	7.352
Lisinopril	Target	7.463
Tetracycline	Target	7.768

Table 4.3A: List of PPCP MRM ions and quadrupole voltages used in LC/MS-MS analysis

Compound	MRM Ions (m/z)		Voltages (V)		
	Precursor	M1	Q1	Q2	Q3
		M2			
		M3			
Metformin	130.4	60.20	-10.0	-15.0	-10.0
		71.20	-11.0	-22.0	-12.0
		85.20	-10.0	-15.0	-15.0
Nicotine	163.3	130.30	-13.0	-22.0	-25.0
		117.30	-12.0	-28.0	-20.0
		132.30	-13.0	-19.0	-25.0
trans-3'-Hydroxycotinine	193.3	80.25	-15.0	-25.0	-15.0
		111.30	-14.0	-13.0	-20.0
		106.30	-15.0	-25.0	-22.0
Acyclovir	226.3	152.30	-10.0	-14.0	-27.0
		135.10	-10.0	-27.0	-26.0
		185.20	-17.0	-8.0	-17.0
Cimetidine	253.3	95.15	-10.0	-31.0	-17.0
		159.15	-10.0	-15.0	-10.0
		117.15	-10.0	-16.0	-21.0
Cotinine	177.3	80.20	-14.0	-26.0	-16.0
		98.25	-14.0	-30.0	-18.0
		136.20	-11.0	-13.0	-25.0
Albuterol	240.4	148.20	-10.0	-19.0	-28.0
		222.25	-10.0	-11.0	-14.0
		166.20	-10.0	-13.0	-17.0
Atenonol	267.3	145.25	-11.0	-26.0	-15.0
		190.25	-11.0	-20.0	-12.0
		225.20	-11.0	-18.0	-14.0
Ranitidine	315.3	176.25	-12.0	-18.0	-11.0

		130.20	-12.0	-26.0	-27.0
		102.20	-12.0	-35.0	-19.0
Azithromycin	591.5	116.10	-22.0	-35.0	-11.0
		158.40	-22.0	-31.0	-29.0
		186.50	-24.0	-37.0	-11.0
Gabapentin	172.4	154.30	-14.0	-14.0	-29.0
		137.30	-14.0	-20.0	-12.0
		95.20	-13.0	-23.0	-16.0
Morphine	286.4	152.20	-11.0	-51.0	-28.0
		201.20	-11.0	-25.0	-13.0
		165.20	-12.0	-40.0	-16.0
Oxymorphone	302.3	284.15	-12.0	-20.0	-19.0
		227.25	-12.0	-29.0	-14.0
		242.25	-12.0	-29.0	-16.0
Clonindine	230.2	44.20	-18.0	-25.0	-17.0
		213.15	-16.0	-26.0	-13.0
		160.25	-17.0	-34.0	-10.0
MDA d5	185.2	168.25	-14.0	-11.0	-11.0
		110.25	-13.0	-22.0	-22.0
		138.25	-14.0	-19.0	-14.0
2-Hydroxy Ibuprofen	221.3	180.25	-16.0	-10.0	-11.0
		121.20	-17.0	-29.0	-22.0
		139.15	-18.0	-19.0	-28.0
+/- Methamphetamine d5	155.2	92.15	-12.0	-21.0	-19.0
		91.15	-12.0	-21.0	-17.0
		121.20	-12.0	-14.0	-23.0
Hydromorphone	286.3	185.20	-12.0	-30.0	-11.0
		157.20	-12.0	-42.0	-15.0
		128.30	-12.0	-54.0	-23.0
Naldolol	310.4	254.35	-12.0	-19.0	-17.0
		201.30	-13.0	-23.0	-13.0
		236.20	-13.0	-21.0	-16.0
Caffeine	195.3	138.25	-15.0	-19.0	-26.0
		42.10	-15.0	-46.0	-14.0
		110.30	-14.0	-23.0	-21.0
Caffeine 13C3	198.1	140.20	-14.0	-19.0	-22.0
		112.20	-14.0	-23.0	-22.0
		43.15	-14.0	-35.0	-15.0
Oxycodone d3	319.2	301.2	-13.0	-20.0	-20.0
		244.20	-12.0	-29.0	-16.0
		259.20	-12.0	-26.0	-17.0
+/- Amphetamine	136.1	65.15	-13.0	-40.0	-26.0

		91.20	-13.0	-20.0	-20.0
		119.25	-13.0	-14.0	-23.0
MDA	180.4	163.25	-10.0	-12.0	-17.0
		105.15	-14.0	-21.0	-10.0
Naloxone	328.4	310.20	-13.0	-20.0	-22.0
		268.30	-13.0	-27.0	-12.0
Sulfathiazole	256.2	92.10	-10.0	-27.0	-16.0
		156.10	-10.0	-15.0	-10.0
		108.15	-10.0	-25.0	-20.0
Aspartame	295.3	120.35	-12.0	-28.0	-22.0
		180.30	-12.0	-15.0	-11.0
		235.25	-12.0	-15.0	-15.0
Penicillin G	335.3	289.15	-13.0	-27.0	-19.0
		128.10	-11.0	-28.0	-27.0
		91.20	-10.0	-42.0	-16.0
Hydrocodone d6	306.2	202.15	-12.0	-32.0	-20.0
		174.15	-12.0	-40.0	-18.0
		128.20	-12.0	-54.0	-23.0
Methamphetamine	150.0	91.20	-27.0	-25.0	-11.0
		65.20	-15.0	-40.0	-11.0
		119.25	-15.0	-15.0	-11.0
Triamterene	254.3	237.20	-10.0	-26.0	-16.0
		141.20	-10.0	-45.0	-13.0
		104.20	-10.0	-40.0	-18.0
Desethylatrazine 13C3	191.1	149.20	-14.0	-16.0	-14.0
		106.10	-14.0	-25.0	-20.0
		80.15	-14.0	-27.0	-16.0
Codeine	300.3	165.30	-12.0	-43.0	-10.0
		215.30	-12.0	-25.0	-13.0
		225.15	-23.0	-27.0	-15.0
Ciprofloxacin d8	340.1	322.25	-13.0	-22.0	-22.0
		235.15	-24.0	-38.0	-15.0
		296.25	-24.0	-19.0	-14.0
Ciprofloxacin	332.3	314.20	-13.0	-21.0	-14.0
		231.35	-13.0	-34.0	-15.0
		288.40	-13.0	-20.0	-13.0
Phentermine	150.0	91.20	-12.0	-35.0	-16.0
		65.10	-13.0	-41.0	-25.0
		39.20	-13.0	-50.0	-14.0
Metoprolol	268.4	116.20	-11.0	-20.0	-20.0
		56.20	-11.0	-29.0	-19.0
		133.25	-11.0	-25.0	-13.0

Sulfamethazine	279.3	186.20	-11.0	-19.0	-12.0
		92.20	-11.0	-31.0	-18.0
		124.20	-11.0	-22.0	-21.0
Sulfomethazine 13C6	285.1	186.10	-11.0	-19.0	-19.0
		124.20	-11.0	-24.0	-25.0
		98.15	-11.0	-29.0	-17.0
Naltrexone	342.4	324.20	-11.0	-23.0	-22.0
		270.30	-14.0	-27.0	-17.0
MDMA	194.4	163.35	-10.0	-14.0	-10.0
		105.15	-10.0	-23.0	-20.0
		135.20	-11.0	-20.0	-28.0
Enrofloxacin	360.3	316.40	-12.0	-20.0	-21.0
		342.35	-14.0	-26.0	-23.0
		245.15	-14.0	-29.0	-16.0
Formoterol	345.4	149.30	-13.0	-21.0	-28.0
		121.20	-11.0	-33.0	-22.0
		327.25	-14.0	-15.0	-23.0
Atrazine-Mercapturate	343.3	214.25	-14.0	-19.0	-14.0
		172.15	-13.0	-30.0	-11.0
		102.10	-14.0	-41.0	-19.0
Hydrocodone	300.3	199.20	-12.0	-29.0	-20.0
		171.15	-12.0	-39.0	-28.0
		128.20	-12.0	-54.0	-21.0
cis-Tramadol	264.0	58.20	-11.0	-22.0	-23.0
Desvenlafaxine	264.4	58.20	-11.0	-21.0	-10.0
		246.25	-11.0	-13.0	-16.0
		107.30	-11.0	-35.0	-20.0
MDEA	208.4	163.35	-11.0	-14.0	-10.0
		105.20	-11.0	-26.0	-18.0
		135.20	-10.0	-20.0	-26.0
Bupropion	240.3	184.20	-10.0	-13.0	-12.0
		131.20	-10.0	-25.0	-25.0
		130.25	-10.0	-40.0	-25.0
Sulfamethoxazole	254.3	92.10	-10.0	-30.0	-19.0
		65.10	-10.0	-44.0	-10.0
		108.25	-10.0	-22.0	-20.0
Sulfomethoxazole 13C6	260.1	162.10	-10.0	-15.0	-10.0
		98.10	-10.0	-27.0	-19.0
		114.10	-10.0	-23.0	-11.0
Ethyl Paraben 13C6	173.2	101.20	-13.0	-17.0	-19.0
		145.20	-13.0	-13.0	-15.0
		83.20	-13.0	-26.0	-16.0

Enalapril	377.4	234.2	-10.0	-20.0	-15.0
		91.15	-10.0	-54.0	-17.0
		117.30	-15.0	-38.0	-22.0
Propanolol	260.3	116.20	-11.0	-20.0	-22.0
		183.25	-11.0	-19.0	-18.0
		56.10	-11.0	-27.0	-22.0
Meripidine	248.4	174.20	-10.0	-20.0	-11.0
		220.35	-10.0	-22.0	-14.0
		70.20	-11.0	-30.0	-27.0
Sulfadimethoxine	311.3	156.25	-10.0	-21.0	-10.0
		92.10	-12.0	-36.0	-17.0
		108.20	-10.0	-33.0	-21.0
Dextromethorphan	272.4	215.25	-11.0	-24.0	-14.0
		171.20	-11.0	-39.0	-17.0
		147.20	-11.0	-29.0	-14.0
Sulfaquinoxaline	301.2	92.10	-12.0	-33.0	-17.0
		137.10	-12.0	-28.0	-26.0
		156.15	-10.0	-16.0	-15.0
Venlafaxine	278.4	58.25	-11.0	-21.0	-10.0
		260.30	-11.0	-13.0	-18.0
		121.20	-11.0	-29.0	-23.0
Diphenhydramine	256.3	167.20	-10.0	-19.0	-17.0
		152.20	-11.0	-36.0	-14.0
		165.20	-10.0	-40.0	-16.0
Diltiazem	415.3	178.20	-10.0	-25.0	-11.0
		150.20	-10.0	-45.0	-15.0
		109.25	-10.0	-55.0	-10.0
10,11-Carbamazepine Epoxide	253.3	180.30	-10.0	-30.0	-19.0
		236.20	-10.0	-11.0	-15.0
		210.15	-19.0	-14.0	-13.0
Promethazine	285.3	86.2	-11.0	-21.0	-16.0
		198.15	-11.0	-24.0	-20.0
		71.20	-11.0	-45.0	-12.0
DEET	192.3	91.20	-15.0	-32.0	-18.0
		119.25	-15.0	-20.0	-11.0
		89.60	-11.0	-19.0	-17.0
Propoxyphene	340.4	58.20	-13.0	-25.0	-10.0
		266.25	-13.0	-10.0	-18.0
		91.10	-14.0	-49.0	-17.0
Fentanyl	337.4	188.40	-14.0	-25.0	-12.0
		105.30	-14.0	-36.0	-20.0
		103.15	-14.0	-50.0	-19.0

Verapamil	455.4	165.30	-11.0	-28.0	-16.0
		150.35	-11.0	-41.0	-16.0
		303.25	-11.0	-28.0	-20.0
Escitalopram	325.4	109.10	-12.0	-28.0	-20.0
		262.20	-10.0	-21.0	-17.0
		234.10	-13.0	-29.0	-25.0
Norsertraline 13C6	281.0	159.05	-20.0	-20.0	-10.0
		123.10	-20.0	-44.0	-25.0
		89.15	-20.0	-54.0	-16.0
Benztropine	308.4	167.35	-12.0	-30.0	-10.0
		152.20	-12.0	-51.0	-15.0
		165.25	-12.0	-54.0	-16.0
Alprazolam d5	314.1	286.15	-12.0	-27.0	-19.0
		210.20	-12.0	-43.0	-21.0
		279.20	-12.0	-27.0	-19.0
Buprenorphine	468.5	396.30	-19.0	-41.0	-14.0
		55.25	-12.0	-47.0	-20.0
		414.35	-12.0	-35.0	-14.0
Fexofenadine	502.4	466.40	-20.0	-29.0	-16.0
		484.30	-20.0	-23.0	-17.0
		171.20	-20.0	-42.0	-11.0
Carbamazepine	237.3	194.25	-10.0	-19.0	-20.0
		192.25	-18.0	-22.0	-19.0
		193.25	-10.0	-32.0	-12.0
Loratadine	383.3	337.15	-15.0	-25.0	-24.0
		267.20	-14.0	-30.0	-18.0
		266.15	-15.0	-46.0	-17.0
Naproxen	185.3	170.20	-14.0	-18.0	-18.0
		141.20	-12.0	-30.0	-27.0
		153.10	-15.0	-21.0	-25.0
Oxazepam	287.2	241.10	-12.0	-23.0	-27.0
		269.10	-12.0	-17.0	-12.0
		104.15	-12.0	-35.0	-18.0
Paroxetine	330.3	192.40	-14.0	-22.0	-13.0
		70.25	-13.0	-29.0	-12.0
		44.20	-14.0	-23.0	-16.0
Fluoxetine	310.2	44.25	-13.0	-13.0	-16.0
		148.30	-13.0	-10.0	-15.0
		115.10	-13.0	-12.0	-16.0
Nordiazepam	271.2	140.25	-11.0	-29.0	-26.0
		226.25	-11.0	-28.0	-16.0
		165.20	-11.0	-28.0	-17.0

Bezafibrate	362.3	139.20	-15.0	-27.0	-13.0
		121.20	-12.0	-30.0	-11.0
		316.15	-14.0	-16.0	-20.0
Nitrazepam	282.3	236.20	-12.0	-25.0	-26.0
		180.25	-12.0	-37.0	-11.0
		207.30	-11.0	-35.0	-13.0
Diazepam d5	290.1	198.20	-11.0	-31.0	-21.0
		154.15	-11.0	-27.0	-16.0
		227.15	-11.0	-28.0	-10.0
Lorazepam	321.3	275.05	-12.0	-21.0	-19.0
		303.10	-13.0	-17.0	-14.0
		229.10	-13.0	-31.0	-15.0
Budesonide	431.4	413.30	-11.0	-13.0	-14.0
		237.35	-10.0	-31.0	-25.0
		173.40	-11.0	-29.0	-17.0
Nortriptyline	264.3	233.25	-11.0	-15.0	-15.0
		91.15	-11.0	-23.0	-17.0
		105.20	-11.0	-22.0	-21.0
Amitriptyline	278.4	233.30	-11.0	-19.0	-10.0
		91.15	-11.0	-28.0	-18.0
		117.30	-11.0	-22.0	-23.0
Methadone	310.4	265.25	-13.0	-16.0	-18.0
		105.25	-13.0	-29.0	-20.0
		77.20	-13.0	-54.0	-14.0
Clonazepam	316.3	270.10	-10.0	-26.0	-18.0
		241.10	-10.0	-36.0	-16.0
		214.25	-10.0	-38.0	-13.0
Alprazolam	309.3	281.15	-12.0	-27.0	-19.0
		205.30	-13.0	-41.0	-21.0
		274.25	-13.0	-26.0	-18.0
Sertraline	306.2	159.10	-12.0	-28.0	-16.0
		275.15	-12.0	-13.0	-12.0
Benzophenone d10	193.2	110.20	-14.0	-17.0	-20.0
		82.20	-14.0	-34.0	-15.0
		54.20	-15.0	-55.0	-21.0
Temazepam	301.2	255.20	-12.0	-23.0	-28.0
		283.15	-12.0	-14.0	-19.0
		177.15	-12.0	-40.0	-11.0
Flunitrazepam	314.2	268.30	-13.0	-27.0	-18.0
		239.15	-13.0	-34.0	-16.0
		183.20	-24.0	-53.0	-18.0
Diazepam	285.3	193.25	-12.0	-33.0	-12.0

		257.20	-12.0	-23.0	-17.0
		154.20	-12.0	-28.0	-15.0
Atorvastatin	559.3	250.00	-22.0	-48.0	-24.0
		440.40	-22.0	-24.0	-15.0
		380.15	-22.0	-31.0	-26.0
Triclocarban	315.2	127.10	-13.0	-29.0	-25.0
		93.15	-13.0	-40.0	-18.0
		128.15	-13.0	-20.0	-13.0
Lisinopril	406.4	84.25	-16.0	-30.0	-15.0
		365.10	-15.0	-16.0	-26.0
		245.40	-30.0	-30.0	-11.0
Tetracycline	445.2	341.10	-11.0	-19.0	-16.0
		429.15	-11.0	-15.0	-14.0
		73.30	-11.0	-38.0	-13.0
Hydorchlorothiazide	296.2	205.20	16.0	20.0	14.0
		121.20	15.0	30.0	11.0
		269.10	16.0	17.0	13.0
Furosemide	329.0	285.25	17.0	15.0	10.0
		205.15	17.0	23.0	21.0
		126.15	17.0	32.0	27.0
Perfluoroocatnoic Acid	413.0	369.15	21.0	10.0	13.0
		169.20	21.0	18.0	11.0
		119.20	22.0	24.0	15.0
Glipizide	444.2	319.25	23.0	22.0	11.0
		170.20	23.0	30.0	17.0
Warfarin	307.1	161.25	15.0	19.0	11.0
		250.30	16.0	23.0	12.0
		117.20	16.0	35.0	12.0
Diclofenac	239.9	250.05	15.0	11.0	12.0
Celecoxib	380.1	316.30	19.0	23.0	11.0
		276.25	19.0	30.0	13.0
		296.30	19.0	25.0	14.0

Table 4.4A: Average %RSD values for all PPCPs detected in water samples

Compound	Average %RSD
Glipizide	4.42%
Atorvastatin	12.04%

Fexofenadine	14.85%
Temazepam	15.09%
Cimetidine	16.56%
MDA	16.60%
cis-Tramadol HCl	16.75%
Nicotine	17.63%
Caffeine	17.92%
Venlafaxine	18.03%
Ranitidine	18.19%
10_11-Carbamazepine epoxide	18.26%
Carbamazepine	19.41%
DEET	19.44%
Triamterene	22.04%
Bupropion	23.74%
Atenolol	26.15%
Sulfamethoxazole	26.96%
Desvenlafaxine	28.68%
Diphenhydramine hydrochloride	30.44%
Cotinine	33.78%
Methadone	34.89%
Dextromethorphan	35.70%
Metoprolol	36.45%
Propranolol	38.49%
Celecoxib	40.96%
Sertraline	50.81%
Diltiazem	51.87%
Furosemide	51.87%
Hydrochlorothiazide	52.69%
Diclofenac	55.85%
Metformin	57.69%
Alprazolam	76.25%

Table 4.5A: Average %RSD values for all PPCPs detected in sediment samples

Compound	Average %RSD
Carbamazepine	2.32%
Caffeine	7.16%
Verapamil	14.56%

Desvenlafaxine	19.54%
Diphenhydramine hydrochloride	20.35%
Metformin	21.04%
Venlafaxine	24.19%
Escitalopram	24.52%
cis-Tramadol HCl	25.26%
Temazepam	25.87%
Nicotine	26.96%
Sertraline	28.69%
Dextromethorphan	29.29%
Triclocarban	29.30%
Nortriptyline	29.82%
Triamterene	30.70%
Fentanyl	30.88%
Fexofenadine	33.78%
Bupropion	35.78%
Propranolol	40.68%
Fluoxetine	41.14%
Methadone	41.49%
Diltiazem	41.86%
Metoprolol	42.17%
DEET	43.06%
Amitriptyline	50.34%
Glipizide	57.96%
Oxymorphone	59.79%
Diclofenac	75.65%
Celecoxib	117.31%
Paroxetine	129.01%
Furosemide	133.69%

Table 4.6A: Average Matrix Spike recovery percentages for all PPCPs water samples

Compound	Average Matrix Spike Recovery
Metformin	0.00%
Azithromycin	0.00%
Gabapentin	0.00%
2-Hydroxy Ibuprofen	0.00%

Hydromorphone	0.00%
Penicillin G	0.00%
(±)-Methamphetamine	0.00%
Codeine	0.00%
Ciprofloxacin	0.00%
Phentermine	0.00%
Naproxen	0.00%
Budesonide	0.00%
Triclocarban	0.00%
Lisinopril	0.00%
Tetracycline	0.00%
Perfluorooctanoic Acid	0.00%
Furosemide	4.52%
Acyclovir	4.54%
Fentanyl	5.90%
Promethazine	10.88%
trans-3'-Hydroxycotinine	12.38%
Hydrochlorothiazide	15.93%
Enrofloxacin	16.17%
Warfarin	23.65%
Flunitrazepam	27.53%
Diazepam	28.13%
Temazepam	29.45%
Fluoxetine	29.50%
Celecoxib	34.57%
Paroxetine	36.17%
Nortriptyline	37.14%
Diclofenac	37.20%
Sertraline	42.15%
Bezafibrate	44.72%
Glipizide	45.76%
Sulfathiazole	46.37%
Amitriptyline	51.40%
Sulfaquinoxaline	52.50%
Hydrocodone	52.63%
Ranitidine	54.62%
Aspartame	54.80%
Cimetidine	55.18%
Escitalopram	55.75%
Benztropine	56.25%
Methadone	56.80%
Diphenhydramine hydrochloride	57.86%

MDMA	59.16%
Nitrazepam	59.18%
Nordiazepam	59.44%
Bupropion	62.07%
Morphine	62.11%
Clonidine	63.69%
Clonazepam	64.46%
Albuterol (Salbutamol)	64.80%
(±)-Lorazepam	65.20%
Propranolol	67.70%
MDEA	69.26%
Dextromethorphan	69.44%
Diltiazem	69.62%
Carbamazepine	71.45%
Meperidine	71.96%
Nicotine	72.58%
Buprenorphine	73.30%
Alprazolam	74.25%
Loratadine	77.34%
Venlafaxine	78.72%
Oxymorphone	82.96%
Sulfamethazine	83.07%
Sulfadimethoxine	84.20%
Oxazepam	85.50%
Cotinine	86.22%
Atrazine_Mercapturate	86.58%
Propoxyphene	90.02%
10_11-Carbamazepine epoxide	91.12%
Verapamil	98.36%
MDA	102.17%
cis-Tramadol HCl	102.93%
Sulfamethoxazole	106.10%
Naltrexone	108.39%
Enalapril	110.95%
Metoprolol	120.76%
Atorvastatin	122.53%
Formoterol	136.05%
DEET	170.64%
Desvenlafaxine	178.64%
Atenolol	200.03%
Naloxone	223.99%
Caffeine	228.09%

Triamterene	236.04%
Fexofenadine	390.07%
Nadolol	607.22%

Table 4.7A: Average Matrix Spike recovery percentages for all PPCPs in sediment samples

Compound	Average Matrix Spike Recovery
trans-3'-Hydroxycotinine	0.00%
Acyclovir	0.00%
Azithromycin	0.00%
Gabapentin	0.00%
2-Hydroxy Ibuprofen	0.00%
Hydromorphone	0.00%
Aspartame	0.00%
Penicillin G	0.00%
(±)-Methamphetamine	0.00%
Codeine	0.00%
Ciprofloxacin	0.00%
Phentermine	0.00%
Enrofloxacin	0.00%
Naproxen	0.00%
Budesonide	0.00%
Atorvastatin	0.00%
Lisinopril	0.00%
Tetracycline	0.00%
Furosemide	0.00%
Bupropion	0.80%
Ranitidine	2.26%
Atrazine_Mercapturate	7.49%
Fentanyl	8.81%
Cimetidine	13.24%
Perfluorooctanoic Acid	19.12%
Enalapril	20.49%
Nicotine	25.12%
Bezafibrate	28.44%
Morphine	28.65%
Oxymorphone	34.13%

Temazepam	42.79%
Diazepam	43.30%
Flunitrazepam	44.59%
Metformin	45.57%
Hydrochlorothiazide	46.42%
Paroxetine	52.85%
Atenolol	54.15%
Albuterol (Salbutamol)	55.62%
Nortriptyline	61.31%
Diclofenac	65.31%
Nordiazepam	69.53%
Caffeine	69.72%
Fluoxetine	71.27%
Sertraline	71.88%
Promethazine	72.06%
DEET	76.97%
Propranolol	77.19%
Amitriptyline	77.53%
Celecoxib	79.82%
Formoterol	80.54%
Warfarin	81.47%
Nitrazepam	81.88%
Clonidine	83.66%
MDA	84.96%
Venlafaxine	85.33%
Methadone	85.77%
MDMA	86.33%
Carbamazepine	87.07%
Benztropine	87.36%
Meperidine	93.57%
Glipizide	94.85%
Sulfaquinoxaline	94.94%
Hydrocodone	94.97%
Dextromethorphan	95.08%
(±)-Lorazepam	95.35%
Clonazepam	96.89%
Oxazepam	97.32%
Buprenorphine	97.69%
Verapamil	98.59%
Loratadine	100.25%
Propoxyphene	101.20%
Sulfathiazole	105.01%

Sulfamethoxazole	108.41%
Triclocarban	111.54%
MDEA	112.22%
Metoprolol	116.47%
Alprazolam	117.13%
Cotinine	117.83%
Diltiazem	119.43%
cis-Tramadol HCl	119.53%
Sulfadimethoxine	121.94%
10_11-Carbamazepine epoxide	124.56%
Nadolol	124.97%
Triamterene	125.45%
Desvenlafaxine	150.68%
Escitalopram	159.00%
Sulfamethazine	174.44%
Naltrexone	192.68%
Fexofenadine	221.85%
Diphenhydramine hydrochloride	227.43%
Naloxone	398.50%

Table 4.8A: % Moisture, % Sand, % Silt, and % Clay for Sediment Samples

Sampling Locaiton	Sampling Trip	% Moisture	% Sand	% Silt	% Clay
HC1	T01	24.87	62.6	32.6	4.7
	T02	44.52	51.5	42.6	5.9
	T03	26.33	31.2	61.2	7.7
HC2	T01	32.83	10.6	73.2	16.2
	T02	53.71	31.8	61.3	7.0
	T03	50.28	17.2	74.1	8.7
	T04	70.81	32.3	60.0	7.7
HC3	T01	50.85	14.5	75.6	9.9
	T02	58.09	9.6	73.1	17.3
	T03	57.67	10.4	76.8	12.7
	T04	67.27	15.5	70.2	14.3
HC4	T01	49.69	15.7	71.1	13.2
	T02	46.29	55.2	38.7	6.1
	T03	50.58	12.6	74.3	13.1
	T04	71.08	25.3	66.1	8.6

HC5	T01	40.96	31.9	59.4	8.7
	T02	53.13	17.3	74.6	8.1
	T03	54.98	14.6	73.8	11.6
	T04	66.61	23.6	66.3	10.1
GC2	T01	58.99	4.8	81.3	13.9
	T02	56.07	5.3	79.1	15.6
	T03	56.66	3.0	83.0	13.9
	T04	73.04	4.8	80.8	14.4
GC3	T01	50.46	1.6	76.6	21.8
	T02	57.99	2.2	69.0	28.8
	T03	45.51	3.0	83.0	13.9
	T04	68.91	28.2	61.2	10.5
FMR3	T01	60.61	12.0	75.8	12.2
	T02	57.76	10.6	77.3	12.1
	T03	72.10	15.7	74.9	9.4
	T04	78.54	3.0	83.0	13.9

Table 4.9A: Total Suspended Matter for all water samples at all sites

Sampling Locaiton	Sampling Trip	TSM mg/L
CB1	T01	117.0
	T02	24.1
	T03	N/A
CR1	T01	9.42
	T02	0.804
	T03	16.3
	T04	23.5
HC1	T01	19.3
	T02	58.8
	T03	217*
	T04	28.9
HC2	T01	N/A
	T02	33.4
	T03	16.3

	T04	50.5
HC3	T01	N/A
	T02	31.9
	T03	14.5
	T04	43.7
HC4	T01	N/A
	T02	23.1
	T03	29.6
	T04	30.6
HC5	T01	N/A
	T02	27.4
	T03	16.4
	T04	69.0
GC1	T01	8.77
	T02	11.9
	T03	8.48
GC2	T01	N/A
	T02	17.8
	T03	5.52
	T04	8.67
GC3	T01	N/A
	T02	152
	T03	10.4
	T04	10.1
FMR1	T01	N/A
	T02	247*
	T03	0.540
	T04	3.67
FMR2	T01	N/A
	T02	240*
	T03	23.2
	T04	20.2
FMR3	T01	N/A
	T02	21.47
	T03	38.93
	T04	72.36
LP1	T01	29.70
	T02	86.04
	T03	23.34

Table 4.10A: PPCP Concentrations in Effluent sample from Alexandria Renew Enterprises in comparison to downstream of the WTP

PPCP	Average Concentration in Alex Renew Effluent (ng/L)	Average Concentration in UHC01 Water Samples (ng/L)	Average Concentration in UHC01 Sediment Samples (ng/g)
Present in Effluent and Downstream (Water, Sediment, or Both)			
Nicotine	272.562	23.005	7.700
Atenolol	3477.397	20.554	0.000
Ranitidine	2949.203	6.127	0.000
Caffeine	902.704	124.103	9.735
Metoprolol	992.189	39.718	2.675
cis-Tramadol HCl	915.646	38.571	9.721
Desvenlafaxine	5329.191	110.062	34.301
Bupropion	1891.388	9.049	0.000
Sulfamethoxazole	4692.180	65.836	0.000
Propranolol	292.333	0.000	3.144
Dextro- methorphan	793.103	0.000	1.283
Venlafaxine	1096.542	3.390	11.196
Diphenhydramine hydrochloride	3930.078	0.000	79.155
Diltiazem	447.568	0.000	2.077
DEET	215.426	63.959	0.312
Fentanyl	13.916	0.000	0.118
Verapamil	495.919	0.000	9.167
Escitalopram	1291.649	0.000	65.863
Fexofenadine	50215.876	387.303	96.499
Carbamazepine	2160.398	21.162	0.000
Celecoxib	1259.775	3.271	0.000
Present in Effluent and but NOT Downstream (Water, Sediment, or Both)			
Loratadine	38.460	0.000	0.000
Oxazepam	89.356	0.000	0.000
Fluoxetine	206.242	0.000	0.000
(±)-Lorazepam	78.727	0.000	0.000
Nortriptyline	42.279	0.000	0.000
Amitriptyline	518.945	0.000	0.000
Methadone	168.184	0.000	0.000
Alprazolam	34.316	0.000	0.000
Sertraline	1522.842	0.000	0.000

Temazepam	272.358	0.000	0.000
Atorvastatin	3687.946	0.000	0.000
Tetracycline	130.894	0.000	0.000
Hydrochlorothiazide	18245.856	0.000	0.000
Glipizide	151.075	0.000	0.000
Diclofenac	34.815	0.000	0.000
10_11-Carbamazepine epoxide	416.563	0.000	0.000
Phentermine	1434.205	0.000	0.000
Meth- amphetamine	1064.801	0.000	0.000
Azithromycin	93799.337	0.000	0.000
Gabapentin	30598.523	0.000	0.000
Triamterene	609.016	0.000	0.000
Metformin	6777.303	0.000	0.000
Not Present in Effluent but present Downstream (Water, Sediment, or Both)			
Cimetidine	0.000	3.955	0.000
Cotinine	0.000	4.939	-0.399
Furosemide	0.000	5.687	0.000
Not Present in Effluent or Downstream (Water or Sediment)			
3'-Hydroxy cotinine	0.000	0.000	0.000
Acyclovir	0.000	0.000	0.000
Albuterol	0.000	0.000	0.000
Morphine	0.000	0.000	0.000
Oxymorphone	0.000	0.000	0.000
Clonidine	0.000	0.000	0.000
2-Hydroxy-Ibuprofen	0.000	0.000	0.000
Hydromorphone	0.000	0.000	0.000
Nadolol	0.000	0.000	0.000
Sulfathiazole	0.000	0.000	0.000
Aspartame	0.000	0.000	0.000
Penicillin G	0.000	0.000	0.000
Naloxone	0.000	0.000	0.000
MDA	0.000	0.000	0.000
Codeine	0.000	0.000	0.000
Ciprofloxacin	0.000	0.000	0.000
Sulfamethazine	0.000	0.000	0.000
Naltrexone	0.000	0.000	0.000
MDMA	0.000	0.000	0.000
Enrofloxacin	0.000	0.000	0.000
Formoterol	0.000	0.000	0.000

Atrazine Mercapturate	0.000	0.000	0.000
Hydrocodone	0.000	0.000	0.000
MDEA	0.000	0.000	0.000
Enalapril	0.000	0.000	0.000
Meperidine	0.000	0.000	0.000
Sulfadimethoxine	0.000	0.000	0.000
Sulfaquinoxaline	0.000	0.000	0.000
Promethazine	0.000	0.000	0.000
Propoxyphene	0.000	0.000	0.000
Benztropine	0.000	0.000	0.000
Buprenorphine	0.000	0.000	0.000
Naproxen	0.000	0.000	0.000
Paroxetine	0.000	0.000	0.000
Nordiazepam	0.000	0.000	0.000
Bezafibrate	0.000	0.000	0.000
Nitrazepam	0.000	0.000	0.000
Budesonide	0.000	0.000	0.000
Clonazepam	0.000	0.000	0.000
Flunitrazepam	0.000	0.000	0.000
Diazepam	0.000	0.000	0.000
Triclocarban	0.000	0.000	0.000
Lisinopril	0.000	0.000	0.000
Warfarin	0.000	0.000	0.000
Perfluorooctanoic Acid	0.000	0.000	0.000

Table 4.11A: PPCP Concentrations in Effluent sample from Arlington Water Pollution Control Plant in comparison to downstream of the WTP

PPCP	Average Concentration in Arlington Water Pollution Control Plant Effluent (ng/L)	Average Concentration in FMR02 Water Samples (ng/L)	Average Concentration in FMR03 Sediment Samples (ng/g)
Present in Effluent and Downstream (Water, Sediment, or Both)			
Metformin	1538.212	4.900	0.000

Nicotine	37.291	76.586	0.000
Cotinine	78.337	9.357	0.000
Atenolol	360.650	8.394	0.000
Caffeine	71.903	283.700	0.000
Triamterene	81.934	5.849	57.690
Metoprolol	255.932	26.768	117.257
cis-Tramadol HCl	139.893	5.690	86.351
Desvenlafaxine	164.097	0.000	69.545
Bupropion	609.411	19.042	5.516
Sulfamethoxazole	228.063	2.514	0.000
Propranolol	47.896	1.172	31.403
Dextromethorphan	67.023	0.342	36.173
Venlafaxine	168.584766	5.293208523	79.4500811
Diphenhydramine hydrochloride	238.339	0.581	784.784
10_11-Carbamazepine epoxide	419.510	12.430	0.000
DEET	71.104	151.327	128.787
Escitalopram	136.271	0.000	407.302
Fexofenadine	13920.538	217.371	354.677
Carbamazepine	572.363	19.817	0.154
Fluoxetine	96.623	0.000	423.837
(±)-Lorazepam	16.333	0.000	0.000
Nortriptyline	12.815	0.000	22.058
Amitriptyline	22.094	0.000	46.639
Methadone	18.012	0.072	54.816
Alprazolam	6.913	0.000	0.000
Sertraline	224.0236	0.000	345.438
Hydrochlorothiazide	4412.220	35.981	0.000
Celecoxib	227.640	1.875	1.451
Present in Effluent and but NOT Downstream (Water, Sediment, or Both)			
Glipizide	14.058	0.000	0.000
Temazepam	55.975	0.000	0.000
Tetracycline	28.516	0.000	0.000
Loratadine	30.398	0.000	0.000
Oxazepam	14.057	0.000	0.000
Fentanyl	0.526	0.000	0.000
Verapamil	17.466	0.000	0.000
Diltiazem	7.394	0.000	0.000
Phentermine	180.086	0.000	0.000
Meth- amphetamine	131.508	0.000	0.000

Azithromycin	6914.168	0.000	0.000
Not Present in Effluent but present Downstream (Water, Sediment, or Both)			
Oxymorphone	0.000	0.000	12.421
MDA	0.000	54.506	0.000
Promethazine	0.000	0.004	0.000
Triclocarban	0.000	0.000	316.673
Not Present in Effluent or Downstream (Water or Sediment)			
3'-Hydroxy cotinine	0.000	0.000	0.000
Acyclovir	0.000	0.000	0.000
Cimetidine	0.000	0.000	0.000
Albuterol	0.000	0.000	0.000
Ranitidine	0.000	0.000	0.000
Gabapentin	0.000	0.000	0.000
Morphine	0.000	0.000	0.000
Clonidine	0.000	0.000	0.000
2-Hydroxy-Ibuprofen	0.000	0.000	0.000
Hydromorphone	0.000	0.000	0.000
Nadolol	0.000	0.000	0.000
Sulfathiazole	0.000	0.000	0.000
Aspartame	0.000	0.000	0.000
Penicillin G	0.000	0.000	0.000
Naloxone	0.000	0.000	0.000
Codeine	0.000	0.000	0.000
Ciprofloxacin	0.000	0.000	0.000
Sulfamethazine	0.000	0.000	0.000
Naltrexone	0.000	0.000	0.000
MDMA	0.000	0.000	0.000
Enrofloxacin	0.000	0.000	0.000
Formoterol	0.000	0.000	0.000
Atrazine Mercapturate	0.000	0.000	0.000
Hydrocodone	0.000	0.000	0.000
MDEA	0.000	0.000	0.000
Enalapril	0.000	0.000	0.000
Meperidine	0.000	0.000	0.000
Sulfadimethoxine	0.000	0.000	0.000
Sulfaquinoxaline	0.000	0.000	0.000
Propoxyphene	0.000	0.000	0.000
Benztropine	0.000	0.000	0.000
Buprenorphine	0.000	0.000	0.000
Naproxen	0.000	0.000	0.000

Paroxetine	0.000	0.000	0.000
Nordiazepam	0.000	0.000	0.000
Bezafibrate	0.000	0.000	0.000
Nitrazepam	0.000	0.000	0.000
Budesonide	0.000	0.000	0.000
Clonazepam	0.000	0.000	0.000
Flunitrazepam	0.000	0.000	0.000
Diazepam	0.000	0.000	0.000
Atorvastatin	0.000	0.000	0.000
Lisinopril	0.000	0.000	0.000
Furosemide	0.000	0.000	0.000
Perfluorooctanoic Acid	0.000	0.000	0.000
Warfarin	0.000	0.000	0.000
Diclofenac	0.000	0.000	0.000

Table 4.12A: Concentrations of PPCPs detected in surface water, pore-water, and sediment samples at sampling sites HC1, HC2 and HC3.

Compound	Environmental Sub-compartment	HC1	HC2	HC4
Metformin	Surface Water Concentration (ng/L)	0.59	3.35	3.08
	Pore-Water Concentration (ng/L)	5.17	4642	1724
	Sediment Concentration (ng/g)	2.83	2.68	0.994
Caffeine	Surface Water Concentration (ng/L)	124		
	Pore-Water Concentration (ng/L)	90.9		
	Sediment Concentration (ng/g)	9.74		
Triamterene	Surface Water Concentration (ng/L)	9.12	0.95	0.95
	Pore-Water Concentration (ng/L)	7.40	2017	41.5
	Sediment Concentration (ng/g)	0.72	9.93	0.33
Metoprolol	Surface Water Concentration (ng/L)	40.2	15.9	
	Pore-Water Concentration (ng/L)	181	856	
	Sediment Concentration (ng/g)	3.67	43.0	
Tramadol	Surface Water Concentration (ng/L)	42.0	15.1	0.62
	Pore-Water Concentration (ng/L)	62.1	33.7	6.85
	Sediment Concentration (ng/g)	10.0	0.32	0.72
Desvenlafaxine	Surface Water Concentration (ng/L)	113	44.2	1.50
	Pore-Water Concentration (ng/L)	522	12.0	1.90
	Sediment Concentration (ng/g)	34.3	0.83	0.89

Bupropion	Surface Water Concentration (ng/L)	11.1	4.12	
	Pore-Water Concentration (ng/L)	95.6	389	
	Sediment Concentration (ng/g)	0.20	0.89	
Propranolol	Surface Water Concentration (ng/L)	1.95		
	Pore-Water Concentration (ng/L)	6.61		
	Sediment Concentration (ng/g)	3.40		
Dextromethorphan	Surface Water Concentration (ng/L)	0.14	0.18	
	Pore-Water Concentration (ng/L)	7.16	0.01	
	Sediment Concentration (ng/g)	2.37	127	
Venlafaxine	Surface Water Concentration (ng/L)	7.93	2.47	
	Pore-Water Concentration (ng/L)	13.6	0.46	
	Sediment Concentration (ng/g)	11.2	69.2	
Diphenhydramine	Surface Water Concentration (ng/L)	0.74		0.74
	Pore-Water Concentration (ng/L)	2.28		0.04
	Sediment Concentration (ng/g)	79.2		14.8
DEET	Surface Water Concentration (ng/L)	64.0		
	Pore-Water Concentration (ng/L)	479		
	Sediment Concentration (ng/g)	0.31		
Carbamazepine	Surface Water Concentration (ng/L)	21.2		
	Pore-Water Concentration (ng/L)	108		
	Sediment Concentration (ng/g)	0.76		
Celecoxib	Surface Water Concentration (ng/L)	3.40		
	Pore-Water Concentration (ng/L)	28.6		
	Sediment Concentration (ng/g)	0.91		

Table 4.13A: % Moisture, % Sand, % Silt, and % Clay for GC2 Core Subsection Sediment Samples

Sampling Locaiton	SubSection	% Moisture	% Sand	% Silt	% Clay
GC2	S01	63.33%	8.39%	77.13%	14.48%
	S02	68.00%	3.82%	79.28%	16.90%
	S03	56.79%	6.61%	76.61%	16.79%
	S04	60.48%	2.24%	76.82%	20.94%
	S05	62.45%	1.55%	77.85%	20.60%
	S06	64.20%	3.47%	75.05%	21.48%
	S07	61.83%	3.22%	75.81%	20.97%
	S08	62.31%	2.92%	75.04%	22.03%
	S09	60.97%	4.27%	74.40%	21.34%

	S10	59.84%	1.28%	75.87%	22.85%
	S11	63.29%	3.93%	74.87%	21.20%
	S12	65.09%	1.10%	74.66%	24.24%
	S13	63.68%	1.13%	74.90%	23.97%
	S14	51.81%	0.85%	75.91%	23.24%
	S15	55.83%	2.11%	76.24%	21.65%
	S16	54.07%	2.63%	74.77%	22.61%
	S17	55.25%	1.87%	74.91%	23.23%
	S18	51.07%	2.28%	76.93%	20.79%
	S19	56.67%	2.68%	71.86%	25.46%
	S20	55.75%	3.60%	75.35%	21.05%
	S21	51.74%	2.03%	75.01%	22.96%
	S22	55.53%	2.24%	75.33%	22.43%
	S23	54.23%	1.30%	74.10%	24.61%
	S24	59.67%	4.92%	74.60%	20.48%
	S25	62.27%	6.14%	76.35%	17.50%
	S26	62.29%	7.78%	73.48%	18.74%
	S27	67.13%	7.12%	75.84%	17.04%
	S28	62.71%	8.29%	76.62%	15.09%
	S29	68.09%	11.40%	75.15%	13.45%

REFERENCES

(1) Meador, J. P.; Yeh, A.; Young, G.; Gallagher, E. P. Contaminants of Emerging Concern in a Large Temperate Estuary. *Environ. Pollut.* **2016**, *213*, 254–267. https://doi.org/10.1016/j.envpol.2016.01.088.

(2) Ebele, A. J.; Abou-Elwafa Abdallah, M.; Harrad, S. Pharmaceuticals and Personal Care Products (PPCPs) in the Freshwater Aquatic Environment. *Emerg. Contam.* **2017**, *3* (1), 1–16. https://doi.org/10.1016/j.emcon.2016.12.004.

(3) Mottaleb, M. A. Use of LC-MS and GC-MS Methods to Measure Emerging Contaminants Pharmaceutical and Personal Care Products (PPCPs) in Fish. *J. Chromatogr. Sep. Tech.* **2015**, *06* (03). https://doi.org/10.4172/2157-7064.1000267.

(4) Deo, R. P. Pharmaceuticals in the Surface Water of the USA: A Review. *Curr. Environ. Health Rep.* **2014**, *1* (2), 113–122. https://doi.org/10.1007/s40572-014-0015-y.

(5) Kolpin, D. W.; Furlong, E. T.; Meyer, M. T.; Thurman, E. M.; Zaugg, S. D.; Barber, L. B.; Buxton, H. T. Pharmaceuticals, Hormones, and Other Organic Wastewater Contaminants in U.S. Streams, 1999−2000: A National Reconnaissance. *Environ. Sci. Technol.* **2002**, *36* (6), 1202–1211. https://doi.org/10.1021/es011055j.

(6) González-Mariño, I.; Quintana, J. B.; Rodríguez, I.; Cela, R. Determination of Drugs of Abuse in Water by Solid-Phase Extraction, Derivatisation and Gas Chromatography–Ion Trap-Tandem Mass Spectrometry. *J. Chromatogr. A* **2010**, *1217* (11), 1748–1760. https://doi.org/10.1016/j.chroma.2010.01.046.

(7) Berset, J.-D.; Brenneisen, R.; Mathieu, C. Analysis of Llicit and Illicit Drugs in Waste, Surface and Lake Water Samples Using Large Volume Direct Injection High Performance Liquid Chromatography – Electrospray Tandem Mass Spectrometry (HPLC–MS/MS). *Chemosphere* **2010**, *81* (7), 859–866. https://doi.org/10.1016/j.chemosphere.2010.08.011.

(8) Lee, S. S.; Paspalof, A. M.; Snow, D. D.; Richmond, E. K.; Rosi-Marshall, E. J.; Kelly, J. J. Occurrence and Potential Biological Effects of Amphetamine on Stream Communities. *Environ. Sci. Technol.* **2016**, *50* (17), 9727–9735. https://doi.org/10.1021/acs.est.6b03717.

(9) Martin, C. B.; Ogden, C. L. Prescription Drug Use in the United States, 2015–2016. **2019**, No. 334, 8.

(10) Arya, G.; Tadayon, S.; Sadighian, J.; Jones, J.; de Mutsert, K.; Huff, T. B.; Foster, G. D. Pharmaceutical Chemicals, Steroids and Xenoestrogens in Water, Sediments and Fish from the Tidal Freshwater Potomac River (Virginia, USA). *J.*

Environ. Sci. Health Part A **2017**, *52* (7), 686–696. https://doi.org/10.1080/10934529.2017.1312975.

(11) de Solla, S. R.; Gilroy, è. A. M.; Klinck, J. S.; King, L. E.; McInnis, R.; Struger, J.; Backus, S. M.; Gillis, P. L. Bioaccumulation of Pharmaceuticals and Personal Care Products in the Unionid Mussel Lasmigona Costata in a River Receiving Wastewater Effluent. *Chemosphere* **2016**, *146*, 486–496. https://doi.org/10.1016/j.chemosphere.2015.12.022.

(12) Parolini, M.; Magni, S.; Castiglioni, S.; Binelli, A. Genotoxic Effects Induced by the Exposure to an Environmental Mixture of Illicit Drugs to the Zebra Mussel. *Ecotoxicol. Environ. Saf.* **2016**, *132*, 26–30. https://doi.org/10.1016/j.ecoenv.2016.05.022.

(13) Andrés-Costa, M. J.; Andreu, V.; Picó, Y. Analysis of Psychoactive Substances in Water by Information Dependent Acquisition on a Hybrid Quadrupole Time-of-Flight Mass Spectrometer. *J. Chromatogr. A* **2016**, *1461*, 98–106. https://doi.org/10.1016/j.chroma.2016.07.062.

(14) Martínez Bueno, M. J.; Uclés, S.; Hernando, M. D.; Fernández-Alba, A. R. Development of a Solvent-Free Method for the Simultaneous Identification/Quantification of Drugs of Abuse and Their Metabolites in Environmental Water by LC–MS/MS. *Talanta* **2011**, *85* (1), 157–166. https://doi.org/10.1016/j.talanta.2011.03.051.

(15) Bradley, P. M.; Journey, C. A.; Button, D. T.; Carlisle, D. M.; Clark, J. M.; Mahler, B. J.; Nakagaki, N.; Qi, S. L.; Waite, I. R.; VanMetre, P. C. Metformin and Other Pharmaceuticals Widespread in Wadeable Streams of the Southeastern United States. *Environ. Sci. Technol. Lett.* **2016**, *3* (6), 243–249. https://doi.org/10.1021/acs.estlett.6b00170.

(16) Bodík, I.; Mackuľak, T.; Fáberová, M.; Ivanová, L. Occurrence of Illicit Drugs and Selected Pharmaceuticals in Slovak Municipal Wastewater. *Environ. Sci. Pollut. Res.* **2016**, *23* (20), 21098–21105. https://doi.org/10.1007/s11356-016-7415-5.

(17) Choi, K.; Kim, Y.; Park, J.; Park, C. K.; Kim, M.; Kim, H. S.; Kim, P. Seasonal Variations of Several Pharmaceutical Residues in Surface Water and Sewage Treatment Plants of Han River, Korea. *Sci. Total Environ.* **2008**, *405* (1–3), 120–128. https://doi.org/10.1016/j.scitotenv.2008.06.038.

(18) Boleda, M. R.; Galceran, M. T.; Ventura, F. Monitoring of Opiates, Cannabinoids and Their Metabolites in Wastewater, Surface Water and Finished Water in Catalonia, Spain. *Water Res.* **2009**, *43* (4), 1126–1136. https://doi.org/10.1016/j.watres.2008.11.056.

(19) Zhang, Y.; Zhang, T.; Guo, C.; Lv, J.; Hua, Z.; Hou, S.; Zhang, Y.; Meng, W.; Xu, J. Drugs of Abuse and Their Metabolites in the Urban Rivers of Beijing, China: Occurrence, Distribution, and Potential Environmental Risk. *Sci. Total Environ.* **2017**, *579*, 305–313. https://doi.org/10.1016/j.scitotenv.2016.11.101.

(20) Stromgaard, K.; Krogsgaard-Larsen, P.; Madsen, U. *Textbook of Drug Design and Discovery, Fourth Edition*; CRC Press, 2009.

(21) WHO | Information sheet on opioid overdose http://www.who.int/substance_abuse/information-sheet/en/ (accessed Jan 28, 2018).
(22) DEA Strategic Intelligence Section. 2015 NDTA Report.Pdf. DEA 2015.
(23) Blau, M. STAT forecast: Opioids could kill nearly 500,000 in U.S. in next decade https://www.statnews.com/2017/06/27/opioid-deaths-forecast/ (accessed Jan 28, 2018).
(24) Klee, H. *Amphetamine Misuse: International Perspectives on Current Trends*; CRC Press, 1997.
(25) Amphetamines | Drug Aware http://drugaware.com.au/getting-the-facts/faqs-ask-a-question/amphetamines/#why-do-people-take-amphetamines (accessed Jan 23, 2018).
(26) CDC Press Releases https://www.cdc.gov/media/releases/2016/p0503-unnecessary-prescriptions.html (accessed Aug 1, 2019).
(27) Antibiotic Overprescribing: Still a Major Concern. *J. Fam. Pract.* **2017**, *66* (12).
(28) Overprescribed: High Cost Isn't America's Only Drug Problem. *STAT*, 2019.
(29) What Is Mental Health? | MentalHealth.gov https://www.mentalhealth.gov/basics/what-is-mental-health (accessed Aug 1, 2019).
(30) FEDERAL WATER POLLUTION CONTROL ACT. **2002**, 234.
(31) Much ado about pharma residue: EPA rule aims to end waste flushing https://www.wastedive.com/news/much-ado-about-pharma-residue-epa-rule-aims-to-end-waste-flushing/545159/ (accessed Oct 10, 2019).
(32) ICPRB; Drive, 30 West Gude; Suite 450; Rockville; Md 20850 301.984.1908. Potomac Basin Facts https://www.potomacriver.org/potomac-basin-facts/ (accessed Aug 1, 2019).
(33) *A Water-Quality Study of the Tidal Potomac River and Estuary: An Overview*; 1984. https://doi.org/10.3133/wsp2233.
(34) Ecology and Vulnerability Coastal: Estuaries & embayments | Massachusetts Wildlife Climate Action Tool http://climateactiontool.org/ecogroup/coastal-estuaries-embayments (accessed Aug 1, 2019).
(35) Infrastructure Overview https://alexrenew.com/helping-our-community/infrastructure-overview (accessed Oct 23, 2019).
(36) Arlington Water Pollution Control Plant Upgrade and Expansion | Balfour Beatty US https://www.balfourbeattyus.com/our-work/project-portfolio/arlington-water-pollution-control-plant-upgrade-an (accessed Oct 23, 2019).
(37) Ent_ovent.Pdf.
(38) About DC Water | DCWater.com https://www.dcwater.com/about-dc-water (accessed Oct 23, 2019).
(39) Land Use.
(40) US Department of Commerce, N. O. and A. A. NOAA's National Ocean Service Education: Estuaries https://oceanservice.noaa.gov/education/kits/estuaries/media/supp_estuar05e_fresh.html (accessed Aug 1, 2019).

(41) Ocean and River Chemistry https://eesc.columbia.edu/courses/ees/lithosphere/hays_tutorial_3/hydro.htm (accessed Aug 1, 2019).
(42) River Chemistry - an overview | ScienceDirect Topics https://www.sciencedirect.com/topics/earth-and-planetary-sciences/river-chemistry (accessed Aug 1, 2019).
(43) Xing, B.; Senesi, N.; Huang, P. M. *Biophysico-Chemical Processes of Anthropogenic Organic Compounds in Environmental Systems*; John Wiley & Sons, 2011.
(44) Salimiasl, S. M.; Mousavi, Z.; Akhgari, M. Comparison of the Modified QuEChERS Method and the Conventional Method of Extraction in Forensic Medicine to Detect Methadone in Post-Mortem Urine by GCMS. *Asia Pac. J. Med. Toxicol.* **2017**, *6* (3), 79–85.
(45) Dulaurent, S.; El Balkhi, S.; Poncelet, L.; Gaulier, J.-M.; Marquet, P.; Saint-Marcoux, F. QuEChERS Sample Preparation Prior to LC-MS/MS Determination of Opiates, Amphetamines, and Cocaine Metabolites in Whole Blood. *Anal. Bioanal. Chem.* **2016**, *408* (5), 1467–1474. https://doi.org/10.1007/s00216-015-9248-3.
(46) The QuEChERS Approach to Determine Pharmaceuticals and Toxins in Whole Blood.Pdf.
(47) QuEChERS 101- The Basics and Beyond.Pdf.
(48) Ramnarine, R.; Voroney, R. P.; Wagner-Riddle, C.; Dunfield, K. E. Carbonate Removal by Acid Fumigation for Measuring the Δ13C of Soil Organic Carbon. *Can. J. Soil Sci.* **2011**, *91* (2), 247–250. https://doi.org/10.1139/CJSS10066.
(49) USGS 01646502 POTOMAC RIVER (ADJUSTED) NEAR WASH, DC https://waterdata.usgs.gov/nwis/inventory?agency_code=USGS&site_no=01646502 (accessed Oct 23, 2019).
(50) USGS 01653000 CAMERON RUN AT ALEXANDRIA, VA https://waterdata.usgs.gov/nwis/inventory?agency_code=USGS&site_no=01653000 (accessed Oct 23, 2019).
(51) USGS 01654000 ACCOTINK CREEK NEAR ANNANDALE, VA https://waterdata.usgs.gov/nwis/inventory?agency_code=USGS&site_no=01654000 (accessed Oct 23, 2019).
(52) USGS 01652500 FOURMILE RUN AT ALEXANDRIA, VA https://waterdata.usgs.gov/nwis/inventory?agency_code=USGS&site_no=01652500 (accessed Oct 23, 2019).
(53) He, W.; Yang, C.; Liu, W.; He, Q.; Wang, Q.; Li, Y.; Kong, X.; Lan, X.; Xu, F. The Partitioning Behavior of Persistent Toxicant Organic Contaminants in Eutrophic Sediments: Coefficients and Effects of Fluorescent Organic Matter and Particle Size. *Environ. Pollut.* **2016**, *219*, 724–734. https://doi.org/10.1016/j.envpol.2016.07.014.
(54) Sheppard, S.; Long, J.; Sanipelli, B.; Sohlenius, G. Solid/Liquid Partition Coefficients (Kd) for Selected Soils and Sediments at Forsmark and Laxemar-Simpevarp. 72.

(55) 20872se8-003,20625se8-010_allegra_lbl.Pdf.
(56) Fekadu, S.; Alemayehu, E.; Dewil, R.; Van der Bruggen, B. Pharmaceuticals in Freshwater Aquatic Environments: A Comparison of the African and European Challenge. *Sci. Total Environ.* **2019**, *654*, 324–337. https://doi.org/10.1016/j.scitotenv.2018.11.072.
(57) Kosonen, J.; Kronberg, L. The Occurrence of Antihistamines in Sewage Waters and in Recipient Rivers. *Environ. Sci. Pollut. Res.* **2009**, *16* (5), 555–564. https://doi.org/10.1007/s11356-009-0144-2.
(58) Archer, E.; Petrie, B.; Kasprzyk-Hordern, B.; Wolfaardt, G. M. The Fate of Pharmaceuticals and Personal Care Products (PPCPs), Endocrine Disrupting Contaminants (EDCs), Metabolites and Illicit Drugs in a WWTW and Environmental Waters. *Chemosphere* **2017**, *174*, 437–446. https://doi.org/10.1016/j.chemosphere.2017.01.101.
(59) 017963s062,018704s021lbl.Pdf.
(60) Batt, A. L.; Kincaid, T. M.; Kostich, M. S.; Lazorchak, J. M.; Olsen, A. R. Evaluating the Extent of Pharmaceuticals in Surface Waters of the United States Using a National-Scale Rivers and Streams Assessment Survey. *Environ. Toxicol. Chem.* **2016**, *35* (4), 874–881. https://doi.org/10.1002/etc.3161.
(61) Maurer, M.; Escher, B.; Richle, P.; Schaffner, C.; Alder, A. Elimination of β-Blockers in Sewage Treatment Plants. *Water Res.* **2007**, *41* (7), 1614–1622. https://doi.org/10.1016/j.watres.2007.01.004.
(62) Gabet-Giraud, V.; Miège, C.; Jacquet, R.; Coquery, M. Impact of Wastewater Treatment Plants on Receiving Surface Waters and a Tentative Risk Evaluation: The Case of Estrogens and Beta Blockers. *Environ. Sci. Pollut. Res.* **2014**, *21* (3), 1708–1722. https://doi.org/10.1007/s11356-013-2037-7.
(63) Fono, L. J.; Kolodziej, E. P.; Sedlak, D. L. Attenuation of Wastewater-Derived Contaminants in an Effluent-Dominated River †. *Environ. Sci. Technol.* **2006**, *40* (23), 7257–7262. https://doi.org/10.1021/es061308e.
(64) Stein, K.; Ramil, M.; Fink, G.; Sander, M.; Ternes, T. A. Analysis and Sorption of Psychoactive Drugs onto Sediment. *Environ. Sci. Technol.* **2008**, *42* (17), 6415–6423. https://doi.org/10.1021/es702959a.
(65) Kasprzyk-Hordern, B.; Dinsdale, R. M.; Guwy, A. J. The Occurrence of Pharmaceuticals, Personal Care Products, Endocrine Disruptors and Illicit Drugs in Surface Water in South Wales, UK. *Water Res.* **2008**, *42* (13), 3498–3518. https://doi.org/10.1016/j.watres.2008.04.026.
(66) Ebele, A. J.; Abou-Elwafa Abdallah, M.; Harrad, S. Pharmaceuticals and Personal Care Products (PPCPs) in the Freshwater Aquatic Environment. *Emerg. Contam.* **2017**, *3* (1), 1–16. https://doi.org/10.1016/j.emcon.2016.12.004.
(67) Buerge, I. J.; Poiger, T.; Müller, M. D.; Buser, H.-R. Caffeine, an Anthropogenic Marker for Wastewater Contamination of Surface Waters. *Environ. Sci. Technol.* **2003**, *37* (4), 691–700. https://doi.org/10.1021/es020125z.
(68) Edwards, Q. A.; Kulikov, S. M.; Garner-O'Neale, L. D. Caffeine in Surface and Wastewaters in Barbados, West Indies. *SpringerPlus* **2015**, *4*. https://doi.org/10.1186/s40064-015-0809-x.

(69) Gardinali, P. R.; Zhao, X. Trace Determination of Caffeine in Surface Water Samples by Liquid Chromatography–Atmospheric Pressure Chemical Ionization–Mass Spectrometry (LC–APCI–MS). *Environ. Int.* **2002**, *28* (6), 521–528. https://doi.org/10.1016/S0160-4120(02)00080-6.
(70) Gonçalves, E. S.; Rodrigues, S.; Silva-Filho, E. V. da. The Use of Caffeine as a Chemical Marker of Domestic Wastewater Contamination in Surface Waters: Seasonal and Spatial Variations in Teresópolis, Brazil; 2017. https://doi.org/10.4136/ambi-agua.1974.
(71) Tp185-C6.Pdf.
(72) Weeks, J. A.; Guiney, P. D.; Nikiforov, A. I. Assessment of the Environmental Fate and Ecotoxicity of N,N-Diethyl-m-Toluamide (DEET). *Integr. Environ. Assess. Manag.* **2012**, *8* (1), 120–134. https://doi.org/10.1002/ieam.1246.
(73) Aronson, D.; Weeks, J.; Meylan, B.; Guiney, P. D.; Howard, P. H. Environmental Release, Environmental Concentrations, and Ecological Risk of N,N-Diethyl-m-Toluamide (DEET). *Integr. Environ. Assess. Manag.* **2012**, *8* (1), 135–166. https://doi.org/10.1002/ieam.271.
(74) Bradley, P. M.; Barber, L. B.; Clark, J. M.; Duris, J. W.; Foreman, W. T.; Furlong, E. T.; Givens, C. E.; Hubbard, L. E.; Hutchinson, K. J.; Journey, C. A.; et al. Pre/Post-Closure Assessment of Groundwater Pharmaceutical Fate in a Wastewater-Facility-Impacted Stream Reach. *Sci. Total Environ.* **2016**, *568*, 916–925. https://doi.org/10.1016/j.scitotenv.2016.06.104.
(75) Huerta-Fontela, M.; Galceran, M. T.; Ventura, F. Ultraperformance Liquid Chromatography−Tandem Mass Spectrometry Analysis of Stimulatory Drugs of Abuse in Wastewater and Surface Waters. *Anal. Chem.* **2007**, *79* (10), 3821–3829. https://doi.org/10.1021/ac062370x.
(76) Silva, A. K. da; Amador, J.; Cherchi, C.; Miller, S. M.; Morse, A. N.; Pellegrin, M.-L.; Wells, M. J. M. Emerging Pollutants – Part I: Occurrence, Fate and Transport. *Water Environ. Res.* **2013**, *85* (10), 1978–2021. https://doi.org/10.2175/106143013X13698672323065.
(77) Wells, M. J. M.; Bell, K. Y.; Traexler, K. A.; Pellegrin, M.-L.; Morse, A. Emerging Pollutants. *Water Environ. Res.* **2010**, *82* (10), 2095–2170. https://doi.org/10.2175/106143010X12756668802292.
(78) Bradley, P. M.; Battaglin, W. A.; Clark, J. M.; Henning, F. P.; Hladik, M. L.; Iwanowicz, L. R.; Journey, C. A.; Riley, J. W.; Romanok, K. M. Widespread Occurrence and Potential for Biodegradation of Bioactive Contaminants in Congaree National Park, USA: Bioactive Contaminants in Congaree National Park. *Environ. Toxicol. Chem.* **2017**, *36* (11), 3045–3056. https://doi.org/10.1002/etc.3873.
(79) Writer, J. H.; Ferrer, I.; Barber, L. B.; Thurman, E. M. Widespread Occurrence of Neuro-Active Pharmaceuticals and Metabolites in 24 Minnesota Rivers and Wastewaters. *Sci. Total Environ.* **2013**, *461–462*, 519–527. https://doi.org/10.1016/j.scitotenv.2013.04.099.
(80) Giebułtowicz, J.; Nałęcz-Jawecki, G. Occurrence of Antidepressant Residues in the Sewage-Impacted Vistula and Utrata Rivers and in Tap Water in Warsaw

(Poland). *Ecotoxicol. Environ. Saf.* **2014**, *104*, 103–109. https://doi.org/10.1016/j.ecoenv.2014.02.020.
(81) Schultz, M. M.; Furlong, E. T.; Kolpin, Dana. W.; Werner, S. L.; Schoenfuss, H. L.; Barber, L. B.; Blazer, V. S.; Norris, D. O.; Vajda, A. M. Antidepressant Pharmaceuticals in Two U.S. Effluent-Impacted Streams: Occurrence and Fate in Water and Sediment, and Selective Uptake in Fish Neural Tissue. *Environ. Sci. Technol.* **2010**, *44* (6), 1918–1925. https://doi.org/10.1021/es9022706.
(82) Hilton, M. J.; Thomas, K. V. Determination of Selected Human Pharmaceutical Compounds in Effluent and Surface Water Samples by High-Performance Liquid Chromatography–Electrospray Tandem Mass Spectrometry. *J. Chromatogr. A* **2003**, *1015* (1–2), 129–141. https://doi.org/10.1016/S0021-9673(03)01213-5.
(83) Clara, M.; Strenn, B.; Kreuzinger, N. Carbamazepine as a Possible Anthropogenic Marker in the Aquatic Environment: Investigations on the Behaviour of Carbamazepine in Wastewater Treatment and during Groundwater Infiltration. *Water Res.* **2004**, *38* (4), 947–954. https://doi.org/10.1016/j.watres.2003.10.058.
(84) Zhang, Y.; Geißen, S.-U.; Gal, C. Carbamazepine and Diclofenac: Removal in Wastewater Treatment Plants and Occurrence in Water Bodies. *Chemosphere* **2008**, *73* (8), 1151–1161. https://doi.org/10.1016/j.chemosphere.2008.07.086.
(85) Tixier, C.; Singer, H. P.; Oellers, S.; Müller, S. R. Occurrence and Fate of Carbamazepine, Clofibric Acid, Diclofenac, Ibuprofen, Ketoprofen, and Naproxen in Surface Waters. *Environ. Sci. Technol.* **2003**, *37* (6), 1061–1068. https://doi.org/10.1021/es025834r.
(86) Schultz, M. M.; Furlong, E. T. Trace Analysis of Antidepressant Pharmaceuticals and Their Select Degradates in Aquatic Matrixes by LC/ESI/MS/MS. *Anal. Chem.* **2008**, *80* (5), 1756–1762. https://doi.org/10.1021/ac702154e.
(87) Bachour, R.-L.; Golovko, O.; Kellner, M.; Pohl, J. Behavioral Effects of Citalopram, Tramadol, and Binary Mixture in Zebrafish (Danio Rerio) Larvae. *Chemosphere* **2020**, *238*, 124587. https://doi.org/10.1016/j.chemosphere.2019.124587.
(88) Fernandes, M. J.; Paíga, P.; Silva, A.; Llaguno, C. P.; Carvalho, M.; Vázquez, F. M.; Delerue-Matos, C. Antibiotics and Antidepressants Occurrence in Surface Waters and Sediments Collected in the North of Portugal. *Chemosphere* **2020**, *239*, 124729. https://doi.org/10.1016/j.chemosphere.2019.124729.
(89) Rúa-Gómez, P. C.; Püttmann, W. Occurrence and Removal of Lidocaine, Tramadol, Venlafaxine, and Their Metabolites in German Wastewater Treatment Plants. *Environ. Sci. Pollut. Res.* **2012**, *19* (3), 689–699. https://doi.org/10.1007/s11356-011-0614-1.
(90) Rezka, P.; Balcerzak, W. Occurrence of Antidepressants – from Wastewater to Drinking Water; 2016. https://doi.org/10.4467/2353737XCT.16.204.5953.
(91) Kumar, A.; Xagoraraki, I. Fate of Pharmaceuticals , Personal Care Products , and Endocrine-Disrupting 1 Chemicals in Water 2 3; 2012.
(92) Bernot, M. J.; Becker, J. C.; Doll, J.; Lauer, T. E. A National Reconnaissance of Trace Organic Compounds (TOCs) in United States Lotic Ecosystems. *Sci. Total Environ.* **2016**, *572*, 422–433. https://doi.org/10.1016/j.scitotenv.2016.08.060.

(93) R_EastmanSOE2013_final_for_web-Web.Pdf.
(94) Klosterhaus, S. L.; Grace, R.; Hamilton, M. C.; Yee, D. Method Validation and Reconnaissance of Pharmaceuticals, Personal Care Products, and Alkylphenols in Surface Waters, Sediments, and Mussels in an Urban Estuary. *Environ. Int.* **2013**, *54*, 92–99. https://doi.org/10.1016/j.envint.2013.01.009.
(95) Duarte, B.; Caçador, M. I. V. *Ecotoxicology of Marine Organisms*; CRC Press, 2019.
(96) Hai, F. I.; Visvanathan, C.; Boopathy, R. *Sustainable Aquaculture*; Springer, 2018.
(97) Prasad, M. N. V.; Vithanage, M.; Kapley, A. *Pharmaceuticals and Personal Care Products: Waste Management and Treatment Technology: Emerging Contaminants and Micro Pollutants*; Butterworth-Heinemann, 2019.
(98) Hummel, D.; Löffler, D.; Fink, G.; Ternes, T. A. Simultaneous Determination of Psychoactive Drugs and Their Metabolites in Aqueous Matrices by Liquid Chromatography Mass Spectrometry †. *Environ. Sci. Technol.* **2006**, *40* (23), 7321–7328. https://doi.org/10.1021/es061740w.
(99) Huerta-Fontela, M.; Galceran, M. T.; Ventura, F. Ultraperformance Liquid Chromatography−Tandem Mass Spectrometry Analysis of Stimulatory Drugs of Abuse in Wastewater and Surface Waters. *Anal. Chem.* **2007**, *79* (10), 3821–3829. https://doi.org/10.1021/ac062370x.
(100) Castiglioni, S.; Zuccato, E.; Crisci, E.; Chiabrando, C.; Fanelli, R.; Bagnati, R. Identification and Measurement of Illicit Drugs and Their Metabolites in Urban Wastewater by Liquid Chromatography−Tandem Mass Spectrometry. *Anal. Chem.* **2006**, *78* (24), 8421–8429. https://doi.org/10.1021/ac061095b.
(101) Ferrer, I.; Heine, C. E.; Thurman, E. M. Combination of LC/TOF-MS and LC/Ion Trap MS/MS for the Identification of Diphenhydramine in Sediment Samples. *Anal. Chem.* **2004**, *76* (5), 1437–1444. https://doi.org/10.1021/ac034794m.
(102) Pharmaceuticals, Personal Care Products, and Perfluoroalkyl Substances in Elliott Bay Sediments: 2013 Data Summary. 15.
(103) Han, K. D.; Bark, K.-M.; Heo, E. P.; Lee, J. K.; Kang, J. S.; Kim, T. H. Increased Phototoxicity of Hydrochlorothiazide by Photodegradation. *Photodermatol. Photoimmunol. Photomed.* **2000**, *16* (3), 121–124. https://doi.org/10.1111/j.1600-0781.2000.160304.x.
(104) Tamat, S. R.; Moore, D. E. Photolytic Decomposition of Hydrochlorothiazide. *J. Pharm. Sci.* **1983**, *72* (2), 180–183. https://doi.org/10.1002/jps.2600720221.
(105) Borowska, E.; Bourgin, M.; Hollender, J.; Kienle, C.; McArdell, C. S.; von Gunten, U. Oxidation of Cetirizine, Fexofenadine and Hydrochlorothiazide during Ozonation: Kinetics and Formation of Transformation Products. *Water Res.* **2016**, *94*, 350–362. https://doi.org/10.1016/j.watres.2016.02.020.
(106) Kim, I.; Tanaka, H. Photodegradation Characteristics of PPCPs in Water with UV Treatment. *Environ. Int.* **2009**, *35* (5), 793–802. https://doi.org/10.1016/j.envint.2009.01.003.
(107) Maldonado-Torres, S.; Gurung, R.; Rijal, H.; Chan, A.; Acharya, S.; Rogelj, S.; Piyasena, M.; Rubasinghege, G. Fate, Transformation, and Toxicological Impacts

of Pharmaceutical and Personal Care Products in Surface Waters. *Environ. Health Insights* **2018**, *12*. https://doi.org/10.1177/1178630218795836.
(108) Martínez-Hernández, V.; Meffe, R.; Herrera, S.; Arranz, E.; de Bustamante, I. Sorption/Desorption of Non-Hydrophobic and Ionisable Pharmaceutical and Personal Care Products from Reclaimed Water onto/from a Natural Sediment. *Sci. Total Environ.* **2014**, *472*, 273–281. https://doi.org/10.1016/j.scitotenv.2013.11.036.
(109) Liu, Y.; Lu, X.; Wu, F.; Deng, N. Adsorption and Photooxidation of Pharmaceuticals and Personal Care Products on Clay Minerals. *React. Kinet. Mech. Catal.* **2011**, *104* (1), 61–73. https://doi.org/10.1007/s11144-011-0349-5.
(110) Li, F. B.; Li, X. Z.; Liu, C. S.; Li, X. M.; Liu, T. X. Effect of Oxalate on Photodegradation of Bisphenol A at the Interface of Different Iron Oxides. *Ind. Eng. Chem. Res.* **2007**, *46* (3), 781–787. https://doi.org/10.1021/ie0612820.
(111) Khetan, S. K.; Collins, T. J. Human Pharmaceuticals in the Aquatic Environment: A Challenge to Green Chemistry. *Chem. Rev.* **2007**, *107* (6), 2319–2364. https://doi.org/10.1021/cr020441w.
(112) Sui, Q.; Huang, J.; Deng, S.; Chen, W.; Yu, G. Seasonal Variation in the Occurrence and Removal of Pharmaceuticals and Personal Care Products in Different Biological Wastewater Treatment Processes. *Environ. Sci. Technol.* **2011**, *45* (8), 3341–3348. https://doi.org/10.1021/es200248d.
(113) Loraine, G. A.; Pettigrove, M. E. Seasonal Variations in Concentrations of Pharmaceuticals and Personal Care Products in Drinking Water and Reclaimed Wastewater in Southern California. *Environ. Sci. Technol.* **2006**, *40* (3), 687–695. https://doi.org/10.1021/es051380x.
(114) Sun, Q.; Lv, M.; Hu, A.; Yang, X.; Yu, C.-P. Seasonal Variation in the Occurrence and Removal of Pharmaceuticals and Personal Care Products in a Wastewater Treatment Plant in Xiamen, China. *J. Hazard. Mater.* **2014**, *277*, 69–75. https://doi.org/10.1016/j.jhazmat.2013.11.056.
(115) Marques dos Santos, M.; Hoppe-Jones, C.; Snyder, S. A. DEET Occurrence in Wastewaters: Seasonal, Spatial and Diurnal Variability - Mismatches between Consumption Data and Environmental Detection. *Environ. Int.* **2019**, *132*, 105038. https://doi.org/10.1016/j.envint.2019.105038.
(116) US EPA, O. DEET https://www.epa.gov/insect-repellents/deet (accessed Aug 13, 2019).
(117) 20872se8-003,20625se8-010_allegra_lbl.Pdf.
(118) CDCTobaccoFree. Data and Statistics https://www.cdc.gov/tobacco/data_statistics/index.htm (accessed Oct 28, 2019).
(119) Abuse, N. I. on D. Tobacco/Nicotine and Vaping https://www.drugabuse.gov/drugs-abuse/tobacconicotine-vaping (accessed Oct 28, 2019).
(120) Kelly-Gerreyn, B.; Hydes, D.; Waniek, J. Control of the Diffusive Boundary Layer on Benthic Fluxes: A Model Study. *Mar. Ecol. Prog. Ser.* **2005**, *292*, 61–74. https://doi.org/10.3354/meps292061.

(121) Environmental Organic Chemistry, 3rd Edition | Wiley https://www.wiley.com/en-us/Environmental+Organic+Chemistry%2C+3rd+Edition-p-9781118767238 (accessed Nov 7, 2019).
(122) Cui, S.; Fu, Q.; Li, T.; Ma, W.; Liu, D.; Wang, M. Sediment-Water Exchange, Spatial Variations, and Ecological Risk Assessment of Polycyclic Aromatic Hydrocarbons (PAHs) in the Songhua River, China. *Water* **2016**, *8* (8), 334. https://doi.org/10.3390/w8080334.
(123) Minick, D. J.; Anderson, K. A. Diffusive Flux of PAHs across Sediment-Water and Water-Air Interfaces at Urban Superfund Sites. *Environ. Toxicol. Chem.* **2017**, *36* (9), 2281–2289. https://doi.org/10.1002/etc.3785.
(124) Berton Fisher, J.; Petty, R. L.; Lick, W. Release of Polychlorinated Biphenyls from Contaminated Lake Sediments: Flux and Apparent Diffusivities of Four Individual PCBs. *Environ. Pollut. Ser. B Chem. Phys.* **1983**, *5* (2), 121–132. https://doi.org/10.1016/0143-148X(83)90041-1.
(125) Koelmans, A. A.; Poot, A.; Lange, H. J. D.; Velzeboer, I.; Harmsen, J.; Noort, P. C. M. van. Estimation of In Situ Sediment-to-Water Fluxes of Polycyclic Aromatic Hydrocarbons, Polychlorobiphenyls and Polybrominated Diphenylethers. *Environ. Sci. Technol.* **2010**, *44* (8), 3014–3020. https://doi.org/10.1021/es903938z.
(126) Kupryianchyk, D.; Noori, A.; Rakowska, M. I.; Grotenhuis, J. T. C.; Koelmans, A. A. Bioturbation and Dissolved Organic Matter Enhance Contaminant Fluxes from Sediment Treated with Powdered and Granular Activated Carbon. *Environ. Sci. Technol.* **2013**, *47* (10), 5092–5100. https://doi.org/10.1021/es3040297.
(127) Fernandez, L. A.; Lao, W.; Maruya, K. A.; Burgess, R. M. Calculating the Diffusive Flux of Persistent Organic Pollutants between Sediments and the Water Column on the Palos Verdes Shelf Superfund Site Using Polymeric Passive Samplers. *Environ. Sci. Technol.* **2014**, *48* (7), 3925–3934. https://doi.org/10.1021/es404475c.
(128) Gergory Foster. *Survey of Micropollutants in Fluvial-Estuarine Sediments and Water from the Hunting Creek Watershed and the Tidal Freshwater Potomac River*; Potomac Environmental Reserach and Education Center, 2019; pp 1–47.
(129) Berner, R. A. The Benthic Boundary Layer from the Viewpoint of a Geochemist. In *The Benthic Boundary Layer*; McCave, I. N., Ed.; Springer US: Boston, MA, 1976; pp 33–55. https://doi.org/10.1007/978-1-4615-8747-7_3.
(130) Zhou, J. L.; Hong, H.; Zhang, Z.; Maskaoui, K.; Chen, W. Multi-Phase Distribution of Organic Micropollutants in Xiamen Harbour, China. *Water Res.* **2000**, *34* (7), 2132–2150. https://doi.org/10.1016/S0043-1354(99)00360-7.
(131) Neff, J. M. Bioaccumulation of Organic Micropollutants from Sediments and Suspended Particulates by Aquatic Animals. *Fresenius Z. Für Anal. Chem.* **1984**, *319* (2), 132–136. https://doi.org/10.1007/BF00584674.
(132) Maskaoui, K.; Zhou, J. L.; Zheng, T. L.; Hong, H.; Yu, Z. Organochlorine Micropollutants in the Jiulong River Estuary and Western Xiamen Sea, China. *Mar. Pollut. Bull.* **2005**, *51* (8), 950–959. https://doi.org/10.1016/j.marpolbul.2004.11.018.

(133) van der Wal, L.; Jager, T.; Fleuren, R. H. L. J.; Barendregt, A.; Sinnige, T. L.; van Gestel, C. A. M.; Hermens, J. L. M. Solid-Phase Microextraction To Predict Bioavailability and Accumulation of Organic Micropollutants in Terrestrial Organisms after Exposure to a Field-Contaminated Soil. *Environ. Sci. Technol.* **2004**, *38* (18), 4842–4848. https://doi.org/10.1021/es035318g.
(134) County, F. Cameron Run Watershed Management Plan. **2007**, 770.
(135) Wimbush, M. The Physics of the Benthic Boundary Layer. In *The Benthic Boundary Layer*; McCave, I. N., Ed.; Springer US: Boston, MA, 1976; pp 3–10. https://doi.org/10.1007/978-1-4615-8747-7_1.
(136) Eek, E.; Cornelissen, G.; Breedveld, G. D. Field Measurement of Diffusional Mass Transfer of HOCs at the Sediment-Water Interface. *Environ. Sci. Technol.* **2010**, *44* (17), 6752–6759. https://doi.org/10.1021/es100818w.
(137) Cumming, B. Limnology: Lake and River Ecosystems. Third Edition. By Robert G Wetzel. *Q. Rev. Biol.* **2003**, *78* (3), 368–369. https://doi.org/10.1086/380040.
(138) Mopper, K.; Qian, J. Water Analysis: Organic Carbon Determinations. In *Encyclopedia of Analytical Chemistry*; Meyers, R. A., Ed.; John Wiley & Sons, Ltd: Chichester, UK, 2000. https://doi.org/10.1002/9780470027318.a0884.
(139) Fukushima, T.; Imai, A.; Matsushige, K.; Aizaki, M.; Otsuki, A. Freshwater DOC Measurements by High-Temperature Combustion: Comparison of Differential (DTC - DIC) and DIC Purging Methods. *Water Res.* **1996**, *30* (11), 2717–2722. https://doi.org/10.1016/S0043-1354(96)00198-4.
(140) Williams, P. M.; Bauer, J. E.; Robertson, K. J.; Wolgast, D. M.; Occelli, M. L. Report on DOC and DON Measurements Made at Scripps Institution of Oceanography, 1988–1991. *Mar. Chem.* **1993**, *41* (1–3), 271–281. https://doi.org/10.1016/0304-4203(93)90130-G.
(141) ChemSpider | Search and share chemistry http://www.chemspider.com/ (accessed Nov 1, 2019).
(142) Santschi, P. H.; Anderson, R. F.; Fleisher, M. Q.; Bowles, W. Measurements of Diffusive Sublayer Thicknesses in the Ocean by Alabaster Dissolution, and Their Implications for the Measurements of Benthic Fluxes. *J. Geophys. Res. Oceans* **1991**, *96* (C6), 10641–10657. https://doi.org/10.1029/91JC00488.
(143) Santschi, P. H.; Bower, P.; Nyffeler, U. P.; Azevedo, A.; Broecker, W. S. Estimates of the Resistance to Chemical Transport Posed by the Deep-Sea Boundary Layer1,2. *Limnol. Oceanogr.* **1983**, *28* (5), 899–912. https://doi.org/10.4319/lo.1983.28.5.0899.
(144) Thibodeaux, L. J.; Valsaraj, K. T.; Reible, D. D. Bioturbation-Driven Transport of Hydrophobic Organic Contaminants from Bed Sediment. *Environ. Eng. Sci.* **2001**, *18* (4), 215–223. https://doi.org/10.1089/109287501753113124.
(145) Eek, E.; Cornelissen, G.; Kibsgaard, A.; Breedveld, G. D. Diffusion of PAH and PCB from Contaminated Sediments with and without Mineral Capping; Measurement and Modelling. *Chemosphere* **2008**, *71* (9), 1629–1638. https://doi.org/10.1016/j.chemosphere.2008.01.051.
(146) Oen, A. M. P.; Schaanning, M.; Ruus, A.; Cornelissen, G.; Källqvist, T.; Breedveld, G. D. Predicting Low Biota to Sediment Accumulation Factors of

PAHs by Using Infinite-Sink and Equilibrium Extraction Methods as Well as BC-Inclusive Modeling. *Chemosphere* **2006**, *64* (8), 1412–1420. https://doi.org/10.1016/j.chemosphere.2005.12.028.

(147) Howell, N. L.; Rifai, H. S. Longitudinal Estimates of Sediment-Water Diffusive Flux of PCB Congeners in the Houston Ship Channel. *Estuar. Coast. Shelf Sci.* **2015**, *164*, 19–27. https://doi.org/10.1016/j.ecss.2015.06.024.

(148) Li, J.; Shang, X.; Zhao, Z.; Tanguay, R. L.; Dong, Q.; Huang, C. Polycyclic Aromatic Hydrocarbons in Water, Sediment, Soil, and Plants of the Aojiang River Waterway in Wenzhou, China. *J. Hazard. Mater.* **2010**, *173* (1–3), 75–81. https://doi.org/10.1016/j.jhazmat.2009.08.050.

(149) (PDF) PCB fluxes from the sediment to the water column following resuspension – A column experiment https://www.researchgate.net/publication/50357135_PCB_fluxes_from_the_sediment_to_the_water_column_following_resuspension_-_A_column_experiment (accessed Nov 2, 2019).

(150) Bioturbation-Driven Release of Buried PCBs and PBDEs from Different Depths in Contaminated Sediments https://pubs.acs.org/doi/pdfplus/10.1021/es100615g (accessed Nov 1, 2019). https://doi.org/10.1021/es100615g.

(151) Kondolf, G. M. PROFILE: Hungry Water: Effects of Dams and Gravel Mining on River Channels. *Environ. Manage.* **1997**, *21* (4), 533–551. https://doi.org/10.1007/s002679900048.

(152) Neal, C.; Leeks, G.; Millward, G.; Harris, J.; Huthnance, J.; Rees, J. Land–Ocean Interaction: Processes, Functioning and Environmental Management from a UK Perspective: An Introduction. *Sci. Total Environ.* **2003**, *314–316*, 3–11. https://doi.org/10.1016/S0048-9697(03)00091-3.

(153) Saeedi, M.; Daneshvar, Sh.; Karbassi, A. R. Role of Riverine Sediment and Particulate Matter in Adsorption of Heavy Metals. *Int. J. Environ. Sci. Technol.* **2004**, *1* (2), 135–140. https://doi.org/10.1007/BF03325826.

(154) Dvoršćak, M.; Fingler, S.; Mendaš, G.; Stipičević, S.; Vasilić, Ž.; Drevenkar, V. Distribution of Organochlorine Pesticide and Polychlorinated Biphenyl Residues in Lake Sediment Cores from the Plitvice Lakes National Park (Croatia). *Arch. Environ. Contam. Toxicol.* **2019**, *77* (4), 537–548. https://doi.org/10.1007/s00244-019-00668-z.

(155) Matić Bujagić, I.; Grujić, S.; Laušević, M.; Hofmann, T.; Micić, V. Emerging Contaminants in Sediment Core from the Iron Gate I Reservoir on the Danube River. *Sci. Total Environ.* **2019**, *662*, 77–87. https://doi.org/10.1016/j.scitotenv.2019.01.205.

(156) Radović, T.; Grujić, S.; Petković, A.; Dimkić, M.; Laušević, M. Determination of Pharmaceuticals and Pesticides in River Sediments and Corresponding Surface and Ground Water in the Danube River and Tributaries in Serbia. *Environ. Monit. Assess.* **2014**, *187* (1), 4092. https://doi.org/10.1007/s10661-014-4092-z.

(157) Wade, T. L.; Velinsky, D. J.; Reinharz, E.; Schlekat, C. E. Tidal River Sediments in the Washington, D.C. Area. II. Distribution and Sources of Organic Contaminants. *Estuaries* **1994**, *17* (2), 321–333. https://doi.org/10.2307/1352666.

(158) Zwolsman, J. J. G.; Berger, G. W.; Van Eck, G. T. M. Sediment Accumulation Rates, Historical Input, Postdepositional Mobility and Retention of Major Elements and Trace Metals in Salt Marsh Sediments of the Scheldt Estuary, SW Netherlands. *Mar. Chem.* **1993**, *44* (1), 73–94. https://doi.org/10.1016/0304-4203(93)90007-B.
(159) Simms, A. R.; Rodriguez, A. B.; Anderson, J. B. Bayhead Deltas and Shorelines: Insights from Modern and Ancient Examples. *Sediment. Geol.* **2018**, *374*, 17–35. https://doi.org/10.1016/j.sedgeo.2018.07.004.
(160) Society, N. G. estuary http://www.nationalgeographic.org/encyclopedia/estuary/ (accessed Nov 3, 2019).
(161) Covaci, A.; Gheorghe, A.; Voorspoels, S.; Maervoet, J.; Steen Redeker, E.; Blust, R.; Schepens, P. Polybrominated Diphenyl Ethers, Polychlorinated Biphenyls and Organochlorine Pesticides in Sediment Cores from the Western Scheldt River (Belgium): Analytical Aspects and Depth Profiles. *Environ. Int.* **2005**, *31* (3), 367–375. https://doi.org/10.1016/j.envint.2004.08.009.
(162) Wang, W.; Bai, J.; Zhang, G.; Wang, X.; Jia, J.; Cui, B.; Liu, X. Depth-Distribution, Possible Sources, and Toxic Risk Assessment of Organochlorine Pesticides (OCPs) in Different River Sediment Cores Affected by Urbanization and Reclamation in a Chinese Delta. *Environ. Pollut.* **2017**, *230*, 1062–1072. https://doi.org/10.1016/j.envpol.2017.06.068.
(163) Venkatesan, M. I.; de Leon, R. P.; van Geen, A.; Luoma, S. N. Chlorinated Hydrocarbon Pesticides and Polychlorinated Biphenyls in Sediment Cores from San Francisco Bay1Institute of Geophysics and Planetary Physics Contribution Number: 4214.1. *Mar. Chem.* **1999**, *64* (1), 85–97. https://doi.org/10.1016/S0304-4203(98)90086-X.
(164) Gong, X.; Qi, S.; Wang, Y.; Julia, E. B.; Lv, C. Historical Contamination and Sources of Organochlorine Pesticides in Sediment Cores from Quanzhou Bay, Southeast China. *Mar. Pollut. Bull.* **2007**, *54* (9), 1434–1440. https://doi.org/10.1016/j.marpolbul.2007.05.006.
(165) Sediment-Sampling.Pdf.
(166) *Scientific Investigations Report*; Scientific Investigations Report; 2004.
(167) DDT, DDE, and DDD - ToxFAQs™. 2.
(168) Jayaraj, R.; Megha, P.; Sreedev, P. Organochlorine Pesticides, Their Toxic Effects on Living Organisms and Their Fate in the Environment. *Interdiscip. Toxicol.* **2016**, *9* (3–4), 90–100. https://doi.org/10.1515/intox-2016-0012.
(169) Adeyinka, A.; Pierre, L. Organophosphates. In *StatPearls*; StatPearls Publishing: Treasure Island (FL), 2019.
(170) US EPA, O. DDT - A Brief History and Status https://www.epa.gov/ingredients-used-pesticide-products/ddt-brief-history-and-status (accessed Nov 5, 2019).
(171) US EPA, O. DDT Ban Takes Effect ddt-ban-takes-effect.html (accessed Nov 5, 2019).
(172) Hung, C.-C.; Gong, G.-C.; Chen, H.-Y.; Hsieh, H.-L.; Santschi, P. H.; Wade, T. L.; Sericano, J. L. Relationships between Pesticides and Organic Carbon Fractions in Sediments of the Danshui River Estuary and Adjacent Coastal Areas of Taiwan.

Environ. Pollut. **2007**, *148* (2), 546–554. https://doi.org/10.1016/j.envpol.2006.11.036.
(173) D-(-)-Morphine | C17H19NO3 | ChemSpider http://www.chemspider.com/Chemical-Structure.4450907.html?rid=2dd525c3-9667-4e11-a7fd-49f01695869e (accessed Feb 7, 2018).
(174) (-)-Tramadol | C16H25NO2 | ChemSpider http://www.chemspider.com/Chemical-Structure.580887.html?rid=39180ff0-2807-4f2f-9dc1-6cd6738eac7a&page_num=0 (accessed Feb 7, 2018).
(175) Buprenorphine | C29H41NO4 | ChemSpider http://www.chemspider.com/Chemical-Structure.559124.html?rid=315e87a7-4a3a-48d5-ac18-b49b18bff265 (accessed Feb 7, 2018).

BIOGRAPHY

Arion Leahigh received her Bachelor of Science from the University of Pittsburgh in 2013. She was employed as a graduate research assistant and graduate teaching assistant at George Mason University for five years and received her Doctor of Philosophy degree in Chemistry and Biochemistry from George Mason University in 2019.